Department of Pharmacology and Toxicology
Faculty of Pharmacy in Hradec Králové
Charles University
Czech Republic

Novel approaches for development of *in vitro* liver cell models

Doctoral dissertation (article-based)

Hradec Králové 2017 Mgr. Tomáš Smutný

I hereby declare that this thesis is my original work which I solely composed by myself under the supervision of **Prof. PharmDr. Petr Pávek, Ph.D.** All used literature and other sources are summarized in the list of references and properly cited. This work has not been submitted for any different or equal degree.

Prohlašuji, že tato práce je mým původním autorským dílem, které jsem vypracoval samostatně pod vedením svého školitele **prof. PharmDr. Petra Pávka, Ph.D.** Veškerá literatura a další zdroje, z nichž jsem při zpracování čerpal, jsou uvedeny v seznamu použité literatury a v práci řádně citovány. Práce nebyla využita k získání jiného nebo stejného titulu.

……..

Mgr. Tomáš Smutný

Acknowledgements

I am pleased to say thank you here to some people who helped me to bring this work to its end. I was working as a doctoral student from 2011-2017. I am deeply grateful to Professor Petr Pávek for his untiring assistance and guidance through all these years. Professor Pávek shaped me by his inspiring ideas and sharing knowledge. I want to thank Professor Pávek for his permanent support through my doctoral study and his enthusiasm. I would also like to warmly thank to Adjunct Professor Yan-Ru Lou who guided me during my research fellowship at the University of Helsinki. I gratefully thank to Adjunct Professor Yan-Ru Lou for her support and inspiring discussion. I would like to thank Professor Marjo Yliperttula for giving me an opportunity to study at University of Helsinki. My thanks also go to all co-authors who contributed to a completion of this dissertation.

I acknowledge all my former and present colleagues at the Faculty of Pharmacy in Hradec Králové. I am very grateful to Dr. Michal Říha for his good advice and enduring friendship.

Liisa Kanninen, Riina Harjumäki, Tuuli Salmi, Mariia Bogacheva, Ara Taalas, Alma Kartal-Hodzic, Johanna Niklander, Leena Pietilä and Timo Oksanen are acknowledged for excellent collaboration and great company. All of them helped me to enjoy wonderful year in Finland. Liisa Kanninen is specially thanked for her excellent team working skills and support. Kiitos paljon.

I wish to thank Lucy who has made my life more beautiful. I thank to my parents, grandparents, brothers and friends for taking part in my everyday life.

At the end, I would like to acknowledge the Charles University Grant Agency (GAUK) 338315 (170/50/55006), the Grant Agency of the Czech Republic (GACR) 303/12/0472, 303/12/G163, and SVV project 260 293 for a support of this work.

Abstract

Charles University
Faculty of Pharmacy in Hradec Králové
Department of Pharmacology and Toxicology
Candidate: Tomáš Smutný, MSc.
Supervisor: Prof. PharmDr. Petr Pávek, Ph.D.
Title of doctoral thesis: Novel approaches for development of in vitro liver cell models.

The liver is a main metabolizing organ in the body. Therefore, the evaluation of hepatic metabolism is a crucial step during drug development. Moreover, a liver damage induced by drugs is another task to be assessed in drug development. *In vitro* liver cell models allow addressing some of these concerns. Up to date, primary human hepatocytes are considered as a "gold" standard of *in vitro* liver cell models. Additionally, other liver model systems are used such as liver tissue slices, subcellular fractions, liver cancer cell lines and hepatocytes derived from stem cells. Despite the significant progress towards right estimation of pharmacokinetic and toxicological parameters of drug candidates during drug development, current *in vitro* systems still suffer from various drawbacks. One of these limitations is their insufficient similarity with *in vivo*-like phenotype associated with low metabolic capacity of the models. In last several years, we were victims of tremendous effort to improve existing models such as 3D models, co-culture and perfusion cultures.

Aims of this thesis can be divided into three parts. Firstly, we tried to enhance metabolic capacity of *in vitro* liver cell models using small molecules, which are activators of crucial nuclear receptors controlling expression of drug-metabolizing enzymes (DMEs). Liver cancer cell lines were predominantly utilized since these cells have fast and unlimited life-span, good availability and easy handling but lack many DMEs. Secondly, we focused on the impact of post-transcriptional and post-translational modifications of key regulators of DMEs, which could also shed some light on the phenomenon of low DMEs expression in common liver cell lines. Finally, we applied *in vitro* liver cell models including stem cell-derived hepatocytes for a hepatotoxicity assessment of newly developed drug candidates and suspected hepatotoxicans-derived from medical plants.

In our first study, we identified MEK1/2 inhibitors as strong activators CYP3A subfamily genes in commonly used hepatocellular carcinoma cell line HepG2. These results are important since CYP3A4 isoform metabolizes more than 30% of all clinically used drugs and it is poorly expressed in this cell line as well as in other liver cell models. Furthermore, we attempted to decipher the mechanism underlying this phenomenon.

Secondly, we identified several new compounds functioning as "pan-xenosensors" ligands. Since nuclear receptors (NRs) such as PXR, CAR and transcription factor AhR are involved in the gene regulation of DMEs, we suppose that these small molecules can be used for the boosting of DME gene expression in *in vitro* liver models.

In another study, we focused on *in silico* prediction of microRNAs (miRNAs) targeting NRs, which are associated with CYP3A4 regulation. We and other groups suggested that the effect of miRNAs on the regulation of NRs could participate in CYP3A4 interindividual expression variability. We can hypothesize that our predicted miRNAs could have an impact on the expression of DMEs in *in vitro* liver cell models.

The better knowledge about the regulatory network controlling PXR (and other NRs) functions can lead to possible modifications of *in vitro* liver models allowing to optimize their properties closer to *in vivo*-like phenotype.

In our next study, we tried to estimate a toxicity of newly synthesized compounds with a potential antituberculotic activity. To fulfill the aim of the study, we used primary human hepatocytes and four different mammalian cell lines including hepatic HuH-7 and HepG2 cells. The mitochondrial activity measured by MTS assay was selected as a marker of a cell viability. Our tested molecules revealed generally low cellular toxicity with several exceptions.

Currently, we evaluate induced hepatocyte-like cells (iHep cells) for toxicological screening in our preparing manuscript (not yet published). For this analysis, we used several hepatotoxic phytochemicals with different mode of toxicity to validate model sensitivity and compared iHep cells with HepG2 cells and primary hepatocytes. We believe that such analysis can bring a reference point for tracking of a position of currently available iHep cells for toxicological applications.

Collectively, our investigation brought some novel small molecules used for the adjustment metabolic capacity of current *in vitro* liver models. Moreover, we

described some aspects of post-transcriptional and post-translational modifications involved in DME regulation. Finally, we applied *in vitro* cell models for the prediction of hepatotoxicity of newly synthesized drug candidates with a potential antituberculotic activity and suspected hepatotoxicans-derived from medical plants.

Abstrakt

Univerzita Karlova
Farmaceutická fakulta v Hradci Králové
Katedra farmakologie a toxikologie
Kandidát: Mgr. Tomáš Smutný
Školitel: prof. PharmDr. Petr Pávek, Ph.D.
Název dizertační práce: Nové přístupy ve vývoji *in vitro* jaterních buněčných modelů

Játra jsou hlavním metabolickým orgánem v lidském těle. Odhad jaterního metabolismu je tak důležitým krokem při vývoji léčiv. Neméně důležité je také vyhodnocení rizika jaterního poškození navozeného potencionálními léčivy. Některé parametry spojené s metabolismem a toxicitou vyvíjených léčiv mohou být predikovány pomocí *in vitro* jaterních buněčných modelů. Dnes jsou za jejich zlatý standard považovány primární lidské hepatocyty. Vedle nich se uplatňují další jaterní modelové systémy, jako jsou jaterní tkáňové řezy, subcelulární frakce, jaterní nádorové buněčné linie a hepatocyty odvozené od kmenových buněk. Soudobé *in vitro* modely mají stále řadu nevýhod, a to i navzdory pokrokům v jejich vývoji. Ty směřují k lepšímu odhadu farmakokinetických a toxikologických parametrů testovaných kandidátních léčiv. Jednou z nevýhod jaterních modelů je jejich nedostatečná podobnost s *in vivo* fenotypem spojená s nízkou metabolickou kapacitou. V posledních několika letech jsme byli svědky ohromujícího postupu nových technologií zaměřujících se na zlepšení stávajících jaterních buněčných modelů (například zavedení 3D modelů, kultivace buněk několika typů v jednom systému nebo využití perfúzních kultur).

Cíle této dizertační práce můžeme rozdělit do tří částí. Nejdříve jsme se pokusili zesílit metabolickou kapacitu *in vitro* jaterních buněčných modelů za použití malých molekul, které jsou aktivátory důležitých jaderných receptorů zapojených v regulaci enzymů metabolizujících léčiva (drug-metabolizing enzymes (DMEs)). Převážně jsme využili jaterní nádorové buněčné linie, protože mají rychlý a neomezený růst, dobrou dostupnost a snadno se s nimi pracuje. Na druhé straně postrádají mnoho DMEs. Posledně jmenovaná skutečnost nás vedla k tomu, abychom se také zabývali vlivem post-transkripčních a post-translačních modifikací klíčových regulátorů DMEs. Tyto modifikace by mohly vnést více světla do fenoménu nízké exprese DMEs v buněčných jaterních linií. Nakonec jsme se zaměřili na využití *in vitro* jaterních modelů (včetně

hepatocytů dovozených od kmenových buněk) pro hodnocení hepatotoxicity nově vyvíjených kandidátních léčiv a suspektních hepatotoxinů odvozených od léčivých rostlin.

V naší první studii jsme identifikovali inhibitory MEK1/2 jako silné aktivátory genů podrodiny CYP3A v běžně používané hepatocelulární nádorové buněčné linii HepG2. Tyto výsledky jsou důležité, neboť izoforma CYP3A4, která metabolizuje více než 30 % všech klinicky používaných léčiv, je omezeně exprimována v této buněčné linii a dalších jaterních buněčných modelech. V této práci jsme se navíc pokusili dešifrovat mechanismus stojící za tímto fenoménem.

V druhé práci jsme identifikovali několik nových látek fungujících jako ligandy významných xenosenzorů (např. jaderných receptorů PXR a CAR a transkripčního faktoru AhR). Xenozenzory jsou zapojené do genové regulace DMEs. Můžeme proto předpokládat, že tyto malé molekuly mouhou být využity k zesílení exprese významných genů DMEs v jaterních *in vitro* modelech.

V další práci jsme se zaměřili na *in silico* predikci microRNAs (miRNAs), které mají potenciál ovlivnit expresi jaderných receptorů zapojených do regulace CYP3A4. Předpokládá se, že účinek miRNAs na regulaci jadernách receptorů by se mohl podílet na interindividuální variabilitě v expresi CYP3A4. Můžeme vyslovit hypotézu, že námi predikované miRNAs by mohly mít dopad na expresi DMEs v jaterních *in vitro* buněčných modelech.

Lepší znalosti o regulatorní síti kontrolující funkce PXR a dalších jaderných receptorů mohou vést k modifikacím *in vitro* jaterních modelů a umožnit optimalizaci jejich vlastností blíže směrem k *in vivo* fenotypu.

V naší další studii jsme se pokusili odhadnout toxicitu nově připravených látek s potenciální antituberkulotickou aktivitou. Pro tento účel jsme použili primární lidské hepatocyty a čtyři odlišné savčí buněčné linie zahrnující jaterní linie HuH-7 a HepG2. Mitochondriální aktivitu (měřenou pomocí MTS testu) jsme zvolili jako znak buněčné viability. Ze studie vyplývá, že námi testované molekuly vykazovaly až na několik výjimek nízkou buněčnou toxicitu.

V současné době vyhodnocujeme uplatnění indukovaných hepatocytům podobných buněk (induced hepatocyte-like cells (iHep cells)) pro toxikologický

screening (připravovaná publikace). Pro validaci modelu jsme v této analýze použili několik hepatotoxických fytochemikálií s rozdílným mechanismem toxicity. Dále jsme porovnali iHep buňky s HepG2 buňkami a primárními hepatocyty. Věříme, že naše připravovaná studie může přinést informace o pozici komerčně dostupných iHep buněk v toxikologických aplikacích.

Náš výzkum přinesl některé nové malé molekuly použitelné pro úpravu metabolické kapacity současných *in vitro* jaterních modelů. Dále jsme popsali některé aspekty post-transkripční a post-translační modifikace stojící za regulací enzymů metabolizujících léčiva. V neposlední řadě jsme využili *in vitro* buněčných modelů pro odhad hepatoxicity nově syntetizovaných kandidátních léčiv s potenciální antituberkulotickou aktivitou a suspektních hepatotoxinů odvozených z léčivých rostlin.

Content

1. General introduction

1.1. The liver

The liver is the largest gland in body having endocrine and exocrine functions and representing about 1/50 of the adult body weight. Importantly, the liver is a principal drug elimination organ. Liver tissue is predominantly composed of parenchymal cells (hepatocytes) which comprise about 78% of a liver volume. Hepatocytes participate in the most metabolic and transport functions in liver. Besides hepatocytes, there are also other cell types (non-parenchymal cells) involving Kupffer cells (intravascular tissue macrophages), hepatic stellate cells (principal producers of extracellular matrix proteins), endothelial cells, cholangiocytes (biliary epithelial cells), and Pit cells (natural killer cells). The extracellular space constitutes about 16% of the liver volume (Ishibashi et al. 2009; Malarkey et al. 2005; Si-Tayeb et al. 2010a).

Since the liver is a key metabolizing organ, it eliminates most clinically used drugs. For that reason, the estimation of hepatic clearance is the important step during the drug development. Moreover, the liver is the target of drug-induced liver injury (DILI). That is why a toxicity assessment of drug candidates regarding to their potential to induce hepatotoxicity is the crucial part of safety management in the early phase of drug development.

1.2. Drug metabolism

Drug metabolism is a biochemical process aiming to an enzymatic conversion of foreign chemicals (xenobiotics) such as drugs to more polar metabolites. The increased water solubility of metabolites promotes their excretion by the kidney. Reactions of drug metabolism can be divided into two main phases. In phase I, xenobiotics are modified by oxidation, reduction or hydrolysis reactions leading to introduction of a polar group into substrates such as hydroxyl or amino groups. Cytochromes P450 (CYPs) are dominant phase I xenobiotic/drug-metabolizing enzymes (DMEs) participating in oxidative reactions (Almazroo et al. 2017; Hollinger 2003; Rang et al. 2015; Vellonen et al. 2014).

In phase II, metabolites are further modified by conjugation reactions with substances such as glucuronic acid, sulfate, glycine or glutathione (GSH). Reactions are catalyzed by clinically important enzymes including UDP-glucuronosyltransferases (UGTs), which are localized in the membrane of endoplasmic reticulum, cytosolic sulfotransferases (SULTs), glutathione S-transferases (GSTs) and N-acetyltransferases (NATs). Generated conjugates are more water soluble than their parent drugs/xenobiotics (Almazroo et al. 2017; Hollinger 2003; Vellonen et al. 2014).

Metabolites can be pharmacologically more active or even more toxic than parent compounds. Some drugs do not undergo both phases of metabolism instead they are only metabolized by either phase I or phase II enzymes. Additionally, some drugs are not a subject of metabolism and are excreted as parent drugs (Hollinger 2003; Vellonen et al. 2014).

Moreover, many drugs alter gene expression and activity of enzymes implicated in drug metabolism and can cause so-called drug-drug interactions (DDIs). A change in enzymatic or even transport activity caused by one drug can affect pharmacokinetics and pharmacodynamics of concomitantly administered drug and eventually lead to lower therapeutic outcomes or toxicity (Amacher 2016; Hollinger 2003; Vellonen et al. 2014).

1.3. Cytochromes P450 (CYPs)

1.3.1. General notes

Cytochromes P450 are hem-containing enzymes embedded in the smooth endoplasmic reticulum of hepatocytes. They are the most important phase I DMEs capable of oxidative reactions. Outcomes of CYP-catalyzed reactions are hydroxylated substrates and water (Vellonen et al. 2014; Hollinger 2003; Rang et al. 2015). CYP families such as CYP1, CYP2 and CYP3 include only several enzymes which, however, metabolize a majority of all drugs used in clinic (Zanger and Schwab 2013).

The regulation of CYPs is complex and it is influenced by many factors such as gender, age, health condition, induction or inhibition by drugs and other xenobiotics, epigenetics, and genetic polymorphisms (Zanger and Schwab 2013).

A few CYP isoforms reveal considerable genetic polymorphisms with highest occurred in CYP2D6 and then CYP2C19, CYP2A6, CYP2B6, CYP2C9 and CYP3A4/5

genes, respectively (Hedrich et al. 2016; Raunio and Rahnasto-Rilla 2012; Zanger and Schwab 2013).

1.3.2. Transcriptional regulators of CYP genes

Ligand-activated nuclear receptors (NRs) control expression of main drug metabolism-related CYP isoforms as well as other DMEs and drug transporters in the liver. Among them, pregnane X receptor (PXR, NR1I2) and constitutive androstane receptor (CAR, NR1I3) have the dominant role. They mediate hepatic respond to various compounds, which a human body is exposed to from environment (Pascussi et al. 2003). Therefore, they are also referred as to "xenosensors" (Tolson and Wang 2010). Additionally, NRs are implicated in a regulation of metabolism of lipids, glucose, bile acids, and steroids. They control immune responses, endocrine homeostasis, and apoptosis (Gao and Xie 2012; Ihunnah et al. 2011; Pascussi et al. 2003; Yang and Wang 2014).

Ligand binding domain is one of structural parts of PXR as well as CAR proteins (Fig. 1). After the ligand binding, NRs undergo conformational changes, which allow them to heterodimerize with another receptor termed as retinoid X receptor α (RXRα, NR2B1). Then, assembled heterodimers bind to their response elements in a promoter regions of target genes such as CYPs. The binding to DNA is mediated via another structural part of NRs called as the DNA binding domain. PXR recognizes a myriad of structurally diverse drugs such as rifampicin, nifedipine, clotrimazole; dietary compounds such as hyperforin, and bile acids such as lithocholic acid to name a few. This characteristic feature can be explained by a flexible ligand binding domain (Akiyama and Gonzalez 2003; Pascussi et al. 2003). In the case of CAR, there is still the lack of known specific, potent and non-toxic ligands. Only several direct ligands of human CAR have been described so far such as 6-(4-Chlorophenyl)imidazo[2,1-*b*][1,3]thiazole-5-carbaldehyde-*O*-(3,4-dichlorobenzyl)oxime (CITCO) and clotrimazole (Smutny et al. 2016). Constitutive activity of CAR is an interesting feature of the NR. It means that CAR can also transactivate target genes in the absence of ligands (Akiyama and Gonzalez 2003; Pascussi et al. 2003; Yang and Wang 2014).

Vitamin D receptor (VDR, NR1I1) and glucocorticoid receptor (GR, NR3C1) are other NRs implicated in a regulation of various cell functions. Notably, they govern

expression of some DMEs. Similarly to CAR and PXR, VDR also heterodimerizes with RXRα after a ligand binding. 1α,25-dihydroxyvitamin D_3 is a model VDR ligand. Contrary, GR forms homodimers without RXRα binding (Fig. 1) (Dvorak and Pavek 2010; Pascussi et al. 2003; Wang et al. 2013).

It is of particular importance that NRs can mutually control their own expression thus forming a tangled regulatory network (Pascussi et al. 2003). As exemplified by GR which was found to be the activator of PXR and CAR expression (Pascussi et al. 2001). Complex cross-talk between NRs is further promoted by sharing ligands, partners and target genes (Pascussi et al. 2003; Pavek 2016).

Besides NRs, a ligand-activated transcription factor aryl hydrocarbon receptor (AhR) also links gene expression of DMEs to xenobiotic exposure. AhR is a member of the basic Helix-Loop-Helix/Per-Arnt-Sim family. Its prototypical ligands are polycyclic compounds such as 2,3,7,8-tetrachlorodibenzo-p-dioxin (TCDD), and benzo[a]pyrene. Upon a ligand-triggered translocation into nucleus, AhR dimerizes with its partner protein termed AhR nuclear translocator (ARNT). Then, AhR/ARNT heterodimer binds to response elements in a promoter of target genes (Bock 2014; Ramadoss et al. 2005).

Along with above mentioned factors, there are also liver-enriched transcription factors implicated in a regulation of CYP genes such as hepatocyte nuclear factor 4 α (HNF4α) and CCAAT/enhancer-binding proteins (C/EBPs) among others (Akiyama and Gonzalez 2003).

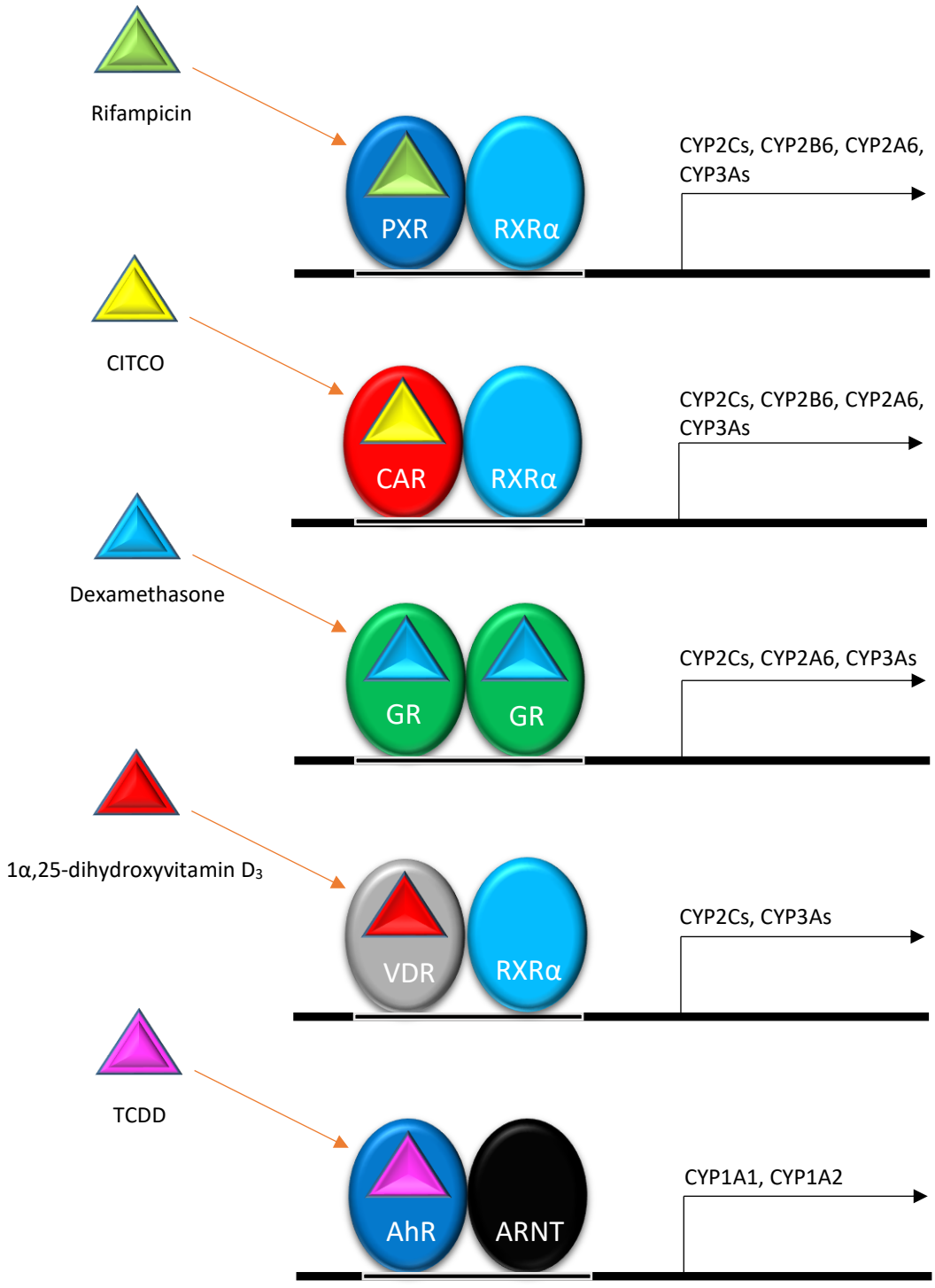

Fig. 1. Transcriptional regulators of CYP genes. Prototypical ligands with corresponding ligand binding domains are depicted as tringles. Indicated CYP genes can be upregulated directly or indirectly by a respective transcriptional factor.

1.3.3. Classification of CYPs

The CYP1A subfamily consists of two members, namely CYP1A1 and CYP1A2 (Zanger and Schwab 2013). The letter is considerably expressed in the liver than in other tissues (Nishimura et al. 2003) accounting for about 13% of the total hepatic P450 protein content (Shimada et al. 1994). On the other hand, CYP1A1 is a primarily extrahepatic enzyme. CYP1A2 contributes to metabolism of various polycyclic aromatic hydrocarbons such as those included in tobacco smoke and industrial combustion products; caffeine and drugs. Both, CYP1A1 and CYP1A2 are inducible mainly via AhR pathway (Ramadoss et al. 2005; Zanger and Schwab 2013).

CYP2A6 is a predominantly hepatic isoform (Nishimura et al. 2003) contributing to about 4% to the total hepatic P450 protein content (Shimada et al. 1994), although with significant variability among individuals. CYP2A6 is involved in e.g. bioactivation of the prodrug tegafur to 5-fluorouracil or the inactivation of nicotine and letrozole. CYP2A6 expression is inducible via PXR, CAR and GR pathways (Raunio and Rahnasto-Rilla 2012; Zanger and Schwab 2013).

CYP2B6 is a minor hepatic CYP isoform representing less than 1% of the total hepatic P450 protein content (Shimada et al. 1994), but it shows a high variability in expression. It is estimated that CYP2B6 participates on metabolism around 8% of all clinically used drugs. CYP2B6 activates prodrug cyclophosphamide and metabolites efavirenz, bupropion and artemisinin to name a few. CYP2B6 is a highly inducible isoform by agonists of CAR and PXR nuclear receptors. Additionally, CYP2B6 is extensively polymorphic CYP isoform (Hedrich et al. 2016; Zanger and Schwab 2013).

CYP2C subfamily comprises four isoforms. Of these, CYP2C8, CYP2C9 and CYP2C19 significantly contribute to liver metabolism. CYP2C proteins represent about 20% of the total hepatic P450 content (Shimada et al. 1994; Zanger and Schwab 2013). Their liver expression decreases in the following order CYP2C9, CYP2C8 and CYP2C19. All of them are inducible via PXR, CAR, GR and VDR pathways, but CYP2C8 is the most potently inducible member. CYP2C9 is involved in the metabolism of warfarin or diclofenac among others. CYP2C8 participates in the transformation e.g. rosiglitazone, pioglitazone or paclitaxel. Eventually, CYP2C19 activates clopidogrel and inactivates proton pump inhibitors (Zanger and Schwab 2013).

CYP2D6 is encoded by a non-inducible *CYP2D6* gene. Its protein level differs significantly between humans mainly as a result of its extensive polymorphism (Zanger and Schwab 2013). Although, CYP2D6 accounts only for about 2% of the total hepatic P450 protein content (Shimada et al. 1994), it takes part in metabolism of approximately 15-25% used drugs spanning across various therapeutic groups such as antidepressants, antipsychotics, analgesics (e.g. codeine and tramadol) (Zanger and Schwab 2013).

CYP2E1 is an abundant liver CYP isoform (about 7% of the total hepatic P450 protein content) (Nishimura et al. 2003; Shimada et al. 1994) with poor correlation between mRNA and protein levels suggesting significant post-transcriptional regulation. CYP2E1 is involved in metabolism of e.g. ethanol and paracetamol (Gonzalez 2007; Zanger and Schwab 2013).

The CYP3A subfamily (about 30% of the total hepatic P450 protein content (Shimada et al. 1994)) includes four genes 3A4, 3A5, 3A7 and 3A43 (Zanger and Schwab 2013). Whereas CYP3A4 and CYP3A5 are main isoforms of adult liver, CYP3A7 occurs predominantly in fetal liver (Nishimura et al. 2003). CYP3A4 is the most abundantly expressed adult CYP3A isoform, which is estimated to catalyse the biotransformation of more than 30% of drugs in use today. Typical CYP3A4 substrates involve cyclosporine, nifedipine, midazolam and testosterone (Martinez-Jimenez et al. 2007). Regarding to its regulation, it was demonstrated that gene encoding CYP3A4 protein is induced via PXR, CAR, VDR and GR nuclear receptors (Martinez-Jimenez et al. 2007; Wang et al. 2013). However, human CAR is the dominant regulator of CYP2B6 relative to CYP3A4 (Faucette et al. 2006). Importantly, CYP3A4 exhibits extremely high expression variation in population caused by a regulatory variability rather than structural polymorphisms as only rare or insignificant allelic variants have been described in case of CYP3A4 gene (Martinez-Jimenez et al. 2007). Polymorphic CYP3A5 is expressed in the liver of about one-quarter of adults. If expressed, CYP3A5 can significantly contribute to drug metabolism, particularly in individuals with low expression of CYP3A4 (Plant 2007; Zanger and Schwab 2013).

1.4. Hepatic drug transport

The interplay between hepatic transporters and DMEs such as CYPs in the drug disposition is well-recognized. Drug uptake from sinusoidal blood into hepatocytes

(sometimes referred as to phase 0) precedes drug metabolism (phase I and II) which is subsequently followed by efflux of drug metabolites either back into blood or into bile (phase III). This process represents the main route of elimination for many drugs (Almazroo et al. 2017; Kim 2002).

Directional movement of a drug from blood into bile is ensured by polarization of hepatocytes (Fig. 2) (Kim 2002) manifested as a structurally and functionally different membrane domain organization. Based on that, hepatocyte plasmatic membrane can be divided into two domains:

- Basolateral membrane domain - the domain receives drugs from blood via fenestrated sinusoidal endothelium. Sinusoidal endothelium allows drugs to pass into a perisinusoidal space of Disse, from where small lipophilic compounds can diffuse directly through the basolateral membrane into hepatocytes. However, a plenty of lipophilic and some polar drugs can pass the hepatocyte basolateral membrane only by active transport meditated via uptake transporters such as members of the solute carrier (SLC) superfamily. Among them organic anion transporting polypeptides (OATPs), organic anion transporters (OATs) and organic cation transporters (OCTs) rank as the most important uptake carriers (Funk 2008; Kim 2002; Vellonen et al. 2014).

- Canalicular membrane domains between neighboring hepatocytes create a bile canaliculus, which is associated with membrane-bound efflux transporters pumping drugs into the canalicular space. These efflux transporters belong to the ABC (ATP-binding cassette) transporter superfamily. Their function is to counteract systemic exposure of drugs. P-glycoprotein (MDR1, ABCB1), bile salt export pump (BSEP, ABCB11), multidrug resistance-associated protein 2 (MRP2, ABCC2) and breast cancer resistance protein (BCRP, ABCG2) are the most important members of ABC superfamily expressed in hepatocyte. Some efflux transporters are also localized on the basolateral membrane (mainly MRP1, ABCC1; MRP3, ABCC3) where they pump drugs back into blood (Almazroo et al. 2017; Funk 2008).

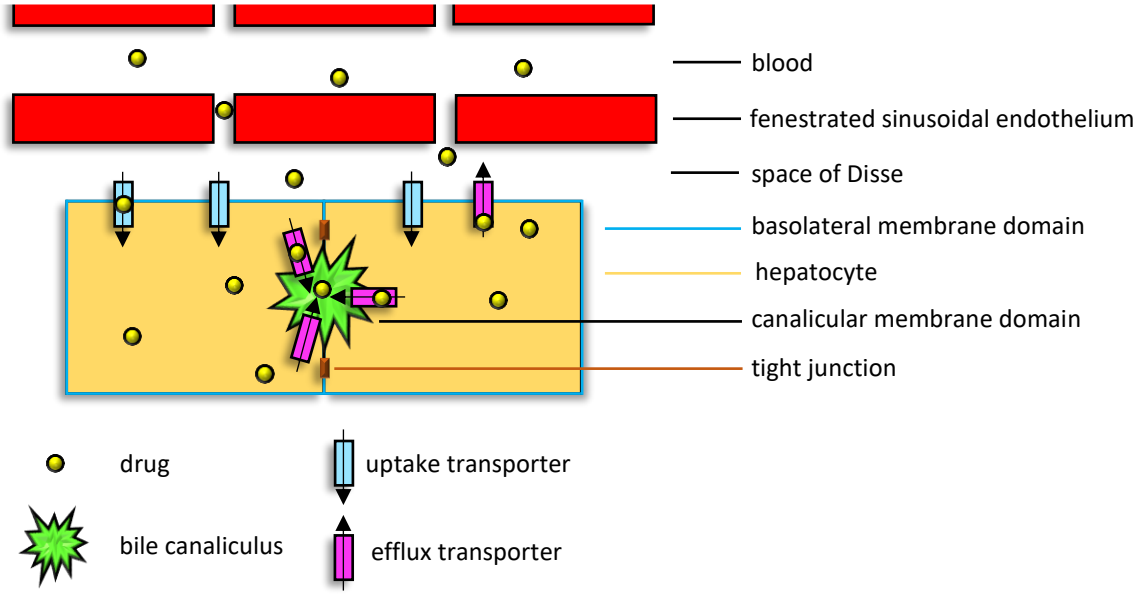

Fig. 2. Hepatocyte polarization and drug transport

The effects of drugs on gene expression of transporters or substrate competition can cause pharmacokinetic interactions and toxicity. As example, hepatic transporters are implicated in hepatobiliary elimination of bile salts, therefore a drug-mediated perturbation of the transport can lead to an accumulation of bile salts in hepatocytes resulting in cholestasis and liver injury (Amacher 2016; Funk 2008).

1.5. Drug-induced liver injury (DILI)

DILI belongs among the most often occurred adverse reactions leading to a drug withdrawal from a market. Between 1998-2008, 15 of total 51 drugs were withdrawn from the US, European or Asian markets due to hepatotoxicity. It makes hepatotoxicity being responsible for almost each third withdrawn drug and a second lead cause of a drug withdrawal after cardiotoxicity (17/51) (MacDonald and Robertson 2009).

One reason for a frequent engagement of the liver in drug-driven toxicity is related to its anatomical location since the liver forms the entrance gate to a systemic circulation for orally administered drugs. Besides, the liver is the important metabolic organ which hosts a plenty of DMEs that can metabolize parent drugs into reactive and toxic metabolites (Grattagliano et al. 2009). Various liver symptoms of DILI can be manifested

like necrosis, cholestatic jaundice, steatosis, hepatitis, cirrhosis and tumors (Pandit et al. 2012).

The early detection of a hepatotoxic potential of drug candidates is still limited by unsatisfactory knowledge about precise mechanisms underlying liver toxicity and damage. While direct toxicity is a dose-dependent and predictable process, idiosyncratic reactions triggered by drugs via unknown mechanism with a proposed role of immune system are unpredictable (Grattagliano et al. 2009).

- Paracetamol is a prototypical drug causing the direct liver toxicity. It is primary metabolized via sulfation and glucuronidation pathway. Additionally, a small amount is catalysed by CYP2E1 resulting in a reactive metabolite N-acetyl-p-benzoquinone imine (NAPQI) which is subsequently inactivated by a conjugation with GSH. However, excessive dose of paracetamol can overcome detoxification capacity and unbound NAPQI can then covalently bind to cell proteins causing massive cell necrosis and liver failure (Grattagliano et al. 2009; Yoon et al. 2016).

- The non-steroidal anti-inflammatory drug (NSAID) nimesulid is an example of a drug inducing the idiosyncratic reaction in the liver. Nimesulid was recently subjected of re-evaluation of its risk/benefit profile due to unpredictable hepatotoxicity (Grattagliano et al. 2009).

There are also other approved and commonly used drugs implicated in causing liver damage. To further illustrate the category of drugs associated with DILI, antidepressants, antitubercular isoniazid and rifampicin, antiepileptic drugs (valproic acid and phenytoin), NSAIDs (diclofenac), anti-retroviral drugs, immunosuppressant azathioprine and antifungals (fluconazole) can be named (Pandit et al. 2012). It is worth mentioning that not only drug- but also herb-induced liver injury (HILI) represent a serious problem for public health. That is even more pronounced since herbal remedies such as those used in traditional Chinese medicine gain growing worldwide popularity (Ekor 2014; Liu et al. 2016).

In vitro assessment of hepatotoxicity can be carried out based on analyses (Bale et al. 2014; Horii and Yamada 2007; Xu et al. 2008):

- gene expression profiling

- cell morphology assessment
- biochemical endpoints measurement reflecting cell viability such as:
    - a mitochondrial damage measured by changes of a mitochondrial membrane potential or mitochondrial activity
    - a release of lactate dehydrogenase (LDH)
    - a reduction of intracellular antioxidant GSH
    - a formation of reactive oxygen species (ROS)

2. *In vitro* liver models for preclinical drug development

2.1. Introduction

Despite the criticism, millions of experimental animals are used in a research worldwide every year (Doke and Dhawale 2015). Arguments supporting the restriction of animals in scientific procedures can be found in fields of ethical issues, cost effectiveness and data interpretation (Ranganatha and Kuppast 2012).

Many acts aim to reduce a distress and a pain of animals, which is in agreement with ethical principles. However, growing requests of authorities result in increased costs of experiments making drug development more expensive. This is mainly due to the fact that experiments become more time consuming and laborious and they need higher demands on skilled manpower and equipped laboratories (Doke and Dhawale 2015). Moreover, interspecies variability is the obstacle for a translatability of data as confirmed by repeated experience (Ranganatha and Kuppast 2012). Taken all these facts together, there is an urgent need for alternative models, which could replace experimental animals.

In vitro approaches could become an effective tool for evaluation of important ADMET parameters. The great potential of *in vitro* models is a reduction of the number of used animals or their full replacement, an identification of potentially undesired effects in the early phase of drug development and a cost effectiveness. The prediction efficacy of *in vitro* models have been already proved throughout pharmaceutical industry for example for assessment of mutagenesis (AMES test; micronucleus test, MNT; Comet), teratogenicity (embryonic stem cell test, EST) and a risk of cardiac arrhythmias (hERG test) (Roth and Singer 2014).

In vitro liver cells represented predominantly by primary human hepatocytes and liver cancer cell lines are used for the evaluation of drug metabolism and prediction of DILI. However, there is still no model, which would fulfill all criteria of differentiated *in vivo*-like hepatocytes with the following characteristics (Si-Tayeb et al. 2010a; Vellonen et al. 2014):

- optimal morphology with functional apical-basal polarization

- normal metabolism such as correct expression spectrum of enzymes and metabolic reactions; inducibility of enzymes
- normal transporter activity such as correct expression profile of transporters, rate and direction of transport
- normal liver-specific functions such as a secretion of bile, urea and liver proteins e.g. albumin

Extrapolation of *in vitro* results to a clinical situation is another complicated task. This is caused by considerable differences between the liver and simplified reductionist cellullar models. Since no current model can fully recapitulate all *in vivo* liver functions, the estimation of medication on liver parameters can be done only with rational consideration of advantages and limitations of each particular model. The progress in technologies allow us to acquire large data sets during experiments and focus on mechanistic endpoints rather than phenomenological observations. Despite impressive update of technologies, it is important to stress that results captured from *in vitro* model can only be as valid as a model reflects *in vivo* situation (Roth and Singer 2014).

2.2. The overview of the current state of the art in *in vitro* liver models

2.2.1. Liver tissue slices

Liver tissue slices are well-established *in vitro* liver models, which retain intact tissue architecture composed of all liver cell types. Liver tissue slices were proofed to be an effective system for toxicity assessment, which unlike primary hepatocytes, permits the evaluation of zonal- and cell-specific toxicity. Additionally, presence of various cell types makes possible to investigate an interactive toxicity where one liver cell type can modulate the toxicity in another one. Compared to primary hepatocytes which are exposed to harmful proteolytic enzymes during their isolation, liver tissues slices are only damaged on the surface of preparation by slicing (Lake and Price 2013).

Liver tissue slices reflect ongoing diseases, age, sex, genome disposition and lifestyle of donors. Therefore, the application of tissue slices generated from different donors allow to encompass clinical diversity of patients in dish (Vickers and Fisher 2013).

The expression of phase I and II DMEs in slices enables to employ metabolic studies. However, the decline of DMEs expression during time leads to changes

in metabolic activities. The metabolic capacity of culture liver tissue slices is further compromised by the fact that particular DMEs can be differentially lost resulting in the expression pattern distinct from that occurred *in vivo*. Other disadvantages of liver slices include degenerative changes in tissue over culture time, limited availability and low throughput applications (Lake and Price 2013).

2.2.2. Liver microsomes, cytosolic and S9 subcellular fractions

Liver microsomes are vesicles formed by artificially fragmented membranes of endoplasmic reticulum containing DMEs such as CYPs. They can be utilized for the prediction of hepatic clearance, the metabolite identification and the evaluation of influence of certain CYP isoforms in drug candidate metabolism. Liver microsomes enable high throughput screening. They are also cost effective. However, the absence of drug transporters and full spectrum of hepatocyte enzymes limit their broader applications (Asha and Vidyavathi 2010; Vellonen et al. 2014).

The liver cytosolic fractions enable to analyse the effect of only some soluble phase II enzymes such as GST, NAT, and SULT. In contrast, S9 fraction includes liver microsomes enriched with cytosolic fraction. This *in vitro* model system therefore contains a more complete battery of metabolic enzymes than respective individual fractions (Asha and Vidyavathi 2010). All mentioned subcellular fractions require the supplementation with cofactors e.g. NADP for proper CYP activity.

Taken all together, all subcellular fractions are rather simple models restricted only to some metabolic studies but they do not enable to assess e.g. enzymatic induction or the interplay between metabolism and drug transporters (Asha and Vidyavathi 2010; Vellonen et al. 2014).

2.2.3. Primary hepatocytes

Human primary hepatocytes are considered as the “gold” standard of *in vitro* liver models for drug metabolism (e.g. for estimation of hepatic clearance, drug-drug interactions and metabolite profiling) and hepatotoxicity assessment (Li 2007; Ramaiahgari et al. 2014). They can be used as a single-celled suspension or plated in a monolayer (Soldatow et al. 2013). Unfortunately, primary hepatocytes are limited by

availability and batch-to-batch variability (Ramaiahgari et al. 2014). Moreover, expression of the most CYP enzymes decrease over culture time in primary hepatocytes due to de-differentiation process triggered by introduction of artificial *in vitro* conditions (Boess et al. 2003). Additionally, some CYPs (e.g. CYP3A4) show high degree of expression variability in human hepatocytes (Martinez-Jimenez et al. 2007).

To overcome the problem with the lack of primary human hepatocytes, technique based on a transduction of proliferating genes in primary human hepatocytes without inducing their immortalization has been developed. This so-called upcyte strategy allows to expand primary hepatocytes through a limited number of cell divisions without changing their phenotype (Ramachandran et al. 2015). Interestingly, small molecules also have a potential to induce proliferation of functional primary human hepatocytes (Shan et al. 2013).

2.2.4. Sandwich-cultured hepatocytes

Culture conditions of hepatocytes can be modified by seeding cells between two layers of hydrated collagen resulting in so-called sandwich system (Fig. 3). It was shown that this *in vitro* cultivation technique allows specific hepatocyte morphology and functions (Dunn et al. 1991). Hepatocytes in the sandwich-cultured configuration form a polar geometry with functional bile canaliculi surrounded by tight junctions. This organisation of hepatocytes predetermines the model for drug transport studies. Indeed, sandwiched hepatocytes allow to conduct the accumulation and efflux studies as well as to evaluate transporter-based drug-drug interactions. Since altered hepatic bile acid transport induced by drugs is one of underlying mechanisms for hepatotoxicity, the sandwich model thus represents the unique tool for assessment of DILI. The preserved expression of DMEs also enables to study interplay between drug metabolism and transport (Swift et al. 2010).

It was demonstrated that addition of a mixture of small molecules such as phenobarbital, dexamethasone and β-naphthoflavone to the culture medium maintains gene expression and enzyme activity of DMEs in sandwich-cultured hepatocytes closer to those occurred *in vivo* (Kienhuis et al. 2007).

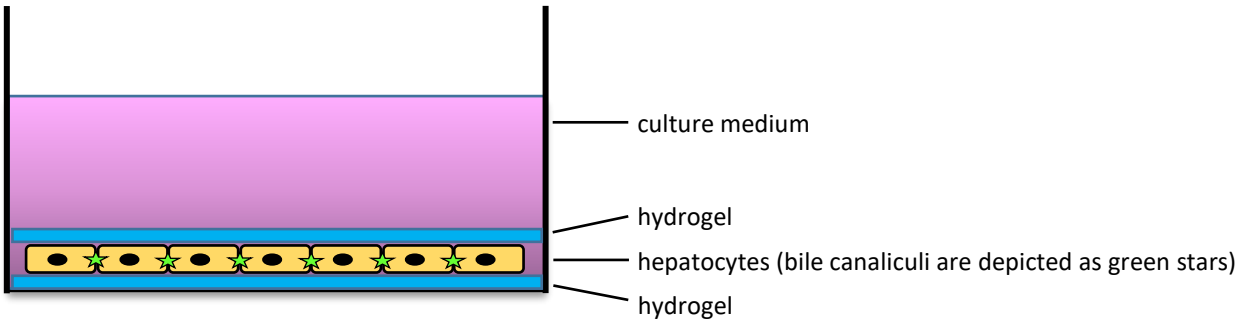

Fig. 3. Hepatocytes cultured in sandwich configuration

2.2.5. Liver cancer cell lines

Immortalized liver cancer cell lines represent alternative to primary human hepatocytes in drug development. Their great benefit is fast and unlimited life span, good availability and easy handling. Each liver cancer cell line has been derived from a single donor, which prevents inter-donor variability. Contrary, cell lines lack a full battery of DMEs and other hallmarks of adult hepatocytes (Vellonen et al. 2014). HepG2 and HepaRG cells belong among the most common liver cell lines used for drug studies.

- **HepG2** is a well-characterized and frequently used liver cancer cell line, which originates from liver tissue of 15-year-old Caucasian male who suffered from hepatocellular carcinoma (Aden et al. 1979). The expression level of phase I DMEs is generally much lower in HepG2 cells compared to that found in primary human hepatocytes (Westerink and Schoonen 2007; Wilkening et al. 2003). CYP3A4 is extremely low in this cell line. On the other hand, CYP3A7 is sufficiently expressed suggesting rather fetal liver phenotype of HepG2 cells than adult one. Fetal-like phenotype of HepG2 cells is further supported by other facts such as expression of a fetal marker alpha-fetoprotein (AFP) (Knowles et al. 1980) and higher expression of CYP1A1 compared to CYP1A2, the phenomenon described in fetal liver (Wilkening et al. 2003). Since, HepG2 cells express different levels of DMEs in comparison with the *in vivo* situation, they are less suitable for metabolic studies (Wilkening et al. 2003). Moreover, it was also shown that enzymatic activity of HepG2 cells depends on the source and culture conditions (Hewitt and Hewitt 2004). Additionally, expression

of DMEs varies based on a number of cell passages (Wilkening and Bader 2003). As rather "metabolically empty", HepG2 cells can be utilized for an incorporation of CYP enzyme of interest. These transgenic cells enable to decipher the role of particular CYP in metabolism and toxicity of a drug candidate. Similarly, the transfection of regulatory nuclear factors have been reported to boost the cells towards increased metabolic capacity (Pelkonen et al. 2013).

- **HepaRG** is a perspective liver cell line, which has been derived from liver tumor of a female patient who suffered from hepatocellular carcinoma consecutive to chronic hepatitis C virus infection (Gripon et al. 2002). HepaRG progenitors exhibit a low expression of liver-specific genes during proliferation phase. After the reaching confluency, bipotent HepaRG cells start to transform into both hepatocyte-like and biliary-like cells. The subsequent exposition to 2% dimethyl sulfoxide further potentiates differentiation of confluent HepaRG cells. Under the defined protocol, HepaRG cells express many phase I and II DMEs at the similar level as in human primary hepatocytes (with the exception of CYP2D6, which is at the limit of a detection). HepaRG cells also express functional nuclear receptors PXR and CAR and several drug transporters. Moreover, HepaRG cells retain relatively stable phenotype making them useful cell system for long-term toxicity studies (Guillouzo et al. 2007).

2.2.6. Hepatocytes derived from stem cells

Since there is a constant lack of available primary human hepatocytes for experimental purposes, the great effort has been made with the aim to find their alternative source. Pluripotent stem (PS) cells can give rise to cells of all three embryonic germ layers, therefore PS cells have potential to become a favorable source of most, if not all cell types of the body including endoderm-derived hepatocytes (Sauer et al. 2014). Typical types of PS cells are embryonic stem cells (ESCs) isolated from the inner cell mass of human blastocysts (Thomson et al. 1998). Other types of PS cells are induced pluripotent stem cells (iPSCs). They were firstly prepared by genetic reprogramming of somatic cells (mouse fibroblasts) in 2006 using the forced expression of four transcription

factors, Oct3/4, Sox2, c-Myc a Klf4, known now as Yamanaka factors (Takahashi and Yamanaka 2006). From that time, many additional innovative strategies leading to generation of iPSCs were developed including somatic cell reprogramming by overexpression of specific miRNAs (Sauer et al. 2014) and using small molecules (Feng et al. 2009).

Recent advances in stem cell biology promoted a rapid development of multitude differentiation protocols enabling to generate induced hepatocyte-like cells (iHep cells) from PS cells (Cai et al. 2008; Chen et al. 2012; Si-Tayeb et al. 2010b; Song et al. 2009). ESCs are less preferred for iHep differentiation than iPSCs owing to ethical concerns associated with embryo destruction in the case of ESCs as well as the incompatibility to establish patient-specific hepatocytes from ESCs (Chiang et al. 2013). Despite benefits of iPSCs, the effect of somatic cell reprogramming warrants further studies since it can affect following iPSCs differentiation into iHep cells (Si-Tayeb et al. 2010b). Protocols typically begin with PS cells and in step-wise fashion mimic conditions occurred during liver embryogenesis leading to definitive endoderm, hepatic-specific endoderm, hepatoblasts followed by hepatocytes (Schwartz et al. 2014). However, iHep cells prepared according to current protocols resemble generally more fetal-like phenotype rather than adult one as demonstrated by the expression of AFP and a considerable reduction of DMEs including CYP3A4 (Cai et al. 2008; Schwartz et al. 2014).

Reproducing all hepatocyte functions is a great challenge. Despite the extensive endeavour, we are still not able to reach fully mature PS cell-derived hepatocytes (Cai et al. 2008). As pointed out in the recent study, iHep cells adapt their phenotype to 2D culturing with regard to expression of CYPs and some transports. Hence, it is highly expected that more *in vivo*-like environment is needed to improve hepatocyte phenotype (Ulvestad et al. 2013). Furthermore, as apparent from the existence of multiple differentiation protocols, it is very difficult to conclude which differentiation method results in more terminally differentiated iHep cells. The reason is that the comparison of iHep cells and human hepatocytes require a broad range of tests confirming correct cellular morphology and functions, although no clear consensus for characterisation of iHep cells exists. Additionally, the evaluation is also complicated by variability of human hepatocytes used as a reference control and the loss of hepatocyte phenotype and functions during cultivation. This comparison can make iHep cells to appear more mature than they really are (Chiang et al. 2013; Schwartz et al. 2014).

It is worth noting that other researchers focused on the direct reprogramming of somatic cells into iHep cells via bypassing the pluripotent stage. Two groups have proved the concept as they converted mouse fibroblasts into iHep cells via forced expression of several transcription factors (Huang et al. 2011; Sekiya and Suzuki 2011).

The potential of iHep cells encompass the toxicity assessment, drug metabolism studies, the disease modelling and the cell therapy. Interestingly, iHep cells derived from individuals carrying their specific genotype represent a promising *in vitro* liver model utilized in a personalized medicine (Yi et al. 2012).

Small molecules have been proposed to have several implications in the stem cell research. They were shown to improve the efficiency and kinetics of somatic cell reprogramming into iPSCs functioning as pluripotency gene activators, self-renewal modulators and reprogramming boosters. These chemicals include DNA methyltransferase inhibitors as well as histone deacetylase inhibitors which can overcome epigenetic barrier and in turn enhance the effect of reprogramming. Interestingly, the dual inhibition (2i) of mitogen-activated protein kinase kinase (MEK) and glycogen synthase kinase-3 (GSK3) signaling by respective inhibitors helped to promote fully competent iPSCs from somatic cells highlighting the importance of signal transduction pathways in the process of somatic cell reprogramming (Feng et al. 2009). Moreover, a class of compounds identified by Shan and colleagues promoted the maturation of human iHep cells (Shan et al. 2013). It is expected that small molecules could replace some expensive growth factors (Chiang et al. 2013) and mitigate variation in quality between batches. One of goals of research might be the discovery a “chemical cocktail”, which could reprogram somatic cells to iPSCs omitting a risk associated with viral-mediated transduction of transcription factors (Feng et al. 2009).

Currently, several vendors offer off-the-shelf iHep cells such as Clontech Laboratories, a Takara Bio Company (Cellartis Enhanced hiPS-HEP), ReproCELL (ReproHepato) and Cellular Dynamics International (iCell Hepatocytes).

2.2.7. 3D models

Human body is organized in three-dimensional manner (3D). For that reason, 2D culture systems composed of cells attached to a plastic surface from one side and with

other side exposed to culture medium can hardly imitate a tissue specific architecture as that found *in vivo*. Additionally, the cells lack sufficient cell-cell interactions in the monolayer as cells contact each other only at their periphery (Ruedinger et al. 2015). It seems reasonable to suppose that a modification of culture environment in a way which stimulates 3D cell organization will move liver cell phenotype closer to *in vivo* situation (Pampaloni et al. 2007).

Indeed, it has been reported that 2D cultured HepG2 cells have a different global gene expression profile compared to cells cultured in 3D conditions. It was also highlighted that HepG2 cells cultivated in 2D monolayer upregulated expression of genes encoding adhesion, extracellular matrix and cytoskeletal proteins whereas 3D counterparts enhanced expression of genes responsible for metabolic and synthetic functions. The transfer of 3D aggregates on cell culture dishes led to the loss of enhanced liver functions demonstrating the importance of 3D organisation (Chang and Hughes-Fulford 2009).

Additionally, 3D culture expands a field of stem cell research as it paves the way for a better recapitulation of *in vivo*-like stem cell niche and embryonic development (Lou et al. 2014).

Taken together, 3D cultures have potential to equalize functional and morphological differences between petri dish-based cell cultures and physiological tissue (Pampaloni et al. 2007).

2.2.7.1. Spheroids

Spheroids are spherical multicellular aggregates based on the cell capacity to self-assemble forming simple three-dimensional systems. They revealed to have some advantages when compared to 2D culture systems. Liver cell spheroids showed long-term survival (Lan et al. 2010), structural apical-basal polarity (Malinen et al. 2014), directional transport (Malinen et al. 2012), higher expression and synthesis of liver-specific hallmarks such as HNF4α (Nakamura et al. 2011), albumin and urea (Verma et al. 2007), increased metabolic activity (Wang et al. 2008), and production of their own extracellular matrix (Glicklis et al. 2000).

3D liver cell-derived spheroids were proposed to be more suitable for drug metabolism and toxicity studies compared to 2D counterparts. 3D system revealed higher expression and metabolic activity of several CYP isoforms such as CYP3A4, CYP2C9 and CYP2D6. Moreover, 3D cultured cells maintained a differentiated phenotype for longer term allowing repeated drug exposures. This increases sensitivity of the system to identify hepatotoxins (Ramaiahgari et al. 2014).

Spheroids can be prepared by various strategies including the cultivation of cells on a non-adherent surface of a plastic dish (Fig. 4A) (Kelm et al. 2003; Koide et al. 1990), the spheroid assembly in rotating petri dishes (Li et al. 1992), rotating wall vessels (Chang and Hughes-Fulford 2009), and spinner vessels (Wu et al. 1996), hanging-drop technique (Fig. 4B) (Kelm et al. 2003; Messner et al. 2013; Takahashi et al. 2015) or gel entrapment (Fig. 4C) (Bhattacharya et al. 2012; Glicklis et al. 2000; Lan et al. 2010; Malinen et al. 2014; Malinen et al. 2012; Semino et al. 2003).

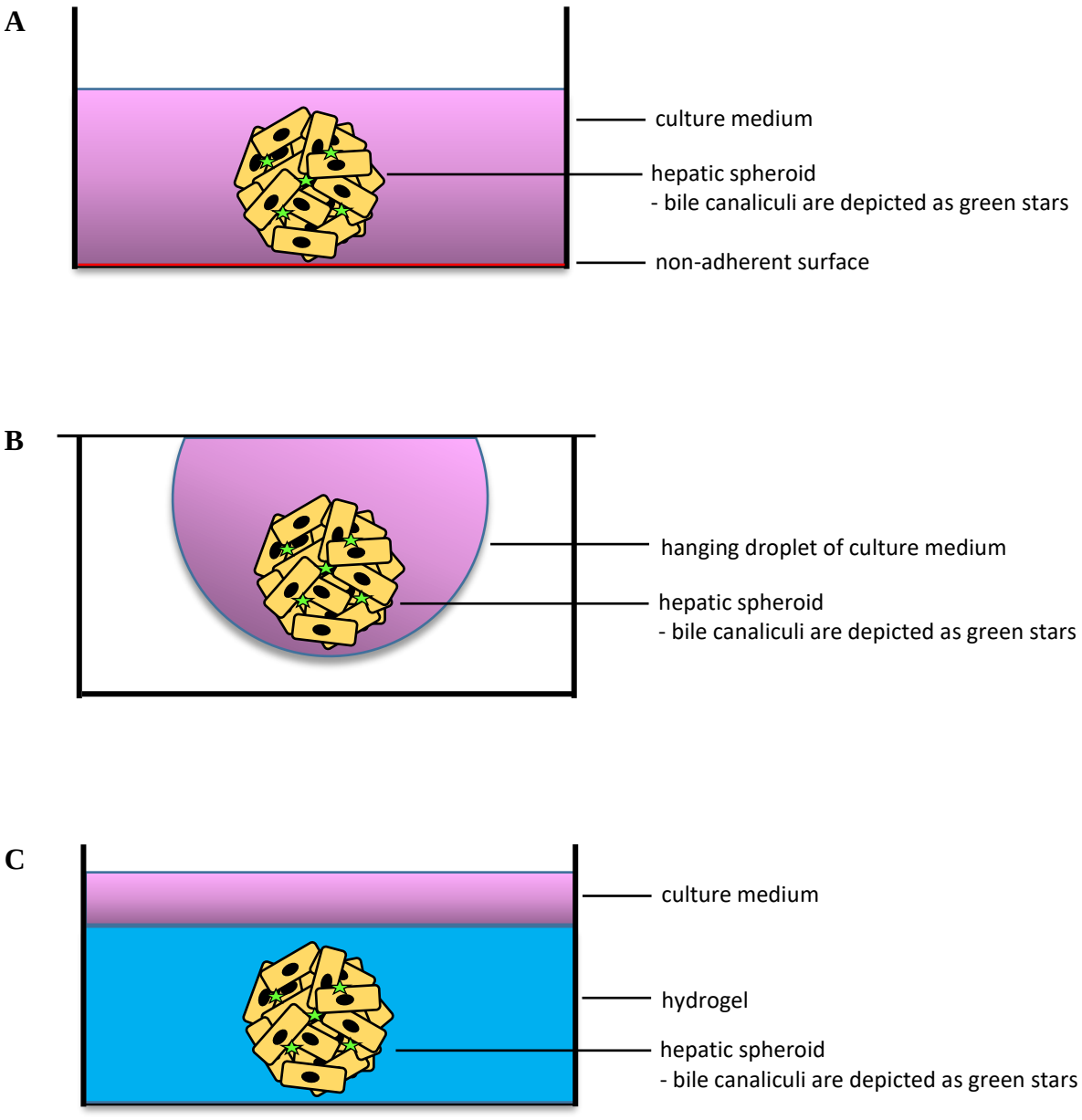

Fig. 4. Spheroid culture yielded from: A) the cultivation of the hepatocytes on the non-adherent surface, B) hanging-drop technique, C) gel entrapment

Additionally, Nanoculture® plates (SCIVAX, Japan) with textured surface like a micro-square pattern are platform enabling formation of adhesive spheroids (Fig. 5) (Nakamura et al. 2011).

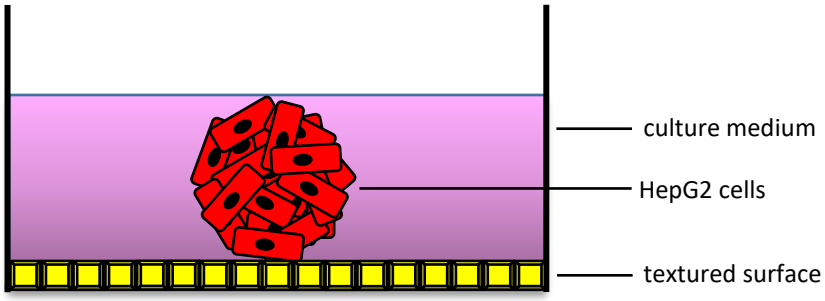

Fig. 5. Spheroid formation induced by a micropattern on the culture surface

Spheroids should reach an optimal size which allows a sufficient diffusion of oxygen. It was reported that central hypoxia can be prevented if a diameter of hepatocyte spheroid do not exceed 100 μm (Glicklis et al. 2004). To meet this criteria, several approaches were adopted to avoid formation of large spheroids such as dexamethasone treatment or increasing of cell adherence to hydrogel in the case of gel entrapment strategy (Wang et al. 2008).

- **Hanging-drop technique**

The gravity-enforced cell aggregation leads to a formation of scaffold-free spheroids in hanging drop of dispersed cells accumulated at the free liquid-air interface (Kelm and Fussenegger 2004; Kelm et al. 2003).

The hanging-drop technique has been adopted for the preparation of spheroids derived from HepG2 or HepaRG liver cells. Yielded spheroids secreted increased amount of liver-specific markers such as albumin and apoliprotein B when compared to same cells cultured in 2D conditions. It is of particular importance that mRNA level of some DMEs like CYP1A2, CYP2B6 and CYP3A4 as well as genes related to glucose and lipid metabolism were also enhanced in HepaRG spheroids. These findings provide clear evidence confirming the effect of the culture environment on liver cell functions. In sharp

contrast, HepG2 spheroids did not show enhanced expression of CYPs which proposes biased cell functions (Takahashi et al. 2015). Similarly, HepG2 cell spheroids formed in the PuraMatrix hydrogel did not display higher expression level of DMEs compared to 2D counterparts. These results indicate that 3D cell organisation do not always guarantee correct expression of DMEs (Malinen et al. 2012).

The hanging-drop method can be performed using commercially available plates such as GravityPLUS Hanging Drop System provided by InSphero.

- **Gel entrapment**

Extracellular matrix

The cells are surrounded by the non-cellular component in tissues known as extracellular matrix (ECM) which functions as the physical scaffold to cells. In addition, ECM regulates cell functions through mechanical and chemical signals. The cell-matrix interactions are realized via cell surface receptors such as integrins (Frantz et al. 2010).

ECM is comprised by two main groups of macromolecules. First, proteoglycans are hydrophilic molecules consisted of glycosaminoglycans connected with specific core proteins. Importantly, proteoglycans form a hydrated gel in the extracellular space, which ensures hydration and force-resistance properties of the tissue. The second class of ECM components are fibrous proteins including collagens, elastins, fibronectins and laminins which provide tensile strength, mediate cell attachment and affect cell functions (Frantz et al. 2010).

ECM also functions as a storage site for various signaling molecules. Indeed, there are growth factors retained in ECM, which can be released into the microenvironment upon ECM degradation (Frantz et al. 2010; Hansen et al. 2015).

ECM is a dynamic structure being under constant enzymatic and non-enzymatic remodelling processes. Unique chemical and mechanical features of ECM varies across different tissues and physiological states (Frantz et al. 2010).

Biomaterials

A natural ECM can be substituted by biomaterials in 3D liver cell models. Optimal biomaterials should correspond to physiological ECM by spatial and chemical composition. In addition, biomaterials have to be biocompatible and should provide a mechanical support and signal information to cells. Such properties of biomaterials enable cell growth, adhesion (although some biomaterials are non-adhesive) and differentiation (Vellonen et al. 2014).

The **hydrogels** belong among the most important biomaterials used for 3D cultivation of hepatocytes. They are formed by hydrophilic polymers with a high number of mutual physical and chemical bonds (Ruedinger et al. 2015). The cells can be cultivated either on the surface (Verma et al. 2007; Wang et al. 2008) or embedded inside hydrogels (Malinen et al. 2014).

The great advantage of hydrogels is their potential for modifications including mechanistic, penetration or signal properties which then meet needs of optimal ECM for a specific cell type.

- Mechanical features such as stiffness and viscoelasticity can be tuned by material composition. Recent trends focus on temporal control of hydrogel stiffening. Materials should be degradable in a controlled fashion to enable cell growth and spreading thus mimicking the dynamic properties of nature ECM (Ruedinger et al. 2015).
- The porous structure of hydrogels allows transfer of compounds (nutrients and metabolites), and oxygen inside and outside the gel by diffusion. Various techniques were adopted to achieve enhanced pores such as freeze-drying and gas foaming (Ruedinger et al. 2015).
- Biomimetic properties of hydrogel can be reached by entrapment of growth factors and introduction of specific cell-binding motifs within hydrogel (Ruedinger et al. 2015).

The hydrogels can be divided according to their origin into **natural** or **synthetic** materials (Ruedinger et al. 2015). These materials can be further classified as highly **defined** like peptide-based materials (PuraMatrix) (Zhang et al. 1995) or **undefined** e.g. the reconstituted basement membrane extracted from the Engelbreth-Holm-Swarm tumor (Matrigel) (Kleinman and Martin 2005; Vukicevic et al. 1992).

- Natural hydrogels derived from animal sources include e.g. collagen, fibrin, and hyaluronic acid. They contain indigenous signal molecules occurred in ECM, which promote cell functions. Their shortcomings are potential batch-to-batch variation, undefined structure as well as risk of a pathogen contamination (Ruedinger et al. 2015).

  Other sources of natural polymers can be found in plants, algae and shells. From this group, wood-derived nanofibrillar cellulose (Bhattacharya et al. 2012; Malinen et al. 2014), alginate (Glicklis et al. 2000; Lan et al. 2010) and chitosan (Verma et al. 2007) have been used for the cultivation of hepatocytes resulting in a spheroid formation.

  Nanofibrillar cellulose (Growdex) forms a non-adhesive hydrogel based on physical interactions between fibers mediated by hydrogen bonds. Undifferentiated HepaRG cells embedded in 3D nanofibrillar cellulose hydrogel yielded spheroids with apical-basal polarity, increased CYP3A4 activity and a functional vectorial molecular transport. These findings suggest that 3D environment expedite differentiation of HepaRG progenitors rather than 2D culture (Malinen et al. 2014). Similar results were also obtained using hyaluronan-gelatin hydrogel (Extracel) (Malinen et al. 2014).

  Alginate sponges represent a non-adherent biomaterial with highly hydrated anionic surface composed of polysaccharide chains. Hepatocytes seeded in alginate scaffolds (prepared by lyophilisation of a frozen cross-linked material) clustered into spheroids. These spheroids matched to pore size of a sponge. Importantly, the alginate-mediated 3D arrangement of hepatocytes promoted albumin secretion (Glicklis et al. 2000). Interestingly, HepG2 cells encapsulated within alginate hydrogel showed a very slow growth keeping a relatively constant amount during a cultivation. The control of a cell density can help to minimalize a variability between experiments (Lan et al. 2010).

  Chitosan is a polysaccharide derived from shells of crabs and shrimps. It was shown to have a similar structure to glycosaminoglycans. Additionally, chitosan can be fabricated into the adhesive film, which was proofed to be an effective biomaterial for the preparation of spheroids composed of HepG2 cells. Formed

3D aggregates produced more albumin and urea than control monolayer (Verma et al. 2007).

- Among synthetic materials e.g. poly(vinyl alcohol) (PVA), poly(ethylene glycol) (PEG) and poly(hydroxyethyl methacrylate) (PHEMA) are utilized for preparation of hydrogels. These materials have a defined structure and quality, however, their synthetic structure does not possess any biological information. To overcome this limit, several semi-synthetic (biohybrid) materials were designed to contain synthetic hydrophilic polymer conjugated with polysaccharide or protein moieties (Ruedinger et al. 2015).

  PuraMatrix is a well-defined porous hydrogel formed by synthetic self-assembling peptide nanofibers (10-20 nm in diameter). The hydrogel is composed mainly of water, which exceeds 99% of a total volume content determining its low mechanical strength (Semino et al. 2003; Wang et al. 2008; Zhang et al. 1995). It has been reported to promote differentiation of rat hepatocyte progenitor cell line Lig-8 into functional hepatocyte-like spheroids (Semino et al. 2003). Moreover, primary rat hepatocytes seeded on a top of PuraMatrix hydrogel generated spheroids and revealed better hepatic functions (Wang et al. 2008). HepG2 cells embedded inside the hydrogel formed spheroids with structural and functional apical-basal polarity (Malinen et al. 2012).

Several aspects dealing with a hydrogel application have to be considered prior rising a successful 3D liver culture. It should be noted that the size of fibers is critically important factor. Diameter of many polymeric fibers are in micron range, which is similar to the diameter of many cell types. Cells embedded in such hydrogels do not truly interface with 3D environment but 2D curved surface (Semino et al. 2003). Another fact is that stiffer hydrogels restrict cell growth and the size of cellular spheroids (Semino et al. 2003). Contrary, if cells are entrapped in too soft hydrogels then cells can end in the bottom of a culture plate.

Since some analysis are limited by thick and highly scattering 3D samples, thus, well-suited high-resolution imaging methods have to be developed to challenge this obstacle (Pampaloni et al. 2007). Moreover, analytical procedures have to be sometimes modified to overcome transport limitations of hydrogels e.g. using higher concentrations of reagents or a longer incubation period (Ruedinger et al. 2015).

2.2.8. Co-culture models

It is unrealistic to expect that the simple single cell type liver model can reflect the real situation occurred *in vivo*. The liver is composed of various specialized cells with different structures and functions. Therefore, models designed to mimic a diversity of cells are anticipated to more closely predict liver-like responses.

Indeed, the hanging-drop technique has been modified to simulate a liver-like cell composition. In this setup, primary human hepatocytes were cultivated along with non-parenchymal cells, Kupffer cells and endothelial cells, resulting in a hepatic microtissue model. This model integrated both structural principles of *in vivo*-like liver tissue such as multi-cell type composition and 3D organisation with heterotypic cell-cell contacts. It was shown that such system can provide a stable phenotype enabling long-term testing. Moreover, the presence of Kupffer cells can enable to study indirect hepatotoxicity of compounds meditated by immune system (Messner et al. 2013).

Other authors described that 3D co-culture of completely mixed HepG2 cells with human umbilical vein endothelial cells (HUVECs) shapes a natural cell-type composition since HUVECs always migrated predominantly to the periphery of formed spheroids (Fig. 6) (Kelm and Fussenegger 2004).

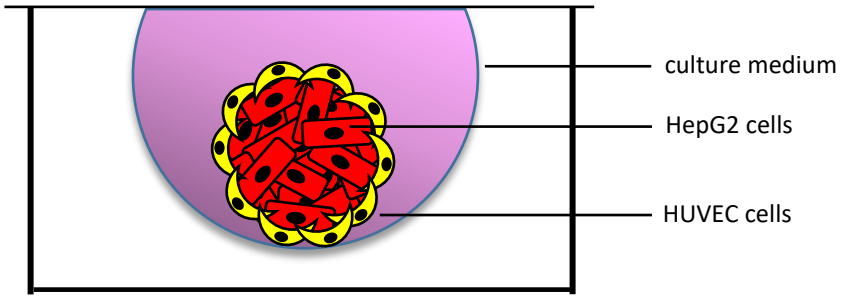

Fig. 6. Co-culture spheroid formed by hanging-drop technique

Various cell types used in co-culture models have to be of a high quality. Additionally, mixing of different cells together contributes to a variability in a cell culture (Roth and Singer 2014).

Several ready to use co-culture models can be obtained such as HμREL hepatic co-cultures (HμREL Corporation) or Human HepatoPac Co-Cultures (Hepregen).

Interestingly, co-culture system consisted of distinct organ tissue slices represent the interesting approach, which makes possible to assess a multiorgan toxicity. In this platform, the tested compound is firstly metabolized by liver tissue slices then the effect of potentially toxic metabolites is evaluated on the extrahepatic tissue (Lake and Price 2013).

2.2.9. Perfusion cultures

The continuous flow of cell culture medium can be incorporated into 2D (Fig. 7) and 3D liver cell platforms thus mimicking blood flow in hepatic sinusoids. Microfluidic-based cell models seem to be superior to static models with regular media changes since they enable to imitate biomechanical stimuli of a physiological shear stress as well as alleviate diffusional limitations within 3D system and control a concentration level of oxygen, delivery of nutrients and removal of metabolic by-products. Especially, the shear stress was shown to be important as a factor affecting hepatocyte morphology and functions (Domansky et al. 2010; Goral and Yuen 2012). Interestingly, liver sinusoidal endothelial cells co-cultured with hepatocytes better resist to de-differentiation in perfused conditions (as proofed by expression of functional marker SE-1) compared to endothelial cells cultivated alone in static conditions (Domansky et al. 2010).

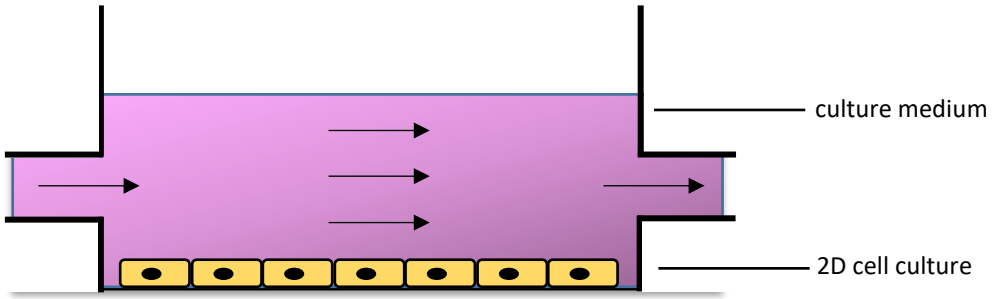

Fig. 7. Microfluidic-based 2D cell model

For cells like hepatocytes which function in highly perfused *in vivo* conditions and have high oxygen demands (the liver uses 20-30% of total oxygen consumed by the body), the microfluidic-based platforms can offer more *in vivo*-like relevant environment (Goral and Yuen 2012). Despite considerable benefits of perfused models,

their complexity could block routine drug testing within pharmaceutical industry (Roth and Singer 2014).

3. References

Aden DP, Fogel A, Plotkin S, Damjanov I, Knowles BB (1979) Controlled synthesis of HBsAg in a differentiated human liver carcinoma-derived cell line. Nature 282(5739):615-6

Akiyama TE, Gonzalez FJ (2003) Regulation of P450 genes by liver-enriched transcription factors and nuclear receptors. Biochim Biophys Acta 1619(3):223-34

Almazroo OA, Miah MK, Venkataramanan R (2017) Drug Metabolism in the Liver. Clin Liver Dis 21(1):1-20 doi:10.1016/j.cld.2016.08.001

Amacher DE (2016) The regulation of human hepatic drug transporter expression by activation of xenobiotic-sensing nuclear receptors. Expert Opin Drug Metab Toxicol 12(12):1463-1477 doi:10.1080/17425255.2016.1223626

Asha S, Vidyavathi M (2010) Role of human liver microsomes in in vitro metabolism of drugs-a review. Appl Biochem Biotechnol 160(6):1699-722 doi:10.1007/s12010-009-8689-6

Bale SS, Vernetti L, Senutovitch N, et al. (2014) In vitro platforms for evaluating liver toxicity. Exp Biol Med (Maywood) 239(9):1180-91 doi:10.1177/1535370214531872

Bhattacharya M, Malinen MM, Lauren P, et al. (2012) Nanofibrillar cellulose hydrogel promotes three-dimensional liver cell culture. J Control Release 164(3):291-8 doi:10.1016/j.jconrel.2012.06.039

Bock KW (2014) Homeostatic control of xeno- and endobiotics in the drug-metabolizing enzyme system. Biochem Pharmacol 90(1):1-6 doi:10.1016/j.bcp.2014.04.009

Boess F, Kamber M, Romer S, et al. (2003) Gene expression in two hepatic cell lines, cultured primary hepatocytes, and liver slices compared to the in vivo liver gene expression in rats: possible implications for toxicogenomics use of in vitro systems. Toxicol Sci 73(2):386-402 doi:10.1093/toxsci/kfg064

Cai J, DeLaForest A, Fisher J, et al. (2008) Protocol for directed differentiation of human pluripotent stem cells toward a hepatocyte fate StemBook. Cambridge (MA)

Doke SK, Dhawale SC (2015) Alternatives to animal testing: A review. Saudi Pharm J 23(3):223-9 doi:10.1016/j.jsps.2013.11.002

Domansky K, Inman W, Serdy J, Dash A, Lim MH, Griffith LG (2010) Perfused multiwell plate for 3D liver tissue engineering. Lab Chip 10(1):51-8 doi:10.1039/b913221j

Dunn JC, Tompkins RG, Yarmush ML (1991) Long-term in vitro function of adult hepatocytes in a collagen sandwich configuration. Biotechnol Prog 7(3):237-45 doi:10.1021/bp00009a007

Dvorak Z, Pavek P (2010) Regulation of drug-metabolizing cytochrome P450 enzymes by glucocorticoids. Drug Metab Rev 42(4):621-35 doi:10.3109/03602532.2010.484462

Ekor M (2014) The growing use of herbal medicines: issues relating to adverse reactions and challenges in monitoring safety. Front Pharmacol 4:177 doi:10.3389/fphar.2013.00177

Faucette SR, Sueyoshi T, Smith CM, Negishi M, Lecluyse EL, Wang H (2006) Differential regulation of hepatic CYP2B6 and CYP3A4 genes by constitutive androstane receptor but not pregnane X receptor. J Pharmacol Exp Ther 317(3):1200-9 doi:10.1124/jpet.105.098160

Feng B, Ng JH, Heng JC, Ng HH (2009) Molecules that promote or enhance reprogramming of somatic cells to induced pluripotent stem cells. Cell Stem Cell 4(4):301-12 doi:10.1016/j.stem.2009.03.005

Frantz C, Stewart KM, Weaver VM (2010) The extracellular matrix at a glance. J Cell Sci 123(Pt 24):4195-200 doi:10.1242/jcs.023820

Funk C (2008) The role of hepatic transporters in drug elimination. Expert Opin Drug Metab Toxicol 4(4):363-79 doi:10.1517/17425255.4.4.363

Gao J, Xie W (2012) Targeting xenobiotic receptors PXR and CAR for metabolic diseases. Trends Pharmacol Sci 33(10):552-8 doi:10.1016/j.tips.2012.07.003

Gerets HH, Tilmant K, Gerin B, et al. (2012) Characterization of primary human hepatocytes, HepG2 cells, and HepaRG cells at the mRNA level and CYP activity in response to inducers and their predictivity for the detection of human hepatotoxins. Cell Biol Toxicol 28(2):69-87 doi:10.1007/s10565-011-9208-4

Glicklis R, Merchuk JC, Cohen S (2004) Modeling mass transfer in hepatocyte spheroids via cell viability, spheroid size, and hepatocellular functions. Biotechnol Bioeng 86(6):672-80 doi:10.1002/bit.20086

Glicklis R, Shapiro L, Agbaria R, Merchuk JC, Cohen S (2000) Hepatocyte behavior within three-dimensional porous alginate scaffolds. Biotechnol Bioeng 67(3):344-53

Gonzalez FJ (2007) The 2006 Bernard B. Brodie Award Lecture. Cyp2e1. Drug Metab Dispos 35(1):1-8 doi:10.1124/dmd.106.012492

Goral VN, Yuen PK (2012) Microfluidic platforms for hepatocyte cell culture: new technologies and applications. Ann Biomed Eng 40(6):1244-54 doi:10.1007/s10439-011-0453-8

Grattagliano I, Bonfrate L, Diogo CV, Wang HH, Wang DQ, Portincasa P (2009) Biochemical mechanisms in drug-induced liver injury: certainties and doubts. World J Gastroenterol 15(39):4865-76

Gripon P, Rumin S, Urban S, et al. (2002) Infection of a human hepatoma cell line by hepatitis B virus. Proc Natl Acad Sci U S A 99(24):15655-60 doi:10.1073/pnas.232137699

Guillouzo A, Corlu A, Aninat C, Glaise D, Morel F, Guguen-Guillouzo C (2007) The human hepatoma HepaRG cells: a highly differentiated model for studies of liver metabolism and toxicity of xenobiotics. Chem Biol Interact 168(1):66-73 doi:10.1016/j.cbi.2006.12.003

Hansen NU, Genovese F, Leeming DJ, Karsdal MA (2015) The importance of extracellular matrix for cell function and in vivo likeness. Exp Mol Pathol 98(2):286-94 doi:10.1016/j.yexmp.2015.01.006

Hedrich WD, Hassan HE, Wang H (2016) Insights into CYP2B6-mediated drug–drug interactions. APSB 6(5):413-425 doi:10.1016/j.apsb.2016.07.016

Hewitt NJ, Hewitt P (2004) Phase I and II enzyme characterization of two sources of HepG2 cell lines. Xenobiotica 34(3):243-56 doi:10.1080/00498250310001657568

Hollinger MA (2003) Introduction to pharmacology. Taylor & Francis, 2nd Edition, Part 1, Chapter 3

Horii I, Yamada H (2007) In vitro hepatotoxicity testing in the early phase of drug discovery. AATEX 14(Special Issue):437-441

Huang P, He Z, Ji S, et al. (2011) Induction of functional hepatocyte-like cells from mouse fibroblasts by defined factors. Nature 475(7356):386-9 doi:10.1038/nature10116

Chang TT, Hughes-Fulford M (2009) Monolayer and spheroid culture of human liver hepatocellular carcinoma cell line cells demonstrate distinct global gene expression patterns and functional phenotypes. Tissue Eng Part A 15(3):559-67 doi:10.1089/ten.tea.2007.0434

Chen YF, Tseng CY, Wang HW, Kuo HC, Yang VW, Lee OK (2012) Rapid generation of mature hepatocyte-like cells from human induced pluripotent stem cells by an efficient three-step protocol. Hepatology 55(4):1193-203 doi:10.1002/hep.24790

Chiang CH, Huo TI, Sun CC, et al. (2013) Induced pluripotent stem cells and hepatic differentiation. J Chin Med Assoc 76(11):599-605 doi:10.1016/j.jcma.2013.07.007

Ihunnah CA, Jiang M, Xie W (2011) Nuclear receptor PXR, transcriptional circuits and metabolic relevance. Biochim Biophys Acta 1812(8):956-63 doi:10.1016/j.bbadis.2011.01.014

Ishibashi H, Nakamura M, Komori A, Migita K, Shimoda S (2009) Liver architecture, cell function, and disease. Semin Immunopathol 31(3):399-409 doi:10.1007/s00281-009-0155-6

Karabanovich G, Zemanova J, Smutny T, et al. (2016) Development of 3,5-Dinitrobenzylsulfanyl-1,3,4-oxadiazoles and Thiadiazoles as Selective Antitubercular Agents Active Against Replicating and Nonreplicating Mycobacterium tuberculosis. J Med Chem 59(6):2362-80 doi:10.1021/acs.jmedchem.5b00608

Kelm JM, Fussenegger M (2004) Microscale tissue engineering using gravity-enforced cell assembly. Trends Biotechnol 22(4):195-202 doi:10.1016/j.tibtech.2004.02.002

Kelm JM, Timmins NE, Brown CJ, Fussenegger M, Nielsen LK (2003) Method for generation of homogeneous multicellular tumor spheroids applicable to a wide variety of cell types. Biotechnol Bioeng 83(2):173-80 doi:10.1002/bit.10655

Kienhuis AS, Wortelboer HM, Maas WJ, et al. (2007) A sandwich-cultured rat hepatocyte system with increased metabolic competence evaluated by gene expression profiling. Toxicol In Vitro 21(5):892-901 doi:10.1016/j.tiv.2007.01.010

Kim RB (2002) Transporters and xenobiotic disposition. Toxicology 181-182:291-7

Kleinman HK, Martin GR (2005) Matrigel: basement membrane matrix with biological activity. Semin Cancer Biol 15(5):378-86 doi:10.1016/j.semcancer.2005.05.004

Knowles BB, Howe CC, Aden DP (1980) Human hepatocellular carcinoma cell lines secrete the major plasma proteins and hepatitis B surface antigen. Science 209(4455):497-9

Koide N, Sakaguchi K, Koide Y, et al. (1990) Formation of multicellular spheroids composed of adult rat hepatocytes in dishes with positively charged surfaces and under other nonadherent environments. Exp Cell Res 186(2):227-35

Lake BG, Price RJ (2013) Evaluation of the metabolism and hepatotoxicity of xenobiotics utilizing precision-cut slices. Xenobiotica 43(1):41-53 doi:10.3109/00498254.2012.734643

Lan SF, Safiejko-Mroczka B, Starly B (2010) Long-term cultivation of HepG2 liver cells encapsulated in alginate hydrogels: a study of cell viability, morphology and drug metabolism. Toxicol In Vitro 24(4):1314-23 doi:10.1016/j.tiv.2010.02.015

Li AP (2007) Human hepatocytes: isolation, cryopreservation and applications in drug development. Chem Biol Interact 168(1):16-29 doi:10.1016/j.cbi.2007.01.001

Li AP, Colburn SM, Beck DJ (1992) A simplified method for the culturing of primary adult rat and human hepatocytes as multicellular spheroids. In Vitro Cell Dev Biol 28A(9-10):673-7

Lin Z, Will Y (2012) Evaluation of drugs with specific organ toxicities in organ-specific cell lines. Toxicol Sci 126(1):114-27 doi:10.1093/toxsci/kfr339

Liu C, Fan H, Li Y, Xiao X (2016) Research Advances on Hepatotoxicity of Herbal Medicines in China. Biomed Res Int 2016:7150391 doi:10.1155/2016/7150391

Lou YR, Kanninen L, Kuisma T, et al. (2014) The use of nanofibrillar cellulose hydrogel as a flexible three-dimensional model to culture human pluripotent stem cells. Stem Cells Dev 23(4):380-92 doi:10.1089/scd.2013.0314

MacDonald JS, Robertson RT (2009) Toxicity testing in the 21st century: a view from the pharmaceutical industry. Toxicol Sci 110(1):40-6 doi:10.1093/toxsci/kfp088

Malarkey DE, Johnson K, Ryan L, Boorman G, Maronpot RR (2005) New insights into functional aspects of liver morphology. Toxicol Pathol 33(1):27-34 doi:10.1080/01926230590881826

Malinen MM, Kanninen LK, Corlu A, et al. (2014) Differentiation of liver progenitor cell line to functional organotypic cultures in 3D nanofibrillar cellulose and hyaluronan-gelatin hydrogels. Biomaterials 35(19):5110-21 doi:10.1016/j.biomaterials.2014.03.020

Malinen MM, Palokangas H, Yliperttula M, Urtti A (2012) Peptide nanofiber hydrogel induces formation of bile canaliculi structures in three-dimensional hepatic cell culture. Tissue Eng Part A 18(23-24):2418-25 doi:10.1089/ten.TEA.2012.0046

Martinez-Jimenez CP, Jover R, Donato MT, Castell JV, Gomez-Lechon MJ (2007) Transcriptional regulation and expression of CYP3A4 in hepatocytes. Curr Drug Metab 8(2):185-94

Messner S, Agarkova I, Moritz W, Kelm JM (2013) Multi-cell type human liver microtissues for hepatotoxicity testing. Arch Toxicol 87(1):209-13 doi:10.1007/s00204-012-0968-2

Mohri T, Nakajima M, Fukami T, Takamiya M, Aoki Y, Yokoi T (2010) Human CYP2E1 is regulated by miR-378. Biochem Pharmacol 79(7):1045-52 doi:10.1016/j.bcp.2009.11.015

Nakajima M, Yokoi T (2011) MicroRNAs from biology to future pharmacotherapy: regulation of cytochrome P450s and nuclear receptors. Pharmacol Ther 131(3):330-7 doi:10.1016/j.pharmthera.2011.04.009

Nakamura K, Kato N, Aizawa K, Mizutani R, Yamauchi J, Tanoue A (2011) Expression of albumin and cytochrome P450 enzymes in HepG2 cells cultured with a nanotechnology-based culture plate with microfabricated scaffold. J Toxicol Sci 36(5):625-33

Nishimura M, Yaguti H, Yoshitsugu H, Naito S, Satoh T (2003) Tissue distribution of mRNA expression of human cytochrome P450 isoforms assessed by high-sensitivity real-time reverse transcription PCR. Yakugaku Zasshi 123(5):369-75

Pampaloni F, Reynaud EG, Stelzer EH (2007) The third dimension bridges the gap between cell culture and live tissue. Nat Rev Mol Cell Biol 8(10):839-45 doi:10.1038/nrm2236

Pan YZ, Gao W, Yu AM (2009) MicroRNAs regulate CYP3A4 expression via direct and indirect targeting. Drug Metab Dispos 37(10):2112-7 doi:10.1124/dmd.109.027680

Pandit A, Sachdeva T, Bafna P (2012) Drug-Induced Hepatotoxicity: A Review. JAPS 2(5):233-243 doi:10.7324/JAPS.2012.2541

Pascussi JM, Drocourt L, Gerbal-Chaloin S, Fabre JM, Maurel P, Vilarem MJ (2001) Dual effect of dexamethasone on CYP3A4 gene expression in human hepatocytes. Sequential role of glucocorticoid receptor and pregnane X receptor. Eur J Biochem 268(24):6346-58

Pascussi JM, Gerbal-Chaloin S, Drocourt L, Maurel P, Vilarem MJ (2003) The expression of CYP2B6, CYP2C9 and CYP3A4 genes: a tangle of networks of nuclear and steroid receptors. Biochim Biophys Acta 1619(3):243-53

Pavek P (2016) Pregnane X Receptor (PXR)-Mediated Gene Repression and Cross-Talk of PXR with Other Nuclear Receptors via Coactivator Interactions. Front Pharmacol 7:456 doi:10.3389/fphar.2016.00456

Pelkonen O, Turpeinen M, Hakkola J, et al. (2013) Preservation, induction or incorporation of metabolism into the in vitro cellular system - views to current opportunities and limitations. Toxicol In Vitro 27(5):1578-83 doi:10.1016/j.tiv.2012.06.002

Plant N (2007) The human cytochrome P450 sub-family: transcriptional regulation, inter-individual variation and interaction networks. Biochim Biophys Acta 1770(3):478-88 doi:10.1016/j.bbagen.2006.09.024

Ramadoss P, Marcus C, Perdew GH (2005) Role of the aryl hydrocarbon receptor in drug metabolism. Expert Opin Drug Metab Toxicol 1(1):9-21 doi:10.1517/17425255.1.1.9

Ramachandran SD, Vivares A, Klieber S, et al. (2015) Applicability of second-generation upcyte(R) human hepatocytes for use in CYP inhibition and induction studies. Pharmacol Res Perspect 3(5):e00161 doi:10.1002/prp2.161

Ramaiahgari SC, den Braver MW, Herpers B, et al. (2014) A 3D in vitro model of differentiated HepG2 cell spheroids with improved liver-like properties for repeated dose high-throughput toxicity studies. Arch Toxicol 88(5):1083-95 doi:10.1007/s00204-014-1215-9

Rang HP, Ritter JM, Flower RJ, Henderson G (2015) Rang & Dale´s Pharmacology Elsevier, 8th Edition, Section 1

Ranganatha N, Kuppast I (2012) A review on alternatives to animal testing methods in drug development Int J Pharm Pharm Sci 4(Suppl 5):28-32

Raunio H, Rahnasto-Rilla M (2012) CYP2A6: genetics, structure, regulation, and function. Drug Metabol Drug Interact 27(2):73-88 doi:10.1515/dmdi-2012-0001

Roth A, Singer T (2014) The application of 3D cell models to support drug safety assessment: opportunities & challenges. Adv Drug Deliv Rev 69-70:179-89 doi:10.1016/j.addr.2013.12.005

Ruedinger F, Lavrentieva A, Blume C, Pepelanova I, Scheper T (2015) Hydrogels for 3D mammalian cell culture: a starting guide for laboratory practice. Appl Microbiol Biotechnol 99(2):623-36 doi:10.1007/s00253-014-6253-y

Sauer V, Roy-Chowdhury N, Guha C, Roy-Chowdhury J (2014) Induced pluripotent stem cells as a source of hepatocytes. Curr Pathobiol Rep 2(1):11-20 doi:10.1007/s40139-013-0039-2

Sekiya S, Suzuki A (2011) Direct conversion of mouse fibroblasts to hepatocyte-like cells by defined factors. Nature 475(7356):390-3 doi:10.1038/nature10263

Semino CE, Merok JR, Crane GG, Panagiotakos G, Zhang S (2003) Functional differentiation of hepatocyte-like spheroid structures from putative liver progenitor cells in three-dimensional peptide scaffolds. Differentiation 71(4-5):262-70 doi:10.1046/j.1432-0436.2003.7104503.x

Shan J, Schwartz RE, Ross NT, et al. (2013) Identification of small molecules for human hepatocyte expansion and iPS differentiation. Nat Chem Biol 9(8):514-20 doi:10.1038/nchembio.1270

Shimada T, Yamazaki H, Mimura M, Inui Y, Guengerich FP (1994) Interindividual variations in human liver cytochrome P-450 enzymes involved in the oxidation of drugs, carcinogens and toxic chemicals: studies with liver microsomes of 30 Japanese and 30 Caucasians. J Pharmacol Exp Ther 270(1):414-23

Schwartz RE, Fleming HE, Khetani SR, Bhatia SN (2014) Pluripotent stem cell-derived hepatocyte-like cells. Biotechnol Adv 32(2):504-13 doi:10.1016/j.biotechadv.2014.01.003

Si-Tayeb K, Lemaigre FP, Duncan SA (2010a) Organogenesis and development of the liver. Dev Cell 18(2):175-89 doi:10.1016/j.devcel.2010.01.011

Si-Tayeb K, Noto FK, Nagaoka M, et al. (2010b) Highly efficient generation of human hepatocyte-like cells from induced pluripotent stem cells. Hepatology 51(1):297-305 doi:10.1002/hep.23354

Smutny T, Bitman M, Urban M, et al. (2014) U0126, a mitogen-activated protein kinase kinase 1 and 2 (MEK1 and 2) inhibitor, selectively up-regulates main isoforms of CYP3A subfamily via a pregnane X receptor (PXR) in HepG2 cells. Arch Toxicol 88(12):2243-59 doi:10.1007/s00204-014-1254-2

Smutny T, Mani S, Pavek P (2013) Post-translational and post-transcriptional modifications of pregnane X receptor (PXR) in regulation of the cytochrome P450 superfamily. Curr Drug Metab 14(10):1059-69

Smutny T, Nova A, Drechslerova M, et al. (2016) 2-(3-Methoxyphenyl)quinazoline Derivatives: A New Class of Direct Constitutive Androstane Receptor (CAR) Agonists. J Med Chem 59(10):4601-10 doi:10.1021/acs.jmedchem.5b01891

Smutny T, Tebbens J, Pavek P (2015) Bioinformatic analysis of miRNAs targeting the key nuclear receptors regulating CYP3A4 gene expression: The challenge of the CYP3A4 “missing heritability” enigma. J Appl Biomed 13(3):181-188 doi:doi.org/10.1016/j.jab.2015.04.002

Soldatow VY, Lecluyse EL, Griffith LG, Rusyn I (2013) In vitro models for liver toxicity testing. Toxicol Res (Camb) 2(1):23-39 doi:10.1039/C2TX20051A

Song Z, Cai J, Liu Y, et al. (2009) Efficient generation of hepatocyte-like cells from human induced pluripotent stem cells. Cell Res 19(11):1233-42 doi:10.1038/cr.2009.107

Swift B, Pfeifer ND, Brouwer KL (2010) Sandwich-cultured hepatocytes: an in vitro model to evaluate hepatobiliary transporter-based drug interactions and hepatotoxicity. Drug Metab Rev 42(3):446-71 doi:10.3109/03602530903491881

Takagi S, Nakajima M, Mohri T, Yokoi T (2008) Post-transcriptional regulation of human pregnane X receptor by micro-RNA affects the expression of cytochrome P450 3A4. J Biol Chem 283(15):9674-80 doi:10.1074/jbc.M709382200

Takahashi K, Yamanaka S (2006) Induction of pluripotent stem cells from mouse embryonic and adult fibroblast cultures by defined factors. Cell 126(4):663-76 doi:10.1016/j.cell.2006.07.024

Takahashi Y, Hori Y, Yamamoto T, Urashima T, Ohara Y, Tanaka H (2015) 3D spheroid cultures improve the metabolic gene expression profiles of HepaRG cells. Biosci Rep 35(3) doi:10.1042/BSR20150034

Takayama K, Kawabata K, Nagamoto Y, et al. (2013) 3D spheroid culture of hESC/hiPSC-derived hepatocyte-like cells for drug toxicity testing. Biomaterials 34(7):1781-9 doi:10.1016/j.biomaterials.2012.11.029

Thomson JA, Itskovitz-Eldor J, Shapiro SS, et al. (1998) Embryonic stem cell lines derived from human blastocysts. Science 282(5391):1145-7

Tolson AH, Wang H (2010) Regulation of drug-metabolizing enzymes by xenobiotic receptors: PXR and CAR. Adv Drug Deliv Rev 62(13):1238-49 doi:10.1016/j.addr.2010.08.006

Ulvestad M, Nordell P, Asplund A, et al. (2013) Drug metabolizing enzyme and transporter protein profiles of hepatocytes derived from human embryonic and

induced pluripotent stem cells. Biochem Pharmacol 86(5):691-702 doi:10.1016/j.bcp.2013.06.029

Vellonen KS, Malinen M, Mannermaa E, et al. (2014) A critical assessment of in vitro tissue models for ADME and drug delivery. J Control Release 190:94-114 doi:10.1016/j.jconrel.2014.06.044

Verma P, Verma V, Ray P, Ray AR (2007) Formation and characterization of three dimensional human hepatocyte cell line spheroids on chitosan matrix for in vitro tissue engineering applications. In Vitro Cell Dev Biol Anim 43(10):328-37 doi:10.1007/s11626-007-9045-1

Vickers AE, Fisher RL (2013) Evaluation of drug-induced injury and human response in precision-cut tissue slices. Xenobiotica 43(1):29-40 doi:10.3109/00498254.2012.732714

Vukicevic S, Kleinman HK, Luyten FP, Roberts AB, Roche NS, Reddi AH (1992) Identification of multiple active growth factors in basement membrane Matrigel suggests caution in interpretation of cellular activity related to extracellular matrix components. Exp Cell Res 202(1):1-8

Wang S, Nagrath D, Chen PC, Berthiaume F, Yarmush ML (2008) Three-dimensional primary hepatocyte culture in synthetic self-assembling peptide hydrogel. Tissue Eng Part A 14(2):227-36 doi:10.1089/tea.2007.0143

Wang Z, Schuetz EG, Xu Y, Thummel KE (2013) Interplay between vitamin D and the drug metabolizing enzyme CYP3A4. J Steroid Biochem Mol Biol 136:54-8 doi:10.1016/j.jsbmb.2012.09.012

Westerink WM, Schoonen WG (2007) Cytochrome P450 enzyme levels in HepG2 cells and cryopreserved primary human hepatocytes and their induction in HepG2 cells. Toxicol In Vitro 21(8):1581-91 doi:10.1016/j.tiv.2007.05.014

Wilkening S, Bader A (2003) Influence of culture time on the expression of drug-metabolizing enzymes in primary human hepatocytes and hepatoma cell line HepG2. J Biochem Mol Toxicol 17(4):207-13 doi:10.1002/jbt.10085

Wilkening S, Stahl F, Bader A (2003) Comparison of primary human hepatocytes and hepatoma cell line Hepg2 with regard to their biotransformation properties. Drug Metab Dispos 31(8):1035-42 doi:10.1124/dmd.31.8.1035

Wu FJ, Friend JR, Hsiao CC, et al. (1996) Efficient assembly of rat hepatocyte spheroids for tissue engineering applications. Biotechnol Bioeng 50(4):404-15 doi:10.1002/(SICI)1097-0290(19960520)50:4<404::AID-BIT7>3.0.CO;2-P

Xu JJ, Henstock PV, Dunn MC, Smith AR, Chabot JR, de Graaf D (2008) Cellular imaging predictions of clinical drug-induced liver injury. Toxicol Sci 105(1):97-105 doi:10.1093/toxsci/kfn109

Yang H, Wang H (2014) Signaling control of the constitutive androstane receptor (CAR). Protein Cell 5(2):113-23 doi:10.1007/s13238-013-0013-0

Yi F, Liu GH, Izpisua Belmonte JC (2012) Human induced pluripotent stem cells derived hepatocytes: rising promise for disease modeling, drug development and cell therapy. Protein Cell 3(4):246-50 doi:10.1007/s13238-012-2918-4

Yoon E, Babar A, Choudhary M, Kutner M, Pyrsopoulos N (2016) Acetaminophen-Induced Hepatotoxicity: a Comprehensive Update. J Clin Transl Hepatol 4(2):131-42 doi:10.14218/JCTH.2015.00052

Zanger UM, Schwab M (2013) Cytochrome P450 enzymes in drug metabolism: regulation of gene expression, enzyme activities, and impact of genetic variation. Pharmacol Ther 138(1):103-41 doi:10.1016/j.pharmthera.2012.12.007

Zhang S, Holmes TC, DiPersio CM, Hynes RO, Su X, Rich A (1995) Self-complementary oligopeptide matrices support mammalian cell attachment. Biomaterials 16(18):1385-93

4. Aims

Aims of this thesis can be divided into three parts:

1. To identify small molecules for the metabolic capacity improvement of *in vitro* hepatocyte cellular models (publications 1, 2).

2. To assess post-transcriptional and post-translational modifications of NRs implicated in a regulation of DMEs, which could at least partially stand behind phenomenon of poor expression of DMEs in *in vitro* hepatocyte cellular models (publications 1, 3, 4).

3. To assess the risk of DILI/HILI of new candidate drugs or hepatotoxic phytochemicals using *in vitro* hepatocyte cellular models (publications 5, U1 unpublished yet).

5. A list of publications

This doctoral dissertation is based on following papers:

1. **Smutny T**, Bitman M, Urban M, Dubecka M, Vrzal R, Dvorak Z, Pavek P. U0126, a mitogen-activated protein kinase kinase 1 and 2 (MEK1 and 2) inhibitor, selectively up-regulates main isoforms of CYP3A subfamily via a pregnane X receptor (PXR) in HepG2 cells. (2014) Arch Toxicol., 88(12):2243-59. (IF 2014/2015: **5.980**)

2. **Smutny T,** Nova A, Drechslerová M, Carazo A, Hyrsova L, Rania Hrušková Z, Kuneš J, Pour M, Špulák M, Pavek P. 2-(3-Methoxyphenyl)quinazoline Derivatives: A New Class of Direct Constitutive Androstane Receptor (CAR) Agonists. (2016) J Med Chem., 59(10):4601-10. (IF 2015 = **5.589**)

3. **Smutny T**, Tebbens J, Pavek P. Bioinformatic Analysis of MiRNAs Targeting the Key Nuclear Receptors Regulating CYP3A4 Gene Expression: the Challenge of the CYP3A4 "Missing Heritability" Enigma. (2015) J Appl Biomed., 13(3):181-188. (IF 2014/2015: **1.302**)

4. **Smutny T**, Mani S, Pavek P. Post-translational and post-transcriptional modifications of pregnane X receptor (PXR) in regulation of the cytochrome P450 superfamily. (2013) Curr Drug Metab., 14(10):1059-69. (IF 2013: **3.487**)

5. Karabanovich G, Zemanová J, **Smutný T**, Székely R, Šarkan M, Centárová I, Vocat A, Pávková I, Čonka P, Němeček J, Stolaříková J, Vejsová M, Vávrová K, Klimešová V, Hrabálek A, Pávek P, Cole ST, Mikušová K, Roh J. Development of 3,5-Dinitrobenzylsulfanyl-1,3,4-oxadiazoles and Thiadiazoles as Selective Antitubercular Agents Active Against Replicating and Nonreplicating Mycobacterium tuberculosis. (2016) J Med Chem., 59(6):2362-80. (IF 2015: **5.589**)

U1. Tomáš Smutný, Riina Harjumäki, Liisa Kanninen, Marjo Yliperttula, Petr Pávek, Yan-Ru Lou. Human induced hepatocyte-like cells as alternative model for evaluation of herb-induced liver injury. (*preparing manuscript, yet unpublished data*)

6. Author´s contribution

This doctoral dissertation is based on papers referred as number 1-5. The candidate is a first author of first four publications.

- In publication 1, the candidate:
  - participated in the design of experiments
  - performed and analysed experiments dealing with qRT-PCR (Fig. 1; Fig. 2A, C; Fig. 4A, B; Fig. 5C, D), gene reporter assays (Fig. 2B, D, E; Fig. 3B, C; Fig. 4C; Fig. 5A, B), ligand binding assays (Fig. 3A, D) and enzymatic activity assays (Fig. 7B)
  - wrote a draft and participated in the finishing of all manuscript

- In publication 2, the candidate:
  - participated in the design of experiments
  - performed and analysed experiments dealing with PXR, AhR and VDR gene reporter assays and recombinant human CYP3A4, CYP2C9 and CYP1A2 activity assays
  - wrote parts of a manuscript concerning his experiments and participated in the finishing of all manuscript

- In publication 3, the candidate:
  - suggested the design of *in silico* analysis
  - performed *in silico* prediction and participated in analysis of results
  - wrote a draft and participated in the finishing of all manuscript

- In publication 4, the candidate:
  - summarized publications covering the topic of the review
  - wrote a draft and participated in the finishing of all manuscript
  - prepared the figure and the table included in the review

- In publication 5, the candidate:

- participated in the design of experiments
- performed and analysed experiments dealing with toxicity assessment of tested compounds on three mammalian cell lines (HeLa, HuH7, MDCKII-MDR1 cells) and primary human hepatocytes using MTS assay
- wrote parts of manuscript concerning his experiments and participated in the finishing of all manuscript

7. The publications not related to this doctoral dissertation

I. Kanninen LK, Harjumäki R, Peltoniemi P, Bogacheva MS, Salmi T, Porola P, Niklander J, **Smutny T**, Urtti A, Yliperttula ML, Lou YR. Laminin-511 and laminin-521-based matrices for efficient hepatic specification of human pluripotent stem cells. (2016) Biomaterials., 103:86-100. (IF 2015: **8.387**)

II. Hyrsova L, **Smutny T**, Carazo A, Moravcik S, Mandikova J, Trejtnar F, Gerbal-Chaloin S, Pavek P. The pregnane X receptor down-regulates organic cation transporter 1 (SLC22A1) in human hepatocytes by competing for (squelching) SRC-1 coactivator. (2016) Br J Pharmacol., 173(10):1703-15. (IF 2015: **5.259**)

III. Hyrsova L, **Smutny T**, Trejtnar F, Pavek P. Expression of human organic cation transporter 1 (OCT1): unique patterns of indirect regulation by nuclear receptors and hepatospecific gene regulation. (2016) Drug Metab Rev., 48(2):139-58. (IF 2015: **4.526**)

IV. Carazo Fernández A, **Smutny T**, Hyrsova L, Berka K, Pavek P. Chyrsin, balcalein and galangin are indirect activators of the human constitutive androstane receptor (CAR). (2015) Toxicol Lett., 233(2):68-77. (IF 2014/2015: **3.262**)

V. **Smutny T**, Pavek P. Resveratrol an inhibitor of Pregnane X receptor (PXR): another lesson in PXR antagonism. (2014) J Pharmacol Sci., 126(2):177-8. (IF 2014/2015: **2.360**)

VI. Karabanovich G, Roh J, **Smutny T**, Nemecek J, Vicherek P, Stolarikova J, Vejsova M, Dufkova I, Vavrova K, Pavek P, Klimesova V, Hrabalek A. 1-Substituted-5-[(3,5-dinitrobenzyl)sulfanyl]-1H-tetrazoles and their isosteric analogs: A new class of selective antitubercular agents active against drug-susceptible and multidrug-resistant mycobacteria. (2014) Eur J Med Chem., 82:324-40. (IF 2014/2015: **3.447**)

VII. Pavek P, **Smutny T**. Nuclear receptors in regulation of biotransformation enzymes and drug transporters in the placental barrier. (2014) Drug Metab Rev., 46(1):19-32. (IF 2014/2015: **5.356**)

VIII. Rulcova A, Krausova L, **Smutny T**, Vrzal R, Dvorak Z, Jover R, Pavek P. Glucocorticoid receptor regulates organic cation transporter 1 (OCT1, SLC22A1) expression via HNF4α upregulation in primary human hepatocytes. (2013) Pharmacol Rep., 65(5):1322-35. (IF 2013: **2.165**)

8. Articles published in journals with impact factor associated with a topic of doctoral dissertation accompanied by candidate´s commentary

1. U0126, a mitogen-activated protein kinase kinase 1 and 2 (MEK1 and 2) inhibitor, selectively up-regulates main isoforms of CYP3A subfamily via a pregnane X receptor (PXR) in HepG2 cells.

Smutny T, Bitman M, Urban M, Dubecka M, Vrzal R, Dvorak Z, Pavek P. U0126, a mitogen-activated protein kinase kinase 1 and 2 (MEK1 and 2) inhibitor, selectictively up-regulates main isoforms of CYP3A subfamily via a pregnane X receptor (PXR) in HepG2 cells. (2014) Arch Toxicol., 88(12):2243-59
(IF 2014/2015: **5.980**)

It was shown that expression of major CYPs is substantially reduced in cell lines derived from a hepatocellular carcinoma (HCC) such as HepG2 cells and in the cancer tissue of patients suffering from HCC. Additionally, it was demonstrated that the extracellular signal-regulated protein kinase (ERK) signaling pathway is involved in hepatocarcinogenesis. Indeed, the elevated phosphorylation level of ERK1/2 has been detected in most human HCC samples as well as constitutively active ERK1/2 were shown to contribute to the proliferation and the invasion of human HCC cells.

Mitogen-activated protein kinases (MAPKs) are serine/threonine kinases, which have key functions in a transduction of extracellular signals from activated cell surface receptors into various cellular responses by interfering with substrates such as transcription factors or downstream kinases. MAPK family includes ERK1 and ERK2. ERK1/2 are a part of ERK signaling pathway receiving phosphorylation signal from upstream mitogen-activated protein kinase kinases 1/2 (MEK1/2).

In this study, we detected a strong impact (>100-fold upregulation of mRNA) of MEK1/2 inhibitors such as U0126 on expression of main isoforms of the CYP3A subfamily in HepG2 cells and the weak effect on CYP3A4 mRNA expression in primary human hepatocytes.

As revealed by gene reporter assays, U0126 activated a reporter construct with CYP3A4 promoter containing PXR response elements compared to construct containing mutated elements. We also found that actinomycin D, a well-known transcriptional inhibitor, abrogated U0126-mediated increase of CYP3A mRNA expression in HepG2 cells proposing a transcriptional level of the regulation.

We further noticed that the upregulation of CYP3A genes is at least partially mediated by a direct binding of U0126 to the PXR ligand binding pocket employing a ligand binding assay and utilizing a PXR mutant expressing an obstructed ligand binding pocket. Additionally, PXR antagonist sulforaphane diminished effect of U0126 on CYP3A4 mRNA expression. In two-hybrid assay, we revealed that U0126 promoted the interaction between PXR and its coactivator SRC1 in HepG2 cells. Taken all these results together, we can suppose that U0126 is an agonist of PXR.

Interestingly, we found that small heterodimer partner (SHP), a repressor of PXR, is dramatically downregulated by U0126. Hence, U0126-induced downregulation of SHP gene expression may participate in CYP3A mRNA induction.

Our findings also suggested cross talk between PXR and the ERK signaling pathway. We showed that a partial inhibition of MEK1 using a MEK1 dominant negative expression vector led to the downregulation of SHP mRNA expression but did not result in significant CYP3A4 mRNA upregulation, even though we confirmed a significant effect on CYP3A4 transactivation in gene reporter assay in HepG2 cells

Our results showed that MEK1/2 inhibitors can enhance expression of CYP3A genes in HepG2 cells via both a direct binding to PXR and an indirect effect involving SHP downregulation. We also found higher CYP3A4 enzymatic activity in HepG2 cells after the treatment with U0126. Based on our data, MEK1/2 inhibitors could lead to the new strategy aiming to the improvement of a metabolic capacity of HepG2 cells.

Arch Toxicol (2014) 88:2243–2259
DOI 10.1007/s00204-014-1254-2

MOLECULAR TOXICOLOGY

U0126, a mitogen-activated protein kinase kinase 1 and 2 (MEK1 and 2) inhibitor, selectively up-regulates main isoforms of CYP3A subfamily via a pregnane X receptor (PXR) in HepG2 cells

Tomas Smutny · Michal Bitman · Michal Urban · Michaela Dubecka · Radim Vrzal · Zdeněk Dvorak · Petr Pavek

Received: 10 January 2014 / Accepted: 15 April 2014 / Published online: 14 May 2014

Abstract Hepatocyte tumor cell lines lack the expression or induction properties of major cytochrome P450 (CYP) enzymes compared to primary human hepatocytes. The Ras/Raf/MEK/ERK signaling cascade contributes to hepatocarcinogenesis, dedifferentiation and loss of hepatocyte drug metabolism in hepatocyte tumors. In the present study, we examined whether MEK1/2 inhibitors can restore the expression of CYP genes in hepatocarcinoma HepG2 cells. We found that U0126, a prototype dual MEK1/2 inhibitor, is a potent inducer of CYP3A4, CYP3A5 and CYP3A7 mRNA expression (>100-fold) in HepG2 cells and CYP3A4 mRNA expression in primary human hepatocytes. This U0126-mediated induction is sensitive to the transcriptional inhibitor actinomycin D and was not detected for CYP2B6 or MDR1 mRNA expression. In gene reporter assays, U0126 activates a CYP3A4 promoter luciferase reporter construct containing PXR response elements (PXREs), but not a construct containing mutated PXREs. Based on a ligand binding assay and the examination of a PXR mutant expressing an obstructed ligand binding pocket, we found that U0126 is a ligand of PXR. We also found that U0126 up-regulates the mRNA expression of the nuclear receptors HNF4α, CAR, VDR and PXR but abolishes small heterodimer partner (SHP) corepressor expression in HepG2 cells. The MEK1/2 inhibitors PD0325901 and PD184352, as well as dominant-negative MEK1 expression, also down-regulate SHP mRNA expression. In contrast, dominant-negative MEK1 expression does not significantly induce CYP3A4 gene in HepG2 cells. In conclusion, we found that U0126 is an atypical PXR ligand that via direct (binding and activation of PXR) and indirect (SHP dowregulation) mechanisms selectively restores CYP3A genes in HepG2 cells.

Keywords Cytochrome P450 · CYP3A4 · Gene regulation · Pregnane X receptor · ERK cascade

Abbreviations

CAR	Constitutive androstane receptor
CDCA	Chenodeoxycholic acid
CDK	Cyclin-dependent kinase
CYP	Cytochrome P450
DMEs	Drug-metabolizing enzymes
DN	Dominant negative
ERK1/2	Extracellular signal-regulated kinases 1/2
FXR	Farnesoid X receptor
HNF4α	Hepatocyte nuclear factor-4 alpha
LBD	Ligand binding domain
MAPK	Mitogen-activated protein kinase
MDR1	Multi-drug resistance 1; ABCB1 gen; P-glycoprotein
MEK1/2	Mitogen-activated/extracellular signal-regulated kinase kinases 1/2
NR	Nuclear receptor
PKA	Cyclic AMP-dependent protein kinase
PKC	Protein kinase C
PXR	Pregnane X receptor
PXRE	Pregnane X receptor response element
SHP	Short/small heterodimer partner (N0B2)
SRC1	Steroid receptor coactivator-1
UTR	Untranslated region

T. Smutny · M. Bitman · M. Urban · M. Dubecka · P. Pavek (✉)
Department of Pharmacology and Toxicology, Faculty of Pharmacy in Hradec Kralove, Charles University in Prague, Heyrovskeho 1203, 500 05 Hradec Kralove, Czech Republic
e-mail: pavek@faf.cuni.cz; petr.pavek@faf.cuni.cz

R. Vrzal · Z. Dvorak
Department of Cell Biology and Genetics, Regional Centre of Advanced Technologies and Materials, Faculty of Science, Palacky University in Olomouc, Slechtitelu 11, 783 71 Olomouc, Czech Republic

Introduction

Cytochrome P450 (CYP) superfamily members are monooxygenases that predominantly catalyze the oxidation of a vast array of exogenous and endogenous compounds, including drugs, toxins and fatty acids. Of these, the CYP3A subfamily comprises the most important group of CYPs that are involved in xenobiotic metabolism due to both the promiscuity to their substrates, which are responsible for the metabolism of up to 50 % of all clinically used drugs, and their abundance in the liver, constituting over 30 % of the total CYP content (Shimada et al. 1994). The CYP3A subfamily includes four members: CYP3A4, CYP3A5, CYP3A7 and CYP3A43. Among these, CYP3A4 is a pivotal drug-metabolizing enzyme (DME) in the adult human liver (Plant 2007).

Several nuclear receptors (NRs), which are ligand-inducible transcription factors, regulate DMEs expression. Of the NRs, the pregnane X receptor (PXR, NR1I2) has been shown to be the primary regulator of CYP3A4 induction (Bertilsson et al. 1998; Blumberg et al. 1998; Goodwin et al. 1999; Lehmann et al. 1998). It is well established that the transcriptional activity of PXR is regulated via direct binding to various ligands. Moreover, numerous studies have indicated that phosphorylation-mediated cellular signaling pathways modulate the functions of NRs, including PXR, with respect to both the basal and ligand-activated transactivation of the CYP3A4 gene (Rochette-Egly 2003; Smutny et al. 2013).

Pregnane X receptor (PXR) has been found to be phosphorylated by protein kinase A (PKA), resulting in alteration of PXR-mediated CYP3A expression in a species-specific manner (Ding and Staudinger 2005a; Lichti-Kaiser et al. 2009b). Furthermore, activation of the protein kinase C (PKC) signaling pathway repressed PXR-mediated induction of Cyp3a11 gene expression in mouse hepatocytes (Ding and Staudinger 2005b). It was also demonstrated that PXR is phosphorylated by cyclin-dependent kinases 2 (CDK2) and 5 (CDK5) to suppress PXR-mediated CYP3A4 expression (Dong et al. 2010; Lin et al. 2008). In addition, p70 S6K, a downstream kinase of the PI3K-Akt pathway, was also found to directly phosphorylate PXR in vitro and negatively regulate PXR transcriptional activity (Pondugula et al. 2009).

The extracellular signal-regulated kinases 1 and 2 (ERK1/2) belong to the mitogen-activated protein kinase (MAPK) family of serine and threonine kinases and play a key role in the integration of extracellular signals to induce different cellular responses by modifying various nuclear and cytosolic substrates, including transcription factors (e.g., Elk1) (De Luca et al. 2012; Shaul and Seger 2007). Briefly, activation of the ERK signaling pathway is initiated by tyrosine kinase receptors (TKRs), such as the EGF receptor (EGFR), upon ligand binding, which then promotes the activation of Ras GTPase. Active Ras facilitates signal transduction via subsequent phosphorylation steps that activate Raf kinase, which in turn induces activation of MEK1/2, which consequently phosphorylate ERK1/2 (Shaul and Seger 2007). ERK1/2 activation has been shown to be critical for cell proliferation via promotion of the G_1/S transition (Meloche and Pouyssegur 2007). Importantly, increased levels of phosphorylated ERK1/2 have been reported in most human hepatocellular carcinoma (HCC) samples (Lee et al. 2006), and constitutively, active ERK1/2 have been found to be important for the proliferation and invasion of human HCC cells (Min et al. 2010; Wiesenauer et al. 2004).

CYP3A4 is highly expressed in normal adult hepatocytes (in the G_0 phase) (Martinez-Jimenez et al. 2007). However, reduced expression of CYP3A4 was detected in vitro in HCC cell lines, such as HepG2 cells (Donato et al. 2008; Rodriguez-Antona et al. 2002), and in tumor tissue from patients suffering from HCC (Haas et al. 2009). Consistently, down-regulation of various CYPs, including CYP3A4, after activation of the ERK signaling pathway was detected in most of these studies (Braeuning 2009). Interestingly, there is a lack of evidence regarding the association between the ERK signaling pathway in hepatocytes or hepatocyte-derived cell lines and PXR activity with respect to the regulation of major CYP isoforms expression.

The aim of the study was to elucidate whether inhibition of the ERK1/2 signaling cascade affects the expression of CYP3A subfamily genes in the HepG2 cell line and in primary human hepatocytes. In the present study, we found that U0126, a prototypical MEK1/2 inhibitor, robustly up-regulates expression of the main isoforms of the CYP3A subfamily in HepG2 cells via a dual mechanism involving both PXR ligand-dependent and PXR ligand-independent induction. Our data also suggest that MEK1/2 inhibition by small molecule inhibitors stimulates PXR-mediated transactivation of CYP3A4, but down-regulates SHP expression and indicate that Ras/Raf/MEK/ERK signaling pathway controls PXR activity in its target gene regulation.

Materials and methods

Chemicals

Rifampicin (a prototypical ligand of the human PXR), 1,4-diamino-2,3-dicyano-1,4-bis(methylthio)butadiene (U0126) (a prototypical MEK1/2 inhibitor), chenodeoxycholic acid (CDCA), PD184352, PD0325901, actinomycin D, SR12813 (a human PXR ligand), dimethyl sulfoxide

(DMSO), sulforaphane (SFN) and nonessential amino acids (NEAA) were purchased from Sigma-Aldrich (St. Louis, MO, USA). U0124 (an inactive analog of U0126 that does not inhibit MEKs) was purchased from Santa Cruz Biotechnology (Santa Cruz, CA, USA). DMEM medium was purchased from both Sigma-Aldrich (St. Louis, MO, USA) and Invitrogen/Life Technologies (Carlsbad, CA, USA). FBS was purchased from PAA (Pasching, Austria). Phenol red-free Opti-MEM® medium was purchased from Invitrogen/Life Technologies (Carlsbad, CA, USA). All other chemicals were of the highest quality that was commercially available. Stock solutions (1,000×) were prepared in DMSO.

Cell lines

The human Caucasian hepatocellular carcinoma (HepG2) cell line was purchased from the European Collection of Cell Cultures (ECACC, Salisbury, UK). HepG2 cells were maintained in antibiotic-free Dulbecco's modified Eagle's medium (DMEM) with 10 % fetal bovine serum (FBS) and 1 % nonessential amino acids at 37 °C in a humidified atmosphere containing 5 % CO_2. The final concentration of DMSO in the culture medium was 0.1 % (v/v) in all experiments.

Primary cultures of human hepatocytes

Hepatocytes were prepared from lobectomy segments resected from adult patients for medical reasons unrelated to our research program. Human tissue acquisition was designed according to procedures complying with the current Czech legislation. The human liver samples used in this study were obtained from four patients: LH18, LH19, LH21 and LH279 (Vrzal et al. 2009). The hepatocyte preparation LH42 was generated from a 60-year-old woman. Human long-term hepatocytes in monolayer (Batch HEP220797, Biopredic International, Saint Gregoire, France) have been prepared from 66-year-old Caucasian female liver with colorectal cancer. Following isolation, the cells were plated on collagen-coated culture dishes at a density of 1.4×10^5 cells/cm^2. The medium was replaced with serum-free medium the day after delivery, and the cultures were allowed to stabilize for an additional 48–72 h prior to treatment. The cultures were maintained at 37 °C in 5 % CO_2 in a humidified incubator and treated with evaluated compounds.

Plasmids

The pA-luc plasmid contains a constitutive liver-enhanced module (CLEM4, −11.4 to −10.5 kb), which is responsible for the constitutive activation of CYP3A4 gene, as well as a distal XREM (−7836/−7208) and a basal promoter sequences (prPXRE, −362/+53). The pC-luc construct contains mutations in all PXREs of the pA-luc construct as we described in our previous report (Pavek et al. 2010). The p3A4-luc reporter construct contains only the XREM and basal promoter sequences. The pER6-luc plasmid contains three copies of the proximal CYP3A4 promoter response element, an everted repeat of the AG(G/T)TCA hexamer separated by six nucleotides (ER-6) and a minimal promoter (Svecova et al. 2008). The expression plasmids for the human PXR and FXR receptors, pSG5-hPXR and pSG5-hFXR, respectively, were kindly provided by Dr. S. Kliewer (University of Texas, Dallas, TX, USA). The pGL5-luc (a luciferase gene reporter vector with five copies of the GAL4 consensus binding site), pGL4.23 and pRL-TK constructs were purchased from Promega (Madison, WI, USA). The mammalian two-hybrid fusion plasmids pM-GAL4-PXR LBDwt, VP16-SRC-1-receptor-interacting domain (RID) and a pM-GAL4-PXR LBDmut (S247W/C284W) mutant construct were described previously (Takeshita et al. 2002; Wang et al. 2007). The construct expressing dominant-negative MEK1 with mutations K97R, S218A and S222A (pMEV-MEK1-DN) and the empty vector were obtained from Biomyx Technology (San Diego, CA, USA). The Elk1 construct (pFA2-Elk1) and the negative control construct pFC2-dbd were purchased from Agilent Technologies, Inc. (Santa Clara, CA, USA) as a component of the PathDetectTrans-Reporting Systems kit to monitor ERK pathway activation. The pGL3-SHP-luc reporter plasmid containing 2,080 bp of human SHP promoter was kindly donated by Dr. S. Mani (Albert Einstein Cancer Institute, Bronx, NY, USA). The reporter construct pGL3-3A4-3′UTR, containing the CYP3A4 gene 3′UTR segment (0–1,130 base pairs from the stop codon), and the pGL3-3A4-3′UTR-27M construct, containing the mutated miR27b MRE, were described and kindly donated by Pan et al. (Pan et al. 2009). The PXR T422 and T248 mutants were described in our previous report (Doricakova et al. 2013). The CYP2B6-luc reporter plasmid (B-1.6k/PB/XREM) has been kindly donated by Dr. Hongbing Wang (University of Maryland School of Pharmacy, Baltimore, MD, USA). The plasmid contains a 1.8 kb of proximal promoter and 400 bp with PBREM and XREM of human CYP2B6 gene inserted into pGL3-luc vector (Wang et al. 2003).

Transient transfection and luciferase gene reporter assays

All of the transient transfection gene reporter assays were performed via lipofection using either Lipofectamine® 2000 transfection reagent (Invitrogen/Life Technologies, Carlsbad, CA, USA) or TransFectin™ (Bio-Rad, Hercules, CA, USA) in HepG2 cells, as described previously

(Rulcova et al. 2010). Briefly, the cells were seeded onto 48-well plates and transfected with a luciferase reporter construct (150, 170 or 200 ng/well), a NR expression plasmid (80 or 100 ng/well) or/with a MEK expression construct (100, 200 or 300 ng per well) together with *Renilla reniformis* luciferase transfection control plasmid (pRL-TK) (30 or 40 ng/well) 24 h later. Then, the cells were stabilized for 24 h prior to treatment and further maintained in phenol red-free Opti-MEM® medium (200 µl) containing the evaluated compounds at the indicated concentrations for additional 24 or 48 h. After treatment, the cells were lysed, and luciferase activity was measured. The data are expressed as the fold change in firefly luciferase activity normalized to *Renilla* luciferase activity in each sample and relative to the vehicle (DMSO 0.1 %)-treated controls, which were normalized to 1. When necessary, an equivalent quantity of empty vector (pSG5, pMEV-2HA(a), pFC2-dbd) was co-transfected to maintain a constant amount of DNA.

Mammalian two-hybrid assays

To analyze the binding of evaluated compounds to the PXR ligand binding domain (LBD) and the interaction between the bound PXR and its coactivator steroid receptor coactivator-1 (SRC1), we used a mammalian two-hybrid assay based on the luciferase reporter gene assay. HepG2 cells were seeded onto 48-well plates and transfected via lipofection using Lipofectamine 2000 reagent with the pGL5-luc luciferase reporter plasmid (150 ng/well), the pVP16-SRC-1 fusion expression plasmid or pVP16 empty vector (100 ng/well), pRL-TK (30 ng/well), the pM-GAL4-PXR LBDwt fusion expression plasmid for wild-type PXR or the double-mutant pM-GAL4-PXR LBDmut (S247W/C284W) expression plasmid co-expressing the yeast GAL4 transcription factor (100 ng/well). The PXR double mutant (S247W/C248W) was generated by substituting serine at position 247, located in the ligand binding pocket of PXR, with the larger tryptophan, which sterically blocks the ligand binding pocket of PXR and ligand binding to receptors (Wang et al. 2007). This replacement possibly explains the ligand-independent and constitutive activation of this mutant receptor (Wang et al. 2007). After 24 h, cells were treated with U0126 (10 µM), U0124 (10 µM), rifampicin (10 µM) or vehicle (DMSO; 0.1 %, v/v) for additional 24 h. Luminescence activity in the cell lysate was measured using a commercially available luciferase detection system (Dual Luciferase Reporter Assay Kit; Promega, Madison, WI, USA).

qRT-PCR assay

Total RNA isolation was performed using commercially available reagent, TRI Reagent® (Invitrogen/Life Technologies, Carlsbad, CA, USA), and RNA purity was determined based on the 260/280 nm ratio. Further, cDNAs were synthesized from 1 µg of the total RNA using Tetro cDNA Synthesis Kit (Bioline, UK) at 45 °C for 30 min in the presence of oligo $(dT)_{18}$ primer mix and terminating reaction by incubation at 85 °C for 5 min. Next, the cDNA was subjected to qRT-PCR as described previously (Pavek et al. 2010, 2012; Rulcova et al. 2010). Semi-qRT-PCR analyses of CYP3A4 (hCYP3A4_Q2), CYP3A5 (hCYP3A5_Q1), CYP3A7 (hCYP3A7_Q2), CYP2B6 (hCYP2B6_Q2), CYP2C9, MDR1 (hABCB1_Q1), SHP (hNR0B2_Q2), HNF4α, RXRα, PXR, vitamin D receptor (VDR), the constitutive androstane receptor (CAR) and hypoxanthine–guanine phosphoribosyltransferase (hHPRT_Q3) mRNA expression in HepG2 cells or primary human hepatocytes were performed using primers containing BHQ1-FAM probes, which were commercially available from Generi-Biotech (Hradec Kralove, Czech republic). qRT-PCR for each gene of interest was performed in triplicate, and the expression values were calculated as their average. Gene expression was evaluated in at least three independent experiments. The expressions of the target genes were normalized against the reference gene HPRT and then processed using the delta–delta method, assuming a PCR efficiency of 2. The data are presented as the fold changes in the activation of gene expression relative to vehicle-treated control (DMSO 0.1 %) samples (set to be 1). Efficiencies of our PCR assays are always higher than 90 % based on 5-point calibration curves.

Western blot

The relative expression of each specific protein in 25–50 µg of HepG2 cells or primary human hepatocytes total lysates was evaluated using Western blot analysis, as reported previously (Pospechova et al. 2009). Antihuman CYP3A4 (HL3: sc-53850; dilution 1:2,000), anti-PXR (mouse monoclonal; H-11: sc-48340; dilution 1:500), primary polyclonal rabbit anti-VDR antibody (sc-1009, D-20, Santa Cruz Biotechnology, CA, USA; dilution 1:500), anti-SHP polyclonal rabbit (H-160; sc-30169; Santa Cruz Biotechnology, CA, USA; 1:1,000) and goat polyclonal anti-actin (clone I-19:1616; the loading control) antibodies were purchased from Santa Cruz Biotechnology (Santa Cruz, CA, USA). Phosphorylated and total ERK were analyzed using Western blot analysis as described in our previous report (Pospechova et al. 2009). All experiments have been repeated at least three times, but representative Western blot figures are presented.

PXR ligand binding assay

The LanthaScreen® TR-FRET PXR Competitive Binding Assay (Invitrogen/Life Technologies, Carlsbad, CA, USA)

was performed to evaluate whether U0126 is a potential PXR ligand. The experiment utilizes a human PXR LBD tagged with glutathione-S-transferase (GST), which is labeled upon binding to a terbium (Tb)-labeled anti-GST antibody. The assay measures the ability of the evaluated compound to replace the fluorescent PXR ligand (Fluormone™ PXR (SXR) Green or "tracer") from the receptor. The competition between the evaluated compound and tracer results in a loss in the fluorescence resonance energy transfer (FRET) signal between the Tb-anti-GST antibody and the tracer, which can be measured. The assay was performed according to the manufacturer's instructions. Briefly, dilution series of U0126 and SR12813 (a PXR ligand used as the positive control; 10 μM SR12813 is established as 100 % relative binding) were dissolved in DMSO. DMSO was used as a negative control (0 % relative binding). Subsequently, 10 μl of each dilution was added in quadruplicate into the wells of a 384-well plate. Next, 5 μl of 4× Fluormone™ PXR (SXR) Green was aliquoted into each well together with 5 μl of DTT/4× Tb-anti-GST antibody/PXR LBD (GST). Finally, the plate was incubated at room temperature for 2 h. The fluorescence was measured using a Synergy 2 Multi-Mode Microplate Reader (BioTek Winooski, VT, USA) at the recommended settings, except for measuring the emission signal at 528 nm instead of 520 nm. The calculation of the TR-FRET ratio was performed by dividing the emission at 528 nm by the emission at 495 nm. The data were presented as the relative binding (%), as described elsewhere (Dong et al. 2010).

CYP3A4 enzymatic activity assays

Human recombinant CYP3A4 protein expressed from cDNA using baculovirus-infected insect cells with human CYP450 reductase and cytochrome b_5 in microsomal fraction (P450-Glo™ CYP3A4 Screening System with Luciferin-PPXE) (Promega, Hercules, CA, USA) was used to evaluate interaction of U0126, PD0325901 and PD184352 with recombinant CYP3A4 in vitro. CYP reactions were performed at a 96-well plate format with the tested compounds at six increasing concentrations (0.1, 1, 5, 7.5, 10 and 20 μM) according to manufacturer's protocol in three independent experiments ($n = 3$). Ketoconazole (5 μM) was used as a prototype CYP3A4 inhibitor. Luminescence was recorded using a plate-reader Synergy 2 (BioTek, Winooski, VT, USA), and values are displayed as relative light units related to control vehicle-treated samples. Data are presented as the mean ± SD of CYP3A4 inhibition related to vehicle-treated membranes (100 %).

The effect of U0126 on in vivo CYP3A4 enzymatic activity in HepG2 cells has been evaluated using the Non-lytic P450-Glo™ CYP3A4 Assay with Luciferin-IPA (Promega) according to manufacturer's protocol with slight modifications. This assay is highly specific for CYP3A4 enzymatic activity, less for CYP3A5 activity, but does not interfere with CYP3A7 activity. HepG2 cells have been seeded at the density of 30×10^3 cells per well in a 48-well plate. After 24 h, HepG2 cells have been treated with U0126 (10 μM), ketoconazole (5 μM) or rifampicin (10 μM) for 48 h and then washed intensively 3 times with PBS, and CYP3A4 enzymatic activity has been analyzed with Luciferin-IPA in Opti-MEM® medium (150 μl per well, final Luciferin-IPA concentration 3 μM) for 1 h. After the incubation, 50 μl of the medium was combined with LDR solution (50 μl) and analyzed after 20 min. Luminescence was recorded using a plate-reader Synergy 2 (BioTek, Winooski, VT). All experiments were carried out at least three times in triplicates and are presented as relative CYP3A4 enzymatic activity related to vehicle-treated (control) cells. Non-specific background signal of samples without LDR solution was subtracted from all other values obtained.

Statistical analysis

All data are presented as the mean ± standard deviations (SDs). Differences between the groups were compared using Student's unpaired two-tailed *t* test. One-way analysis of variance (ANOVA) with Dunnett's post hoc test was applied to the data if more than two groups were analyzed. All of the statistical analyses were performed using GraphPad Prism 6 Software (GraphPad Software Inc., San Diego, CA) form at least three independent experiments ($n = 3$). p value <0.05 was considered to be statistically significant.

Results

U0126 and other MEK1/2 inhibitors, PD0325901 and PD184352, strongly induce expression of CYP3As mRNA in HepG2 cells

To determine the effects of MEK1/2 inhibitors on the mRNA expression of important CYP3A subfamily genes, we treated HepG2 cells with either MEK1/2 inhibitors (U0126, PD0325901 or PD184352, 10 μM), rifampicin (RIF, 20 μM, positive control) or U0124 (an inactive analog of U0126, 10 μM, negative control) or vehicle (DMSO; 0.1 %, v/v) for 24 h. As expected, rifampicin poorly induced mRNA expression of the major isoforms of the CYP3A subfamily in HepG2 cells without co-transfection with the PXR expression construct due to the low activity and expression of endogenous PXR in HepG2 cells (Novotna et al. 2011). Remarkably, all of the MEK1/2 inhibitors applied led to robust up-regulation of CYP3A mRNAs (Fig. 1a). U0126 was found to be the most potent inducer (Fig. 1a); therefore, we mainly use the compound in next experiments.

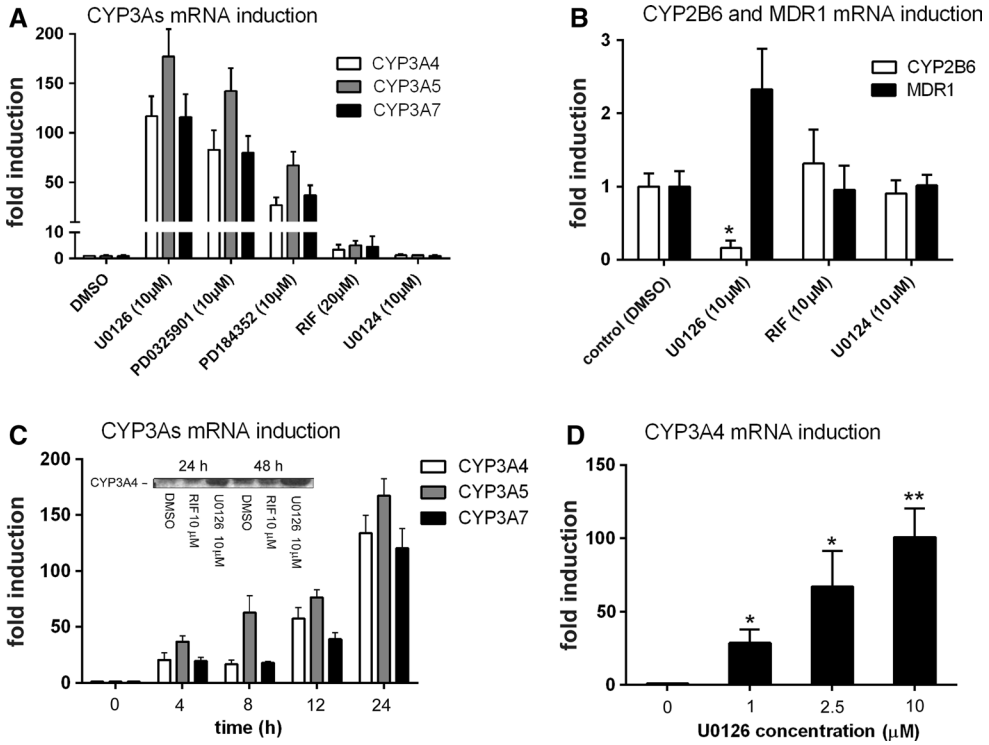

Fig. 1 MEK1/2 inhibitors induce the mRNA expression of CYP3A genes in HepG2 cells. HepG2 cells were treated with a MEK1/2 inhibitors (U0126, PD0325901 or PD184352, 10 μM), rifampicin (RIF, 20 μM), U0124 (10 μM, negative control inactive analog of U0126) or vehicle (DMSO; 0.1 %, v/v) for 24 h. Total RNA was isolated, and the CYP3A4/5/7 mRNA levels (**a**) or CYP2B6 and MDR1 mRNAs levels (**b**) were assessed via qRT-PCR. The data are presented as the mean ± SD from three experiments ($n = 3$) performed in triplicates and are expressed as the fold change in induction relative to vehicle-treated cells (normalized to 1). The values were normalized to HPRT mRNA as a reference gene. **c** HepG2 cells were treated with 10 μM U0126 for 4, 8, 12 or 24 h, respectively. Total RNA was isolated, and the CYP3A4/5/7 mRNA levels were assessed via qRT-PCR. The data are presented as the mean ± SD from triplicate measurements of a representative experiment and are expressed as the fold change in induction relative to vehicle-treated cells at time zero (normalized to 1). The values were normalized to HPRT mRNA as a reference gene. The insert represents immunoreactivity against CYP3A4 in HepG2 cells treated with 10 μM U0126, 10 μM rifampicin (RIF) or vehicle (DMSO; 0.1 %, v/v) for either 24 or 48 h (Fig. 1c, inset). **d** HepG2 cells were treated with U0126 at a concentration of 1, 2.5 or 10 μM or with vehicle (DMSO; 0.1 %, v/v) for 24 h. Total RNA was isolated, and CYP3A4 mRNA levels were assessed via qRT-PCR. The data are presented as the mean ± SD from three independent experiments ($n = 3$) performed in triplicates and are expressed as the fold change in induction relative to vehicle-treated cells (normalized to 1). The values were normalized to HPRT mRNA as a reference gene. $*p < 0.05$ and $**p < 0.01$ indicate a statistically significant effect compared to vehicle-treated cells (ANOVA with Dunnett's post hoc test)

We further analyzed the mRNA expression other PXR target genes, including CYP2B6 and MDR1, in HepG2 cells. Rifampicin treatment did not affect the expression of these genes in HepG2 cells. Interestingly, we found statistically significant ($p < 0.05$) suppression of CYP2B6 mRNA expression and a slight increase in MDR1 mRNA expression due to U0126 treatment in HepG2 cells (Fig. 1b).

Next, in time-dependent experiments, the mRNA expression of CYP3A4, CYP3A5 and CYP3A7 was assessed after 4, 8, 12 or 24 h treatment with U0126 (at a range of concentrations from 1 to 10 μM). We found that U0126 significantly up-regulates the expression of the major CYP3A genes in a time- and concentration-dependent manner (Fig. 1c, d). Consistent with the induction of CYP3A4 mRNA, the CYP3A4 protein level in HepG2 cells also increased due to U0126 treatment in a time-dependent manner (24, 48 h) (Fig. 1c, inset).

These data indicate that U0126 treatment selectively up-regulates CYP3A mRNAs but not CYP2B6 or MDR1 mRNA in HepG2 cells. Moreover, induction of CYP3A mRNAs in HepG2 cells is much more potent in response to MEK1/2 inhibitors compared to rifampicin, a prototypical CYP3A inductor via PXR.

U0126 regulates the expression of CYP3A subfamily genes at the transcriptional level via involvement of PXR in HepG2 cells

To elucidate the mechanism by which U0126 up-regulates the expression of CYP3A subfamily genes, we pre-treated

HepG2 cells with actinomycin D, a well-known transcriptional inhibitor, for 1 h and then treated the cells with 10 μM U0126 for an additional 24 h (Fig. 2a). Notably, pretreatment of HepG2 cells with actinomycin D abolished the effect of U0126 on the induction of CYP3A genes mRNA expression (Fig. 2a). Actinomycin D itself exhibits no significant effect on CYP3A genes expression.

Next, using transient transfection gene reporter assays, we found that all of the MEK1/2 inhibitors evaluated significantly enhanced CYP3A4 luciferase reporter (pA-luc) activity in HepG2 cells co-transfected with the PXR expression construct (Fig. 2b). In the transient transfection CYP3A4 (pA-luc) gene reporter assays in HepG2 cells that were not co-transfected with the PXR expression vector, only U0126 significantly up-regulated the activation of the CYP3A4 construct (Fig. 2b). The lack of a statistically significant effect of rifampicin in these experiments corresponds well with the low transcriptional activity and expression of endogenous PXR in HepG2 cells (Harmsen et al. 2008; Novotna et al. 2011). Subsequently, we treated HepG2 cells with either 10 μM U0126 alone or together with SFN (20 μM), which has been shown to be a PXR antagonist (Zhou et al. 2007), for 24 h (Fig. 2c). SFN significantly ($p < 0.01$) diminished the U0126-mediated up-regulation of CYP3A4 mRNA expression. Consistently, CYP3A4 mRNA induction by U0126 (10 μM) was significantly suppressed (by 25 %, $p < 0.05$) by another PXR inhibitor, A792611 (Healan-Greenberg et al. 2008) (*data not shown*). These results provide further evidence that the U0126-induced up-regulation of CYP3A genes is mediated by PXR activation.

Finally, we transfected HepG2 cells with either an alternative CYP3A4 gene luciferase reporter construct (pA-luc or pER6-luc), a pC-luc construct expressing mutated PXREs or the empty vector pGL4.23. We found that the U0126-mediated up-regulation of CYP3A4 reporter activity is dependent on the presence of PXR binding sites (PXREs) in the luciferase reporter constructs (Fig. 2d).

Recently, Pan et al. demonstrated that miR-27b targets the 3′-untranslated region (3′UTR) of CYP3A4, leading to post-transcriptional down-regulation of CYP3A4 expression (Pan et al. 2009). Therefore, we also examined whether U0126 up-regulates CYP3A4 mRNA expression via miR-27b down-regulation. We transiently transfected HepG2 cells with reporter constructs containing the 3′UTR segment inserted downstream of the firefly luciferase gene, as described elsewhere (Pan et al. 2009). Notably, we detected the same effects of U0126 and rifampicin on the CYP3A4 reporter construct containing the 3′UTR segment expressing either the functional or mutated miR-27b response element (Fig. 2d). These results indicate that the effect of U0126 on CYP3A4 gene expression is not mediated by miR-27b in HepG2 cells.

Consistently with qRT-PCR data presented in Fig. 1b, U0126 treatment suppressed CYP2B6 luciferase gene reporter construct transactivation in transiently transfected HepG2 cells in the presence or absence of exogenous PXR (Fig. 2e).

Thus, we can conclude that U0126 specifically up-regulates CYP3As, but not CYP2B6, mRNA expression at the transcriptional level through the involvement of the PXR.

U0126 is a PXR ligand and stimulates the interaction of PXR with the SRC1 coactivator based on the two-hybrid assay

As U0126 displayed a significant inductive effect on PXR-mediated CYP3A4 expression, we aimed to investigate whether U0126 could be a direct ligand of PXR. We used a TR-FRET-based competitive binding assay to evaluate the ability of U0126 to bind directly to human PXR. We found that U0126 can displace the fluorescent PXR ligand similar to the model PXR ligand, SR12813. These findings suggest that U0126 binds to PXR (Fig. 3a). Interestingly, U0126 displays a lower IC_{50} than SR12813 (IC_{50} = 0.02 and 0.37 μM, respectively), but U0126 is not able to displace more than approximately 25 % of the fluorescent ligand.

Next, we analyzed whether U0126 affects the recruitment of the SRC1 coactivator to either the wild-type (wt) PXR LBD or the constitutively active mutant of PXR (S247W/C284W), which contains a defective ligand binding pocket (Wang et al. 2007). Rifampicin was used as a positive control. We observed that U0126 (10 μM) significantly ($p < 0.05$) strengthened the interaction between the wt PXR LBD and SRC1, as detected by the up-regulation of pGL5-luc reporter activity (2.7-fold activation) in HepG2 cells (Fig. 3b). On the other hand, U0126 did not stimulate an interaction between the mutant PXR LBD and SRC1. These results support the concept that U0126 is an agonist of the LBD of PXR that stimulates recruitment of coactivators to PXR.

To further confirm our hypothesis, we used PXR T422D and T248D mutants to evaluate the effect of U0126 on PXR-mediated p3A4-luc reporter activation in HepG2 cells. Recently, we reported that the residues T248 and T422 of PXR comprised structural determinants of PXR activity (Doricakova et al. 2013). The PXR T248D mutant was shown to be constitutively activated and not inducible by rifampicin. On the other hand, the PXR T422D mutant exhibits decreased rifampicin-mediated PXR activity. We observed a different pattern of PXR T422D activation between U0126 and rifampicin but no significant effect of U0126 or rifampicin on the activation of the T248D PXR mutant (Fig. 3c).

In final experiment, we tested whether other MEK1/2 dual inhibitors PD0325901 and PD184352 interact with

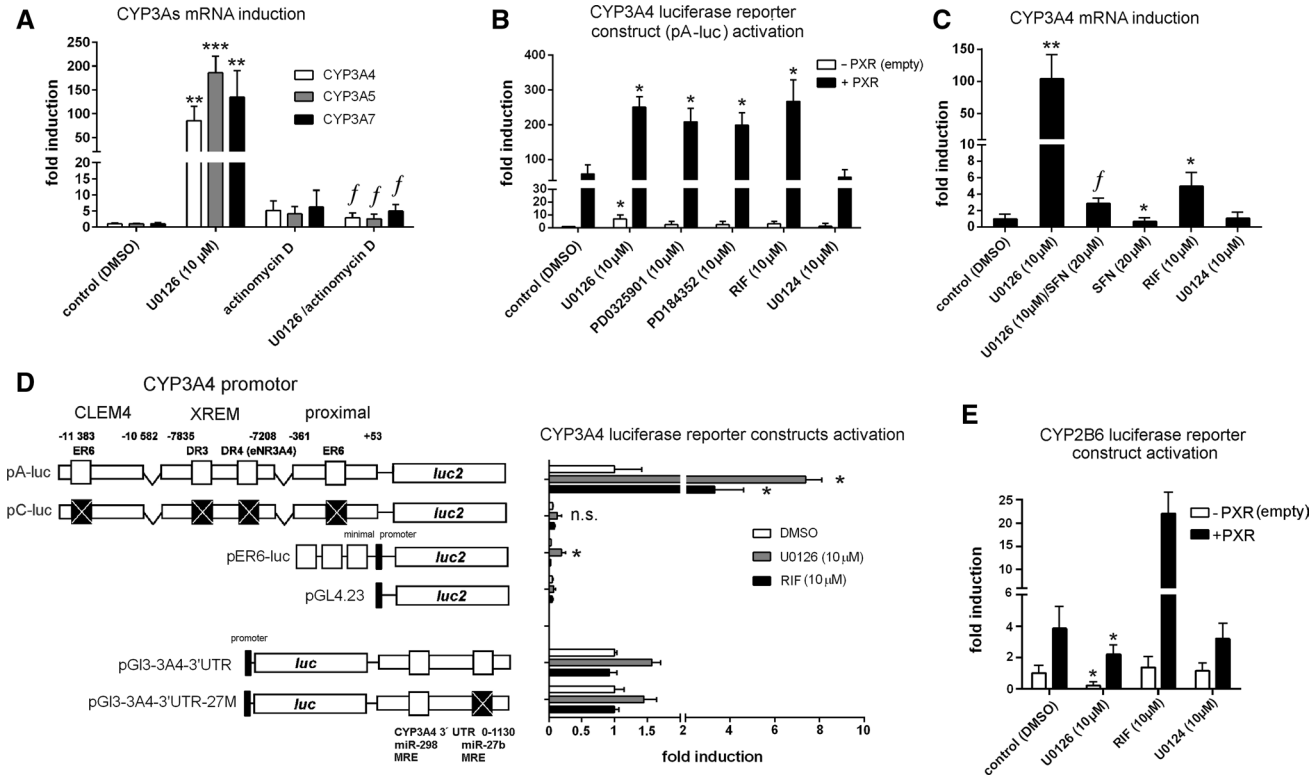

Fig. 2 U0126 transcriptionally regulates CYP3A gene expression via PXR. **a** HepG2 cells were pre-treated with either actinomycin D (3.2 μM) or vehicle (DMSO; 0.1 %, v/v) for 1 h, followed by treatment with either 10 μM U0126 or vehicle (DMSO; 0.1 %, v/v) for an additional 24 h. Total RNA was isolated, and the CYP3A4/5/7 mRNA levels were assessed via qRT-PCR. The data are presented as the mean ± SD from three independent experiments ($n = 3$) performed in triplicate measurements and are expressed as the fold change in induction relative to vehicle pre-treated and treated cells (normalized to 1). The values were normalized to HPRT mRNA as a reference gene. Similar data were acquired from three independent experiments. $^{**}p < 0.01$ and $^{***}p < 0.001$ indicate statistically significant difference compared to vehicle pre-treated and treated cells (ANOVA with Dunnett's post hoc test); $^{f}p < 0.01$—statistically significant compared to vehicle pre-treated, U0126-treated cells (Student's unpaired *t* test). **b** HepG2 cells were transiently transfected with the reporter plasmid (pA-luc; 200 ng per well in 48-well plate) and either the pSG5-PXR expression plasmid or the empty vector (100 ng per well), as well as the pRL-TK control plasmid (30 ng per well) for transfection normalization. After 24 h of stabilization, the cells were treated with the MEK1/2 inhibitor U0126, PD0325901 or PD184352 (10 μM), 10 μM rifampicin (RIF), 10 μM U0124 or vehicle (DMSO; 0.1 %, v/v) for an additional 24 h. After treatment, the cells were lysed and assayed for both firefly and *Renilla* luciferase activities. The data are presented as the mean ± SD from three independent experiments ($n = 3$) and are expressed as the fold change in induction of the activities relative to the vehicle-treated cells transfected with the empty vector (normalized to 1). $^{*}p < 0.05$ indicates statistically significant difference compared to vehicle-treated cells transfected with pSG5-PXR or empty vector (ANOVA with Dunnett's post hoc test). **c** HepG2 cells were treated with 10 μM U0126, 20 μM SFN, both U0126 and SFN together, 10 μM rifampicin (RIF), 10 μM U0124 or vehicle (DMSO; 0.1 %, v/v) for 24 h. Total RNA was isolated, and the CYP3A4 mRNA levels were assessed via qRT-PCR. The data are presented as the mean ± SD from three independent experiments ($n = 3$) performed in triplicate measurements and are expressed as the fold change in induction relative to vehicle-treated cells (normalized to 1). The values were normalized to HPRT mRNA as a reference gene. $^{*}p < 0.05$ and $^{**}p < 0.01$ indicate statistically significant difference compared to vehicle-treated cells (ANOVA with Dunnett's post hoc test); $^{f}p < 0.01$—statistically significant compared to U0126-treated cells (Student's unpaired *t* test). **d** HepG2 cells were transiently transfected with the CYP3A4 gene reporter construct pA-luc, pC-luc, pER6-luc or the pGL4.23 empty reporter vector (200 ng per well in 48-well plates) or the pGl3-3A4-3′UTR or pGl3-3A4-3′UTR-27M reporter plasmids (150 ng per well in 48-well plates) together with the pRL-TK control plasmid (30 ng per well) for transfection normalization. No PXR expression construct was included. After 24 h of stabilization, the cells were treated with 10 μM U0126, 10 μM rifampicin (RIF) or vehicle (DMSO; 0.1 %, v/v) for an additional 24 h. After treatment, the cells were lysed and assayed for both firefly and *Renilla* luciferase activities. The data are presented as the mean ± SD from triplicate measurements of a representative experiment. The results are expressed as the fold change in induction of firefly luciferase activities relative to vehicle-treated cells transfected with either the pA-luc or pGl3-3A4-3′UTR and pGl3-3A4-3′UTR-27M constructs (normalized to 1). $^{*}p < 0.05$ indicates statistically significant difference from vehicle-treated cells transfected with appropriate reporter construct (ANOVA with Dunnett's post hoc test). **e** HepG2 cells were transiently transfected with the CYP2B6-luc reporter plasmid (B-1.6k/PB/XREM, 200 ng per well in 48-well plates) together with either pSG5-PXR or the pSG5 empty vector (100 ng per well), as well as the pRL-TK control plasmid (30 ng per well) for transfection normalization. After 24 h of stabilization, the cells were treated with 10 μM MEK1/2 inhibitor U0126, 10 μM rifampicin (RIF), 10 μM U0124 or vehicle (DMSO; 0.1 %, v/v) for an additional 24 h. After treatment, the cells were lysed and assayed for both firefly and *Renilla* luciferase activities. The data are presented as the mean ± SD from three independent experiments ($n = 3$) performed in triplicate measurements and are expressed as the fold change in induction of firefly luciferase activities relative to vehicle-treated cells transfected with the empty vector (normalized to 1). $^{*}p < 0.05$ indicates statistically significant difference compared to vehicle-treated cells transfected with either the empty vector or the PXR expression construct (ANOVA with Dunnett's post hoc test)

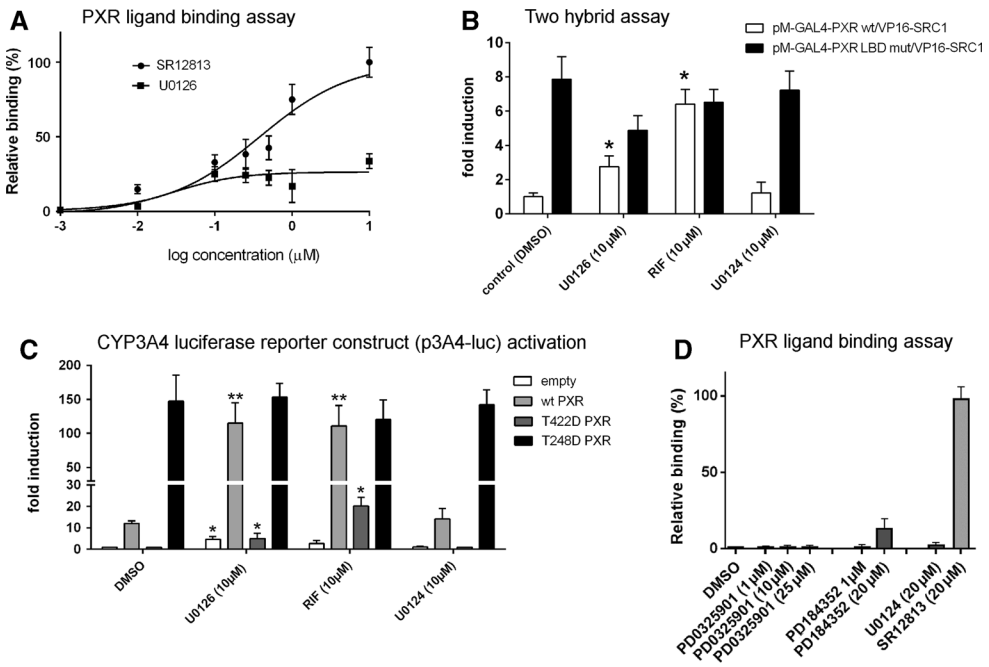

Fig. 3 U0126 binds to the PXR LBD. **a** The LanthaScreen® TR-FRET PXR Competitive Binding Assay was performed to determine the ability of U0126 to directly bind PXR LBD. SR12813, a model PXR agonist, was used as a positive control. The relative binding was calculated as described in the "Materials and methods." The data are presented as the mean ± SD from three independent experiments ($n = 3$) performed in triplicate measurements. **b** The mammalian two-hybrid assay in HepG2 cells transiently transfected with the pGL5-luc reporter plasmid (150 ng per well in 48-well plates) together with either pM-GAL4-PXR LBDwt or pM-GAL4-PXR LBDmut (S247W, C248W) (100 ng per well) fusion expression plasmid, the VP16-SRC1 fusion expression plasmid or the VP16 empty vector (100 ng per well), as well as the pRL-TK control plasmid (30 ng per well) for transfection normalization. After 24 h of stabilization, the cells were treated with U0126 (10 μM), rifampicin (RIF, 10 μM), U0124 (10 μM) or vehicle (DMSO; 0.1 %, v/v) for an additional 24 h. **c** HepG2 cells were transiently transfected with the p3A4-luc reporter plasmid (170 ng per well in 48-well plates) together with either the wt PXR, T422D PXR or T248D PXR expression plasmid (100 ng per well), as well as with the pRL-TK control plasmid (40 ng per well) for transfection normalization. After 24 h of stabilization, the cells were treated with U0126 (10 μM), rifampicin (RIF, 10 μM), U0124 (10 μM) or vehicle (DMSO; 0.1 %, v/v) for an additional 24 h. After treatment, the cells were lysed and assayed for both firefly and *Renilla* luciferase activities. The data are presented as the mean ± SD from three independent experiments ($n = 3$) and are expressed as the fold change in induction of the normalized firefly activities relative to vehicle-treated cells transfected with pM-GAL4-PXR LBDwt and VP16-SRC1 or p3A4-luc without PXR expression vector (normalized to 1). $*p < 0.05$ and $**p < 0.01$ indicate statistically significant difference compared to vehicle-treated cells transfected with the appropriate expression construct (ANOVA with Dunnett's post hoc test). **d** The LanthaScreen® TR-FRET PXR Competitive Binding Assay was performed to determine the ability of the dual MEK1/2 inhibitors PD0325901 and PD184352 to directly bind to the PXR LBD. SR12813, a model PXR agonist, was used as positive control. Similar data were acquired from two independent experiments. The data are presented as the mean ± SD from three independent experiments ($n = 3$) performed in triplicate measurements

PXR. We found that these MEK1/2 inhibitors display either no or limited interaction with PXR (Fig. 3d).

These results suggest that the significant U0126-mediated up-regulation of CYP3A mRNAs is at least partially due to both direct binding of U0126 to the PXR LBD and interaction between the activated PXR and the SCR1 coactivator. On the other hand, these data also suggest that MEK1/2 inhibition by small molecule inhibitors stimulates PXR-mediated transactivation of CYP3A4 and indicate that Ras/Raf/MEK/ERK signaling pathway controls activity of PXR in its target genes regulation. These results also suggest that the T422 residue plays a different role in U0126- and rifampicin-mediated activation of PXR.

U0126 alters the expression of NR genes in HepG2 cells

In the next experiment, we examined the effect of U0126 on the mRNA expression of key NRs involved in the transcriptional regulation of CYP3A genes. Notably, we found that U0126 significantly increased PXR, CAR, HNF4α and VDR mRNA expression after treatment for 24 h in HepG2 cells (Fig. 4a). These results are consistent with the finding by Osabe et al., who also detected up-regulation of CAR mRNA after treatment with U0126 in HepG2 cells (Osabe et al. 2009). Using Western blot analysis, we did not detect significant up-regulation of either PXR or VDR after treatment with U0126 (10 μM) in HepG2 cells (Fig. 4a, inset).

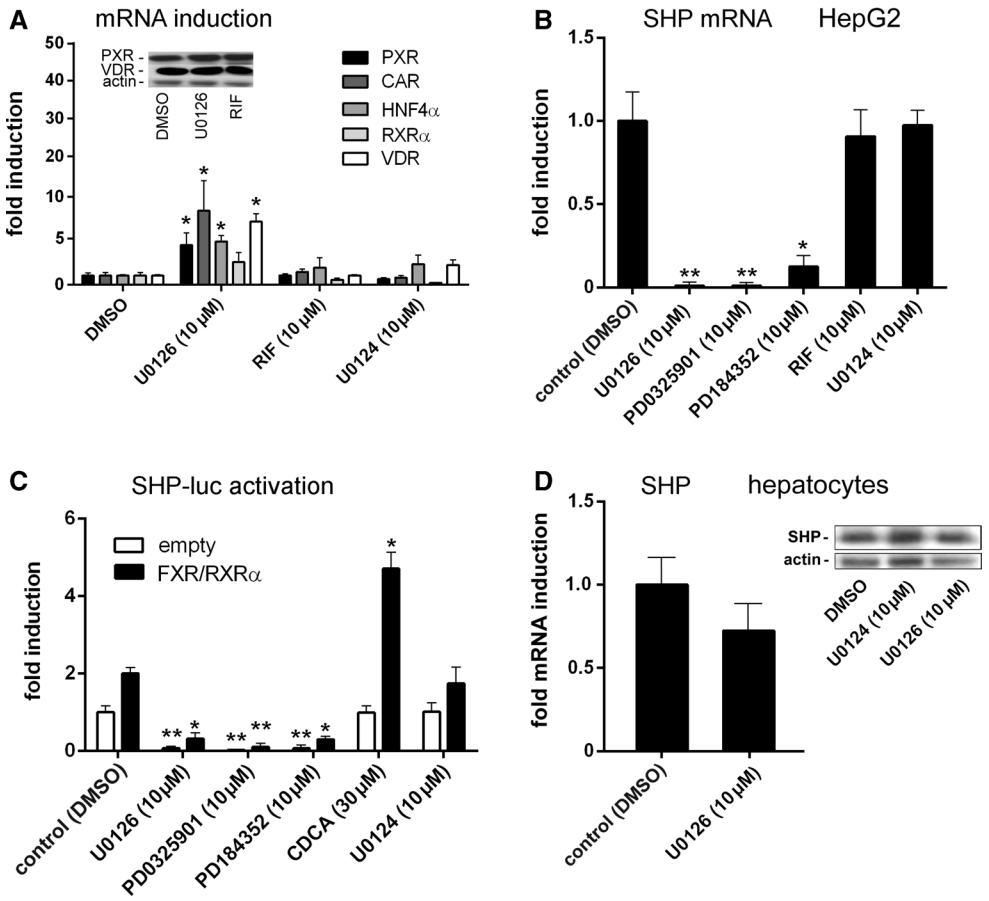

Fig. 4 Effect of U0126 on the expression of important NRs involved in the regulation of CYP3A genes in HepG2 cells. HepG2 cells were treated with U0126 (10 μM), rifampicin (RIF; 10 μM), U0124 (10 μM), PD0325901 (10 μM), PD184352 (10 μM) or vehicle (DMSO; 0.1 %, v/v) for 24 h. Total RNA was isolated, and the PXR, CAR, HNF4α, RXRα, VDR (**a**) and SHP (**b**) mRNA levels were assessed via qRT-PCR. The data are presented as the mean ± SD from three experiments ($n = 3$) and are expressed as the fold change in induction relative to vehicle-treated cells (normalized to 1). The values were normalized to HPRT mRNA as a reference gene. Inset, Western blot using anti-PXR or anti-VDR antibodies of HepG2 cells treated with vehicle (DMSO, 0.1 %), U0126, RIF or U0124 (all at 10 μM) for 24 h (Fig. 4a, inset). **c** HepG2 cells were transiently transfected with the pGL3-SHP-luc reporter plasmid (150 ng per well in 48-well plates) together with either the pSG5-FXR and pSG5-RXRα (100 ng per well) expression plasmids or the pSG5 empty plasmid (200 ng per well), as well as the pRL-TK control plasmid (30 ng per well) for transfection normalization. After 24 h of stabilization, the cells were treated with 10 μM of a MEK1/2 inhibitor (U0126, PD0325901 or PD184352), 30 μM chenodeoxycholic acid (CDCA, a FXR agonist), U0124 (10 μM) or vehicle (DMSO; 0.1 %, v/v) for an additional 24 h. After treatment, the cells were lysed and assayed for both firefly and *Renilla* luciferase activities. The data are presented as the mean ± SD from three experiments ($n = 3$) performed in triplicate measurements and are expressed as the fold change in induction of firefly luciferase activities relative to vehicle-treated cells (normalized to 1). **d** U0126 (10 μM) does not significantly down-regulate SHP mRNA and protein in primary human hepatocytes. Three independent primary human hepatocyte preparations (LH19, LH21 and HEP220797) have been treated with U0126 or U0124 (10 μM) for 24 h. Data are presented as the mean ± SD and are expressed as the fold change related to vehicle-treated (DMSO) cells or presented as a representative Western blotting experiment (hepatocytes batch HEP220797). $*p < 0.05$ and $**p < 0.01$ indicate statistically significant difference compared to vehicle-treated cells (for qRT-PCR) transfected with the empty vector construct (for gene reporter assay) (ANOVA with Dunnett's post hoc test)

Furthermore, we examined whether the effect of MEK1/2 inhibitors on PXR-mediated CYP3A genes expression could be due to an alteration in short heterodimer partner (SHP) gene expression. SHP is an orphan NR that binds to and inhibits the function of several NRs, including PXR (Ourlin et al. 2003). Surprisingly, we found that treatment with U0126, PD0325901 or PD184352 (10 μM) significantly diminished the expression of SHP mRNA after treatment for 24 h in HepG2 cells (Fig. 4b). Rifampicin displays no effect on SHP mRNA, which we have reported previously (Pavek et al. 2012), although contradictory data have also been reported (Li and Chiang 2006).

Moreover, we performed the transient transfection gene reporter assay using the SHP luciferase reporter construct co-transfected with either the FXR and RXRα expression

constructs or the empty expression vector. FXR and its ligand CDCA were used as a control because FXR has been demonstrated to target the SHP promoter and up-regulates SHP gene expression (Goodwin et al. 2000). Consistently, we found that MEK1/2 inhibitors significantly ($p < 0.01$ or $p < 0.05$) suppressed SHP luciferase reporter activity (Fig. 4c).

In next experiments, we examined whether U0126 (10 μM) down-regulates SHP mRNA and protein expression in primary human hepatocytes. We found only non-significant decrease in SHP mRNA expression and no apparent SHP protein down-regulation in primary human hepatocytes (Fig. 4d).

Taken together, these results suggest that SHP down-regulation may be involved in the mechanism by which U0126 and other MEK1/2 inhibitors restore CYP3A4 gene expression in HepG2 cells. It is also possible that moderate up-regulation of PXR, CAR, HNF4α and VDR mRNA expression after treatment with U0126 might play some positive role in the regulation of CYP3A gene expression, as all of these factors transactivate CYP3A4 (Martinez-Jimenez et al. 2007; Pavek et al. 2010).

The effect of ERK signaling pathway inhibition via dominant-negative MEK1 expression on CYP3A4 and SHP mRNA expression

First, we measured the efficiency of dominant-negative (DN) MEK1 to inhibit the ERK signaling pathway. We analyzed the activation of the Elk1 protein, a downstream transcription factor activated by ERK signaling, to measure ERK activity. As expected, U0126 treatment significantly ($p < 0.05$) suppressed Elk1 activation by approximately 75 % (Fig. 5a). DN MEK1 also significantly ($p < 0.05$) suppressed Elk1 activity based on the gene reporter assay, but the effect was less than that of U0126 (Fig. 5a).

Second, using the gene reporter assay, HepG2 cells were co-transfected with either the pMEV-MEK1-DN expression vector or the pMEV-2HA(a) empty vector together with either the PXR expression vector or the empty vector. Transfection of the pMEV-MEK1-DN construct alone significantly ($^{\dagger}p < 0.05$) induced the activity of the CYP3A4 luciferase reporter construct either with or without co-transfection with the PXR expression construct (Fig. 5b), suggesting a positive effect of the ERK pathway inhibition on PXR transcriptional activity. Notably, treatment with U0126 amplified the DN MEK1-mediated up-regulation of CYP3A4 luciferase reporter construct activity ($^{f}p < 0.05$). This amplification is likely due to either the direct binding of U0126 to PXR or the U0126-mediated inhibition of MEK2, which can substitute for MEK1 function (Favata et al. 1998; Min et al. 2011).

In the next experiments, we transfected HepG2 cells with either pMEV-MEK1-DN or the pMEV-2HA(a) empty vector (200, 300 or 400 ng per well) and analyzed the effect of MEK1 inhibition on CYP3A4 and SHP mRNA expression. We only found a statistically significant effect of pMEV-MEK1-DN (400 ng per well) transfection on SHP mRNA expression (Fig. 5c, d). The effect on CYP3A4 was not statistically significant, although we detected some up-regulation of CYP3A4 mRNA (Fig. 5c).

These results indicate that (partial) inhibition of MEK1 and the ERK signaling pathway itself does not result in significant CYP3A4 mRNA up-regulation, even though we detected a significant effect on CYP3A4 transactivation via transient transfection gene reporter assays (Fig. 5b).

U0126 induces CYP3A4 expression in primary human hepatocytes

Next, we examined the effect of U0126 on CYP3A4 expression in primary human hepatocytes. Primary human hepatocytes are a cellular model of quiescent cells (G_0 phase) that express high levels of endogenous NRs, including PXR (Castell et al. 2006). We found that only CYP3A4 mRNA expression is significantly induced in primary human hepatocytes after treatment with 10 μM U0126, which is consistent with the results using HepG2 cells (Fig. 1a, b). In contrast to HepG2 cells, CYP2B6 mRNA was not down-regulated in primary human hepatocytes (Fig. 6a).

Consistent with the qRT-PCR results, the CYP3A4 protein was significantly up-regulated after treatment with U0126 (10 or 25 μM). Expression of PXR and VDR proteins was not affected by U0126 treatment in human hepatocytes (Fig. 6b).

These data indicate that U0126 also induces CYP3A4 mRNA expression in quiescent cells that are not engaged in the cell cycle. This excludes the hypothesis that U0126-mediated MEK/ERK pathway inhibition up-regulates CYP3A4 only via cell cycle inhibition.

U0126 up-regulates CYP3A4 enzymatic activity in HepG2 cells

In CYP3A4 enzymatic assays, we found that U0126 acts as a potent CYP3A4 inhibitor, whereas PD0325901 and PD184352 showed only weak CYP3A4 inhibition (Fig. 7a). The highest CYP3A4 inhibition effect of U0126 was detected at 20 μM concentration, and IC_{50} was estimated to be at the concentration of about 3.3 μM. These data contradict to the published results in rat hepatocytes analyzed using 6β-hydroxylation of testosterone (Andrieux et al. 2004).

In next experiments, we examined whether U0126 up-regulates CYP3A4 enzymatic activity in HepG2 cells. Since we found in preliminary in vitro CYP3A4 enzymatic assays (Fig. 7a) that U0126 significantly inhibits CYP3A4 catalytic activity, we intensively washed HepG2 cells with PBS after

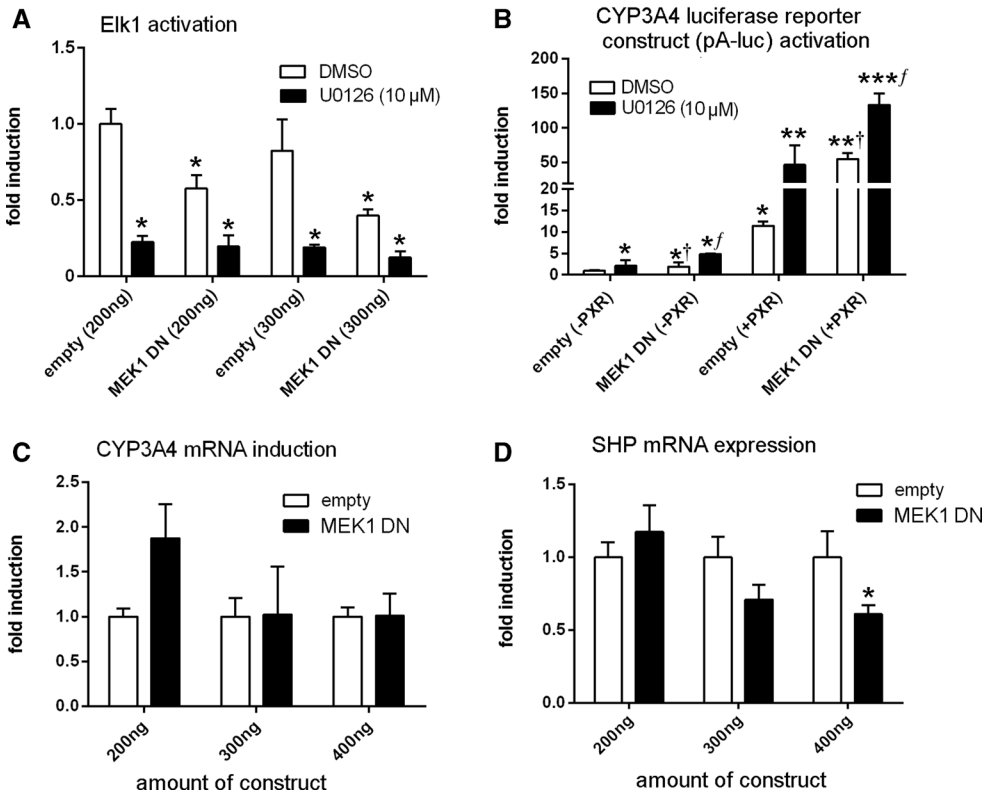

Fig. 5 Effect of ERK signaling pathway inhibition via dominant-negative MEK1 expression on CYP3A4 and SHP mRNA expression. **a** HepG2 cells were transiently transfected with the pGL5-luc reporter plasmid (150 ng per well in 48-well plates) together with either pMEV-MEK1-DN or the pMEV-2HA(a) empty vector (200 or 300 ng per well), as well as the pFA2-Elk1 expression plasmid (100 ng per well) or pFC2-dbd control construct and the pRL-TK control plasmid (30 ng per well) for transfection normalization. After 24 h of stabilization, the cells were treated with 10 μM U0126 or vehicle (DMSO; 0.1 %, v/v) for an additional 24 h. After treatment, the cells were lysed and assayed for both firefly and *Renilla* luciferase activities. The data are presented as the mean ± SD from three independent experiments ($n = 3$) performed in triplicate measurements and are expressed as the fold change in induction of firefly luciferase activities relative to vehicle-treated cells transfected with 200 ng of the pMEV-2HA(a) empty vector (normalized to 1). $^{*}p < 0.05$—statistically significant difference compared to vehicle-treated cells transfected with the pMEV-2HA(a) empty vector (200 ng) (ANOVA with Dunnett's post hoc test). **b** HepG2 cells were transiently transfected with the CYP3A4 reporter plasmid (pA-luc; 150 ng per well in 48-well plates) together with the pSG5-PXR expression plasmid or the pSG5 empty vector (80 ng per well) and either the pMEV-MEK1-DN expression plasmid or the pMEV-2HA(a) empty vector (100 ng per well), as well as the pRL-TK control plasmid (30 ng per well) for transfection normalization. After 24 h of stabilization, the cells were treated with 10 μM U0126 or vehicle (DMSO; 0.1 %, v/v) for an additional 24 h. After treatment, the cells were lysed and assayed for both firefly and *Renilla* luciferase activities. The data are presented as the mean ± SD from three independent experiments ($n = 3$) performed in triplicate measurements and are expressed as the fold change in induction of firefly luciferase activities relative to vehicle-treated cells transfected with both empty vectors (normalized to 1). $^{*}p < 0.05$, $^{**}p < 0.01$ and $^{***}p < 0.001$ indicate statistically significant difference compared to vehicle-treated cells transfected with both empty vectors (ANOVA with Dunnett's post hoc test). $^{\dagger}p < 0.05$—statistically significant effect of pMEV-MEK1-DN compared to the pMEV-2HA(a) empty vector-transfected cells (Student's unpaired t test); $^{f}p < 0.05$—statistically significant effect of U0126 compared to vehicle-treated cells transfected with pMEV-MEK1-DN (Student's unpaired t test). **c**, **d** HepG2 cells were transiently transfected with either pMEV-MEK1-DN or the pMEV-2HA(a) empty vector (200, 300 or 400 ng per well in 12-well plates). After 24 h of stabilization, total RNA was isolated, and CYP3A4 (**c**) and SHP (**d**) mRNA levels were assessed via qRT-PCR. The data are presented as the mean ± SD from triplicate measurements and are expressed as the fold change in induction relative to cells transfected with the pMEV-2HA(a) empty vector (normalized to 1). $^{*}p < 0.05$ indicates statistically significant difference compared to cells transfected with the corresponding amount of the pMEV-2HA(a) empty vector. The data are presented as the mean ± SD from three independent experiments ($n = 3$) performed in triplicate measurements

treatment to remove remaining U0126 from wells. Consistently with previous findings, we observed that HepG2 cells treated with U0126 significantly increase CYP3A4 enzymatic activity. In opposite, cells treated with rifampicin displayed no significant CYP3A4 enzymatic activity up-regulation (Fig. 7b). Ketoconazole, a CYP3A4 inhibitor, abolished the effect of U0126 on CYP3A4 activity in HepG2 cells (Fig. 7b).

These data altogether indicate that U0126 induces CYP3A4 and its catalytic activity in HepG2 cells at the transcriptional level.

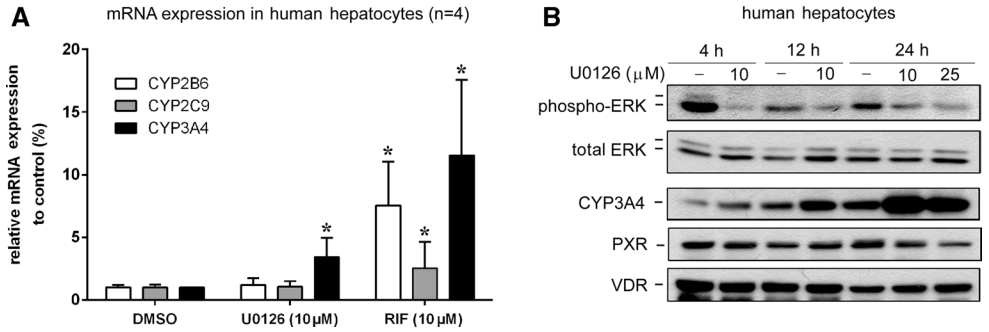

Fig. 6 U0126 induces CYP3A4 expression in primary human hepatocytes. Four primary human hepatocyte cultures ($n = 4$) were treated with either U0126 (10 µM), rifampicin (RIF, 10 µM) or vehicle (DMSO; 0.1 %, v/v) for 24 h. **a** Total RNA was isolated after treatment, and the CYP3A4, CYP2C9 and CYP2B6 mRNA levels were assessed via qRT-PCR. The values were normalized to HPRT mRNA as a reference gene. The data are presented as the mean ± SD from four independent hepatocyte preparations ($n = 4$) and are expressed as the fold change in induction relative to vehicle-treated cells (normalized to 1). $*p < 0.05$ indicates statistically significant difference compared to vehicle-treated cells. **b** Western blot assays using primary human hepatocytes (LH42). Protein levels of CYP3A4, PXR and VDR, as well as phosphorylated and total ERK (a loading control), were examined using specific antibodies after treatment with U0126 (10 or 25 µM) for 4, 12 or 24 h. The experiment has been repeated in three hepatocyte preparations with the same results. A representative Western blotting figure is shown

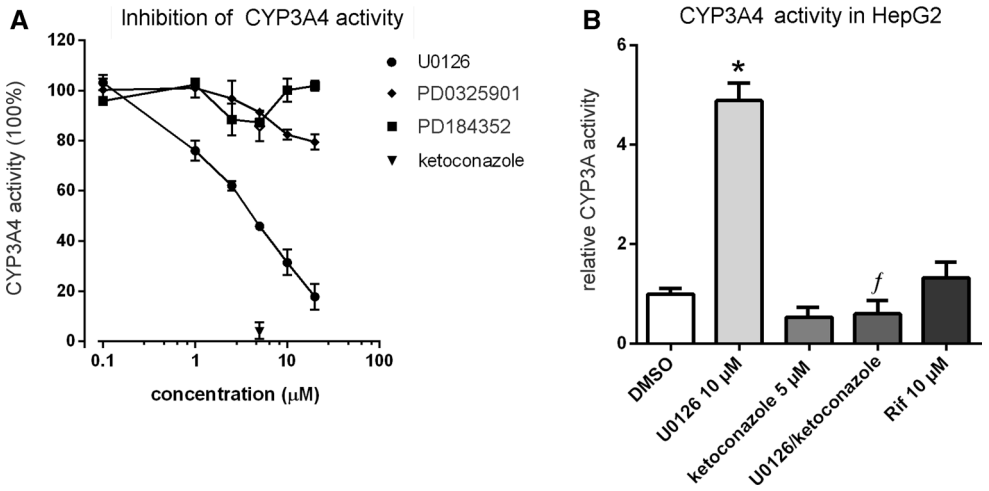

Fig. 7 U0126 up-regulates CYP3A4 enzymatic activity in HepG2 cells. **a** Human recombinant CYP3A4 protein expressed from cDNA using a baculovirus-infected insect cells with human CYP450 reductase and cytochrome b_5 (P450-Glo™ CYP3A4 Screening System with Luciferin-PPXE) was used to evaluate interaction of U0126, PD0325901 and PD184352 with CYP3A4 activity. Ketoconazole (5 µM) was used as a prototype CYP3A4 inhibitor. CYP3A4 reactions were performed according to manufacturer's protocol in three independent experiments ($n = 3$) in triplicates. Luminescence was recorded using a plate reader, and values are displayed as relative light units related to control vehicle-treated samples. Data are presented as the mean ± SD of CYP3A4 inhibition related to vehicle-treated membranes (100 %). **b** The effect of U0126 on in vivo CYP3A4 enzymatic activity in HepG2 cells has been evaluated using Non-lytic P450-Glo™ CYP3A4 Assay with Luciferin-IPA. HepG2 cells have been treated with U0126 (10 µM), ketoconazole (5 µM) or rifampin (10 µM) for 48 h, washed with PBS and analyzed for CYP3A4 enzymatic activity with Luciferin-IPA. Luminescence was recorded using a plate reader, and values are displayed as relative CYP3A4 catalytic activity of control vehicle-treated samples (set to be 1). All experiments were carried out at least three times in triplicate, and data are presented as the meam ± SD from three independent experiments ($n = 3$)

Discussion

In the present study, we provide evidence demonstrating a dramatic effect of the MEK1/2 inhibitor U0126 on the expression of major isoforms of the CYP3A subfamily in HepG2 cells. We demonstrate that this effect is at least partially mediated by direct binding of U0126 to the PXR LBD, which subsequently results in SRC1 coactivator recruitment and binding of PXR to NR response elements within the CYP3A4 promoter. In addition, we reveal that inhibition of MEK activity, a component of the Ras/Raf/MEK/ERK signaling cascade using either a MEK1/2 small molecule inhibitor or expression of a dominant-negative MEK1 plasmid down-regulates SHP repressor mRNA

expression in HepG2 cells. This repressor inhibits the activity of PXR and other NRs involved in the transactivation of CYP3A genes (Ourlin et al. 2003). We also demonstrate that partial inhibition of MEK1 activity using the dominant-negative MEK1 construct does not itself result in significant up-regulation of the CYP3A4 gene expression in HepG2 cells.

Therefore, we propose that U0126 up-regulates the CYP3A4, CYP3A5 and CYP3A7 genes in HepG2 cells via a dual mechanism that primarily involves PXR activation and ERK signaling cascade inhibition-mediated down-regulation of the SHP repressor. This hypothesis is supported by the result that the U0126-mediated induction of CYP3A genes is sensitive to the transcriptional inhibitor actinomycin D (Fig. 2a), as well as to the PXR inhibitor sulforaphane (Fig. 2c). Because U0126 has no effect on a reporter construct containing the 3′UTR segment of the CYP3A4 gene inserted downstream of firefly luciferase, it is unlikely that U0126 affects the posttranscriptional stabilization of CYP3A4 mRNA (Fig. 2d).

Other interesting findings of our study include the results that U0126 and other examined MEK1/2 inhibitors substantially induce CYP3A mRNA expression in HepG2 cells, while the prototypical PXR ligand rifampicin has a negligible effect on the induction of CYP3A mRNA. The transient expression of the T422D PXR mutant in HepG2 cells stimulates the activation of the CYP3A4 reporter construct only after treatment with rifampicin, but not after treatment with U0126 (Fig. 3c). Notably, we detected the opposite effect of U0126 treatment on CYP2B6 mRNA expression and transactivation in HepG2 cells compared to CYP3A genes, although all of these genes are targets of PXR (Figs. 1b, 2e) (Goodwin et al. 2001). We suppose that coactivators squelching may contribute to the opposite effects of U0126 treatment on CYP3A4 and CYP2B6 mRNA expression in HepG2 cell line since robust PXR-mediated transactivation of CYP3A genes may deplete coactivators for CYP2B6 expression.

Thus, these data illustrate the unique activity of U0126 compared to the prototypical PXR ligand rifampicin and document the complex and gene-specific effects of U0126 on PXR-mediated target gene transactivation, which also likely involves MEK1/2 signaling inhibition. Because there is a substantial effect of U0126 on the mRNA expression of CYP3A genes, but only a moderate effect of U0126 on CYP3A4 reporter gene constructs activation, we cannot exclude an epigenetic mechanism by which MEK inhibition mediates the induction of CYP3A genes in HepG2 cells. In addition, we used gene reporter construct which may not include all transcription factor response elements involved in U0126-mediated induction of CYP3A4 mRNA in HepG2; therefore, cooperation of some transcriptional factors could be omitted in our gene reporter assay. We did not detect any interaction between U0126 and either CAR or VDR, which also transactivate CYP3A4 genes (Martinez-Jimenez et al. 2007) (*data not shown*). However, further experiments are required to confirm this speculation.

The growing body of evidence suggests that PXR is a target for site-specific phosphorylation by various kinases, which has predominantly been reported to lead to the down-regulation of its activity (Smutny et al. 2013). Recently, Lichti-Kaiser et al. predicted the phosphorylation sites of PXR via MAPK based on in silico analysis (Lichti-Kaiser et al. 2009a). Therefore, we can hypothesize that ERK signaling could decrease the PXR-mediated expression of its primary target genes. Consistent with this hypothesis, we demonstrate that dominant-negative MEK1 significantly enhanced PXR-mediated CYP3A4 transactivation via a gene reporter assay, although this effect was not detected with respect to CYP3A4 mRNA expression (Fig. 5b, c). However, we were not able to inhibit ERK cascade signaling using dominant-negative MEK1 (or using siRNA targeting MEK1/2 or ERK1/2—*data not shown*) to the same degree as using the small molecule MEK inhibitor U0126 (as indicated by the Elk1 activation assay—Fig. 5a). This might be partly due to lower transfection efficiency, although we carefully optimized our experimental conditions. Therefore, we propose that only substantial inhibition of the kinase activity of MEKs results in significant induction of CYP3A genes in HepG2 cells. This hypothesis should be addressed in our following experiments using more effective MEK/ERK silencing methods.

These data also encourage further efforts to link the potential phosphorylation sites of PXR (or its heterodimer or coactivators) to the ERK and other mitogen-activated signaling pathways. We should also investigate the cross talk between ERK signaling and the cyclin-dependent kinases (CDKs) that control the cell cycle, as MAPK signaling regulates the cell cycle in many cell types (Wilkinson and Millar 2000). Recently, CDK2 has been found to directly phosphorylate PXR and negatively regulate CYP3A4 expression (Lin et al. 2008). Similarly, CDK5, another cyclin-dependent kinase, has been shown to attenuate both the basal and the rifampicin-induced activity of the wt PXR, although CDK5 is not involved in cell cycle regulation (Dong et al. 2010). We and others have found that treatment of HepG2 cells with U0126 decreases the number of cells in the S phase (Wiesenauer et al. 2004), when the activity of CDK2 peaks (Lin et al. 2008), which likely indirectly stimulates PXR activity in HepG2 cells. In our experiments, U0126 (10 μM) reduced the number of cells in S phase from 21 to 12 % after 24 h. Therefore, we cannot exclude the possibility that the MEK inhibitors stimulate PXR activity via a CDK or other kinases involved in cell cycle regulation, although U0126 has been reported not to inhibit CDKs (Favata et al. 1998).

Small heterodimer partner (SHP) is well established as an orphan NR that binds to and inhibits the activity of other NRs, including PXR (Ourlin et al. 2003). Interestingly, we found that all of the MEK1/2 inhibitors evaluated significantly attenuate SHP mRNA expression and SHP promoter transactivation in HepG2 cells (Fig. 4b, c). Moreover, we also observed that transfection with the dominant-negative MEK1 vector (400 ng per well) affects SHP mRNA expression in HepG2 cells (Fig. 5d). In opposite, in primary human hepatocytes, we observed no significant effect of U0126 on SHP expression (Fig. 4d). These data indicate that SHP down-regulation via MEK inhibition may participate in the robust PXR-mediated induction of CYP3A genes in HepG2 cells since SHP has been demonstrated as potent repressor of PXR-mediated transactivation (Ourlin et al. 2003; Pavek et al. 2012). Further experiments with siSHP or using immunoprecipitation should confirm the idea. Furthermore, we have also demonstrated moderate up-regulation of the mRNA expression of the NRs, such as PXR, CAR, HNF4α and VDR, involved in the transcriptional regulation of CYP3A genes after U0126 treatment in HepG2 cells (Fig. 4a), although we did not detect significant up-regulation of PXR or VDR protein. These data may imply a more complex mechanism by which MEK1/2 inhibitors regulate CYP3A gene expression and may suggest that MEK1/2 inhibition in HepG2 cells restores hepatocyte phenotype-specific expression of NRs.

Our results might have several pharmacological implications. First, small molecule inhibitors such as U0126 are often used to analyze the interaction between the ERK signaling pathway and NR-mediated CYP expression. Therefore, our data caution against the use of U0126 to examine ERK cascade signaling-mediated CYP gene regulation, as U0126 mediates the activation of PXR via its direct binding, which could lead to misinterpretation of the role of the ERK signaling pathway in CYP gene regulation. This confound has also been shown with respect to the U0126-mediated AHR transactivation of CYP1A expression (Andrieux et al. 2004; Bachleda and Dvorak 2008).

Second, the primary disadvantage of the use of hepatocyte tumor-derived cell lines for metabolic studies is the general lack of metabolic activity compared to freshly isolated human hepatocytes (Fasinu et al. 2012). HepG2 cells lack CYP3A4 enzymatic activity compared to primary hepatocytes (Rodriguez-Antona et al. 2002). In the present report, we indicate that MEK1/2 inhibitors could significantly up-regulate the expression of CYP3A genes in HepG2 cells. We also found that treatment of HepG2 cells with U0126 significantly induced CYP3A4 enzymatic activity in HepG2 cells (Fig. 7b). However, additional analysis is required to propose this approach as a surrogate of primary human hepatocytes for drug metabolism studies.

In conclusion, we found a dramatic effect of the MEK1/2 inhibitor U0126 on the expression of major isoforms of the CYP3A subfamily in HepG2 cells. We demonstrate that this effect is at least partially mediated by direct binding of U0126 to the PXR LBD. The results also indicate cross talk between PXR and the ERK signaling cascade, thus transactivating CYP3A genes. In addition, we also reveal that MEK inhibition in HepG2 cells significantly down-regulates the repressor SHP in HepG2 cells, which may contribute to indirect PXR activation and specific CYP3A gene induction. Partial inhibition of the ERK signaling cascade has no effect on CYP3A gene expression in HepG2 cells. Further studies of this phenomenon should provide important insights regarding the regulation of PXR activity in both hepatocarcinoma cells and normal human hepatocytes via the Ras/Raf//MEK/ERK signaling cascade. Finally, these studies elucidate the link between the activity of PXR to regulate CYP genes and the role of ERK signaling during liver regeneration or tumorigenesis.

Acknowledgments This research has been supported by the Czech Scientific Agency GACR303/12/0472 (to P.P.) and by SVV 170/50/33904-3 Project.

Conflict of interest None.

References

Andrieux L, Langouet S, Fautrel A et al (2004) Aryl hydrocarbon receptor activation and cytochrome P450 1A induction by the mitogen-activated protein kinase inhibitor U0126 in hepatocytes. Mol Pharmacol 65(4):934–943. doi:10.1124/mol.65.4.934

Bachleda P, Dvorak Z (2008) Pharmacological inhibitors of JNK and ERK kinases SP600125 and U0126 are not appropriate tools for studies of drug metabolism because they activate aryl hydrocarbon receptor. Gen Physiol Biophys 27(2):143–145

Bertilsson G, Heidrich J, Svensson K et al (1998) Identification of a human nuclear receptor defines a new signaling pathway for CYP3A induction. Proc Natl Acad Sci USA 95(21):12208–12213

Blumberg B, Sabbagh W Jr, Juguilon H et al (1998) SXR, a novel steroid and xenobiotic-sensing nuclear receptor. Genes Dev 12(20):3195–3205

Braeuning A (2009) Regulation of cytochrome P450 expression by Ras- and β-catenin-dependent signaling. Curr Drug Metab 10(2):138–158

Castell JV, Jover R, Martinez-Jimenez CP, Gomez-Lechon MJ (2006) Hepatocyte cell lines: their use, scope and limitations in drug metabolism studies. Expert Opin Drug Metab Toxicol 2(2):183–212

De Luca A, Maiello MR, D'Alessio A, Pergameno M, Normanno N (2012) The RAS/RAF/MEK/ERK and the PI3K/AKT signalling pathways: role in cancer pathogenesis and implications for therapeutic approaches. Expert Opin Ther Targets 16(Suppl 2):S17–S27. doi:10.1517/14728222.2011.639361

Ding X, Staudinger JL (2005a) Induction of drug metabolism by forskolin: the role of the pregnane X receptor and the protein kinase a signal transduction pathway. J Pharmacol Exp Ther 312(2):849–856

Ding X, Staudinger JL (2005b) Repression of PXR-mediated induction of hepatic CYP3A gene expression by protein kinase C. Biochem Pharmacol 69(5):867–873

Donato MT, Lahoz A, Castell JV, Gomez-Lechon MJ (2008) Cell lines: a tool for in vitro drug metabolism studies. Curr Drug Metab 9(1):1–11

Dong H, Lin W, Wu J, Chen T (2010) Flavonoids activate pregnane X receptor-mediated CYP3A4 gene expression by inhibiting cyclin-dependent kinases in HepG2 liver carcinoma cells. BMC Biochem 11:23. doi:10.1186/1471-2091-11-23

Doricakova A, Novotna A, Vrzal R, Pavek P, Dvorak Z (2013) The role of residues T248, Y249 and T422 in the function of human pregnane X receptor. Arch Toxicol 87(2):291–301. doi:10.1007/s00204-012-0937-9

Fasinu P, Bouic PJ, Rosenkranz B (2012) Liver-based in vitro technologies for drug biotransformation studies—a review. Curr Drug Metab 13(2):215–224

Favata MF, Horiuchi KY, Manos EJ et al (1998) Identification of a novel inhibitor of mitogen-activated protein kinase kinase. J Biol Chem 273(29):18623–18632

Goodwin B, Hodgson E, Liddle C (1999) The orphan human pregnane X receptor mediates the transcriptional activation of CYP3A4 by rifampicin through a distal enhancer module. Mol Pharmacol 56(6):1329–1339

Goodwin B, Jones SA, Price RR et al (2000) A regulatory cascade of the nuclear receptors FXR, SHP-1, and LRH-1 represses bile acid biosynthesis. Mol Cell 6(3):517–526

Goodwin B, Moore LB, Stoltz CM, McKee DD, Kliewer SA (2001) Regulation of the human CYP2B6 gene by the nuclear pregnane X receptor. Mol Pharmacol 60(3):427–431

Haas S, Merkelbach-Bruse S, Justenhoven C, Brauch H, Fischer HP (2009) Expression of xenobiotic and steroid hormone metabolizing enzymes in hepatocellular tumors of the non-cirrhotic liver. Pathol Res Pract 205(10):716–725. doi:10.1016/j.prp.2009.06.003

Harmsen S, Koster AS, Beijnen JH, Schellens JH, Meijerman I (2008) Comparison of two immortalized human cell lines to study nuclear receptor-mediated CYP3A4 induction. Drug Metab Dispos 36(6):1166–1171. doi:10.1124/dmd.107.017335

Healan-Greenberg C, Waring JF, Kempf DJ, Blomme EA, Tirona RG, Kim RB (2008) A human immunodeficiency virus protease inhibitor is a novel functional inhibitor of human pregnane X receptor. Drug Metab Dispos 36(3):500–507. doi:10.1124/dmd.107.019547

Lee HC, Tian B, Sedivy JM, Wands JR, Kim M (2006) Loss of Raf kinase inhibitor protein promotes cell proliferation and migration of human hepatoma cells. Gastroenterology 131(4):1208–1217. doi:10.1053/j.gastro.2006.07.012

Lehmann JM, McKee DD, Watson MA, Willson TM, Moore JT, Kliewer SA (1998) The human orphan nuclear receptor PXR is activated by compounds that regulate CYP3A4 gene expression and cause drug interactions. J Clin Invest 102(5):1016–1023

Li T, Chiang JY (2006) Rifampicin induction of CYP3A4 requires pregnane X receptor cross talk with hepatocyte nuclear factor 4alpha and coactivators, and suppression of small heterodimer partner gene expression. Drug Metab Dispos 34(5):756–764

Lichti-Kaiser K, Brobst D, Xu C, Staudinger JL (2009a) A systematic analysis of predicted phosphorylation sites within the human pregnane X receptor protein. J Pharmacol Exp Ther 331(1):65–76

Lichti-Kaiser K, Xu C, Staudinger JL (2009b) Cyclic AMP-dependent protein kinase signaling modulates pregnane x receptor activity in a species-specific manner. J Biol Chem 284(11):6639–6649

Lin W, Wu J, Dong H, Bouck D, Zeng FY, Chen T (2008) Cyclin-dependent kinase 2 negatively regulates human pregnane X receptor-mediated CYP3A4 gene expression in HepG2 liver carcinoma cells. J Biol Chem 283(45):30650–30657. doi:10.1074/jbc.M806132200

Martinez-Jimenez CP, Jover R, Donato MT, Castell JV, Gomez-Lechon MJ (2007) Transcriptional regulation and expression of CYP3A4 in hepatocytes. Curr Drug Metab 8(2):185–194

Meloche S, Pouyssegur J (2007) The ERK1/2 mitogen-activated protein kinase pathway as a master regulator of the G1- to S-phase transition. Oncogene 26(22):3227–3239. doi:10.1038/sj.onc.1210414

Min L, He B, Hui L (2010) Mitogen-activated protein kinases in hepatocellular carcinoma development. Semin Cancer Biol. doi:10.1016/j.semcancer.2010.10.011

Min L, He B, Hui L (2011) Mitogen-activated protein kinases in hepatocellular carcinoma development. Semin Cancer Biol 21(1):10–20. doi:10.1016/j.semcancer.2010.10.011

Novotna A, Doricakova A, Vrzal R, Pavek P, Dvorak Z (2011) Construction and characterization of hepatocyte nuclear factor HNF4alpha1 over-expressing cell line derived from human hepatoma HepG2 cells. Eur J Pharmacol 669(1–3):45–50. doi:10.1016/j.ejphar.2011.07.049

Osabe M, Sugatani J, Takemura A et al (2009) Up-regulation of CAR expression through Elk-1 in HepG2 and SW480 cells by serum starvation stress. FEBS Lett 583(5):885–889. doi:10.1016/j.febslet.2009.01.051

Ourlin JC, Lasserre F, Pineau T et al (2003) The small heterodimer partner interacts with the pregnane X receptor and represses its transcriptional activity. Mol Endocrinol 17(9):1693–1703. doi:10.1210/me.2002-0383

Pan YZ, Gao W, Yu AM (2009) MicroRNAs regulate CYP3A4 expression via direct and indirect targeting. Drug Metab Dispos 37(10):2112–2117. doi:10.1124/dmd.109.027680

Pavek P, Pospechova K, Svecova L et al (2010) Intestinal cell-specific vitamin D receptor (VDR)-mediated transcriptional regulation of CYP3A4 gene. Biochem Pharmacol 79(2):277–287. doi:10.1016/j.bcp.2009.08.017

Pavek P, Stejskalova L, Krausova L, Bitman M, Vrzal R, Dvorak Z (2012) Rifampicin does not significantly affect the expression of small heterodimer partner in primary human hepatocytes. Front Pharmacol 3:1. doi:10.3389/fphar.2012.00001

Plant N (2007) The human cytochrome P450 sub-family: transcriptional regulation, inter-individual variation and interaction networks. Biochim Biophys Acta 1770(3):478–488. doi:10.1016/j.bbagen.2006.09.024

Pondugula SR, Brimer-Cline C, Wu J, Schuetz EG, Tyagi RK, Chen T (2009) A phosphomimetic mutation at threonine-57 abolishes transactivation activity and alters nuclear localization pattern of human pregnane X receptor. Drug Metab Dispos 37(4):719–730

Pospechova K, Rozehnal V, Stejskalova L et al (2009) Expression and activity of vitamin D receptor in the human placenta and in choriocarcinoma BeWo and JEG-3 cell lines. Mol Cell Endocrinol 299(2):178–187. doi:10.1016/j.mce.2008.12.003

Rochette-Egly C (2003) Nuclear receptors: integration of multiple signalling pathways through phosphorylation. Cell Signal 15(4):355–366

Rodriguez-Antona C, Donato MT, Boobis A et al (2002) Cytochrome P450 expression in human hepatocytes and hepatoma cell lines: molecular mechanisms that determine lower expression in cultured cells. Xenobiotica 32(6):505–520. doi:10.1080/00498250210128675

Rulcova A, Prokopova I, Krausova L et al (2010) Stereoselective interactions of warfarin enantiomers with the pregnane X nuclear receptor in gene regulation of major drug-metabolizing cytochrome P450 enzymes. J Thromb Haemost 8(12):2708–2717

Shaul YD, Seger R (2007) The MEK/ERK cascade: from signaling specificity to diverse functions. Biochim Biophys Acta 1773(8):1213–1226. doi:10.1016/j.bbamcr.2006.10.005

Shimada T, Yamazaki H, Mimura M, Inui Y, Guengerich FP (1994) Interindividual variations in human liver cytochrome P-450

enzymes involved in the oxidation of drugs, carcinogens and toxic chemicals: studies with liver microsomes of 30 Japanese and 30 Caucasians. J Pharmacol Exp Ther 270(1):414–423

Smutny T, Mani S, Pavek P (2013) Post-translational and post-transcriptional modifications of pregnane X receptor (PXR) in regulation of the cytochrome P450 superfamily. Curr Drug Metab 14(10):1059–1069

Svecova L, Vrzal R, Burysek L et al (2008) Azole antimycotics differentially affect rifampicin-induced pregnane X receptor-mediated CYP3A4 gene expression. Drug Metab Dispos 36(2):339–348. doi:10.1124/dmd.107.018341

Takeshita A, Taguchi M, Koibuchi N, Ozawa Y (2002) Putative role of the orphan nuclear receptor SXR (steroid and xenobiotic receptor) in the mechanism of CYP3A4 inhibition by xenobiotics. J Biol Chem 277(36):32453–32458

Vrzal R, Stejskalova L, Monostory K et al (2009) Dexamethasone controls aryl hydrocarbon receptor (AhR)-mediated CYP1A1 and CYP1A2 expression and activity in primary cultures of human hepatocytes. Chem Biol Interact 179(2–3):288–296

Wang H, Faucette S, Sueyoshi T et al (2003) A novel distal enhancer module regulated by pregnane X receptor/constitutive androstane receptor is essential for the maximal induction of CYP2B6 gene expression. J Biol Chem 278(16):14146–14152. doi:10.1074/jbc.M212482200

Wang H, Huang H, Li H et al (2007) Activated pregnenolone X-receptor is a target for ketoconazole and its analogs. Clin Cancer Res 13(8):2488–2495

Wiesenauer CA, Yip-Schneider MT, Wang Y, Schmidt CM (2004) Multiple anticancer effects of blocking MEK-ERK signaling in hepatocellular carcinoma. J Am Coll Surg 198(3):410–421. doi:10.1016/j.jamcollsurg.2003.10.004

Wilkinson MG, Millar JB (2000) Control of the eukaryotic cell cycle by MAP kinase signaling pathways. FASEB J 14(14):2147–2157. doi:10.1096/fj.00-0102rev

Zhou C, Poulton EJ, Grun F et al (2007) The dietary isothiocyanate sulforaphane is an antagonist of the human steroid and xenobiotic nuclear receptor. Mol Pharmacol 71(1):220–229

2. A New Class of Direct Constitutive Androstane Receptor (CAR) Agonists

Smutny T, Nova A, Drechslerová M, Carazo A, Hyrsova L, Rania Hrušková Z, Kuneš J, Pour M, Špulák M, Pavek P. 2-(3-Methoxyphenyl)quinazoline Derivatives: A New Class of Direct Constitutive Androstane Receptor (CAR) Agonists. (2016) J Med Chem., 59(10):4601-10
(IF 2015 = **5.589**)

In this paper, we focused on the development of new selective and potent agonists of CAR receptor since only poor or non-selective ligands have been reported so far. This fact is a bottleneck for more in-depth investigation of CAR functions. A random screening of a group of compounds previously prepared as potential antituberculotics resulted in a hit of CAR activator derived from 2-(3-methoxyphenyl)quinazoline and other CAR activators were then synthetized based on the structure of the lead compound. The further analysis, however, revealed that discovered small molecules are activators of other NRs such as PXR, AhR and VDR. Importantly, CAR, PXR, AhR and VDR are major transcription factors controlling hepatic expression of many DMEs.

Although, we were not able to identify selective CAR ligand, our results are still very promising because our small molecules showed a strong potency to activate CAR. Hence, discovered molecules might provide a molecular basis for a future synthesis of selective and strong CAR agonists.

Besides, as confirmed to be “pan-xenosensors” ligands, our discovered compounds can be used as molecules for boosting of DME expression in *in vitro* liver models. The treatment by these compounds could improve metabolic functions in liver cell models with an insufficient metabolic capacity.

Journal of Medicinal Chemistry

Article

pubs.acs.org/jmc

2-(3-Methoxyphenyl)quinazoline Derivatives: A New Class of Direct Constitutive Androstane Receptor (CAR) Agonists

Tomas Smutny,[†] Alice Nova,[†,§] Marcela Drechslerová,[‡] Alejandro Carazo,[†] Lucie Hyrsova,[†] Zuzana Rania Hrušková,[‡] Jiří Kuneš,[‡] Milan Pour,[‡] Marcel Špulák,*[,‡] and Petr Pavek*[,†]

[†]Department of Pharmacology and Toxicology, [‡]Department of Inorganic and Organic Chemistry, Faculty of Pharmacy, Charles University, Heyrovského 1203, Hradec Kralove CZ-500 05, Czech Republic

[§]Institute of Molecular and Translation Medicine, Faculty of Medicine, Palacky University in Olomouc, Hnevotinska 5, CZ-779 00 Olomouc, Czech Republic

Supporting Information

ABSTRACT: Constitutive androstane receptor (CAR) is a key regulator of xenobiotic and endobiotic metabolism. Together with pregnane X (PXR) and aryl hydrocarbon (AHR) receptors, it is referred to as "xenobiotic receptor". The unique properties of human CAR, such as its high constitutive activity, both direct (ligand-binding domain-dependent) and indirect activation have hindered the discovery of direct selective human CAR ligands. Herein, we report a novel class of direct human CAR agonists in a group of 2-(3-methoxyphenyl)quinazoline derivatives. The compounds are even more potent activators of human CAR than is prototype 6-(4-chlorophenyl)imidazo[2,1-*b*][1,3]thiazole-5-carbaldehyde *O*-(3,4-dichlorobenzyl)oxime (CITCO). The three most potent ligands are at the same time extremely potent activators of the other xenobiotic or hormonal receptors, namely PXR, AHR, and vitamin D receptor, which regulate major xenobiotic-metabolizing enzymes and efflux transporters. Thus, the novel CAR ligands can be also considered as constituting the first class of potent pan-xenobiotic receptor ligands that can serve as potential antidotes boosting overall metabolic elimination of xenobiotic or toxic compounds.

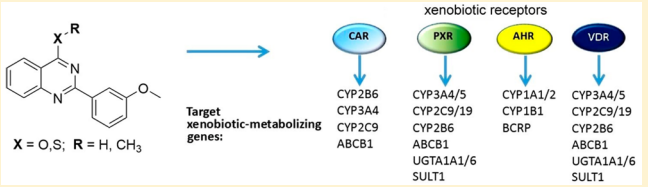

INTRODUCTION

Constitutive androstane receptor (CAR, NR1I3), together with pregnane X receptor (PXR, NR1I2) and aryl hydrocarbon receptor (AHR), are ligand-activated transcription factors that play pivotal roles in xenobiotic clearance. These transcription factors control gene expression across a broad spectrum of target genes that encode key phase I and phase II drug metabolizing enzymes (DMEs) and some drug transporters.[1] They are activated by a variety of exogenous ligands that include drugs, environmental toxicants, industrial chemicals, and herbal compounds. They are therefore sometimes referred to as "xenosensors" or "xenobiotic receptors."[2]

Although CAR was originally identified as a "xenosensor" of environmental, dietary, natural, and synthetic ligands,[3,4] recent findings suggest that CAR also plays important roles in energy metabolism of fatty acids, bile acids, lipids, and glucose, in thyroid hormone metabolism, in cell-cycle regulation, and in cell−cell interaction.[5,6] CAR is composed of three domains: a highly conserved DNA-binding domain, a hinge region, and a divergent ligand binding/dimerization/transcriptional activation domain.[7] In contrast to other nuclear receptors, activation of this receptor is complex. Both ligand-binding domain (LBD)-dependent and independent activation of human CAR have been shown. These release CAR from its cytoplasmic tethering complex and translocate the receptor into the nucleus, where CAR transactivates CAR-inducible genes as a heterodimer with retinoid X receptor α (RXRα) nuclear receptor. Dephosphorylation-induced translocation of CAR to the nucleus is a key step for indirect activation.[8]

Numerous ligands, agonists, antagonists, as well as inverse agonists have been reported for human CAR. There is discrepancy in assigning a CAR-interacting compound because validated methods are not widely used for direct human CAR ligand identification or distinguishing between indirect activators (such as acetaminophen, bilirubin, and phenobarbital) and ligands interacting within its ligand-binding domain.[3,4] Moreover, CAR is constitutively active and it is localized in the nucleus in model tumor cell lines as opposed to its cytoplasmic localization in normal hepatocytes. CAR activation by ligands is determined by their effect on the position of the C-terminal helix12 that binds coactivators of corepressors. In addition, there are significant species differences in the ligand specificity of CAR ligands.[4] Currently, there is *no* specific high-affinity agonist for human CAR that would help decipher the diverse physiological functions of CAR. Known to date is 6-(4-chlorophenyl)imidazo[2,1-*b*]thiazole-5-carbaldehyde-*O*-(3,4-dichlorobenzyl)oxime (CITCO, **1**), which is a potent human, but not mouse, CAR agonist.[9] However, this unstable compound also activates PXR.[9] The potent mouse CAR ligand 1,4-bis[(3,5-dichloropyridine-2-yl)oxy]benzene (TCPOBOP, **2**) does not activate human or rat CAR.[10] Reported activators

Received: December 7, 2015
Published: May 4, 2016

DOI: 10.1021/acs.jmedchem.5b01891
J. Med. Chem. 2016, 59, 4601−4610

of human CAR identified to date include pesticides such as pyrethroids (permethrin, cypermethrin), the carbamate benfuracarb, and organochlorines (e.g., methoxychlor), synthetic compounds such as CITCO, FL81, octicizer, thiazolidin-4-ones, 6-arylpyrrolo[2,1-*d*][1,5]benzothiazepine derivatives, and sulfonamides, and natural flavonoids such as chrysin and drugs (e.g., artemisinin derivatives, nevirapine, nicardipine, efavirenz, carbamazepine).[4,11−17]

In this work, a library of compounds previously prepared as potential antituberculotics was subjected to random screening. The screening revealed that 2-(3-methoxyphenyl)-3,4-dihydroquinazolin-4-one (**3**) displayed promising activation of the CAR receptor comparable to that of CITCO in reporter gene assay. We therefore synthesized other derivatives of 2-(3-methoxyphenyl)quinazoline and analyzed their interaction with the human CAR receptor. Interaction of the compounds with the additional "xenoreceptors" PXR and AHR as well as with other nuclear receptors controlling expression of certain drug metabolism genes, such as vitamin D receptor (VDR) and glucocorticoid receptors (GR),[18] was analyzed simultaneously.

Herein we report that three 2-(3-methoxyphenyl)quinazoline derivatives are robust ligands of CAR as well as of the other "xenobiotic receptors" PXR and AHR and even exceed their prototype ligands in their potencies to activate the receptors in cell-based reporter gene assays.

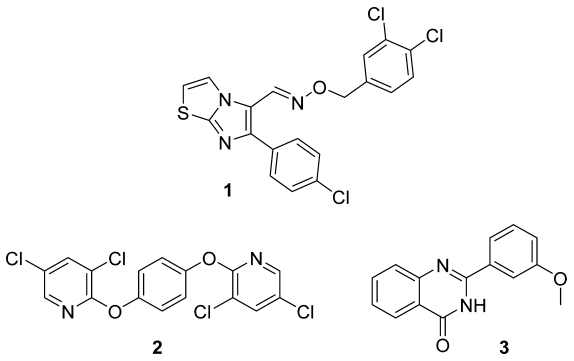

RESULTS

In a random screening of a library previously prepared as potential antituberculotics, we identified a hit compound 2-(3-methoxyphenyl)-3,4-dihydroquinazolin-4-one (**3**) that displayed promising activation of the CAR receptor comparable to that of CITCO. Quinazolinone **3** (Scheme 1) was therefore prepared[19] in order to confirm its activity in relationship to the CAR receptor. Thus, 3-methoxybenzoic acid (**4**) was converted to its chloride **5** which was subsequently treated with 2-aminobenzonitrile to yield amide **6**. Compound **6** was then cyclized to afford the title quinazoline **3** in 55% overall yield. The repeated evaluation of 2-(3-methoxyphenyl)-3,4-dihydroquinazolin-4-one (**3**) in reporter gene assays fully confirmed the ability to activate the CAR receptor.

Scheme 1. Synthesis of 2-(3-Methoxyphenyl)-3,4-dihydroquinazolin-4-one

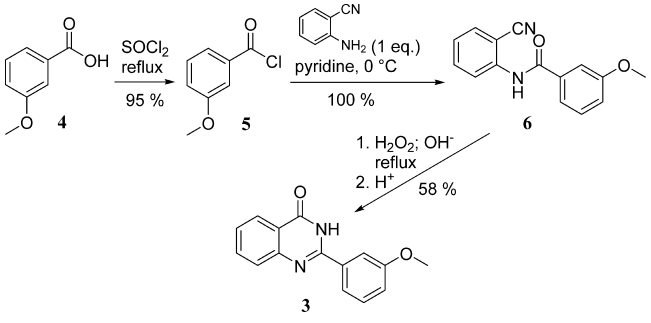

A library of six 2-(3-methoxyphenyl)quinazolines was subsequently prepared via simple alkylation conditions using $RX/NaI/K_2CO_3$ at reflux in acetone (Scheme 2). In contrast to the alkylation of 3,4-dihydroquinazolin-4-one,[20] we observed no *N*3-alkylated products. The reactions afforded only *O*-alkylated species, the structures of which were clearly confirmed by ^{13}C NMR shifts of $-O-CH_n-$ carbon atom (Table 1).[20]

Scheme 2. Alkylation of Quinazoline 3 with Various Primary Halides

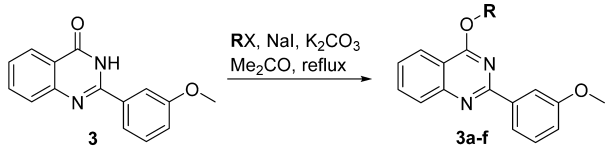

Table 1. Isolated Yields and ^{13}C NMR Chemical Shifts in $CDCl_3$ of C(1′) Group of Compounds 3a−f

compd	yield (%)	δC (ppm)
3a	85	54.0
3b	91	62.7
3c	88	68.3
3d	78	72.8
3e	58	67.3
3f	78	68.2

Quinazoline derivative **7a** bearing methylsulfanyl moiety in position 4 was further synthesized. The starting 2-(3-methoxyphenyl)-3,4-dihydroquinazolin-4-one **3** was first converted into its sulfur analogue **7**, followed by the same alkylation protocol (Scheme 3).

Scheme 3. Preparation of 4-Methylsulfanyl Derivative 7a

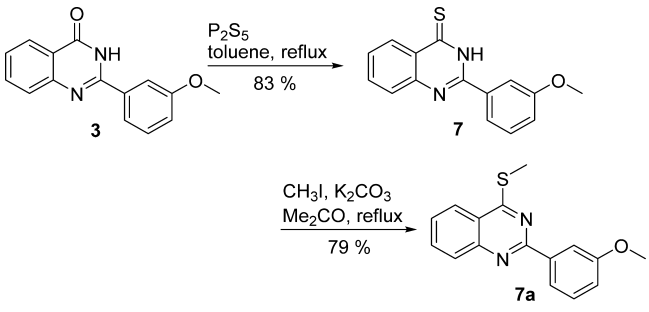

Library Screening and Ligands Identification. We randomly screened a library of compounds previously prepared as potential antituberculotics for activation of the human CAR receptor using a reporter gene assay with $p(ER6)_3$-luc construct transfected together with human CAR expression vector into HepG2 cells. This assay showed itself to be a sensitive test for selecting several potential activators of CAR. 2-(3-Methox-

DOI: 10.1021/acs.jmedchem.5b01891
J. Med. Chem. 2016, 59, 4601−4610

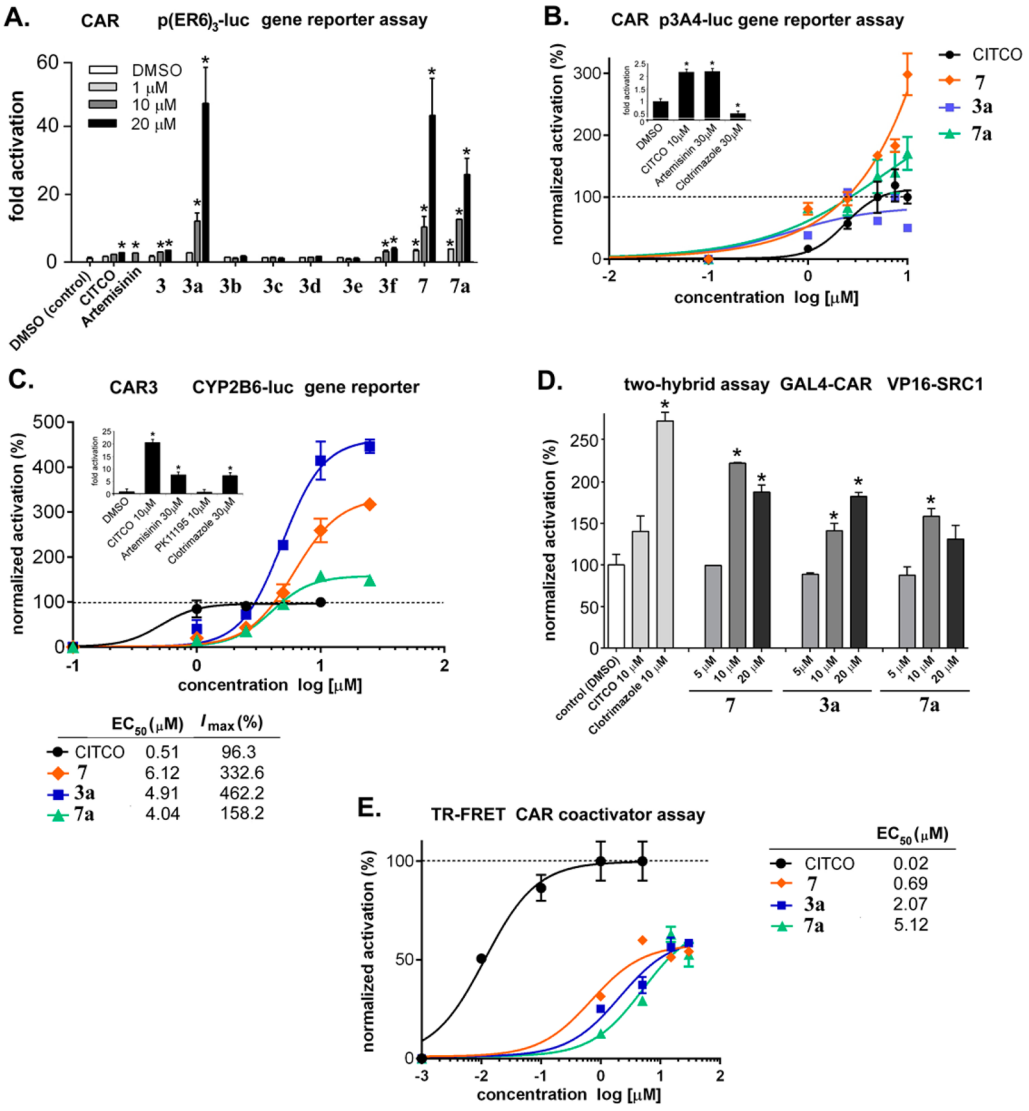

Figure 1. Compounds **7**, **3a**, and **7a** activate human wild-type CAR and its CAR variant **3** in transient transfection reporter gene assays and in TR-FRET CAR coactivation assays.

yphenyl)-3,4-dihydroquinazolin-4-one (**3**) displayed the most promising activation of CAR in the assay and was used as the "lead" compound.

In the next series of experiments, we tested the interactions of the newly synthesized compounds **3a**–**f**, **7**, and **7a** with CAR using the same assay (Figure 1A). Interestingly, we found even more robust activation of the CAR-responsive assay with derivatives **3a**, **7**, and **7a**. The activation was even more potent than that produced by the prototype CAR activator/ligand CITCO in equimolar concentrations (Figure 1A).

Next, the compounds **3**, **3a**, **7**, and **7a** were tested using luciferase gene reporter vectors with promoter responsive sequences of CAR target genes CYP3A4 and CYP2B6. We found that **7**, **3a**, and **7a** compounds significantly activated CYP3A4-luc and CYP2B6-luc reporter constructs in a dose-dependent manner through both wild-type CAR (CAR) characterized by high constitutive activity as well as its variant **3** (CAR3) with low constitutive activity[21] (Figure 1B,C). All tested compounds appeared as lower affinity but high potency activators of human CAR and CAR3 receptors in the assays, as indicated by the EC_{50} and I_{max} parameters (Figure 1C). No effects of compounds **7**, **3a**, and **7a** on HepG2 cell viability have been observed (Figure 1, Supporting Information).

In next set of experiments, we employed mammalian two hybrid assay with GAL4-CAR LBD and VP16-SRC1 fusion constructs. All tested compounds **7**, **3a**, and **7a** significantly stimulated interaction of CAR ligand binding domain with steroid receptor coactivator 1 (SRC1)-VP16 fusion protein (Figure 1D).

Finally, we used the in vitro LanthaScreen time-resolved (TR)-FRET constitutive androstane receptor (CAR) coactivator assay that monitors ligand-dependent, but not indirect phenobarbital activator-dependent, interaction with CAR ligand binding domain (LBD) as we have shown in our previous report.[22] We observed that the tested compounds **7**, **3a**, and **7a** all activated the assay, thus suggesting direct interaction with human CAR LBD (Figure 1E). These activations were, however, weaker than that of CITCO, therefore indicating potential indirect cellular signaling-dependent effects of the quinazoline compounds on CAR activation or a ligand specific interactions of CAR with its coactivators SRC-1 (Figure 1D) and PGC1α (Figure 1E) or corepressors based on position of helix 12 determined by the ligands.[23,24]

DOI: 10.1021/acs.jmedchem.5b01891
J. Med. Chem. 2016, 59, 4601−4610

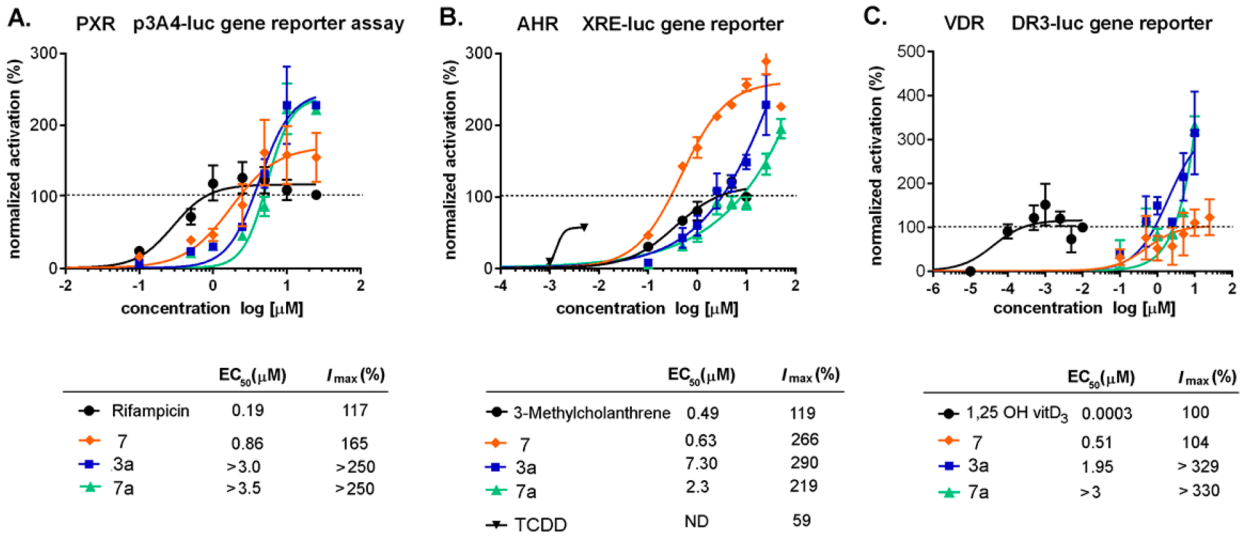

	EC_{50}(μM)	I_{max}(%)
Rifampicin	0.19	117
7	0.86	165
3a	>3.0	>250
7a	>3.5	>250

	EC_{50}(μM)	I_{max}(%)
3-Methylcholanthrene	0.49	119
7	0.63	266
3a	7.30	290
7a	2.3	219
TCDD	ND	59

	EC_{50}(μM)	I_{max}(%)
1,25 OH vitD_3	0.0003	100
7	0.51	104
3a	1.95	> 329
7a	>3	> 330

Figure 2. Compounds 7, **3a**, and **7a** activate PXR, AHR, and VDR receptors in transient transfection reporter gene assays.

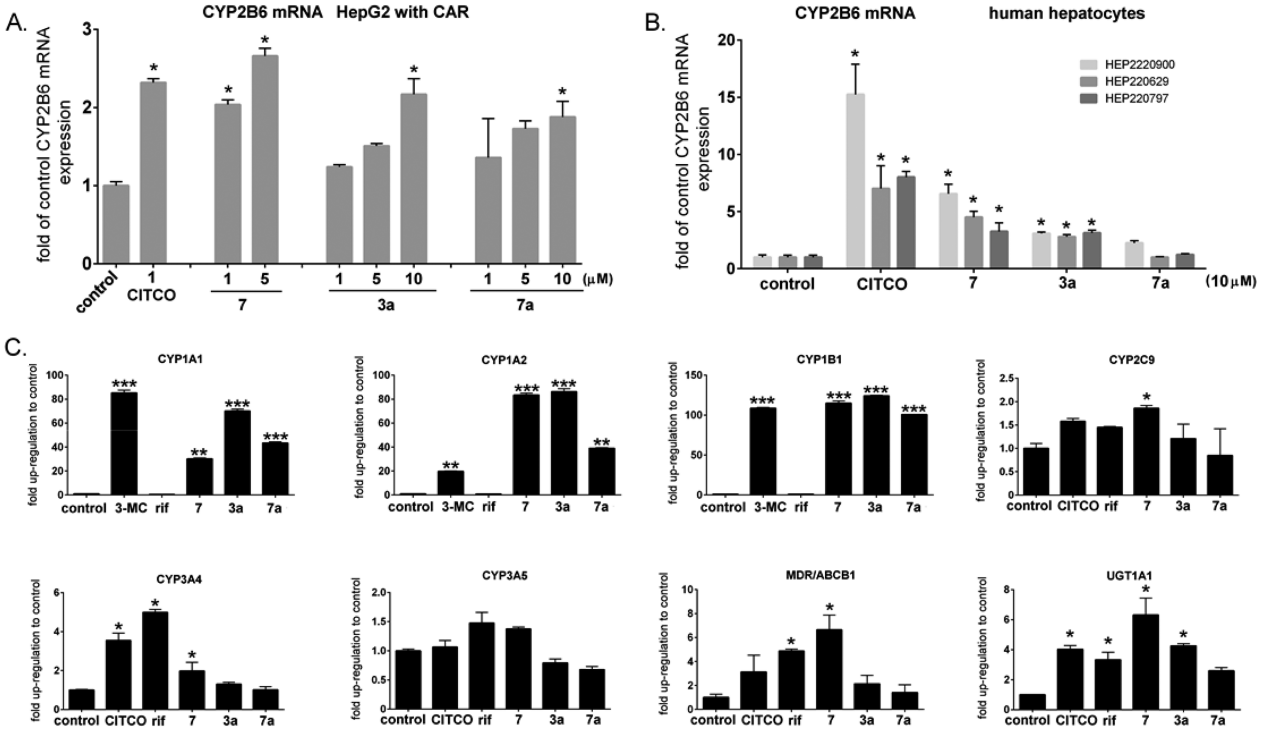

Figure 3. Compounds 7 and **3a** induce target genes expression in CAR-expressing HepG2, HepaRG cells, or in primary human hepatocytes.

Compounds 7, 3a, and 7a Activate PXR, AHR, and VDR Receptors. In the next set of experiments, we analyzed whether 7, **3a**, and **7a** compounds activate other xenobiotic receptors, such as PXR, AHR, and VDR, which control expression of many xenobiotic metabolizing enzymes in the liver and intestine.[25] We found that compounds 7, and, to a lesser extent **3a** and **7a**, significantly activated both PXR and AHR receptors, as indicated by low micromolar EC_{50} and high I_{max} (Figure 2A,B). In addition, compound 7 significantly activated the vitamin D receptor (VDR) in transient transfection reporter gene assay in low micromolar concentrations (EC_{50} = 0.51 μM) (Figure 2C). Glucocorticoid receptor was not significantly activated by the compounds (data not shown).

Compounds 7, 3a, and 7a Induce Prototype CAR Target Gene CYP2B6 mRNA in HepG2 Cells and in Primary Human Hepatocytes. We analyzed whether compounds 7, **3a**, and **7a** induce CYP2B6 mRNA expression in HepG2 cells expressing exogenous human CAR or in three primary human hepatocyte preparations. CYP2B6 is the most responsive target gene of the CAR receptor. We found statistically significant induction of CYP2B6 mRNA expression both in CAR-expressing HepG2 cells and in human hepatocytes after treatment with compounds 7, **3a**, and CITCO (Figure 3A,B). Compound **7a** most likely undergoes fast metabolism in metabolically competent primary human hepatocytes because we did not observe CYP2B6 mRNA induction (Figure 3B).

Compounds 7 and 3a Upregulate other Major Inducible Xenobiotic-Metabolizing Enzymes and P-Glycoprotein Transporter mRNAs. Compounds 7, **3a**, and

DOI: 10.1021/acs.jmedchem.5b01891
J. Med. Chem. 2016, 59, 4601−4610

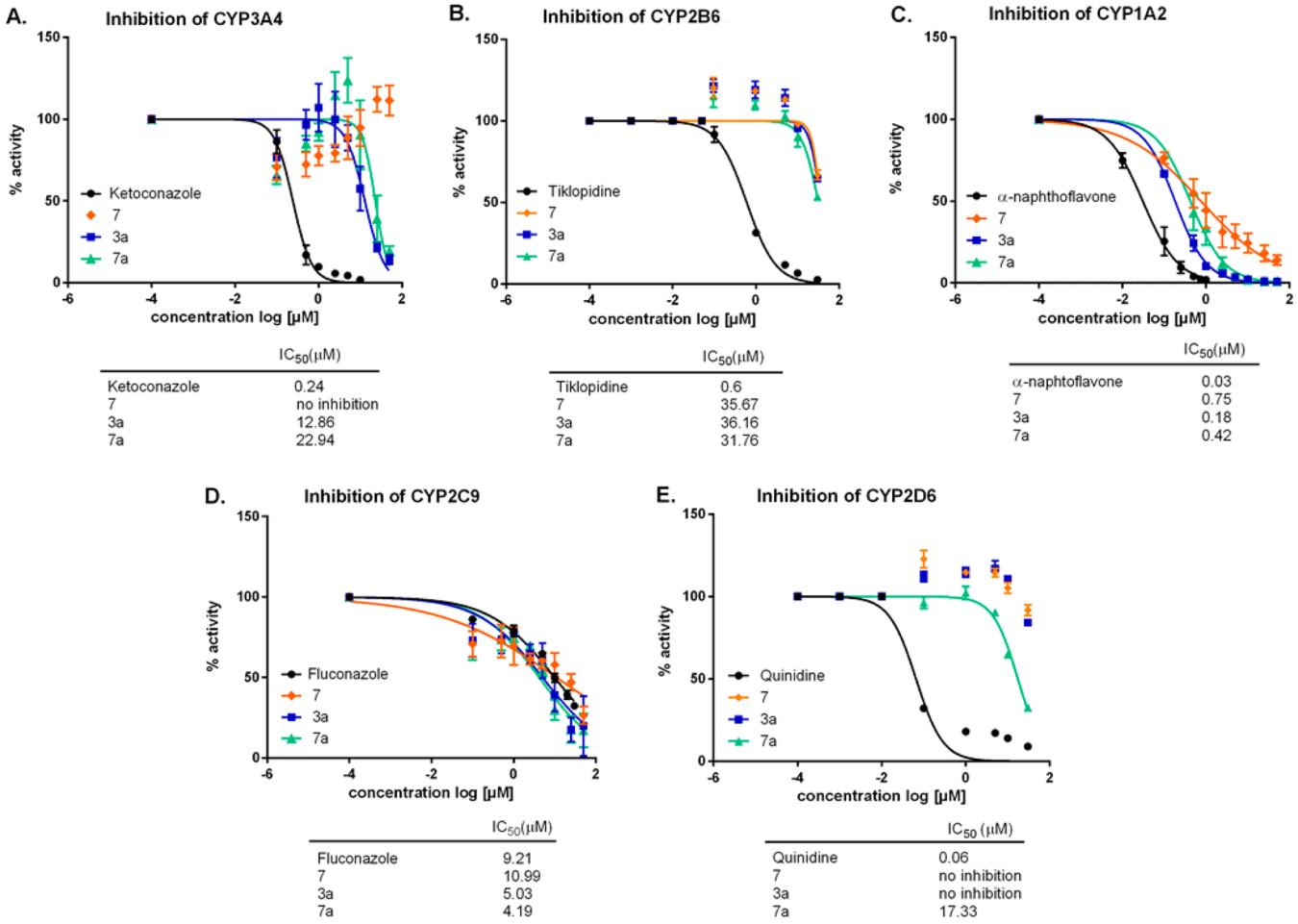

Figure 4. Inhibition of recombinant human CYP3A4, CYP2B6, CYP1A2, CYP2C9, and CYP2D6 enzymes with compounds **7**, **3a**, and **7a**.

7a also significantly induced CYP3A4, CYP3A5, CYP2C9, MDR1/P-glycoprotein genes controlled by CAR, PXR, and VDR as well as AHR target genes CYP1A1, CYP1A2 (also regulated by CAR), CYP1B1, and UGT1A1 (also regulated by PXR) (Figure 3C).

Compounds 7, 3a, and 7a Do Not Significantly Inhibit Major Cytochrome P450 Enzymes CYP3A4 and CYP2C9. Finally, we analyzed if compounds **7**, **3a**, and **7a** interfere enzymatic activities of the most abundant liver CYP enzymes induced by CAR, PXR, VDR, and AHR receptors. We found that tested compound do not significantly affect CYP3A4 and CYP2B6 enzyme activities (Figure 4A,B). On the other hand, compounds **7**, **3a**, and **7a** inhibit enzymatic activity of CYP1A2 enzyme, which activates numerous procarcinogens to active carcinogens in the liver (Figure 4C). In the case of CYP2C9, the IC_{50} were at concentrations leading to CAR, PXR, or VDR nuclear receptors activation (Figure 4D). We observed no significant interaction of tested compounds with CYP2D6 enzyme (Figure 4E).

These data thus indicate that enzymatic activities of the major induced CYP liver enzymes via CAR, PXR, and VDR are not significantly affected with the compounds and that compound **7** least interferes with the enzymes.

DISCUSSION

CAR is one of the key regulators of xenobiotic and endobiotic metabolism. Recently, the therapeutic potential for treatment of such metabolic disorders as obesity, type 2 diabetes mellitus, insulin resistance, dyslipidemia, and atherosclerosis has been indicated in animal models using a ligand of rodent CAR.[26] However, there exists no potent, specific, and nontoxic agonist of *human* CAR receptor that can serve as a chemical tool to address various biological functions of CAR or to consider CAR as a therapeutic target. The unique properties of human CAR, such as its high constitutive activity and the complexity of the related signaling, make discovery of specific ligands difficult. In addition, the lack of robust and validated cell-based assays to study direct interactions of compounds with the CAR ligand-binding pocket (LBP) hinders the discovery of selective human CAR ligands. Therefore, the ligand specificity of human CAR as well as of high-affinity endogenous ligands remains obscure.[11]

Our aim was to discover novel compounds that would interact with the human CAR receptor as a direct agonist with high potency. We randomly screened a library comprising about 400 compounds for the activation of human CAR receptor using a reporter gene assay with pER6-luc construct transfected together with human CAR expression vector into HepG2 cells. This assay provided to be a sensitive test for selecting the lead compound based on 2-(3-methoxyphenyl)-3,4-dihydroquinazolin-4-one (**3**) structure (Figure 1A). The synthesized compounds **7**, **3a**, and **7a** displayed even more potent activation of CAR in transient transfection reporter gene assays (Figure 1A,B), in two hybrid CAR LBD/SRC-1 interaction assay (Figure 1D), and in induction experiments in HepG2 cells transfected with exogenous CAR (Figure 3A).

DOI: 10.1021/acs.jmedchem.5b01891
J. Med. Chem. 2016, 59, 4601−4610

At the same time, we observed activation of variant **3** of the human CAR gene with compounds **7**, **3a**, and **7a** (Figure 1C), which was found to be a ligand-activated low-constitutive activity receptor variant. CAR3 differs from CAR1 by a 5 amino acid insertion outside of the ligand binding pocket.[21,27] Interestingly, in TR-FRET-based coactivator LBD competitive assay, CITCO activated the system more significantly at equimolar concentrations than did compounds **7**, **3a**, and **7a** (Figure 1E). This phenomenon might reflect additional cellular or epigenetic effects of compounds **7**, **3a**, and **7a** that stimulate CAR transactivation[23] or indicate ligand dependent coactivation with PGC1α.

Unlike other NRs that have evolved as receptors for specific high-affinity endogenous ligands, CAR and PXR are highly promiscuous. Only two human CAR crystal structures with agonist bound have been reported to date.[28] The CAR LBD sequence creates a ligand-binding pocket with volume ranging from 525 to 675 Å.[5,28] The LBD cavity has flexible and hydrophobic character, which correlates with the structural promiscuity of CAR ligands.[4,7] The apo-PXR binding cavity volume is even double (approximately1150 Å^3) and can extend in the presence of ligands to 1290−1540 Å^3. Cavity of VDR is larger but narrower than that of CAR (870 Å^3) (Figure 2, Supporting Information). A single residue (T350M) difference in the C-terminal region of the mouse versus human CAR might account for the extensive species selectivity for some agonists.[7] The coactivator recruitment appears to play a central role in fixing ligands in the correct arrangement in large CAR and PXR cavities. In addition, it was clearly shown that ligands determine helix12 position, which is critical for coactivator or corepressor binding and subsequent CAR activation.[24]

The ligand pockets of CAR, PXR, as well as VDR are lined by mostly hydrophobic residues. The 27 residues of the murine CAR pocket create a highly hydrophobic environment, with only a quarter of them being polar. Similarly, the cavity of PXR is lined by 28 amino acids, of which eight have polar or charged side chains.[5,29] Therefore, van der Waals forces play crucial roles in the interactions of the ligand with CAR and hydrogen bonding is rare. For example, CITCO form no hydrogen bonds and makes weak electrostatic interactions with His203, Asn165, and Tyr326. Another CAR agonist 5β-pregnanedione forms a single hydrogen bond with His-203[5,30] but display hydrophobic interactions with Phe161, Ile164, Leu206, Phe217, Tyr224, Phe234, and Leu242 in human CAR cavity.[28] In our docking study, we found that compounds **7** and **3a** form hydrophobic bonding with three amino acids, Phe161, Phe234, and Leu242, that also interact with CITCO and 5β-pregnanedione (Figure 2, Supporting Information).

CAR appears to cross-talk with other two members of subfamily NR1I PXR (NR1I2) and VDR (NR1I1) because these receptors recognize similar response elements, coactivators, and corepressors and share a number of similar target genes involved in xenobiotic detoxification.[31] CAR, PXR, and VDR mainly control inducible expression of such major xenobiotic-metabolizing enzymes of cytochrome P450 as CYP3A4, CYP2C9, CYP2B6, or P-glycoprotein efflux transporter in the hepatocytes or in enterocytes.[32]

Aryl hydrocarbon receptor (AHR) is another key ligand-activated "xenosensor", although it belongs to the basic helix−loop−helix/Per-Sim-ARNT (bHLH/PAS) family of transcription factors. It controls another set of genes involved in the metabolism and transport of xenobiotics including CYP1A1, CYP1A2, CYP1B1, GST1, UGT1A1, UGT1A6, NQO1, ALDH3A1, and BCRP transporter.[33,34] The AHR ligands comprise a wide variety of known toxic and highly hydrophobic environmental contaminants such as halogenated aromatic hydrocarbons including 2,3,7,8-tetrachlorodibenzo-*p*-dioxin (TCDD), polychlorinated biphenyls (PCBs), and the polycyclic aromatic hydrocarbons (PAHs) benzopyrene and 3-methylcholanthrene (MC).[35] Many AHR agonists represent planar aromatic chemicals; however, the SAR analysis showed that absolute planarity is not necessary for ligand binding of polychlorinated biphenyls. It was estimated that an AhR ligand are hydrophobic, electronegative compounds with hydrogenbonding properties between 12−14 Å in length, less than 12 Å in width, and no more than 5 Å deep.[35]

Because of enormous substrate ligand variability of xenosensors PXR, CAR, and AHR, the receptors are sometimes supposed not to strictly discriminate between molecules on the basis of size or chemical structure. The only one 3D QSAR model has been published for human CAR.[24] Considering our tested compounds structural features, we can see that methylation of oxygen or sulfur in position 4 of the quinazoline ring significantly increases activation of CAR (Figure 1A). On the contrary, alkylation of quinazoline **3** employing longer-chain alkyl halides (**b**−**f**) abolish activity toward CAR activation. This correlates with our docking experiment showing reasonable positioning of compounds **7** and **3a** in CAR LBD (Figure 2, Supporting Information).

CONCLUSION

In summary, we have shown that compounds **7**, **3a**, and **7a** are potent ligands of human CAR receptor. We also observed in the study that compounds **7**, **3a**, and **7a** are at the same time highly potent ligands of the xenobiotic receptors PXR and AHR. We can therefore suppose that the compounds boost overall xenobiotic metabolism via induction of their target genes. To our knowledge, this is the first group of such xenobiotic metabolism "boosters" and pan-xenobiotic receptor agonists with potential application as antidotes to toxic compounds dominantly cleared from the body through metabolism. We assume that such antidotes could be seriously considered for treatment of intoxication by some natural compounds (such as mycotoxins) or synthetic toxic compounds, or, in cases of drug-induced liver injury (DILI),[36] under the assumption that the toxicants are mainly eliminated by biotransformation and are not significantly bioactivated to reactive intermediates by the xenobiotic detoxification system. Second, the new class of metabolism activators might be considered in some cases for controlled and stimulated activation of prodrugs.

Additional experiments should further characterize the toxicological properties of the compounds and consider their applications as antidotes in several intoxications or as prodrug activators. In addition, the compound could help us to more precisely characterize the limits of xenobiotic metabolism in different tissues or in the organism as a whole. We are currently synthesizing further set of quinazoline derivatives with a view to identify either more potent human CAR ligands or more selective human CAR agonists.

EXPERIMENTAL SECTION

Biology. *Activation of Human CAR in Transient Transfection Reporter Gene Assays (Figure 1).* HepG2 (A,B) or COS-1 (C) cells were transiently transfected with either p(ER6)$_3$-luc (A), CYP3A4-luc (B), or CYP2B6-luc (C) luciferase gene reporter constructs together

DOI: 10.1021/acs.jmedchem.5b01891
J. Med. Chem. 2016, 59, 4601−4610

with wild-type CAR expression vector (A,B) or its low-constitutive activity variant CAR3 (C) and pRL-TK control plasmid for transfection normalization. After 24 h of stabilization, the cells were treated with the tested compounds **7**, **3a**, and **7a**, CITCO, and artemisinin (CAR agonists), clotrimazole (an inverse agonist) in indicated concentrations or with vehicle (DMSO; 0.1%, v/v) for an additional 48 h (A) or 24 h (B,C). HepG2 cells transfected with CYP3A4-luc and wild-type CAR have been in parallel treated with androstenol (5 μM) to suppress high basal activity (Figure 1B). In experiments with CAR3, RXRα has been cotransfected into COS-1 cells (100 ng/well). After treatment, the cells were lysed and assayed for both firefly and *Renilla* luciferase activities. The data are presented as the means ± SD from triplicate measurements of a representative experiment (A) or as means of three independent experiments (n = 3). The results are expressed as the fold-change in inducing firefly luciferase activities relative to vehicle-treated cells (normalized to 1) *p < 0.05, statistically significant. (D) Compounds **7**, **3a**, and **7a** activate interaction of CAR ligand binding domain with SRC-1 coactivator in a two-hybrid assay. HepG2 cells have been transfected with GAL4-CAR LBD construct together with the VP16-SRC1 construct and the pGL5-luc reporter vector. After 24 h of stabilization, cells were treated with tested compounds, CITCO, and clotrimazole (known ligands of CAR, 10 μM) or vehicle (0.1%, control) for 24 h. Cells were lysed and analyzed for firefly and *Renilla* luciferase activities. The results are expressed as the fold-change in inducing firefly luciferase activities relative to vehicle-treated cells (normalized to 1). (E) Effect of compounds **7**, **3a**, and **7a** on CAR activation in the TR-FRET LanthaScreen CAR coactivator assay. Compounds were tested in a serial dilution together with the prototype CAR agonist CITCO. Data are presented as the relative activation to background activity (no CAR LBD in the reaction mixture, set to 0%) and to the effect of CITCO (1 μM) set as 100% activation. The dotted line represents the constitutive activity of CAR LBD (vehicle-treated samples). Data are presented as the means and SD from three independent experiments (n = 3). EC_{50} indicates the xenobiotic concentration required to achieve half-maximum activation and relative I_{max} represents the overall maximal calculated activation produced by the tested compound (i.e., maximal efficacy).

Activation of PXR, AHR, and VDR Receptors in Transient Transfection Reporter Gene Assays (Figure 2). HepG2 (A,B) or Huh-7 (C) cells were transiently transfected with either p3A4-luc (A), pXRE-luc (B), or pDR_3-luc (C) luciferase gene reporter constructs together with appropriate expression vectors pSG5-PXR (A) or pSG5-VDR (C) and pRL-TK control plasmid for transfection normalization. After 24 h of stabilization, the cells were treated with the tested compounds **7**, **3a**, and **7a**, 3-methylcholantrene (an AHR ligand), rifampicin (a PXR ligand), and 1α,25-dihydroxyvitamin D_3 (1,25OHvit D3, a VDR ligand) at the concentration range indicated for an additional 24 h. After treatment, the cells were lysed and assayed for both firefly and *Renilla* luciferase activities. The results are expressed as the relative change in induction of firefly luciferase activities versus vehicle-treated cells (normalized to 1) when activation with maximal tested concentration of 3-methylcholantrene (10 μM), rifampicin (25 μM), and 1,25OHvitD3 (100 nM) was set to 100%. The data are presented as the relative means ± SD from triplicate measurements of three independent experiments (n = 3). EC_{50} (xenobiotic concentration required to achieve half-maximum promoter activation) and relative I_{max} (representing the overall maximal calculated induction produced by the tested compound, i.e., maximal efficacy) values were determined using GraphPad Prism Software.

Induction of Target Genes mRNA Expression in CAR-Expressing HepG2 Cells, HepaRG Cells, or in Primary Human Hepatocytes (Figure 3). (A) HepG2 cells were transfected with CAR expression plasmid and 24 h later treated with the tested compounds **7**, **3a**, and **7a** (1, 5, or 10 μM) or CITCO (1 μM) or vehicle (DMSO; 0.1%, v/v) for 24 h. (B) Three primary human hepatocyte preparation have been treated with tested compounds **7**, **3a**, and **7a** (10 μM) or CITCO (10 μM) or vehicle (DMSO; 0.1%, v/v) for 24 h. (C) Primary human hepatocytes (batch no. 2220900, Biopredic) or HepaRG cells (for CYP1A1 and CYP1B1) have been treated with 3-methylcholanthrene (3-MC, an AHR prototype ligand, 10 μM), rifampicin (rif, a prototype PXR ligand, 10 μM), CITCO (CAR ligand, 10 μM), and tested compounds **7**, **3a**, and **7a** (10 μM). Total RNA was isolated and CYP2B6 (the gene dominantly controlled by CAR) or CYP1A1, CYP1A2, CYP1B1, CYP2C9, CYP3A4, CYP3A5, MDR1/ABCB1, and UGT1A1 genes mRNAs were assessed via qRT-PCR. The data in Figure 3A are presented as the means ± SD from three experiments (n = 3) performed in triplicates and are expressed as the fold-change in CYP2B6 mRNA induction relative to vehicle-treated cells (normalized to 1). In Figure 3B,C, experiments were performed with three samples for each treatment. The values were normalized to HPRT mRNA as a reference gene. *p < 0.05 indicates statistically significant difference from vehicle-treated cells transfected with appropriate reporter construct (ANOVA with Dunnett's post hoc test).

*Inhibition of Recombinant Human CYP3A4, CYP2B6, CYP1A2, CYP2C9, and CYP2D6 Enzymes with Compounds **7**, **3a**, and **7a** (Figure 4).* Assays with recombinant human enzymes CYP3A4, CYP2B6, CYP1A2, CYP2C9, and CYP2D6 have been performed according to manufacturer's protocols (Promega). IC_{50} (xenobiotic concentration required to achieve half-maximum enzyme inhibition) was determined using GraphPad Prism Software fitting for each compound.

Transient Transfection and Luciferase Reporter Gene Assays. All transient transfection assays were carried out using TransFectin transfection reagent purchased from Bio-Rad (Hercules, CA, USA) in HepG2, HuH7, or COS-1 cells, as described previously.[37] DNA constructs are described in the Supporting Information. Briefly, cells were seeded into 48-well plates and transfected with a luciferase reporter construct (150 ng/well), an expression plasmid (100 ng/well), and the *Renilla reniformis* luciferase transfection control plasmid (pRL-TK) (30 ng/well) 24 h later. In the case of the mammalian two-hybrid assay, HepG2 cells have been transfected with GAL4-CAR LBD (100 ng/well), VP-16-SRC-1 (100 ng/well), and pGL5-luc (150 ng/well) constructs in 48-well plate format. Cells were maintained in a phenol-red-free medium (220 μL) supplemented with 10% charcoal/dextran-stripped FBS and treated with the tested compounds (at indicated concentrations in a range from 0.1 up to 30 μM) or reference compounds CITCO, artemisinin,[38] and clotrimazole (CAR ligands and agonists, 10 μM), 1,25OHvitD_3 (10 nM, a VDR receptor ligand), rifampicin (10 μM, PXR ligand), and 3-methylcholantrene (10 μM, an AHR ligand) for 24 h. Reference compound have been purchased from Sigma-Aldrich. Luminescence activity in the cell lysate was measured using a commercially available luciferase detection system (Dual Luciferase Reporter Assay Kit, Promega). The data are expressed as the fold-change of firefly luciferase activity normalized to *Renilla* luciferase activity in each sample and relative to the vehicle (DMSO 0.1%)-treated controls, which were set equal to 1. Activity of a reference agonist at the maximum tested concentration has been set equal to 100% activation.

Primary Cultures of Human Hepatocytes and HepaRG Cells. Preparation of primary human hepatocytes and information about donors is described in the Supporting Information. HepaRG cells were cultivated as we described recently.[39]

TR-FRET Constitutive Androstane Receptor (CAR) Coactivator Assay. LanthaScreen time-resolved (TR)-FRET constitutive androstane receptor (CAR) coactivator assay was performed according to the recently published protocol.[22] Data are presented as means and SD from three independent experiments, and the curve fitting was performed using a sigmoidal dose response (variable slope) algorithm in GraphPad software version 6. Activity of CITCO at the maximum tested concentration has been set equal to 100% activation.

qRT-PCR Analysis. Total RNA was isolated from HepG2 or HepaRG cells, and primary human hepatocytes were treated with the tested compounds or with CITCO (1 μM), rifampicin (10 μM), and 3-MC (10 μM) for 24 h. qRT-PCR expression analyses were performed as previously described.[37] In expression experiments with CAR-expressing HepG2 cells, 2×10^5 cells were seeded into 12-well plates and transiently transfected with the pCR3-hCAR expression construct. After 24 h of stabilization, the cells were treated with the

DOI: 10.1021/acs.jmedchem.5b01891
J. Med. Chem. 2016, 59, 4601−4610

tested compounds for 24 h in the indicated concentrations. The data are presented as the fold-changes in gene expression relative to the vehicle-treated control (DMSO 0.1%) samples (set equal to 1). Statistical analyses were performed using the means of at least three independent experiments (n = 3) performed in triplicate.

Chemistry. *General.* The structural identities of the prepared compounds were confirmed by ^{1}H NMR and ^{13}C NMR spectroscopy (Varian Mercury-Vx BB 300 and Varian VNMR S500 spectrometers). Each of the reported compounds had ≥95% purity, as determined by combustion analysis (CHNS-OCE FISONS EA1110CE automatic microanalyzer instrument).

Experimental Procedure for the Preparation of Compound ***3****.* A mixture of 3-methoxybenzoic acid **4** (9.700 g, 63.8 mmol) and thionyl chloride (30 mL) was heated under reflux for 3 h. The resultant carboxylic acid chloride **5** was purified by distillation with 95% yield and immediately used for the next reaction step.

Chloride **5** (7.165 g, 42.0 mmol) was slowly added to a cooled (0 °C) solution of 2-aminobenzonitrile (4.962 g, 42.0 mmol) and dry pyridine (17 mL). The reaction mixture was stirred at 0 °C for 4 h, then pyridine was removed under reduced pressure and crude product was recrystallized from an ethanol−water (2:1) mixture with quantitative yield.

A mixture of the resultant amide **6** (7.291 g, 28.9 mmol), sodium hydroxide (32 g), and aqueous hydrogen peroxide solution (30%, 48 mL) in water (200 mL) was heated at 100 °C for 1 h. After cooling to room temperature, the reaction mixture was acidified with concentrated aqueous hydrogen chloride solution (36%) to pH ≅ 4. The product crystallized out of the solution, after which it was filtered, washed with water, and dried to afford 2-(3-methoxyphenyl)-3,4-dihydroquinazolin-4-one (**3**) in 58% yield. White crystalline compound, mp 214 °C, mp lit.[40] 209−210 °C. ^{1}H NMR: (300 MHz, DMSO-d_6) δ 12.52 (1H, bs, OH), 8.14−8.18 (1H, m, Ar), 7.85−7.71 (4H, m, Ar), 7.54−7.21 (2H, m, Ar), 7.15−7.11 (1H, m, Ar), 3.83 (3H, s, OCH_3). ^{13}C NMR: (75 MHz, DMSO-d_6) δ 162.5, 159.5, 152.3, 148.8, 134.8, 134.2, 129.9, 127.7, 126.8, 126.1, 121.2, 120.3, 117.8, 112.7, 55.6. IR: 1047, 1148, 1223, 1251, 1267, 1286, 1310, 1445, 1471, 1482, 1586, 1612, 1670, 3038 cm^{-1}. LRMS (APCI): m/z (relative intensity) 253.6 $[M + H]^+$ (100), 130.6 (3), 88.6 (1.5), 87.6 (6), 73.6 (8). Anal. Calcd for $C_{15}H_{12}N_2O_2$: C, 71.42; H, 4.79; N, 11.10. Found: C, 71.38; H, 5.00; N, 11.21.

General Experimental Procedure for the Preparation of Compounds ***3a−f****.* A mixture of 2-(3-methoxyphenyl)-3,4-dihydroquinazolin-4-one (**3**, 0.5 mmol), sodium iodide (0.05 mmol), potassium carbonate (2.5 mmol), and an appropriate alkylating agent (2.5 mmol) in acetone (5 mL) was heated under reflux for 24 h. The resultant mixture was diluted with ethyl acetate (10 mL), washed with brine (10 mL), and the organic phase dried with sodium sulfate. Crude products were purified by column chromatography (hexane−ethyl acetate 9:1).

*4-Methoxy-2-(3-methoxyphenyl)quinazoline (****3a****).* Yield: 85%. Yellowish crystalline compound, mp 92−94 °C. ^{1}H NMR: (500 MHz, $CDCl_3$) δ 8.22−8.15 (3H, m, Ar), 8.03−7.99 (1H, m, Ar), 7.86−7.8 (1H, m, Ar), 7.55−7.41 (2H, m, Ar), 7.08−7.03 (1H, m, Ar), 4.30 (3H, s, OCH_3), 3.96 (3H, s, OCH_3). ^{13}C NMR: (125 MHz, $CDCl_3$) δ 167.0, 159.8, 159.8, 151.8, 139.7, 133.4, 129.4, 128.0, 126.4, 123.4, 121.1, 116.6, 115.3, 113.4, 55.4, 54.0. IR: 1047, 1108, 1184, 1195, 1282, 1327, 1355, 1380, 1443, 1453, 1509, 1561, 1574, 1620, 2966 cm^{-1}. LRMS (APCI): m/z (relative intensity) 267.6 $[M + H]^+$ (100), 252.6 (75), 224.6 (7), 223.6 (25), 148.6 (7). Anal. Calcd for $C_{16}H_{14}N_2O_2$: C, 72.17; H, 5.30; N, 10.52. Found: C, 72.26; H, 5.37; N, 10.43.

*4-Ethoxy-2-(3-methoxyphenyl)quinazoline (****3b****).* Yield: 91%. Yellowish crystalline compound, mp 93 °C, mp lit.[41] not mentioned. ^{1}H NMR: (300 MHz, $CDCl_3$) δ 8.24−8.14 (3H, m, Ar), 8.02−7.97 (1H, m, Ar), 7.84−7.77 (1H, m, Ar), 7.5−7.41 (2H, m, Ar), 7.08−7.03 (1H, m, Ar), 4.8−4.72 (2H, q, J = 7.2 Hz, OCH_2), 3.94 (3H, s, OCH_3), 1.56−1.51 (3H, t, J = 7.2 Hz, CH). ^{13}C NMR: (75 MHz, $CDCl_3$) δ 166.5, 159.7, 159.7, 151.6, 139.6, 133.2, 129.3, 127.8, 126.2, 123.4, 120.9, 116.4, 115.3, 113.3, 62.7, 55.3, 14.3. IR: 1023, 1050, 1105, 1161, 1282, 1322, 1346, 1356, 1380, 1426, 1458, 1507, 1561, 1575, 2989 cm^{-1}. LRMS (APCI): m/z (relative intensity) 281.5 $[M + H]^+$ (24), 255.5 (2), 254.4 (13), 253.6 (100), 238.5 (4), 210.5 (6), 91.5 (5). Anal. Calcd for $C_{17}H_{16}N_2O_2$: C, 72.84; H, 5.75; N, 9.99. Found: C, 72.81; H, 5.64; N, 10.08.

*2-(3-Methoxyphenyl)-4-propoxyquinazoline (****3c****).* Yield: 88%. Yellowish amorphous compound. ^{1}H NMR: (300 MHz, $CDCl_3$) δ 8.24−8.17 (3H, m, Ar), 8.02−7.98 (1H, m, Ar), 7.83−7.78 (1H, m, Ar), 7.53−7.41 (2H, m, Ar), 7.07−7.03 (1H, m, Ar), 4.65 (2H, t, J = 7.0 Hz, OCH_2), 3.93 (3H, s, OCH_3), 2.06−1.93 (2H, m, CH_2), 1.15 (3H, t, J = 7.0 Hz, CH_3). ^{13}C NMR: (75 MHz, $CDCl_3$) δ 166.7, 159.7, 151.7, 139.6, 133.3, 129.3, 127.8, 126.2, 123.4, 121.0, 116.4, 115.3, 113.3, 68.3, 55.3, 22.1, 10.6. IR: 1046, 1105, 1162, 1252, 1279, 1346, 1363, 1421, 1499, 1561, 1575, 1965 cm^{-1}. LMRS (APCI): m/z (relative intensity) 295.6 $[M + H]^+$ (16), 254.4 (12.5), 253.6 (100), 238.6 (3), 210.6 (3). Anal. Calcd for $C_{18}H_{18}N_2O_2$: C, 73.45; H, 6.16; N, 9.52. Found: C, 73.12; H, 6.00; N, 9.31.

*4-Isobutyloxy-2-(3-methoxyphenyl)quinazoline (****3d****).* Yield: 78%. Yellowish amorphous compound. ^{1}H NMR: (300 MHz, $CDCl_3$) δ 8.23−8.15 (3H, m, Ar), 8.01−7.97 (1H, m, Ar), 7.82−7.77 (1H, m, Ar), 7.52−7.41 (2H, m, Ar), 7.07−7.03 (1H, m, Ar), 4.49 (2H, d, J = 6.8 Hz, OCH_2), 3.95 (3H, s, OCH_3), 2.35−2.22 (1H, m, CH), 1.14 (6H, d, J = 6.8 Hz, CH_3). ^{13}C NMR: (75 MHz, $CDCl_3$) δ 166.7, 159.8, 159.7, 151.7, 139.7, 133.3, 129.3, 127.9, 126.2, 123.4, 121.0, 116.4, 115.4, 113.3, 72.8, 55.3, 27.9, 19.3. IR: 1047, 1107, 1162, 1253, 1280, 1344, 1385, 1421, 1461, 1499, 1561, 1575, 1620, 2959 cm^{-1}. LRMS (APCI): m/z (relative intensity) 309.6 $[M + H]^+$ (7.5), 255.5 (2), 254.4 (16), 253.6 (100), 238.6 (2.5), 210.6 (3). Anal. Calcd for $C_{19}H_{20}N_2O_2$: C, 74.00; H, 6.54; N, 9.08. Found: C, 73.87; H, 6.44; N, 9.21.

*4-Allyloxy-2-(3-methoxyphenyl)quinazoline (****3e****).* Yield: 58%. Yellowish crystalline compound, mp 50−52 °C. ^{1}H NMR: (300 MHz, $CDCl_3$) δ 8.22 (3H, m, Ar), 8.02−7.98 (1H, m, Ar), 7.82−7.77 (1H, m, Ar), 7.52−7.4 (2H, m, Ar), 7.07−7.03 (1H, m, Ar), 6.31−6.18 (1H, m, CH), 5.56 (1H, d, J = 17.2 Hz, =CH_2 A), 5.37 (1H, d, J = 10.4 Hz, =CH_2 B), 5.21 (2H, d, J = 5.5 Hz, OCH_2), 3.95 (3H, s, OCH_3). ^{13}C NMR: (75 MHz, $CDCl_3$) δ 166.1, 159.7, 159.5, 151.7, 139.5, 133.4, 132.6, 129.3, 127.9, 126.3, 123.4, 120.9, 118.3, 116.5, 115.2, 113.3, 67.3, 55.3. IR: 1001, 1052, 1109, 1217, 1280, 1317, 1339, 1355, 1408, 1457, 1500, 1561, 1574, 1619, 2939 cm^{-1}. LRMS (APCI): m/z (relative intensity) 293.6 $[M + H]^+$ (100), 291.7 (2.5), 265.6 (3), 264,6 (11), 253.6 (50), 250.7 (9), 210.6 (2). Anal. Calcd for $C_{18}H_{16}N_2O_2$: C, 73.95; H, 5.52; N, 9.58. Found: C, 74.16; H, 5.65; N, 9.42.

*4-Benzyloxy-2-(3-methoxyphenyl)quinazoline (****3f****).* Yield: 78%. White crystalline compound, mp 109−111 °C. ^{1}H NMR: (300 MHz, $CDCl_3$) δ 8.32−8.17 (3H, m, Ar), 8.07−8.03 (1H, m, Ar), 7.84−7.78 (1H, m, Ar), 7.64−7.6 (2H, m, Ar), 7.52−7.37 (5H, m, Ar), 7.13−7.08 (1H, m, Ar), 5.76 (2H, s, OCH_2), 3.97 (3H, s, OCH_3). ^{13}C NMR: (75 MHz, $CDCl_3$) δ 166.2, 159.7, 159.5, 151.7, 139.4, 136.4, 133.3, 129.3, 128.4, 128.1, 128.0, 127.8, 126.3, 123.3, 120.9, 116.5, 115.1, 113.2, 68.2, 55.2. IR: 1041, 1091, 1222, 1255, 1280, 1331, 1342, 1356, 1416, 1459, 1500, 1563, 1575, 1600, 1619, 2940 cm^{-1}. LRMS (APCI): m/z (relative intensity) 343.6 $[M + H]^+$ (65), 253.5 (1), 92.5 (7.5), 91.5 (100). Anal. Calcd for $C_{22}H_{18}N_2O_2$: C, 77.17; H, 5.30; N, 8.18. Found: C, 77.01; H, 5.32; N, 8.34.

Experimental Procedure for the Preparation of Compound ***7****.* A mixture of 2-(3-methoxyphenyl)-3,4-dihydroquinazolin-4-one (**3**, 1.000 g, 4.0 mmol) and phosphorus pentasulfide (0.880 g, 4.0 mmol) in toluene (10 mL) was heated under reflux for 4 h. The reaction mixture was poured onto ice and washed with chloroform (3 × 20 mL). Collected organic layers were dried with sodium sulfate. Crude product was purified by column chromatography (hexane−ethyl acetate 1:1) to afford thiol **7** in 83% yield. Yellow crystalline compound, mp 222−225 °C, mp lit.[42] not mentioned. ^{1}H NMR: (500 MHz, DMSO-d_6) δ 13.84 (1H, bs, SH), 8.64−8.57 (1H, m, Ar), 7.92−7.86 (1H, m, Ar), 7.8−7.63 (3H, m, Ar), 7.6−7.55 (1H, m, Ar), 7.48−7.43 (1H, m, Ar), 7.16−7.12 (1H, m, Ar), 3.87 (3H, s, OCH_3). ^{13}C NMR: (125 MHz, DMSO-d_6) δ 187.9, 159.4, 151.4, 144.5, 135.6, 133.5, 129.8, 129.5, 128.5, 128.2, 127.8, 121.0, 118.0, 113.3, 55.6. IR: 1029, 1040, 1154, 1189, 1222, 1252, 1263, 1339, 1492, 1508, 1570,

DOI: 10.1021/acs.jmedchem.5b01891
J. Med. Chem. 2016, 59, 4601−4610

2985 cm^{-1}. LRMS (APCI): *m/z* (relative intensity) 269.9 $[M + H]^+$ (100), 253.6 (9), 235.5 (19), 226.5 (6), 210.6 (3); Anal. Calcd for $C_{15}H_{12}N_2OS$: C, 67.14; H, 4.51; N, 10.44; S, 11.95. Found: C, 67.01; H, 4.42; N, 10.28; S, 11.90.

Experimental Procedure for the Preparation of Compound ***7a***. A mixture of 2-(3-methoxyphenyl)-3,4-dihydroquinazolin-4-thione (**7**, 0.5 mmol), potassium carbonate (2.5 mmol), and an methyl iodide (2.5 mmol) in acetone (5 mL) was heated under reflux for 24 h. The resultant mixture was diluted with ethyl acetate (10 mL), washed with brine (10 mL), and the organic phase dried with sodium sulfate. The crude product was purified by column chromatography (hexane−ethyl acetate 9:1) to afford 2-(3-methoxyphenyl)-4-methylsulfanylquinazoline (**7a**) in 79% yield. Yellowish crystalline compound, mp 89−91 °C. ^1H NMR: (300 MHz, $CDCl_3$) δ 8.28−8.21 (2H, m, Ar), 8.11−8.01 (2H, m, Ar), 7.86−7.8 (1H, m, Ar), 7.56−7.41 (2H, m, Ar), 7.09−7.4 (1H, m, Ar), 3.95 (3H, s, OCH_3), 2.83 (3H, s, SCH_3). ^{13}C NMR: (75 MHz, $CDCl_3$) δ 171.4, 159.8, 158.6, 148.6, 139.5, 133.6, 129.5, 129.0, 126.7, 123.7, 122.6, 121.1, 116.7, 113.4, 55.4, 12.6. IR: 1039, 1217, 1249, 1328, 1348, 1429, 1483, 1494, 1559, 1600, 2924 cm^{-1}. LMRS (APCI): *m/z* (relative intensity) 283.6 $[M + H]^+$ (100), 268.5 (7), 250.6 (3.5), 236.5 (5.5), 235.6 (38), 192.6 (1). Anal. Calcd for $C_{16}H_{14}N_2OS$: C, 68.06; H, 5.00; N, 9.92; S, 11.35. Found: C, 68.31; H, 4.89; N, 10.11; S, 11.17.

■ ASSOCIATED CONTENT

Ⓢ Supporting Information

The Supporting Information is available free of charge on the ACS Publications website at DOI: 10.1021/acs.jmedchem.5b01891.

General experimental procedures, supplementary data, and copies of ^1H and ^{13}C NMR spectra of compounds **3**, **3a−f**, **7**, **7a** (PDF)

Molecular formula strings (CSV)

■ AUTHOR INFORMATION

Corresponding Authors

*For M.Š.: phone, +420 495 067 348; fax, +420 495 067 166; E-mail, spulak@faf.cuni.cz.

*For P.P.: phone, +420 495 067 334; fax, +420 495 067 170; E-mail, petr.pavek@faf.cuni.cz.

Notes

The authors declare no competing financial interest.

■ ACKNOWLEDGMENTS

This work was supported by projects nos. 303/12/0472 (biology) and 15-07332S (chemistry) of the Czech Science Foundation. Postgraduate student Z.R.H. acknowledges Charles University for financial support (project no. 398315).

■ ABBREVIATIONS USED

AhR, aryl hydrocarbon receptor; CAR, constitutive androstane receptor; CYP450, cytochrome P450; GR, glucocorticoid receptor; LBD, ligand binding domain; MRP2, multidrug resistance-associated protein; NR, nuclear receptor; PGC1α, peroxisome proliferator-activated receptor gamma, coactivator 1α (PPARGC1A); PXR, pregnane X receptor; SLC, solute carrier family; SRC-1, steroid receptor coactivator 1 (NCOA1); TCDD, 2,3,7,8-tetrachlorodibenzo-*p*-dioxin; XME, xenobiotic-metabolizing enzyme

■ REFERENCES

(1) Chen, Y.; Tang, Y.; Guo, C.; Wang, J.; Boral, D.; Nie, D. Nuclear receptors in the multidrug resistance through the regulation of drug-metabolizing enzymes and drug transporters. *Biochem. Pharmacol.* **2012**, *83*, 1112−1126.

(2) Pascussi, J. M.; Gerbal-Chaloin, S.; Duret, C.; Daujat-Chavanieu, M.; Vilarem, M. J.; Maurel, P. The tangle of nuclear receptors that controls xenobiotic metabolism and transport: crosstalk and consequences. *Annu. Rev. Pharmacol. Toxicol.* **2008**, *48*, 1−32.

(3) Hernandez, J. P.; Mota, L. C.; Baldwin, W. S. Activation of CAR and PXR by Dietary, Environmental and Occupational Chemicals Alters Drug Metabolism, Intermediary Metabolism, and Cell Proliferation. *Curr. Pharmacogenomics Pers. Med.* **2009**, *7*, 81−105.

(4) Molnar, F.; Kublbeck, J.; Jyrkkarinne, J.; Prantner, V.; Honkakoski, P. An update on the constitutive androstane receptor (CAR). *Drug Metab. Drug Interact.* **2013**, *28*, 79−93.

(5) di Masi, A.; De Marinis, E.; Ascenzi, P.; Marino, M. Nuclear receptors CAR and PXR: Molecular, functional, and biomedical aspects. *Mol. Aspects Med.* **2009**, *30*, 297−343.

(6) Wada, T.; Gao, J.; Xie, W. PXR and CAR in energy metabolism. *Trends Endocrinol. Metab.* **2009**, *20*, 273−279.

(7) Ingraham, H. A.; Redinbo, M. R. Orphan nuclear receptors adopted by crystallography. *Curr. Opin. Struct. Biol.* **2005**, *15*, 708−715.

(8) Osabe, M.; Negishi, M. Active ERK1/2 protein interacts with the phosphorylated nuclear constitutive active/androstane receptor (CAR; NR1I3), repressing dephosphorylation and sequestering CAR in the cytoplasm. *J. Biol. Chem.* **2011**, *286*, 35763−35769.

(9) Maglich, J. M.; Parks, D. J.; Moore, L. B.; Collins, J. L.; Goodwin, B.; Billin, A. N.; Stoltz, C. A.; Kliewer, S. A.; Lambert, M. H.; Willson, T. M.; Moore, J. T. Identification of a novel human constitutive androstane receptor (CAR) agonist and its use in the identification of CAR target genes. *J. Biol. Chem.* **2003**, *278*, 17277−17283.

(10) Tzameli, I.; Pissios, P.; Schuetz, E. G.; Moore, D. D. The xenobiotic compound 1,4-bis[2-(3,5-dichloropyridyloxy)]benzene is an agonist ligand for the nuclear receptor CAR. *Mol. Cell. Biol.* **2000**, *20*, 2951−2958.

(11) Kublbeck, J.; Jyrkkarinne, J.; Molnar, F.; Kuningas, T.; Patel, J.; Windshugel, B.; Nevalainen, T.; Laitinen, T.; Sippl, W.; Poso, A.; Honkakoski, P. New in vitro tools to study human constitutive androstane receptor (CAR) biology: discovery and comparison of human CAR inverse agonists. *Mol. Pharmaceutics* **2011**, *8*, 2424−2433.

(12) Kublbeck, J.; Laitinen, T.; Jyrkkarinne, J.; Rousu, T.; Tolonen, A.; Abel, T.; Kortelainen, T.; Uusitalo, J.; Korjamo, T.; Honkakoski, P.; Molnar, F. Use of comprehensive screening methods to detect selective human CAR activators. *Biochem. Pharmacol.* **2011**, *82*, 1994−2007.

(13) Faucette, S. R.; Zhang, T. C.; Moore, R.; Sueyoshi, T.; Omiecinski, C. J.; LeCluyse, E. L.; Negishi, M.; Wang, H. Relative activation of human pregnane X receptor versus constitutive androstane receptor defines distinct classes of CYP2B6 and CYP3A4 inducers. *J. Pharmacol. Exp. Ther.* **2007**, *320*, 72−80.

(14) Yao, R.; Yasuoka, A.; Kamei, A.; Kitagawa, Y.; Rogi, T.; Taieishi, N.; Tsuruoka, N.; Kiso, Y.; Misaka, T.; Abe, K. Polyphenols in alcoholic beverages activating constitutive androstane receptor CAR. *Biosci., Biotechnol., Biochem.* **2011**, *75*, 1635−1637.

(15) Burk, O.; Piedade, R.; Ghebreghiorghis, L.; Fait, J. T.; Nussler, A. K.; Gil, J. P.; Windshugel, B.; Schwab, M. Differential effects of clinically used derivatives and metabolites of artemisinin in the activation of constitutive androstane receptor isoforms. *Br. J. Pharmacol.* **2012**, *167*, 666−681.

(16) Anderson, L. E.; Dring, A. M.; Hamel, L. D.; Stoner, M. A. Modulation of constitutive androstane receptor (CAR) and pregnane X receptor (PXR) by 6-arylpyrrolo[2,1-*d*][1,5]benzothiazepine derivatives, ligands of peripheral benzodiazepine receptor (PBR). *Toxicol. Lett.* **2011**, *202*, 148−154.

(17) Lynch, C.; Pan, Y.; Li, L.; Ferguson, S. S.; Xia, M.; Swaan, P. W.; Wang, H. Identification of novel activators of constitutive androstane receptor from FDA-approved drugs by integrated computational and biological approaches. *Pharm. Res.* **2013**, *30*, 489−501.

DOI: 10.1021/acs.jmedchem.5b01891
J. Med. Chem. 2016, 59, 4601−4610

(18) Dvorak, Z.; Pavek, P. Regulation of drug-metabolizing cytochrome P450 enzymes by glucocorticoids. *Drug Metab. Rev.* **2010**, *42*, 621−635.
(19) Bandgar, B. P. Synthesis of quinazolin-4-(3*H*)-ones from *o*-amidobenzonitriles using urea hydrogen peroxide. *Synth. Commun.* **1997**, *27*, 2065−2068.
(20) Spulak, M.; Novak, Z.; Palat, K.; Kunes, J.; Pourova, J.; Pour, M. The unambiguous synthesis and NMR assignment of 4-alkoxy and 3-alkylquinazolines. *Tetrahedron* **2013**, *69*, 1705−1711.
(21) Auerbach, S. S.; Stoner, M. A.; Su, S.; Omiecinski, C. J. Retinoid X receptor-alpha-dependent transactivation by a naturally occurring structural variant of human constitutive androstane receptor (NR1I3). *Mol. Pharmacol.* **2005**, *68*, 1239−1253.
(22) Carazo, A.; Pavek, P. The Use of the LanthaScreen TR-FRET CAR Coactivator Assay in the Characterization of Constitutive Androstane Receptor (CAR) Inverse Agonists. *Sensors* **2015**, *15*, 9265−9276.
(23) Mutoh, S.; Sobhany, M.; Moore, R.; Perera, L.; Pedersen, L.; Sueyoshi, T.; Negishi, M. Phenobarbital indirectly activates the constitutive active androstane receptor (CAR) by inhibition of epidermal growth factor receptor signaling. *Sci. Signaling* **2013**, *6*, ra31.
(24) Jyrkkarinne, J.; Windshugel, B.; Ronkko, T.; Tervo, A. J.; Kublbeck, J.; Lahtela-Kakkonen, M.; Sippl, W.; Poso, A.; Honkakoski, P. Insights into ligand-elicited activation of human constitutive androstane receptor based on novel agonists and three-dimensional quantitative structure-activity relationship. *J. Med. Chem.* **2008**, *51*, 7181−7192.
(25) Svecova, L.; Vrzal, R.; Burysek, L.; Anzenbacherova, E.; Cerveny, L.; Grim, J.; Trejtnar, F.; Kunes, J.; Pour, M.; Staud, F.; Anzenbacher, P.; Dvorak, Z.; Pavek, P. Azole antimycotics differentially affect rifampicin-induced pregnane X receptor-mediated CYP3A4 gene expression. *Drug Metab. Dispos.* **2008**, *36*, 339−348.
(26) Gao, J.; Xie, W. Targeting xenobiotic receptors PXR and CAR for metabolic diseases. *Trends Pharmacol. Sci.* **2012**, *33*, 552−558.
(27) Auerbach, S. S.; Ramsden, R.; Stoner, M. A.; Verlinde, C.; Hassett, C.; Omiecinski, C. J. Alternatively spliced isoforms of the human constitutive androstane receptor. *Nucleic Acids Res.* **2003**, *31*, 3194−3207.
(28) Xu, R. X.; Lambert, M. H.; Wisely, B. B.; Warren, E. N.; Weinert, E. E.; Waitt, G. M.; Williams, J. D.; Collins, J. L.; Moore, L. B.; Willson, T. M.; Moore, J. T. A structural basis for constitutive activity in the human CAR/RXRalpha heterodimer. *Mol. Cell* **2004**, *16*, 919−928.
(29) Watkins, R. E.; Wisely, G. B.; Moore, L. B.; Collins, J. L.; Lambert, M. H.; Williams, S. P.; Willson, T. M.; Kliewer, S. A.; Redinbo, M. R. The human nuclear xenobiotic receptor PXR: structural determinants of directed promiscuity. *Science* **2001**, *292*, 2329−2333.
(30) Chai, S. C.; Cherian, M. T.; Wang, Y. M.; Chen, T. Small-molecule modulators of PXR and CAR. *Biochim. Biophys. Acta, Gene Regul. Mech.* **2016**, DOI: 10.1016/j.bbagrm.2016.02.013.
(31) Moore, D. D.; Kato, S.; Xie, W.; Mangelsdorf, D. J.; Schmidt, D. R.; Xiao, R.; Kliewer, S. A. International Union of Pharmacology. LXII. The NR1H and NR1I receptors: constitutive androstane receptor, pregnene X receptor, farnesoid X receptor alpha, farnesoid X receptor beta, liver X receptor alpha, liver X receptor beta, and vitamin D receptor. *Pharmacol. Rev.* **2006**, *58*, 742−759.
(32) Urquhart, B. L.; Tirona, R. G.; Kim, R. B. Nuclear receptors and the regulation of drug-metabolizing enzymes and drug transporters: implications for interindividual variability in response to drugs. *J. Clin. Pharmacol.* **2007**, *47*, 566−578.
(33) Barouki, R.; Aggerbeck, M.; Aggerbeck, L.; Coumoul, X. The aryl hydrocarbon receptor system. *Drug Metab. Drug Interact.* **2012**, *27*, 3−8.
(34) Stejskalova, L.; Pavek, P. The function of cytochrome P450 1A1 enzyme (CYP1A1) and aryl hydrocarbon receptor (AhR) in the placenta. *Curr. Pharm. Biotechnol.* **2011**, *12*, 715−730.
(35) Stejskalova, L.; Dvorak, Z.; Pavek, P. Endogenous and exogenous ligands of aryl hydrocarbon receptor: current state of art. *Curr. Drug Metab.* **2011**, *12*, 198−212.
(36) Marschall, H. U.; Wagner, M.; Zollner, G.; Trauner, M. Clinical hepatotoxicity. Regulation and treatment with inducers of transport and cofactors. *Mol. Pharmaceutics* **2007**, *4*, 895−910.
(37) Rulcova, A.; Prokopova, I.; Krausova, L.; Bitman, M.; Vrzal, R.; Dvorak, Z.; Blahos, J.; Pavek, P. Stereoselective interactions of warfarin enantiomers with the pregnane X nuclear receptor in gene regulation of major drug-metabolizing cytochrome P450 enzymes. *J. Thromb. Haemostasis* **2010**, *8*, 2708−2717.
(38) Burk, O.; Arnold, K. A.; Nussler, A. K.; Schaeffeler, E.; Efimova, E.; Avery, B. A.; Avery, M. A.; Fromm, M. F.; Eichelbaum, M. Antimalarial artemisinin drugs induce cytochrome P450 and MDR1 expression by activation of xenosensors pregnane X receptor and constitutive androstane receptor. *Mol. Pharmacol.* **2005**, *67*, 1954−1965.
(39) Hyrsova, L.; Smutny, T.; Carazo, A.; Moravcik, S.; Mandikova, J.; Trejtnar, F.; Gerbal-Chaloin, S.; Pavek, P. The pregnane X receptor down-regulates organic cation transporter 1 (SLC22A1) in human hepatocytes by squelching SRC-1 coactivator. *Br. J. Pharmacol.* **2016**, *173*, 1703−1715.
(40) Zhou, J.; Fang, J. One-Pot Synthesis of Quinazolinones via Iridium-Catalyzed Hydrogen Transfers. *J. Org. Chem.* **2011**, *76*, 7730−7736.
(41) Kuo, S.-c.; Hour, M.-j.; Huang, L.-j.; Lee, K.-h. Preparation of 2-phenyl-4-quinazolinones and 2-phenyl-4-alkoxy-quinazolines as anti-cancer and antiplatelet drugs. U.S. Pat. Appl. Publ. US 6479499 B1, 2002.
(42) Zheng, Y.; Bian, M.; Deng, X.-Q.; Wang, S.-B.; Quan, Z.-S. Synthesis and Anticonvulsant Activity Evaluation of 5-Phenyl-[1,2,4]-triazolo[4,3-*c*]quinazolin-3-amines. *Arch. Pharm. (Weinheim, Ger.)* **2013**, *346*, 119−126.

DOI: 10.1021/acs.jmedchem.5b01891
J. Med. Chem. 2016, 59, 4601−4610

3. Bioinformatic Analysis of MiRNAs Targeting the Key Nuclear Receptors Regulating CYP3A4 Gene Expression: the Challenge of the CYP3A4 "Missing Heritability" Enigma.

Smutny T, Tebbens J, Pavek P. Bioinformatic Analysis of MiRNAs Targeting the Key Nuclear Receptors Regulating CYP3A4 Gene Expression: the Challenge of the CYP3A4 "Missing Heritability" Enigma. (2015) J Appl Biomed., 13(3):181-188.
(IF 2014/2015: **1.302**)

It was suggested that the post-transcriptional modification mediated by microRNAs (miRNAs) can affect expression and consequently the activity of DMEs. MiRNAs are short non-coding RNAs that can bind to mRNA of target genes leading to mRNA degradation or a translation inhibition. In our analysis, we attempted to summarize potential miRNAs targeting key NRs involved in CYP3A4 regulation based on several *in silico* programs. Since CYP3A4 shows a high interindividual expression variability, we and others proposed that the effect of miRNAs on the regulation of NRs could participate in this phenomenon.

As revealed by our *in silico* analysis, PXR, CAR, VDR, HNF4α, RXRα, SHP, and GR mRNA could be potentially regulated by a plenty of miRNAs. We also speculated that some miRNAs may have a role of master regulators of NRs because they are estimated to target more than three genes.

With respect to *in vitro* liver cell models, we can hypothesize here that the strategy affecting deregulated miRNAs implicated in NRs regulation such as miRNAs inhibition could be used to increase expression of NRs and in turn enhance DME expression.

Available online at www.sciencedirect.com

ScienceDirect

journal homepage: http://www.elsevier.com/locate/jab

Original Research Article

Bioinformatic analysis of miRNAs targeting the key nuclear receptors regulating CYP3A4 gene expression: The challenge of the CYP3A4 ''missing heritability'' enigma

Tomas Smutny [a], *Jurjen Duintjer Tebbens* [b], *Petr Pavek* [a,*]

[a] *Department of Pharmacology and Toxicology, Faculty of Pharmacy in Hradec Kralove, Charles University in Prague, Heyrovskeho 1203, Hradec Kralove CZ-500 05, Czech Republic*

[b] *Department of Biophysics and Physical Chemistry, Faculty of Pharmacy in Hradec Kralove, Charles University in Prague, Heyrovskeho 1203, Hradec Kralove CZ-500 05, Czech Republic*

ARTICLE INFO

Article history:
Received 31 March 2015
Accepted 9 April 2015
Available online 21 April 2015

Keywords:
miRNA
Gene regulation
CYP3A4
Cytochrome P450
Metabolism

ABSTRACT

The expression of the main cytochrome P450 enzyme CYP3A4 displays enormous interindividual variability. Studies addressing the genetic variability of either the CYP3A4 gene itself or its key transcription factors have not found any crucial polymorphism contributing to this variability in expression, a phenomenon is referred to as the ''missing heritability of CYP3A4 variability.'' Several reports have recently described microRNAs (miRNAs) targeting the CYP3A4 gene and/or its major transcription factors.

A comprehensive bioinformatic analysis was performed using the miRDB, PITA, miRanda and TargetScan programs in the search for hypothetical miRNAs targeting 3′-untranslated regions of PXR, CAR, VDR, HNF4α, RXRα, SHP and GRα genes controlling CYP3A4 expression.

We propose several novel miRNAs identified parallelly by at least three algorithms to the target analyzed genes. In particular, we found novel promising miRNAs which may be involved in the indirect PXR-mediated CYP3A4 gene expression such as miR-18a and miR-18b, miR-449a, miR-449b and miR-34a. We also hypothesize that some miRNAs may play the role of a master regulator of NRs since they are predicted to target more than three genes.

The identification of miRNAs determining CYP3A4 interindividual variability might be an important step toward progress in pharmacogenetics and personalized medicine.

* *Corresponding author*. Tel.: +420 495 067 334; fax: +420 495 067 170.
E-mail address: petr.pavek@faf.cuni.cz (P. Pavek).

1214-021X/$ – see front matter
http://dx.doi.org/10.1016/j.jab.2015.04.002

Introduction

MiRNAs are small (~22 nt), non-coding and evolutionarily conserved RNAs that post-transcriptionally regulate gene expression by binding to particular response elements mostly within the 3′-untranslated region (3′-UTR) of a target mRNA, resulting in mRNA degradation or translational inhibition (Bartel, 2004). Based on *in silico* prediction, it has been proposed that miRNAs regulate among 30–90% human genes (Lewis et al., 2005; Miranda et al., 2006). They are involved in the majority of cellular processes including cell differentiation, apoptosis, proliferation and carcinogenesis (Friedman and Jones, 2009). At the present time more than 2500 mature miRNAs have been identified in humans (miRBase, release 20) (Griffiths-Jones, 2006; Griffiths-Jones et al., 2008; Kozomara and Griffiths-Jones, 2014).

Cytochrome P450 CYP3A4 (CYP3A4) represents the most important drug metabolizing enzyme (DME), one which metabolizes approximately 50% of all current clinically used drugs. Substrates of CYP3A4 can be found almost in all pharmacotherapeutic groups and include key drugs used in the treatment of widespread and life-threating diseases such as macrolide antibiotics, immunosuppressive agents, HIV antivirals, statins, calcium channel blockers and numerous anticancer drugs (Martinez-Jimenez et al., 2007; Plant, 2007; Singh et al., 2013).

There is enormous interindividual variability in CYP3A4 mRNA and protein expression in the liver and intestine in the human population (Lindell et al., 2003; Bucher et al., 2011; Klein and Zanger, 2013). Besides environmental, hormonal, dietary and gender factors, structural or regulatory polymorphisms in CYP3A4 gene could help explain this interindividual variation. Genetic influence on the CYP3A4 phenotype has been estimated to account for 66–88% of the interindividual variation in phenotype (Klein and Zanger, 2013). However, polymorphisms in the CYP3A4 gene have low allele frequency in populations or lack a phenotypic effect (including reported CYP3A4*22 and *1B); genetic association studies have shown that genetic variability does not account for a significant part of CYP3A4 phenotype variability. In addition, comprehensive study of CYP3A4 mRNA, protein and catalytic activity levels in a microsomal bank suggests that regulatory rather than structural genetic factors contribute to CYP3A4 variability (Sy et al., 2002). However, major variants of two key transcription factors of the CYP3A4 gene – the pregnane X receptor and constitutive androstane receptor – have not been conclusively associated with significant effects on CYP3A4 expression variability (Wang and Sadee, 2012; Klein and Zanger, 2013). Consequently the enigma of the CYP3A4 variability in populations has been referred to as the ''missing heritability of CYP3A4 phenotype variability'' (Klein and Zanger, 2013).

Several nuclear receptors (NRs) have been shown to play an important regulatory role in both the constitutive and inducible expression of the CYP3A4 gene. Among the most studied NRs forming the regulatory network of CYP3A4 gene are the constitutive androstane receptor (CAR, NR1I3), pregnane X receptor (PXR, NR1I2), hepatocyte nuclear factor 4α (HNF4α, NR2A1), vitamin D receptor (VDR, NR1I1), small heterodimer partner (SHP, NR0B2), retinoid X receptor (RXRα, NR2B1) and glucocorticoid receptor α (GRα, NR3C1) (Pascussi et al., 2008; Zanger and Schwab, 2013; Pavek and Smutny, 2014). While many research papers have indicated the function of NRs or their coregulators/corepressors in the transcriptional regulation of CYP3A4 and the other DMEs, so far the regulation of NRs themselves has not been fully clarified.

Recently, microRNAs have opened up a new field of DMEs gene regulation (Nakajima and Yokoi, 2011; Smutny et al., 2013) and it has been suggested to provide a partial explanation regarding CYP3A4 interindividual variability (Pan et al., 2009; Ramamoorthy and Skaar, 2011). At the present time the growing body of evidence already indicates that miRNAs may participate in the complex regulatory network of DMEs expression, including CYP1B1 (Tsuchiya et al., 2006), CYP1A1 (Choi et al., 2012), CYP3A4 (Pan et al., 2009), CYP2E1 (Mohri et al., 2010), CYP2C8 (Zhang et al., 2012) and corresponding transcriptional regulators such as the nuclear receptors PXR (Takagi et al., 2008), VDR (Mohri et al., 2009; Pan et al., 2009), HNF4α (Takagi et al., 2010; Ramamoorthy et al., 2012; Wang and Burke, 2013), GR (Vreugdenhil et al., 2009) and RXRα (Ji et al., 2009; Adlakha et al., 2013; Oda et al., 2014).

In addition, SNPs in 3′-UTRs of CYP mRNA have recently been predicted to interfere with miRNA targeting, thus initiating a new era in miRNA pharmacogenetics (Ramamoorthy and Skaar, 2011). Although, several miRNAs have been experimentally confirmed to target CYP3A4 and NRs mRNAs, a comprehensive analysis of miRNAs predicted to target important NRs involved in CYP3A4 regulation based on recent bioinformatic algorithms has not as yet been reported.

In the present work, based on a comprehensive bioinformatic analysis of four different programs using the latest algorithms, we attempted to revise the current list of miRNAs predicted to target key important NRs involved in CYP3A4 regulation.

We identified many miRNAs that could target key NRs such as PXR, CAR, VDR, HNF4α, RXRα, SHP and GRα involved in CYP3A4 expression and thus hypothetically contribute to interindividual variability in CYP3A4 gene expression and in the variable metabolism and response to numerous drugs. Moreover, we highlighted miRNAs with a great probability of targeting selected genes with respect to their tissue expression, an emphasis which may be helpful for the future experimental validation of miRNAs-mediated regulation of CYP3A4 expression. Finally, we identified 4 miRNAs which may regulate at least five selected genes. These miRNAs may be crucial regulators of xenobiotic-induced NRs and consequently their xenobiotic-metabolizing target genes.

Methods

We used four different open-access online programs to carry out the bioinformatic analysis for the identification of miRNAs predicted to target NRs involved in the CYP3A4 regulation.

Theory/calculation

The **PITA** program (Kertesz et al., 2007), (http://genie.weizmann.ac.il/pubs/mir07/mir07_prediction.html) uses target site

accessibility as a critical factor in miRNA-mRNA interaction, which is rated based on interaction energy, ΔΔG value, representing the difference between microRNA-target hybridization energy and the energy required to make the target site accessible for miRNA binding. For our analysis we set as a minimum seed size of length 8 bases with no single mismatches but allowing a single G:U wobble. A zero flank was selected to obtain the target score, which additionally integrates multiple sites with ΔΔG scores for the particular miRNA on the same 3′-UTR of the target gene when more than one binding site exists for unique miRNA on 3′-UTR. The 3′-UTR of NRs were identified using RefSeq annotation from the genetic sequence database GenBank (http://www.ncbi.nlm.nih.gov/genbank/). The mature miRNAs sequences were downloaded from the miRBase Sequence database (release 20) (Griffiths-Jones, 2006; Griffiths-Jones et al., 2008; Kozomara and Griffiths-Jones, 2014). In our bioinformatic analysis we considered as functional a miRNA putative site with a target score equal to or below −10.

MirTarget2 is a prediction algorithm which uses a machine learning method such as a support vector machine (SVM) and which integrates relevant features associated with miRNA target binding identified by analyzing a large microarray dataset for algorithm training (Wang and El Naqa, 2008). This algorithm was further validated with independent experimental data. The predicted targets for miRNAs are scored to rank their evaluated significance. We used a target score equal to or above 60 as the confidence level for potentially functional miRNA targets. At the present time all the predicted targets based on the MirTarget2 algorithm have been imported into a freely accessible miRDB database (ver. 4.0; http://mirdb.org) (Wang, 2008). Currently, miRDB hosts mature miRNA sequences and miRNA nomenclature derived from miRBase (release 18) (Griffiths-Jones, 2006; Griffiths-Jones et al., 2008; Kozomara and Griffiths-Jones, 2014).

MiRanda (Betel et al., 2008; Betel et al., 2010; John et al., 2004), (http://www.microrna.org/microrna/getGeneForm.do) is another target prediction algorithm using several principles such as base pairing between miRNA and 3′-UTR of mRNA, the binding energy of the RNA–RNA duplex and the evolutionary conservation of the target site. Moreover, it promotes miRNAs with multiple binding sites within 3′-UTR. In our analysis we included these parameters: a mirSVR score equal to or below −0.1, conserved miRNA, PhastCons equal to or above 0 and at least 6mer seed complementarity. The last available version of miRanda (release 2010) uses mature miRNA sequences and miRNA nomenclature derived from miRBase (release 15) (Griffiths-Jones, 2006; Griffiths-Jones et al., 2008; Kozomara and Griffiths-Jones, 2014).

The **TargetScanHuman** algorithm, http://www.targetscan.org/, (release 6.2) is based on miRNA-mRNA complementarity and site conservation (Lewis et al., 2005; Grimson et al., 2007). Other characteristics used by the algorithm include type of seed matching, pairing contribution outside the seed region, AU content 30 nt upstream and downstream of the predicted site and the location of the sites to the nearest end of the 3′-UTR of the target gene. For our analysis we chose a context+ score equal to or below −0.20 and selected both conserved and non-conserved miRNAs. The current version of this algorithm uses mature miRNA sequences and miRNA nomenclature derived from miRBase (release 17) (Griffiths-Jones, 2006; Griffiths-Jones et al., 2008; Kozomara and Griffiths-Jones, 2014).

Since different miRBase database releases were used by different programs, to compare our results we standardized the miRNA nomenclature according to the recent names for each miRNAs provided by miRBase (release 20). The liver and intestine miRNA expression profiles were obtained from mimiRNA (Ritchie, 2010), (http://mimirna.centenary.org.au/mep/formulaire.html) integrating eight and two data files for liver and intestine (jejunum) tissues, respectively.

Results

In the present study we attempted to comprehensively update the current list of *in silico* identified miRNAs predicted to regulate NRs involved in CYP3A4 expression (Fig. 1) with respect to newly discovered human miRNAs and advances in bioinformatic prediction algorithms. (Pascussi et al., 2003; Vrzal et al., 2009; Pavek et al., 2010).

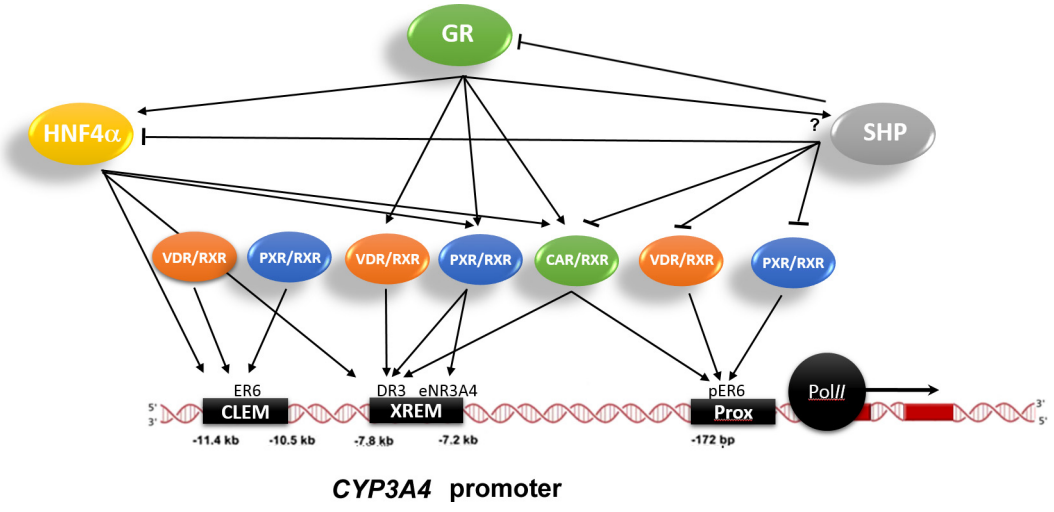

Fig. 1 – Nuclear receptor network involved in CYP3A4 gene transcription regulation.

Table 1 – *In silico* prediction of miRNAs targeting 3′-UTR of selected NRs employing four different algorithms.

NRs Gene	GenBank accession	3′-UTR length (bp)	Number of unique miRNAs[a]	Overlap (%)[b]
SHP (NR0B2)	NM_021969	367	66	2 (3.0)
VDR (NR1I1)	NM_000376	3225	384	23 (6.0)
PXR (NR1I2)	NM_003889	1302	176	25 (14.2)
CAR (NR1I3)	NM_001077482	137	24	3 (12.5)
HNF4α (NR2A1)	NM_000457	1725	323	46 (14.2)
RXRα (NR2B1)	NM_002957	3996	427	8 (1.9)
GRα (NR3C1)	NM_000176	3958	248	9 (3.6)

[a] Total number of unique mature miRNAs targeting a selected gene predicted by all the software.
[b] Total number of unique mature miRNAs targeting a selected gene predicted by at least two software.

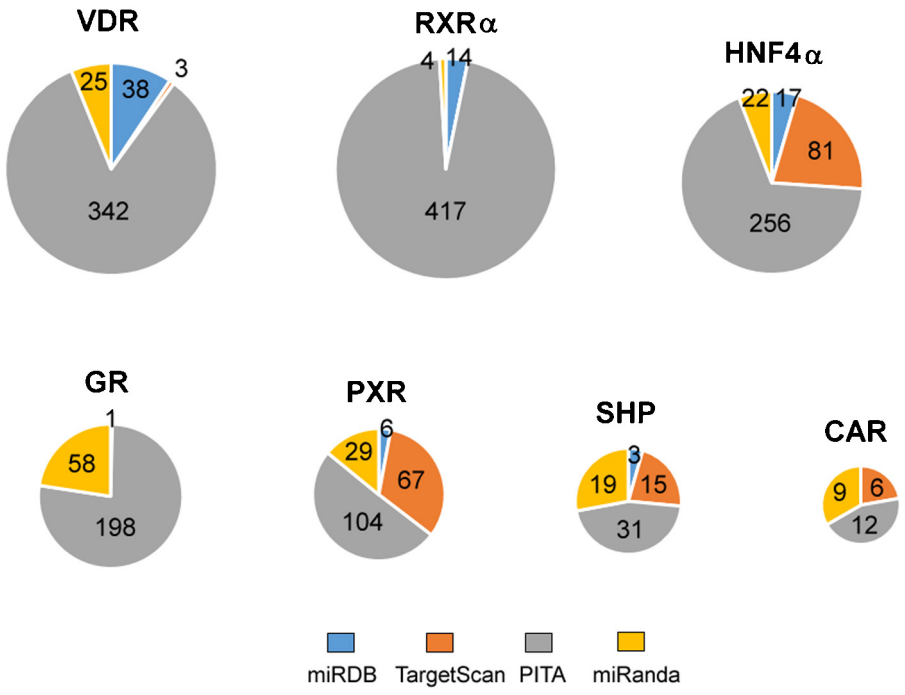

Fig. 2 – Total number of unique mature miRNAs targeting a selected gene predicted by each individual software.

Table 2 – Overview of mature miRNAs targeting selected genes predicted by at least three programs.

Selected genes/Predicted miRNAs	Prediction software				Sum	miRNA expression liver/intestine[a]
	miRDB	TargetScan	PITA	miRanda		
VDR (NR1I1)						
hsa-miR-214 (hsa-miR-214-3p)	1	0	1	1	3	+/+
PXR (NR1I2)						
hsa-miR-18a (hsa-miR-18a-5p)	0	1	1	1	3	+/+
hsa-miR-18b (hsa-miR-18b-5p)	0	1	1	1	3	+/–
hsa-miR-34a (hsa-miR-34a-5p)	0	1	1	1	3	+/+
hsa-miR-449a	0	1	1	1	3	–/n.f
hsa-miR-449b (hsa-miR-449b-5p)	0	1	1	1	3	n.f./n.f
HNF4α (NR2A1)						
hsa-miR-216b (hsa-miR-216b-5p)	1	0	1	1	3	n.f./n.f.
hsa-miR-4434	1	1	1	0	3	n.f./n.f.
hsa-miR-4516	1	1	1	0	3	n.f./n.f.
hsa-miR-4739	1	1	1	0	3	n.f./n.f.
hsa-miR-4756-5p	1	1	1	0	3	n.f./n.f.
hsa-miR-661	1	1	1	0	3	n.f./n.f.
hsa-miR-765	1	1	1	0	3	+/n.f.

[a] miRNA expression in the liver or intestine (jejunum) according to mimiRNA (Ritchie et al., 2010).
+ expression; – expression is not significant or undetectable; n.f. – not found.

Table 3 – Predicted miRNAs by at least one programs that target simultaneously five of the tested genes.

Predicted miRNAs	Prediction software				Sum	Genes
	miRDB	TargetScan	PITA	miRanda		
hsa-miR-3194-5p	0	0	1	0	1	GRα
	0	1	0	0	1	SHP
	0	0	1	0	1	VDR
	0	0	1	0	1	RXRα
	0	0	1	0	1	HNF4α
hsa-miR-5196-5p	0	0	1	0	1	GRα
	0	0	1	0	1	VDR
	0	0	1	0	1	RXRα
	0	0	1	0	1	PXR
	0	0	1	0	1	HNF4α
hsa-miR-6747-5p	0	0	1	0	1	GRα
	0	0	1	0	1	SHP
	0	0	1	0	1	VDR
	0	0	1	0	1	RXRα
	0	0	1	0	1	HNF4α
hsa-miR-6842-5p	0	0	1	0	1	SHP
	0	0	1	0	1	VDR
	0	0	1	0	1	RXRα
	0	0	1	0	1	PXR
	0	0	1	0	1	HNF4α

Using four different prediction programs, we found that all NRs selected for our study can be predicted to be regulated by miRNAs (Table 1 and Fig. 2, Table S1). Importantly, we found that 13 miRNAs were predicted to target selected NR by at least 3 programs (Table 2) and 116 miRNAs by at least 2 programs (Table S2). In addition, we considered the tissue expression of miRNAs predicted in at least three programs regarding the main organs expressing CYP3A4 including the liver and/or intestine (Table 2) obtained from miRNA tissue expression profiler, mimiRNA (Ritchie, 2010). A statistically significant correlation was found between the total number of unique miRNAs predicted by all programs and the length of 3′-UTR of genes ($r^2 = 0.71$) (Fig. 3).

Supplementary Tables S1 and S2 related to this article can be found, in the online version, at doi:10.1016/j.jab.2015.04.002.

We also analyzed whether some miRNAs may target multiple NRs; 32 miRNAs were predicted by at least one program to target four different NRs and 4 miRNAs were found to target five NRs (Table 3 and Table S3). These data thus demonstrate the potential existence of master regulator miRNAs in the regulation of NRs expression and secondarily in CYP3A4 expression.

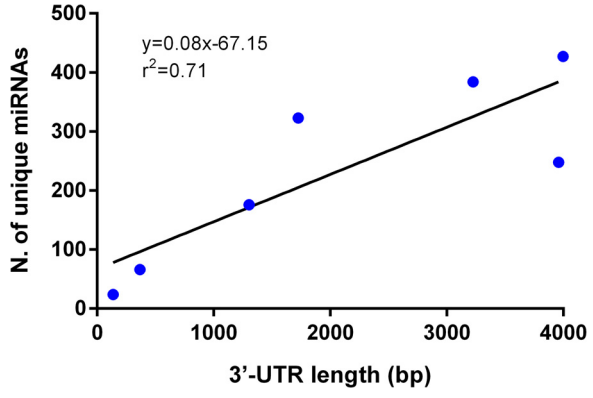

Fig. 3 – Correlation between 3′-UTR length (nt) of selected genes and the number of unique miRNAs predicted by all used algorithms.

Supplementary Table S3 related to this article can be found, in the online version, at doi:10.1016/j.jab.2015.04.002.

Taken together, we identified many new miRNAs targeting the 3′-UTR of the evaluated nuclear receptors mRNA using the latest computational algorithms and approaches.

Discussion

CYP3A4 metabolizes approximately 50% of all current clinically used drugs. Although CYP3A4 expression varies widely between individuals, the contribution of genetic or epigenetic factors remains unclear. Considerable interpersonal variability in CYP3A4 expression and enzyme activity has been attributed to genetic and non-genetic factors (Shimada et al., 1994; Schellens et al., 1988; Westlind et al., 1999). Genetic factors have been estimated to contribute to almost 88% of interindividual variation in its phenotype (Klein and Zanger, 2013), although until now no polymorphisms have been found to significantly affect CYP3A4 activity except for the recently described *22 or *1B alleles (www.cypalleles.ki.se/cyp3a4.htm) (Wang and Sadee, 2012). However, the function of the promoter SNP *CYP3A4*1B* (rs2740574, −392A>G, 5.4% in Caucasians and 35% in non-Caucasians) remains controversial. Similarly, although SNP *CYP3A4*22*, located in CYP3A4 intron 6 (rs35599367, 15389C>T, global minor allele frequency (MAF) 2.1%, 3–8% allele frequency in Caucasians), has been shown to be associated with decreased CYP3A4 mRNA hepatic expression, its low frequency limits more significant contribution to

overall CYP3A4 variability in populations (Wang and Sadee, 2012; Klein and Zanger, 2013; Zanger and Schwab, 2013).

Several studies identified coding or regulatory region SNPs in PXR and CAR, findings which suggest that these polymorphisms could have the potential to affect CYP3A4 expression. Nevertheless, these SNPs likely participate only in a portion of the inter-individual variability in CYP3A4 expression and enzyme activity, the situation being complicated by environmental conditions that affect the expression of multiple transcription factors (Klein et al., 2012; Wang and Sadee, 2012). A recent report by Klein et al. shows an association of the peroxisome proliferator-activated receptor-α (PPARA) SNP (rs4253728) with the CYP3A4 phenotype, although these novel genetic factors explain less than 10% CYP3A4 activity variation (Klein et al., 2012).

CYP3A4 expression appears to be post-transcriptionally regulated by miR-27b (Pan et al., 2009). In addition, CYP3A4 expression can be regulated indirectly by miR-148a or miR-27b *via* targeting PXR (Takagi et al., 2008; Smutny et al., 2013) or VDR (Pan et al., 2009), respectively. It is supposed that these regulatory molecules may contribute to the large inter-individual variability of hepatic CYP3A4, although comprehensive association studies are needed.

Moreover, SNPs in the 3′-UTR of CYP3A4 or NRs could also provide additional clues regarding variable CYP3A4 expression. Indeed, the occurrence of two SNPs – rs3732359 and rs3732360 – in the 3′-UTR region of PXR has been shown to be associated with higher midazolam clearance *in vivo* in African-American subjects (Oleson et al., 2010). Thus despite numerous studies on a genome-wide scale, the genetic factors contributing to CYP3A4 phenotype variability are still not completely understood.

In this paper we chose the principal NRs involved in the regulation of CYP3A4 expression to identify whether they could be targets of miRNAs using four different computational algorithms. We demonstrated that all selected NRs were predicted to be targets of many miRNAs (Table 1 and Table S1). The extensive number of predicted miRNAs for each gene and the finding that more targets were predicted for several miRNAs (*e.g.* miR-3194-5p, miR-5196-5p, miR-6747-5p and miR-6842-5p; Table 3 and Table S3) suggest that miRNAs may form complex and mutually interconnected regulatory networks controlling xenobiotic detoxification. Similarly to the recent report, which correlated the length of 3′-UTR of drug metabolizing CYP mRNAs with the number of predicted miRNAs based on *in silico* approaches (Ramamoorthy and Skaar, 2011), we also confirmed that number of unique miRNAs likely targeting selected NRs correlates significantly with the length of 3′-UTR of NR mRNAs (Fig. 3).

Another finding of our analysis is that different algorithms predicted a different number of miRNAs for the selected target gene (Table 1). This interalgorithm variability may be explained by at least two factors. Firstly, the total score of miRNA-mRNA interactions is calculated based on the different emphases placed on the particular parameters used by each program such as complementarity of miRNA/mRNA, evolutionary conservation and secondary structure accessibility (see Section 'Methods'). Secondly, the different mirBase database releases used by PITA (rel. 20), miRDB (rel. 18), TargetScan (rel. 17), miRanda (rel. 15) may also account for variability among programs.

As mentioned elsewhere (Witkos et al., 2011), prediction criteria for miRNA–mRNA interaction are still not fully elucidated; consequently, there is no universal prediction program (Witkos et al., 2011). Since, computational algorithms continue to lack sufficient sensitivity and specificity as well as rely on various prediction principles, it is a common practice of experimental scientists to use multiple prediction tools and focus on their intersection to reduce false positive/negative results (Dweep et al., 2013). For our work, we proposed that miRNAs predicted by at least three programs to target select gene would be a promising candidate for experimental validation, although, we realized that some programs share similar prediction criteria, so the strength of the prediction may vary with different combinations of programs. Moreover, until now, none of miRNAs presented in Table 2 were confirmed experimentally to directly target predicted genes which warrant further studies.

Interestingly, as shown in Table 2, we identified PXR as hypothetical target for miR-34a *in silico*. Recently, Lamba et al. reported that expression miR-34a negatively correlates with expression of NRs (*e.g.* PXR and HNF4α) and CYPs (*e.g.* CYP3A4 and CYP2C9) in human liver samples ($n = 50$) suggesting miR-34a as potential factor in interindividual variability of DMEs (Lamba et al., 2014). Moreover, miR-34a negatively regulates expression of other key transcription factors of DMEs such as RXRα (Oda et al., 2014) and HNF4α (Takagi et al., 2010; Ramamoorthy et al., 2012; Wang and Burke, 2013) in the liver. Besides miRNA-34a, miR-449a was validated to alter HNF4α expression (Ramamoorthy et al., 2012; Wang and Burke, 2013). In our *in silico* analysis, this miRNA was predicted to strongly target 3′-UTR of PXR mRNA implying potential complex indirect role of miR-449a in CYP3A4 regulation.

To date, the vast majority of studies confirming miRNA-directed gene regulation have been performed using *in vitro* cellular models. In these experiments, the ectopic expression of the miRNA of interest is performed in cells and then changes in the relative levels of presumable target mRNAs and corresponding proteins are examined. Therefore there is an urgent need to corroborate these findings with *in vivo* studies.

Transcription factors such as PXR, CAR, GRα, HNF4α, VDR, SHP and RXRα coordinately sense environmental or hormonal stimuli to fine-tune the network controlling CYP3A4 expression. Therefore genetic variants or epigenetic factors of more genes rather than one individual factor coordinately result in a substantial variation in CYP3A4 activity (Lamba et al., 2010; Sadee, 2012). MiRNAs predominantly bind to the 3′-UTR of mRNAs; however, it also appears to bind to the complementary sequences in coding regions, promoters and 5′-UTR sequences (Kim et al., 2008; Rigoutsos, 2009; Da Sacco and Masotti, 2012). Thus the study of the ''missing hereditability of CYP3A4 variation'' has been extended yet again in complexity. It seems that system approaches rather than molecular biology can help us in the future to address this enigma.

Conclusion

The present data provides important insights into the potential complexity of the miRNA-mediated regulation of NRs with an impact on CYP3A4 interindividual variability.

Based on findings such as those in our study, a growing body of evidence confirming NRs as significant targets for miRNAs can be anticipated. Further studies should confirm whether these hypothetical miRNA-mRNA interactions contribute to the interindividual variability of CYP3A4 gene expression and to the variable metabolism and response to the numerous drugs biotransformed by CYP3A4. In addition, since the studied NRs are also involved in the transcriptional regulation of other key cytochrome P450 enzymes such as phase I enzymes CYP3A5, CYP2C9, CYP2C8, CYP2C19 and CYP2B6 as well as phase II conjugation enzymes UGT1A1 and SULT2A1, results like those presented here may have pharmacogenetic implications for a much larger range of current medications.

Conflict of interest

Authors declare no conflict of interest.

Acknowledgements

The manuscript has been read and approved by all the authors and all authors contributed to the paper. The research has been funded by the Czech Scientific Agency (No. 303/12/G163 to P.P.) and SVV 260 185.

REFERENCES

Adlakha, Y.K., Khanna, S., Singh, R., Singh, V.P., Agrawal, A., Saini, N., 2013. Pro-apoptotic miRNA-128-2 modulates ABCA1, ABCG1 and RXRalpha expression and cholesterol homeostasis. Cell Death Dis. 4, e780.

Bartel, D.P., 2004. MicroRNAs: genomics, biogenesis, mechanism, and function. Cell 116, 281–297.

Betel, D., Wilson, M., Gabow, A., Marks, D.S., Sander, C., 2008. The microRNA.org resource: targets and expression. Nucleic Acids Res. 36, D149–D153.

Betel, D., Koppal, A., Agius, P., Sander, C., Leslie, C., 2010. Comprehensive modeling of microRNA targets predicts functional non-conserved and non-canonical sites. Genome Biol. 11, R90.

Bucher, J., Riedmaier, S., Schnabel, A., Marcus, K., Vacun, G., Weiss, T.S., Thasler, W.E., Nussler, A.K., Zanger, U.M., Reuss, M., 2011. A systems biology approach to dynamic modeling and inter-subject variability of statin pharmacokinetics in human hepatocytes. BMC Syst. Biol. 5, 66.

Da Sacco, L., Masotti, A., 2012. Recent insights and novel bioinformatics tools to understand the role of microRNAs binding to 5′ untranslated region. Int. J. Mol. Sci. 14, 480–495.

Dweep, H., Sticht, C., Gretz, N., 2013. *In-silico* algorithms for the screening of possible microRNA binding sites and their interactions. Curr. Genomics 14, 127–136.

Friedman, J.M., Jones, P.A., 2009. MicroRNAs: critical mediators of differentiation, development and disease. Swiss Med. Wkly. 139, 466–472.

Griffiths-Jones, S., 2006. miRBase: the microRNA sequence database. Methods Mol. Biol. 342, 129–138.

Griffiths-Jones, S., Saini, H.K., van Dongen, S., Enright, A.J., 2008. miRBase: tools for microRNA genomics. Nucleic Acids Res. 36, D154–D158.

Grimson, A., Farh, K.K., Johnston, W.K., Garrett-Engele, P., Lim, L.P., Bartel, D.P., 2007. MicroRNA targeting specificity in mammals: determinants beyond seed pairing. Mol. Cell 27, 91–105.

Choi, Y.M., An, S., Lee, E.M., Kim, K., Choi, S.J., Kim, J.S., Jang, H. H., An, I.S., Bae, S., 2012. CYP1A1 is a target of miR-892a-mediated post-transcriptional repression. Int. J. Oncol. 41, 331–336.

Ji, J., Zhang, J., Huang, G., Qian, J., Wang, X., Mei, S., 2009. Over-expressed microRNA-27a and 27b influence fat accumulation and cell proliferation during rat hepatic stellate cell activation. FEBS Lett. 583, 759–766.

John, B., Enright, A.J., Aravin, A., Tuschl, T., Sander, C., Marks, D. S., 2004. Human microRNA targets. PLoS Biol. 2, e363.

Kertesz, M., Iovino, N., Unnerstall, U., Gaul, U., Segal, E., 2007. The role of site accessibility in microRNA target recognition. Nat. Genet. 39, 1278–1284.

Kim, D.H., Saetrom, P., Snove Jr., O., Rossi, J.J., 2008. MicroRNA-directed transcriptional gene silencing in mammalian cells. Proc. Natl. Acad. Sci. U. S. A. 105, 16230–16235.

Klein, K., Zanger, U.M., 2013. Pharmacogenomics of cytochrome P450 3A4: recent progress toward the missing heritability problem. Front. Genet. 4, 12.

Klein, K., Thomas, M., Winter, S., Nussler, A.K., Niemi, M., Schwab, M., Zanger, U.M., 2012. PPARA: a novel genetic determinant of CYP3A4 *in vitro* and *in vivo*. Clin. Pharmacol. Ther. 91, 1044–1052.

Kozomara, A., Griffiths-Jones, S., 2014. miRBase: annotating high confidence microRNAs using deep sequencing data. Nucleic Acids Res. 42, D68–D73.

Lamba, V., Panetta, J.C., Strom, S., Schuetz, E.G., 2010. Genetic predictors of interindividual variability in hepatic CYP3A4 expression. J. Pharmacol. Exp. Ther. 332, 1088–1099.

Lamba, V., Ghodke, Y., Guan, W., Tracy, T.S., 2014. microRNA-34a is associated with expression of key hepatic transcription factors and cytochromes P450. Biochem. Biophys. Res. Commun. 445, 404–411.

Lewis, B.P., Burge, C.B., Bartel, D.P., 2005. Conserved seed pairing, often flanked by adenosines, indicates that thousands of human genes are microRNA targets. Cell 120, 15–20.

Lindell, M., Karlsson, M.O., Lennernas, H., Pahlman, L., Lang, M. A., 2003. Variable expression of CYP and Pgp genes in the human small intestine. Eur. J. Clin. Invest. 33, 493–499.

Martinez-Jimenez, C.P., Jover, R., Donato, M.T., Castell, J.V., Gomez-Lechon, M.J., 2007. Transcriptional regulation and expression of CYP3A4 in hepatocytes. Curr. Drug Metab. 8, 185–194.

Miranda, K.C., Huynh, T., Tay, Y., Ang, Y.S., Tam, W.L., Thomson, A.M., Lim, B., Rigoutsos, I., 2006. A pattern-based method for the identification of microRNA binding sites and their corresponding heteroduplexes. Cell 126, 1203–1217.

Mohri, T., Nakajima, M., Takagi, S., Komagata, S., Yokoi, T., 2009. MicroRNA regulates human vitamin D receptor. Int. J. Cancer 125, 1328–1333.

Mohri, T., Nakajima, M., Fukami, T., Takamiya, M., Aoki, Y., Yokoi, T., 2010. Human CYP2E1 is regulated by miR-378. Biochem. Pharmacol. 79, 1045–1052.

Nakajima, M., Yokoi, T., 2011. MicroRNAs from biology to future pharmacotherapy: regulation of cytochrome P450s and nuclear receptors. Pharmacol. Ther. 131, 330–337.

Oda, Y., Nakajima, M., Tsuneyama, K., Takamiya, M., Aoki, Y., Fukami, T., Yokoi, T., 2014. Retinoid X receptor alpha in human liver is regulated by miR-34a. Biochem. Pharmacol. 90, 179–187.

Oleson, L., von Moltke, L.L., Greenblatt, D.J., Court, M.H., 2010. Identification of polymorphisms in the 3′-untranslated region of the human pregnane X receptor (PXR) gene

associated with variability in cytochrome P450 3A (CYP3A) metabolism. Xenobiotica 40, 146–162.
Pan, Y.Z., Gao, W., Yu, A.M., 2009. MicroRNAs regulate CYP3A4 expression via direct and indirect targeting. Drug Metab. Dispos. 37, 2112–2117.
Pascussi, J.M., Gerbal-Chaloin, S., Drocourt, L., Maurel, P., Vilarem, M.J., 2003. The expression of CYP2B6, CYP2C9 and CYP3A4 genes: a tangle of networks of nuclear and steroid receptors. Biochim. Biophys. Acta 1619, 243–253.
Pascussi, J.M., Gerbal-Chaloin, S., Duret, C., Daujat-Chavanieu, M., Vilarem, M.J., Maurel, P., 2008. The tangle of nuclear receptors that controls xenobiotic metabolism and transport: crosstalk and consequences. Annu. Rev. Pharmacool. Toxicol. 48, 1–32.
Pavek, P., Smutny, T., 2014. Nuclear receptors in regulation of biotransformation enzymes and drug transporters in the placental barrier. Drug Metab. Rev. 46, 19–32.
Pavek, P., Pospechova, K., Svecova, L., Syrova, Z., Stejskalova, L., Blazkova, J., Dvorak, Z., Blahos, J., 2010. Intestinal cell-specific vitamin D receptor (VDR)-mediated transcriptional regulation of CYP3A4 gene. Biochem. Pharmacol. 79, 277–287.
Plant, N., 2007. The human cytochrome P450 sub-family: transcriptional regulation, inter-individual variation and interaction networks. Biochim. Biophys. Acta 1770, 478–488.
Ramamoorthy, A., Skaar, T.C., 2011. *In silico* identification of microRNAs predicted to regulate the drug metabolizing cytochrome P450 genes. Drug Metab. Lett. 5, 126–131.
Ramamoorthy, A., Li, L., Gaedigk, A., Bradford, L.D., Benson, E.A., Flockhart, D.A., Skaar, T.C., 2012. *In silico* and *in vitro* identification of microRNAs that regulate hepatic nuclear factor 4alpha expression. Drug Metab. Dispos. 40, 726–733.
Rigoutsos, I., 2009. New tricks for animal microRNAS: targeting of amino acid coding regions at conserved and nonconserved sites. Cancer Res. 69, 3245–3248.
Ritchie, W., Flamant, S., Rasko, J.E., 2010. mimiRNA: a microRNA expression profiler and classification resource designed to identify functional correlations between microRNAs and their targets. Bioinformatics 26, 223–227.
Sadee, W., 2012. The relevance of missing heritability in pharmacogenomics. Clin. Pharmacol. Ther. 92, 428–430.
Shimada, T., Yamazaki, H., Mimura, M., Inui, Y., Guengerich, F. P., 1994. Interindividual variations in human liver cytochrome P-450 enzymes involved in the oxidation of drugs, carcinogens and toxic chemicals: studies with liver microsomes of 30 Japanese and 30 Caucasians. J. Pharmacol. Exp. Ther. 270, 414–423.
Schellens, J.H., Soons, P.A., Breimer, D.D., 1988. Lack of bimodality in nifedipine plasma kinetics in a large population of healthy subjects. Biochem. Pharmacol. 37, 2507–2510.
Singh, T.R., Gupta, A., Suravajhala, P., 2013. Challenges in the miRNA research. Int. J. Bioinform. Res. Appl. 9, 576–583.
Smutny, T., Mani, S., Pavek, P., 2013. Post-translational and post-transcriptional modifications of pregnane X receptor (PXR) in regulation of the cytochrome P450 superfamily. Curr. Drug Metab. 14, 1059–1069.
Sy, S.K., Ciaccia, A., Li, W., Roberts, E.A., Okey, A., Kalow, W., Tang, B.K., 2002. Modeling of human hepatic CYP3A4 enzyme kinetics, protein, and mRNA indicates deviation from log-normal distribution in CYP3A4 gene expression. Eur. J. Clin. Pharmacol. 58, 357–365.
Takagi, S., Nakajima, M., Mohri, T., Yokoi, T., 2008. Post-transcriptional regulation of human pregnane X receptor by micro-RNA affects the expression of cytochrome P450 3A4. J. Biol. Chem. 283, 9674–9680.
Takagi, S., Nakajima, M., Kida, K., Yamaura, Y., Fukami, T., Yokoi, T., 2010. MicroRNAs regulate human hepatocyte nuclear factor 4alpha, modulating the expression of metabolic enzymes and cell cycle. J. Biol. Chem. 285, 4415–4422.
Tsuchiya, Y., Nakajima, M., Takagi, S., Taniya, T., Yokoi, T., 2006. MicroRNA regulates the expression of human cytochrome P450 1B1. Cancer Res. 66, 9090–9098.
Vreugdenhil, E., Verissimo, C.S., Mariman, R., Kamphorst, J.T., Barbosa, J.S., Zweers, T., Champagne, D.L., Schouten, T., Meijer, O.C., de Kloet, E.R., Fitzsimons, C.P., 2009. MicroRNA 18 and 124a down-regulate the glucocorticoid receptor: implications for glucocorticoid responsiveness in the brain. Endocrinology 150, 2220–2228.
Vrzal, R., Stejskalova, L., Monostory, K., Maurel, P., Bachleda, P., Pavek, P., Dvorak, Z., 2009. Dexamethasone controls aryl hydrocarbon receptor (AhR)-mediated CYP1A1 and CYP1A2 expression and activity in primary cultures of human hepatocytes. Chem. Biol. Interact. 179, 288–296.
Wang, D., Sadee, W., 2012. The making of a CYP3A biomarker panel for guiding drug therapy. J. Personal. Med. 2, 175–191.
Wang, X., 2008. miRDB: a microRNA target prediction and functional annotation database with a wiki interface. RNA 14, 1012–1017.
Wang, X., El Naqa, I.M., 2008. Prediction of both conserved and nonconserved microRNA targets in animals. Bioinformatics 24, 325–332.
Wang, Z., Burke, P.A., 2013. The role of microRNAs in hepatocyte nuclear factor-4alpha expression and transactivation. Biochim. Biophys. Acta 1829, 436–442.
Westlind, A., Lofberg, L., Tindberg, N., Andersson, T.B., Ingelman-Sundberg, M., 1999. Interindividual differences in hepatic expression of CYP3A4: relationship to genetic polymorphism in the 5′-upstream regulatory region. Biochem. Biophys. Res. Commun. 259, 201–205.
Witkos, T.M., Koscianska, E., Krzyzosiak, W.J., 2011. Practical aspects of microRNA target prediction. Curr. Mol. Med. 11, 93–109.
Zanger, U.M., Schwab, M., 2013. Cytochrome P450 enzymes in drug metabolism: regulation of gene expression, enzyme activities, and impact of genetic variation. Pharmacol. Ther. 138, 103–141.
Zhang, S.Y., Surapureddi, S., Coulter, S., Ferguson, S.S., Goldstein, J.A., 2012. Human CYP2C8 is post-transcriptionally regulated by microRNAs 103 and 107 in human liver. Mol. Pharmacol. 82, 529–540.

4. Post-translational and post-transcriptional modifications of pregnane X receptor (PXR) in regulation of the cytochrome P450 superfamily.

Smutny T, Mani S, Pavek P. Post-translational and post-transcriptional modifications of pregnane X receptor (PXR) in regulation of the cytochrome P450 superfamily. (2013) Curr Drug Metab., 14(10):1059-69.
(IF 2013: **3.487**)

NRs are regulated not only by a direct ligand binding but also indirectly via post-translational modifications governed by cell singling pathways. PXR was reported to be a subject for phosphorylation, SUMOylation, ubiquitination and acetylation. In the presented review, we extensively summarized the effect of these modifications on PXR-mediated CYP regulation.

The knowledge about the regulatory network controlling PXR (and other NRs) functions can shed a light on possible modifications of *in vitro* liver models enabling to improve their properties towards more *in vivo*-like phenotype.

Published in final edited form as:
Curr Drug Metab. 2013 December ; 14(10): 1059–1069.

Post-translational and Post-transcriptional Modifications of Pregnane X Receptor (PXR) in Regulation of the Cytochrome P450 Superfamily

Tomas Smutny[a], **Sridhar Mani**[b], and **Petr Pavek**[a,*]

[a]Faculty of Pharmacy in Hradec Králové, Charles University in Prague, Heyrovského 1203, Hradec Králové 500 05, Czech Republic

[b]Albert Einstein Cancer Center, Albert Einstein College of Medicine, 1300 Morris Park Avenue, Chanin 302D-1, New York, New York 10461, USA

Abstract

Pregnane X receptor (PXR) is a member of the nuclear receptor (NR) superfamily of ligand-activated transcription factors and is activated by a huge variety of endobiotics and xenobiotics, including many clinical drugs. PXR plays key roles not only as a xenosensor in the regulation of both major phase I and II drug metabolism and transporters but also as a physiological sensor in the modulation of bile acid and cholesterol metabolism, glucose and lipid metabolism, and bone and endocrine homeostasis.

Post-translational modifications such as phosphorylation have been shown to modulate the activity of many NRs, including PXR, and constitute an important mechanism for crosstalk between signaling pathways and regulation of genes involved in both xenobiotic and endobiotic metabolism. In addition, microRNAs have recently been shown to constitute another level of PXR activity regulation.

The objective of this review is to comprehensively summarize current understanding of post-transcriptional and post-translational modifications of PXR in regulation of xenobiotic-metabolizing cytochrome P450 (CYP) genes, mainly in hepatic tissue. We also discuss the importance of PXR in crosstalk with cell signaling pathways, which at the level of transcription modify expression of genes associated with some physiological and pathological stages in the organs. Finally, we indicate that these PXR modifications may have important impacts on CYP-mediated biotransformation of some clinically used drugs.

Keywords

Cytochrome P450; gene regulation; induction; post-transcriptional; post-translational modification; pregnane X receptor; PXR

*Address correspondence to this author at the Faculty of Pharmacy in Hradec Králové, Charles University in Prague, Heyrovského 1203, Hradec Králové 500 05, Czech Republic, European Union; Tel: 00420 495067334; Fax: 00420495067170; pavek@faf.cuni.cz.

CONFLICT OF INTEREST

The authors confirm that this article content has no conflicts of interest.

We declare no conflict of interest.

1. INTRODUCTION

Most of the detoxification mechanisms are under control of nuclear receptors (NRs) or ligand-activated transcription factors that trigger transcriptional upregulation of drug-metabolizing enzymes (DMEs). In 1994, aryl hydrocarbon receptor (AHR) and constitutive androstane receptor (CAR) were the first xenosensors discovered, although their roles as the molecular targets of the classic hepatic enzymes inductors has been discovered later on [1,2]. Four years later, mouse *Pxr* was discovered as an orphan nuclear receptor from a mouse liver cDNA library according to its sequence homology to ligand-binding domains of known nuclear receptors [3]. In parallel, the human ortholog of PXR was independently described by three research groups and termed the pregnane activated receptor (PAR), the pregnane X receptor (PXR), or the steroid and xenobiotic receptor (SXR) [4–6].

More recently, PXR receptor has been shown to be a critical factor in transactivation of most important DMEs and transporters. In addition, a growing body of evidence suggests its role in the regulation of endogenous metabolism.

2. PREGNANE X RECEPTOR

2.1. PXR – General Remarks

Pregnane X receptor (PXR, NR1I2) is a member of the nuclear receptors superfamily of ligand-dependent transcriptional factors, subfamily NR1I, and it has been identified as a xenobiotic/metabolite sensor regulating the expression of a wide variety of genes involved in transport, metabolism and elimination of xenobiotics and some endogenous substances [7–9].

It has been shown that PXR is predominantly expressed in the liver and intestine [3–6,10]. This expression pattern correlates with major cytochrome P450 (CYP) genes which encode important enzymes involved in the metabolism of xenobiotics. However, to a much lesser extent, PXR may also be found in such other tissues as kidney, stomach, brain, bone, lung, uterus, heart, adrenal glands, bone marrow, skeletal muscle, and testis [10–12].

Like other typical nuclear receptors, PXR contains both a DNA-binding domain (DBD) at the N-terminus that facilitates binding to DNA responsive elements and a ligand-binding domain (LBD) at the C-terminus which is responsible for ligand binding and interaction with co-regulators [13] (Fig. 1). The crystal structure of human PXR-LBD is characterized by a ligand-binding cavity which is notably larger in volume compared with that of other NRs and is hydrophobic with only small number of polar residues. Thus, the character of the ligand-binding pocket reflects the structure of PXR ligands which are commonly hydrophobic with several polar groups [13–15].

The mechanism underlying PXR transactivation of target genes involves ligand binding to PXR which in turn results in binding to a regulatory DNA sequence termed a response element within the promoter of a target gene. However, PXR requires heterodimerization with retinoid X receptor (RXR) for high-affinity DNA binding [13,16].

It has been reported that coactivators such as the steroid receptor coactivator-1 (SRC-1) [3,5], SRC-2, SRC-3 and the peroxisome proliferator-activated receptor-binding protein (PBP) associate with activated PXR and promote recruitment of transcription machinery at the promoters of the target genes by decompacting the chromatin structure [17]. This could occur through endogenous histone acetyltransferase (HAT) activity of coactivators or by facilitating recruitment of other regulators with HAT activity to activated PXR [17]. In contrast, the silencing mediator for retinoid and thyroid receptors (SMRT) binds to PXR in

the absence of ligand and suppresses its transcriptional activity [18,19]. Similarly, small heterodimer partner (SHP), an atypical orphan nuclear receptor, has been shown to interact directly with PXR and repress its activity [20].

2.2. Pregnane X Receptor and Regulation of Xenobiotic and Endogenous Metabolism

CYP3A4 and several other CYP isoforms, such as CYP2B6 [21] and CYP2C isoforms [18,22], are induced through PXR activation in response to a myriad of natural and synthetic compounds [23,24]. In humans, CYP3A4 is the most important CYP enzyme involved in drug metabolism. There are two main reasons: (*i*) CYP3A4 is abundantly expressed in liver and intestine, which are major organs participating in xenobiotic metabolism; and (*ii*) it has broad substrate specificity responsible for biotransformation of more than 50% of all clinically used drugs [25–27]. In addition to regulating phase I DMEs, PXR also controls the expression of some phase II DMEs and transporters for xenobiotic detoxification and elimination [9]. These facts highlight a protective role of PXR against potentially toxic compounds jeopardizing the body. However, PXR also constitutes a molecular basis for potential drug–drug, herb–drug and food–drug interactions in cases when patients use combinations of chemicals. One PXR activator might, for instance, increase target CYP expression, which could then promote the clearance of other concurrently administered drugs and lead to therapeutic failure in patients. For that reason, drug interactions pose significant obstacles in developing new drug candidates and it is necessary to characterize these in early phases of preclinical development [8,23,28]. In addition to direct binding and activation of PXR, many xenobiotics alter multiple kinase pathways involved in post-translational modifications (PTMs) of PXR, thus resulting in alterations of PXR transcriptional activity and further contributing to drug–drug interactions [29].

In addition to its central role in regulation of xenobiotic metabolism, PXR also crosstalks with endogenous metabolism and inflammation [30–32]. It has been shown that PXR is also involved in modulation of hepatic glucose and lipid metabolism [7,33,34], bone homeostasis [35], endocrine homeostasis [36], and other processes [7,8,12,13,35].

3. POST-TRANSLATIONAL REGULATION OF PXR

While it is well known that the transcriptional activity of PXR is governed by direct binding of ligands, many reports have indicated that cellular signaling pathways modulate the functions of nuclear receptors, including PXR. These aspects shed some light on possible non-liganded mechanisms of receptor activation [37]. Herein, we comprehensively summarize recent evidence interfacing cell signaling pathways with PXR post-translational modification and its impact on CYPs regulation. Thus far, PXR has been shown to be a subject for phosphorylation, SUMOylation, ubiquitination and acetylation (Table 1; Fig. 1).

3.1. Phosphorylation of PXR

It is well established that many nuclear receptor superfamily members exist as phosphoproteins and that their phosphorylation is a dynamically changing process modulating their activities [50].

There is a growing body of evidence that site-specific phosphorylation of PXR provides an important mechanism for PXR-mediated regulation of CYP expression. It has been shown that series of kinases such as p70 S6K [42,45,51], PKA [43–45], PKC [38,45], Cdk2 [39,40,52] and Cdk5 [41] can phosphorylate and regulate PXR transcriptional activity. Along that same line, immunopurified human PXR also has been found to be a target for phosphorylation by such other kinases as glycogen synthase kinase 3 (GSK3), casein kinase II (CK2) and Cdk1 [44] (Fig. 1).

The effects of site-specific phosphorylation of PXR by kinases interfere with a wide variety of its functions involving subcellular localization, dimerization, DNA binding, and co-regulator interaction [38,43–45,47,51]. While phosphorylation generally may contribute to both activation or termination activity in NRs [50], direct phosphorylation in the case of human PXR leads mostly to negative response in its transcriptional activity [9].

3.1.1. PXR Phosphorylation and Inflammation—The activity of hepatic CYP genes is considerably suppressed during inflammation [53]. Recent data give rise to a hypothesis of there being bidirectional negative crosstalk between PXR and NF-κB, the known transcriptional regulator of immune and inflammatory responses, and thus making a connection between xenobiotic metabolism and inflammatory disease [30–32].

Importantly, the cyclic AMP-dependent protein kinase A (PKA) is part of the glucagon mediated pathway and has been shown to have increased activity during acute inflammation [44,54]. There are inconsistent results regarding PKA signaling's effect on the modulation of PXR transcriptional activity via phosphorylation. In mice, activation of the PKA signaling potentiated Pxr-mediated Cyp3a11 gene expression in mouse hepatocytes [43,44]). However, it has a repressive effect on PXR/Pxr transcriptional activity in both human and rat hepatocytes, which indicates PKA to work in a species-specific manner in regulating PXR/Pxr activity [44]. In addition, human PXR was shown to be a substrate for PKA, which was confirmed by *in vitro* kinase assay [43,44]. It was further discovered that PXR exists as a phosphoprotein *in vivo* and that the extent of threonine phosphorylation is enhanced by PKA signaling, which was confirmed by Western blot analysis using specific antibodies directed against phosphothreonine [44]. Finally, PKA signaling promotes interaction of mouse Pxr with coactivators such as SRC-1 and PBP [43] and NCoR with human PXR [44]. Taken together, these results demonstrate that PKA signaling probably modulates PXR activity through modulation of its phosphorylation status, but specific phosphorylation sites for PKA remain obscure [43–45].

It is worthy of note that the phenomenon of PXR activity repression in both cell-based reporter gene assays and in hepatocytes was also observed when protein kinase C (PKC)-dependent intra-cellular signaling pathway, which is also involved in inflammation, was activated [38]. The initiation of PKC signaling during inflammation is mediated upon cytokines stimulation of hepatocytes. In particular, IL-1, IL-6 and TNF-α activate PKC signaling in hepatocytes [55]. It has been well documented that release of proinflammatory cytokines downregulates CYP genes expression in liver [56–58]. The potential molecular basis for negative regulation of PXR transcription activity by PKC includes increasing the strength of interaction between PXR and corepressor NCoR while also disrupting ligand-dependent interaction between PXR and SRC-1. The role of alteration in the phosphorylation status in PXR or co-factors (NCoR and SRC-1) by PKC signaling remains to be evaluated. Interestingly, treatment of hepatocytes with okadaic acid (OA), the known inhibitor of protein phosphatase PP1/2A, diminishes ligand-dependent PXR activity, thus further suggesting a role of protein phosphorylation in regulating PXR activity [38].

Taken together, the available data shed light on the mechanism involved in repressing CYP genes associated with inflammation and presumed molecular links between signaling cascades and CYP expression in the liver.

3.1.2. PXR Phosphorylation and Cell Proliferation—Numerous studies have shown that CYPs are greatly reduced during liver development or regeneration [59]. It has been well established that downregulation of CYP isoenzymes' activities occurs when hepatocytes are exposed to human growth factors such as HGF [60], which potently induces

hepatocyte proliferation [61]. Similarly, findings linking EGF and TGFα with alteration of CYP expression in human hepatocytes have also been reported [62,63].

In recent work pioneered by Lin *et al*. [39], these authors speculate that the activity of PXR changes while cells pass through the various phases of the cell cycle. That study provided compelling evidence about a connection between attenuation of PXR activity during cell cycle progression with the activity of cyclin-dependent kinase 2 (Cdk2), which is one of the key regulators of the cell cycle [39]. The study showed that PXR-mediated activation of CYP3A4 luciferase gene reporter in transient transfection assays was decreased with activation of Cdk2 in HepG2 cells. Consistently, PXR transcriptional activity was substantially reduced in the S phase of the cell cycle, which is when Cdk2 activity increases. In addition, PXR protein was found to be a good substrate for Cdk2 in *in vitro* kinase assay. A putative Cdk2 phosphorylation site at Ser350 position was suggested, but this does not exclude that other phosphorylation sites for Cdk2 may exist within PXR. Furthermore, the phosphorylation-deficient mutation (S350A) rendered partial resistance to the suppressive effects of Cdk2 on activation of the CYP3A4 luciferase gene reporter. By contrast, phosphomimetic mutation (S350D) negatively altered PXR function [39].

Similarly, a study by Sugatani *et al*. [40] provides evidence that Cdk2 negatively regulates the expression of several genes related to xenobiotic metabolism. In contrast to Cdk4, silencing of Cdk2 by siRNA led to upregulation of CYP3A4 and CYP2B6 protein levels in HepG2 cells. Moreover, the treatment of HepG2 cells with HGF, which has been shown to be an anti-mitogenic factor for some tumor cell lines, led to negative regulation of Cdk2 activity. It is likely this occurred via increased expression of p16, p21 and p27, the known Cdk2/Cdk4 inhibitors [40,64], and upregulation of CYP2B6 expression [40]. Importantly, this effect is the inverse of the effect observed in human hepatocytes, where HGF is a strong mitogen and attenuates the expression and activity of CYP isoenzymes [60,61]. In addition, the dissociation between the expression of activated Cdk2 and the expression of CYP2B6 and CYP3A4 was apparent when cells were released into a synchronous cell cycle after S phase blocking by thymidine, which further links cell cycle progression with negative effect on CYP expression [40].

In a more recent work, the mechanism behind the increased CYP3A4 expression in confluent Huh7 cells compared to sub-confluent control cells was examined. The evidence indicates that Cdk2 plays an important role in decreasing PXR-mediated CYP3A4 expression. In proliferative cells, silencing of Cdk2 by siRNA resulted in increase of both CYP3A4 and PXR proteins. Additionally, the PXR mutant S350A induced CYP3A4 expression in HepG2 cells [65].

In parallel, it was observed that Cdk5 negatively regulates PXR activity [41]. In contrast to Cdk2, Cdk5 is not involved in cell-cycle progression but primarily participates in development of the central nervous system and maintaining neuronal survival. The expression of Cdk5 is not restricted only to neuronal tissue since it has also been detected in other non-neuronal cells [66]. Dong *et al.* [41] indicated that Cdk5 and its regulatory subunit p35 are expressed together in HepG2 cells. Otherwise, when Cdk5 was overexpressed in this cell line, there was significant repression of both basal and rifampicin-induced PXR activity in transient transfection CYP3A4 gene reporter assay. In the same line, the increase in PXR activity was detected after siRNA-mediated downregulation of Cdk5. *In vitro* kinase assay outlined direct phosphorylation of PXR by Cdk5 as a possible mechanism in attenuating PXR transcriptional activity [41].

The PI3K-Akt pathway transduces signals from cell-surface tyrosine kinase receptors (TKRs) after their stimulation by insulin and other growth factors to downstream kinases

involved in regulating mRNA transcription and protein translation [54]. Recently, p70 S6K, a downstream kinase of the PI3K-Akt pathway was identified as a negative regulator of PXR transcriptional activity and was shown to directly phosphorylate PXR *in vitro*. Based on bioinformatics predictions, Thr57, a highly conserved phosphorylation site within DBD of human NRs as well as in PXR orthologues from various species, was found to be a putative phosphorylation site for p70 S6K. Site-directed mutagenesis provides a phosphomimetic mutant (T57D) of PXR, which leads to loss of PXR transcriptional activity in transient transfection CYP3A4 luciferase gene reporter in HepG2 cells probably due to disruption of PXR binding to the CYP3A4 gene promoter. Moreover, PXR mutant T57D exhibits a distinctive (punctate) nuclear distribution pattern and does not influence the interaction between PXR and transcriptional coactivator SRC-1. On the other hand, a phosphorylation-deficient mutation (T57A) of PXR renders partial resistance to p70 S6K-mediated negative regulation of PXR activity [42].

Mitogen-activated protein kinases (MAPKs) are serine/threonine kinases, which play an important role in transduction of extracellular signals from activated receptors on the cell surface to different cellular responses by interfering with various substrates such as transcriptional factors or downstream kinases. Importantly, MAPK signaling governs several cellular events, including growth, differentiation and survival. The best studied group of MAPKs consist of extracellular signal-regulated protein kinases (ERK1 and ERK2) [67]. Once activated, ERK may directly phosphorylate an array of NRs. Generally, this occurs at serine and threonine amino acid residues surrounded by proline and leading to either positive or negative regulation of NR transcriptional activity [68]. Based on *in silico* analysis of consensus phosphorylation sites for common protein kinases, Lichti-Kaiser *et al*. recently predicted human PXR to be a target for direct phosphorylation by a MAPK [45]. In our work, we have consistently observed that specific inhibition of mitogen-activated/extracellular signal-regulated kinase kinases 1/2 (MEK1/2), upstream kinases of ERK1/2, leads to activation of PXR transcriptional activity in gene reporter assay in HepG2 cells (*our unpublished data*). Thus, we provide indirect evidence for negative PXR regulation by MEKs. Taken together, we suppose that the MEK/ERK pathway negatively alters its transcriptional activity through direct PXR phosphorylation. Further studies, which will clarify the interplay between PXR and MEK/ERK signaling, are underway in our laboratory.

In an attempt to broaden our understanding of how phosphorylation regulates PXR activity, Lichti-Kaiser *et al*. [45] described comprehensively 18 potentially important serine and threonine amino acid residues within PXR which *in silico* prediction had suggested to be putative kinase phosphorylation sites. Six of the 18 potential phosphorylation sites within PXR were then selected for further characterization according to their ability to alter PXR transcriptional activity in gene reporter assay. This study showed that phosphorylation at Ser8, Thr57, Ser208, Ser305, Ser350 and Thr408 sites altered such various PXR functions as ability for DNA binding, RXRα heterodimerization, interaction with protein cofactors and PXR subcellular localization. Moreover, Thr90 was investigated due to its position within an evolutionarily highly conserved second zinc-finger motif of DBD-PXR. The effects of phosphomimetic and phosphorylation-deficient site mutants within PXR on distinct biological PXR roles are summarized in Table 1. It is unknown to date whether phosphorylation at these sites has any physiological significance, and subsequent studies should aim to prove the various effects of PXR modulation *in vivo*. The authors of the aforementioned work have reported some discrepancies among the data they have obtained. For instance, both phosphorylation-deficient and phosphomimetic mutations at Thr90 have lower binding ability to the CYP3A4 gene ER6 response element in comparison with wild-type PXR, although this does not substantially impact on PXR transcriptional activity in reporter gene assay [45]. Likewise, mutation at Ser350D disrupts RXRα heterodimerization with PXR but does not alter PXR's binding to its response element together with RXRα.

Only basal but not rifampicin-induced transactivation capacity of Ser350D mutant PXR was reported as repressed. These results differ from those observed by Lin *et al*. [39], wherein a phosphomimetic mutant at Ser350D decreased both basal and rifampicin-induced PXR activity in gene reporter assay. This could be due to the different model cell lines (CV-1 vs. HepG2 cells) used in the experiments [39,45].

In a follow-up study, Doricakova *et al*. [47] characterized the roles of other putative phosphorylation sites at T248, T422 [45] and Y249 of PXR. These sites were selected on the basis of *in silico* consensus kinase site prediction analysis. The effects on PXR biological functions using phosphomimetic and phosphorylation-deficient mutants of human PXR at the chosen amino acid residues are summarized in Table 1. These results suggest that residues T248 and T422 within PXR might be structural determinants for PXR function [47], which is in agreement with a report by Ueda *et al*. [46], who showed that hydrogen-bonding interaction of T248 with T422 in α-helix 12 is important for rifampicin-mediated activation of PXR. In addition, ligand-mediated recruitment of SRC-1 coactivator with AF2 domain of PXR was disrupted when phosphorylation-deficient mutants T248A or T248V were used in mammalian two-hybrid assay [46]. Notably, both phosphomimetic and phospho-deficient mutants at T422 abrogate PXR activity, thus indicating that phosphorylation at T422 is not likely a cause for loss of PXR function but that another mechanism should be presumed [47].

Recently, using mass spectrometry Elias *et al*. [69] identified S114, T133/135, S167, and S200 residues phosphorylated within PXR following an *in vitro* kinase assay using Cdk2 and phosphorylation at S114, T133, and T135 *in vivo* in the cells. Closer inspection showed that only dual phosphomimetic mutant T133D/T135D and phosphomimetic mutant S114D attenuate the transcriptional activity of PXR [69].

3.2. Ubiquitination of PXR

To date, the regulatory mechanisms involved in ubiquitination and degradation of PXR and their impacts on PXR-mediated CYP expression have been poorly investigated and require more experimental attention.

The degradation of proteins, including NRs, via proteasomes is targeted by conjugation of selected proteins with a polyubiquitin chain. This process is governed by a sequential pathway of three different enzymes (E1, E2 and E3) and results in covalent binding of ubiquitin to a selective substrate [70].

The first study searching for the connection between PXR and proteasome signaling has been carried out using a yeast two-hybrid protein interaction assay. It was shown that progesterone-occupied PXR interacts with suppressor for gal 1 (SUG1) [71], a known subunit of the 26S proteasome complex [72], but no interactions have been observed in the presence of the other PXR activators such as phthalic acid and nonylphenol. This finding highlights the fact that various PXR activators may alter PXR degradation differently, and it suggests another pathway in regulating PXR-mediated gene expression. The distinct interaction between PXR and SUG1 may be explained by conformational changes which occur within PXR upon binding of various agonists. Subsequently, the same group provided additional evidence supporting the hypothesis that PXR may be degraded by the proteasome. Notably, levels of PXR protein in nuclear fraction extracted from mouse mammary cancer (BALB-MC) cells were elevated when cells were treated with proteasome inhibitors. Consistent with that, overexpression of SUG1 in BALB-MC cells led to the appearance of proteolytic PXR fragments while the addition of proteasome inhibitor eliminated their generation, thus further suggesting an involvement of a proteasome. Moreover, the interaction between PXR and SUG1 depended on the presence of progesterone since

proteolytic PXR derivatives did not appear in the absence of this steroid [74], which is in agreement with results of Masuyama *et al* [71]. Finally, overexpression of SUG1 suppressed progesterone- and PXR-mediated activation of CYP3A1 transcription in gene reporter assays [74].

Recently, Staudinger *et al*. [29] showed that the level of ubiquitinated PXR was elevated in response to MG132, the known inhibitor of 26S proteasome. Notably, PKA activation also led to increase in ubiquitinated PXR protein. It is worthy of note that inhibition of proteasomal degradation inhibited PXR-mediated transcriptional activity in the activation of the CYP3A4 luciferase gene reporter construct [29].

Also noteworthy is that the E3 ubiquitin ligase RBCK1 (Ring-B-box-coiled-coil protein interacting with protein kinase C-1) directly binds and ubiquitinates PXR, resulting in PXR's degradation. The ectopic overexpression of RBCK1 in human hepatocytes leads to downregulation of rifampicin-mediated induction of PXR target genes (such as *CYP2C9* and *CYP3A4*), presumably as a result of endogenous PXR protein degradation although other mechanisms involved or effects on PXR synthesis remain to be elucidated [49].

Taken together, the results provide evidence that some PXR ligands could prolong the lifespan of PXR, in part by disrupting the association between PXR and the proteasome component SUG1 [71,74]. In addition, it has been suggested that PXR is ubiquitinated directly, which may constitute a plausible way for regulating PXR transcriptional activity [29,49].

3.3. SUMOylation of PXR

Post-translational modification of proteins through conjugation with ubiquitin-like proteins – and mainly involving the small ubiquitin-related modifier (SUMO) family members – has been demonstrated to play important roles in modulating NR function. In humans, the SUMO family is comprised of three members known as SUMO-1, SUMO-2 and SUMO-3. SUMOylation, like ubiquitination, utilizes reversible conjugation and deconjugation pathways, but they differ in the array of enzymes which are involved in these processes. For the most part, SUMOylated NRs display repression of their transcriptional activity, which suggests another level of the NRs-mediated regulation of their target genes [73,75].

The SUMO pathway constitutes a conserved enzymatic cascade wherein SUMO conjugation to the target protein is initiated by E1 activating enzyme, which transfers the activated SUMO protein to the E2 conjugating enzyme (Ubc9). Finally, SUMOlation of lysine amino group residues within the substrate is completed by the E2, which usually requires another enzyme among those referred to as E3 ligases. Inverse to conjugation, the substrate may be SUMO deconjugated, which is accomplished by such SUMO isopeptidases as SENP [73,75].

As in the case of phosphorylation, SUMOlyation of PXR could be involved in regulating CYP expression during inflammation. Four potential sites for SUMOylation within PXR have been found by bioinformatic analysis. Consequently, PXR was shown to be a substrate for SUMOylation using an *in vitro* approach [48]. Furthermore, subsequent results have provided evidence that PXR probably is SUMOylated *in vivo* by SUMO-3 chains after stimulation of the hepatocytes by TNFα, which further leads to PXR-mediated repression of NF-κB target gene expression. On the other hand, SUMOlation of PXR has little effect on CYP3A gene expression. These findings indicate an interesting way as to how PXR modification could preferentially regulate the inflammatory response without significant targeting of CYP3A's expression [48]. PXR is not a substrate for SUMO-1 (*unpublished data, Mani Lab, Albert Einstein College of Medicine, Bronx, NY*).

3.4. Acetylation of PXR

A recent study has focused on the involvement of acetylation in regulating PXR function [29,37]. This has been confirmed by other laboratories [52]. Acetylation constitutes a common mechanism for post-translational modification of proteins, including NRs [76]. It has been demonstrated that PXR is acetylated *in vivo* and rifampicin-mediated activation of PXR leads to its deacetylation. In addition, the histone deacetylase SIRT1 was shown to be associated with PXR and partially involved in PXR deacetylation [77]. The given data also suggest that other deacetylases may participate in deacetylation of PXR. To date, however, it is unclear which lysine residues undergo acetylation and which HATs are responsible for PXR acetylation [37].

4. POST-TRANSCRIPTIONAL REGULATION OF PXR

MicroRNAs (miRNA) are short (about 22 nucleotides in length), noncoding RNA molecules. They are capable of regulating target genes by binding to complementary regions of transcripts, which results in repression of their translation or in mRNA degradation. Based on computational prediction, it is estimated that about 60% of all human mRNAs may be under the control of miRNA [78].

Recent data indicate the possibility of miRNA-mediated PXR post-transcriptional regulation. Takagi *et al*. [79] have noted that the level of PXR protein was not associated with PXR mRNA level in human liver samples from the Japanese population, thus pointing to the involvement of a post-transcriptional regulation. They have further evidenced that miR-148a recognizes the complementary sequence in the 3′-untranslated region of human PXR mRNA that leads to downregulation of PXR protein and, subsequently, of its target genes such as CYP3A4 [79].

On the other hand, in a follow-up study, Wei *et al*. [80] did not confirm the results of Takagi *et al*., as they found linear correlation between PXR mRNA and protein levels in human liver samples of Chinese donors. Moreover, no significant correlation of miR-148a with expression of PXR or CYP3A4 was detected [80]. Those authors concluded that ethnic differences between Japanese (N=25) [79] and Chinese Han (N=24) populations might play an important role and contribute to the inconsistent conclusions [80]. Similarly, an absence of correlation between miR-148 and either PXR or CYP3A4 mRNAs has been reported for Caucasian human liver donors (N=92) [81]. The results clearly demonstrate that PXR is not the only translational factors controlling basal expression of CYP3A4. Other nuclear receptors and transcription factors (such as CAR, HNF4α, C/EBPs etc.) are critical for CYP3A4 basal expression and its expression variability in human liver [26].

5. EXPERT OPINION

It is tempting to assume that mutually competitive modifications between SUMOylation and such other PTMs as acetylation and ubiquitination at lysine residues of PXR may occur [73]. However, further analysis is warranted to obtain more evidence as to the purposes of the individual PTMs in relation to PXR activity and their interplay in the context of PXR-mediated CYP expression.

Moreover, it has been noted that depending upon the target protein, phosphorylation may send either a positive or negative regulatory signal which directs the protein to SUMOlation [73]. It is not yet known whether phosphorylation of PXR may regulate its SUMOlation and, if so, how.

It is important to note that cell signaling pathways are mutually interconnected. For that reason, future research should be directed to obtaining a more comprehensive view that integrates multiple cell stimuli in the regulation of PXR-mediated activity. In addition, devoting more effort to the regulation of PXR activity through post-transcriptional and post-translational modifications would provide us new insight into drug metabolism by CYPs and the efficiency of drug therapy during the various physiological and pathological states.

The promiscuity among PXR and other NRs in binding to response element sites of target genes [27] further raises the question of how different post-transcriptional and post-translational modifications of individual NRs alter their role in CYPs' regulation.

Moreover, it should be noted that co-regulators of NRs are also phosphorylation substrates that represent another level in the regulation of PXR-mediated activity [82].

Acknowledgments

The text has been supported by funds from the Czech Scientific Agency GACR303/12/G163 and GACR303/12/0472.

ABBREVIATIONS

AF2	Activation function 2
Akt	Protein kinase B
CAR	Constitutive androstane receptor
Cdk	Cyclin-dependent kinase
CK2	Casein kinase II
CYP	Cytochrome P450
DBD	DNA binding domain
DMEs	Drug-metabolizing enzymes
EGF	Epidermal growth factor
ERK1/2	Extracellular signal-regulated protein kinases 1/2
gal1	Yeast galactokinase Gal1
GSK3	Glycogen synthase kinase 3
HAT	Histone acetyltransferase
HDAC	Histone deacetylase
HGF	Hepatocyte growth factor
IL-1,6	Interleukin-1,6
LBD	Ligand-binding domain
MEK1/2	Mitogen-activated/extracellular signal-regulated kinase kinase 1/2
miRNA	MicroRNA
NCoR	Nuclear receptor corepressor
NF-κB	Nuclear factor-kappa B
NR	Nuclear receptor

OA	Okadaic acid
P70 S6K	70-kDa form of ribosomal protein S6 kinase
PAR	Pregnane activated receptor
PBP	Peroxisome proliferator-activated receptor-binding protein
PI3K	Phosphatidylinositol 3-kinase
PKA	Cyclic AMP-dependent protein kinase
PKC	Protein kinase C
PP1/2A	Protein phosphatase 1/2A
PTMs	Post-translational modifications
PXR	Pregnane X receptor
RBCK1	Ring-B-box-coiled-coil protein interacting with protein kinase C-1
RXR	Retinoid X receptor
SHP	Short/Small heterodimer partner (N0B2)
siRNA	Small interfering RNA
SIRT1	Sirtuin 1, Silent mating type information regulation 2 homolog 1
SMRT	Nuclear receptor corepressor 2; silencing mediator for retinoid and thyroid hormone receptors
SRC-1	Steroid receptor coactivator-1
SUG1	Suppressor for gal 1
SUMO	Small Ubiquitin-related Modifier
SXR	Steroid and xenobiotic receptor
TKR	Tyrosine kinase receptor
TNFα	Tumor necrosis factor alpha

References

1. Ema M, Matsushita N, Sogawa K, Ariyama T, Inazawa J, Nemoto T, Ota M, Oshimura M, Fujii-Kuriyama Y. Human arylhydrocarbon receptor: Functional expression and chromosomal assignment to 7p21. J Biochem. 1994; 116(4):845–851. [PubMed: 7883760]
2. Baes M, Gulick T, Choi HS, Martinoli MG, Simha D, Moore DD. A new orphan member of the nuclear hormone receptor superfamily that interacts with a subset of retinoic acid response elements. Mol Cell Biol. 1994; 14(3):1544–1552. [PubMed: 8114692]
3. Kliewer SA, Moore JT, Wade L, Staudinger JL, Watson MA, Jones SA, McKee DD, Oliver BB, Willson TM, Zetterstrom RH, Perlmann T, et al. An orphan nuclear receptor activated by pregnanes defines a novel steroid signaling pathway. Cell. 1998; 92(1):73–82. [PubMed: 9489701]
4. Bertilsson G, Heidrich J, Svensson K, Asman M, Jendeberg L, Sydow-Backman M, Ohlsson R, Postlind H, Blomquist P, Berkenstam A. Identification of a human nuclear receptor defines a new signaling pathway for cyp3a induction. Proc Natl Acad Sci U S A. 1998; 95(21):12208–12213. [PubMed: 9770465]
5. Lehmann JM, McKee DD, Watson MA, Willson TM, Moore JT, Kliewer SA. The human orphan nuclear receptor pxr is activated by compounds that regulate cyp3a4 gene expression and cause drug interactions. J Clin Invest. 1998; 102(5):1016–1023. [PubMed: 9727070]

6. Blumberg B, Sabbagh W Jr, Juguilon H, Bolado J Jr, van Meter CM, Ong ES, Evans RM. Sxr, a novel steroid and xenobiotic-sensing nuclear receptor. Genes Dev. 1998; 12(20):3195–3205. [PubMed: 9784494]
7. Wada T, Gao J, Xie W. Pxr and car in energy metabolism. Trends Endocrinol Metab. 2009; 20(6): 273–279. [PubMed: 19595610]
8. Ma X, Idle JR, Gonzalez FJ. The pregnane x receptor: From bench to bedside. Expert Opin Drug Metab Toxicol. 2008; 4(7):895–908. [PubMed: 18624678]
9. Wang YM, Ong SS, Chai SC, Chen T. Role of car and pxr in xeno-biotic sensing and metabolism. Expert Opin Drug Metab Toxicol. 2012; 8(7):803–817. [PubMed: 22554043]
10. Nishimura M, Naito S, Yokoi T. Tissue-specific mrna expression profiles of human nuclear receptor subfamilies. Drug Metab Pharmacokinet. 2004; 19(2):135–149. [PubMed: 15499180]
11. Pavek P, Dvorak Z. Xenobiotic-induced transcriptional regulation of xenobiotic metabolizing enzymes of the cytochrome p450 superfamily in human extrahepatic tissues. Curr Drug Metab. 2008; 9(2):129–143. [PubMed: 18288955]
12. Zhou C, Verma S, Blumberg B. The steroid and xenobiotic receptor (sxr), beyond xenobiotic metabolism. Nucl Recept Signal. 2009; 7:e001. [PubMed: 19240808]
13. di Masi A, De Marinis E, Ascenzi P, Marino M. Nuclear receptors car and pxr: Molecular, functional, and biomedical aspects. Mol Aspects Med. 2009; 30(5):297–343. [PubMed: 19427329]
14. Watkins RE, Wisely GB, Moore LB, Collins JL, Lambert MH, Williams SP, Willson TM, Kliewer SA, Redinbo MR. The human nuclear xenobiotic receptor pxr: Structural determinants of directed promiscuity. Science. 2001; 292(5525):2329–2333. [PubMed: 11408620]
15. Ekins S, Chang C, Mani S, Krasowski MD, Reschly EJ, Iyer M, Kholodovych V, Ai N, Welsh WJ, Sinz M, Swaan PW, et al. Human pregnane x receptor antagonists and agonists define molecular requirements for different binding sites. Mol Pharmacol. 2007; 72(3):592–603. [PubMed: 17576789]
16. Cai Y, Konishi T, Han G, Campwala KH, French SW, Wan YJ. The role of hepatocyte rxr alpha in xenobiotic-sensing nuclear receptor-mediated pathways. Eur J Pharm Sci. 2002; 15(1):89–96. [PubMed: 11803135]
17. Rosenfeld MG, Lunyak VV, Glass CK. Sensors and signals: A coactivator/corepressor/epigenetic code for integrating signal-dependent programs of transcriptional response. Genes Dev. 2006; 20(11):1405–1428. [PubMed: 16751179]
18. Synold TW, Dussault I, Forman BM. The orphan nuclear receptor sxr coordinately regulates drug metabolism and efflux. Nat Med. 2001; 7(5):584–590. [PubMed: 11329060]
19. Takeshita A, Taguchi M, Koibuchi N, Ozawa Y. Putative role of the orphan nuclear receptor sxr (steroid and xenobiotic receptor) in the mechanism of cyp3a4 inhibition by xenobiotics. J Biol Chem. 2002; 277(36):32453–32458. [PubMed: 12072427]
20. Ourlin JC, Lasserre F, Pineau T, Fabre JM, Sa-Cunha A, Maurel P, Vilarem MJ, Pascussi JM. The small heterodimer partner interacts with the pregnane x receptor and represses its transcriptional activity. Mol Endocrinol. 2003; 17(9):1693–1703. [PubMed: 12805410]
21. Goodwin B, Moore LB, Stoltz CM, McKee DD, Kliewer SA. Regulation of the human cyp2b6 gene by the nuclear pregnane x receptor. Mol Pharmacol. 2001; 60(3):427–431. [PubMed: 11502872]
22. Gerbal-Chaloin S, Pascussi JM, Pichard-Garcia L, Daujat M, Waechter F, Fabre JM, Carrere N, Maurel P. Induction of cyp2c genes in human hepatocytes in primary culture. Drug Metab Dispos. 2001; 29(3):242–251. [PubMed: 11181490]
23. Staudinger JL, Ding X, Lichti K. Pregnane x receptor and natural products: Beyond drug-drug interactions. Expert Opin Drug Metab Toxicol. 2006; 2(6):847–857. [PubMed: 17125405]
24. Sinz M, Kim S, Zhu Z, Chen T, Anthony M, Dickinson K, Rodrigues AD. Evaluation of 170 xenobiotics as transactivators of human pregnane x receptor (hpxr) and correlation to known cyp3a4 drug interactions. Curr Drug Metab. 2006; 7(4):375–388. [PubMed: 16724927]
25. Li AP, Kaminski DL, Rasmussen A. Substrates of human hepatic cytochrome p450 3a4. Toxicology. 1995; 104(1–3):1–8. [PubMed: 8560487]

26. Martinez-Jimenez CP, Jover R, Donato MT, Castell JV, Gomez-Lechon MJ. Transcriptional regulation and expression of cyp3a4 in hepatocytes. Curr Drug Metab. 2007; 8(2):185–194. [PubMed: 17305497]
27. Plant N. Use of reporter genes to measure xenobiotic-mediated activation of cyp gene transcription. Methods Mol Biol. 2006; 320:343–354. [PubMed: 16719405]
28. Lin JH. Cyp induction-mediated drug interactions: *In vitro* assessment and clinical implications. Pharm Res. 2006; 23(6):1089–1116. [PubMed: 16718615]
29. Staudinger JL, Xu C, Biswas A, Mani S. Post-translational modification of pregnane x receptor. Pharmacol Res. 2011
30. Gu X, Ke S, Liu D, Sheng T, Thomas PE, Rabson AB, Gallo MA, Xie W, Tian Y. Role of nf-kappab in regulation of pxr-mediated gene expression: A mechanism for the suppression of cytochrome p-450 3a4 by proinflammatory agents. J Biol Chem. 2006; 281(26):17882–17889. [PubMed: 16608838]
31. Zhou C, Tabb MM, Nelson EL, Grun F, Verma S, Sadatrafiei A, Lin M, Mallick S, Forman BM, Thummel KE, Blumberg B. Mutual repression between steroid and xenobiotic receptor and nf-kappab signaling pathways links xenobiotic metabolism and inflammation. J Clin Invest. 2006; 116(8):2280–2289. [PubMed: 16841097]
32. Shah YM, Ma X, Morimura K, Kim I, Gonzalez FJ. Pregnane x receptor activation ameliorates dss-induced inflammatory bowel disease via inhibition of nf-kappab target gene expression. Am J Physiol Gastrointest Liver Physiol. 2007; 292(4):G1114–1122. [PubMed: 17170021]
33. Kodama S, Koike C, Negishi M, Yamamoto Y. Nuclear receptors car and pxr cross talk with foxo1 to regulate genes that encode drug-metabolizing and gluconeogenic enzymes. Mol Cell Biol. 2004; 24(18):7931–7940. [PubMed: 15340055]
34. Bhalla S, Ozalp C, Fang S, Xiang L, Kemper JK. Ligand-activated pregnane x receptor interferes with hnf-4 signaling by targeting a common coactivator pgc-1alpha. Functional implications in hepatic cholesterol and glucose metabolism. J Biol Chem. 2004; 279(43):45139–45147. [PubMed: 15322103]
35. Igarashi M, Yogiashi Y, Mihara M, Takada I, Kitagawa H, Kato S. Vitamin k induces osteoblast differentiation through pregnane x receptor-mediated transcriptional control of the msx2 gene. Mol Cell Biol. 2007; 27(22):7947–7954. [PubMed: 17875939]
36. Zhai Y, Pai HV, Zhou J, Amico JA, Vollmer RR, Xie W. Activation of pregnane x receptor disrupts glucocorticoid and mineralo-corticoid homeostasis. Mol Endocrinol. 2007; 21(1):138–147. [PubMed: 16973756]
37. Biswas A, Pasquel D, Tyagi RK, Mani S. Acetylation of pregnane x receptor protein determines selective function independent of ligand activation. Biochem Biophys Res Commun. 2011; 406(3): 371–376. [PubMed: 21329659]
38. Ding X, Staudinger JL. Repression of pxr-mediated induction of hepatic cyp3a gene expression by protein kinase c. Biochem Pharmacol. 2005; 69(5):867–873. [PubMed: 15710363]
39. Lin W, Wu J, Dong H, Bouck D, Zeng FY, Chen T. Cyclin-dependent kinase 2 negatively regulates human pregnane x receptor-mediated cyp3a4 gene expression in hepg2 liver carcinoma cells. J Biol Chem. 2008; 283(45):30650–30657. [PubMed: 18784074]
40. Sugatani J, Osabe M, Kurosawa M, Kitamura N, Ikari A, Miwa M. Induction of ugt1a1 and cyp2b6 by an antimitogenic factor in hepg2 cells is mediated through suppression of cyclin-dependent kinase 2 activity: Cell cycle-dependent expression. Drug Metab Dispos. 2010; 38(1):177–186. [PubMed: 19797611]
41. Dong H, Lin W, Wu J, Chen T. Flavonoids activate pregnane x receptor-mediated cyp3a4 gene expression by inhibiting cyclin-dependent kinases in hepg2 liver carcinoma cells. BMC Biochem. 2010; 11(23)
42. Pondugula SR, Brimer-Cline C, Wu J, Schuetz EG, Tyagi RK, Chen T. A phosphomimetic mutation at threonine-57 abolishes transactivation activity and alters nuclear localization pattern of human pregnane x receptor. Drug Metab Dispos. 2009; 37(4):719–730. [PubMed: 19171678]
43. Ding X, Staudinger JL. Induction of drug metabolism by forskolin: The role of the pregnane x receptor and the protein kinase a signal transduction pathway. J Pharmacol Exp Ther. 2005; 312(2):849–856. [PubMed: 15459237]

44. Lichti-Kaiser K, Xu C, Staudinger JL. Cyclic amp-dependent protein kinase signaling modulates pregnane x receptor activity in a species-specific manner. J Biol Chem. 2009; 284(11):6639–6649. [PubMed: 19141612]
45. Lichti-Kaiser K, Brobst D, Xu C, Staudinger JL. A systematic analysis of predicted phosphorylation sites within the human pregnane x receptor protein. J Pharmacol Exp Ther. 2009; 331(1):65–76. [PubMed: 19617467]
46. Ueda A, Matsui K, Yamamoto Y, Pedersen LC, Sueyoshi T, Negishi M. Thr176 regulates the activity of the mouse nuclear receptor car and is conserved in the nr1i subfamily members pxr and vdr. Biochem J. 2005; 388(Pt 2):623–630. [PubMed: 15610065]
47. Doricakova A, Novotna A, Vrzal R, Pavek P, Dvorak Z. The role of residues t248, y249 and t422 in the function of human pregnane x receptor. Arch Toxicol. 2013; 87(2):291–301. [PubMed: 22976785]
48. Hu G, Xu C, Staudinger JL. Pregnane x receptor is sumoylated to repress the inflammatory response. J Pharmacol Exp Ther. 2010; 335(2):342–350. [PubMed: 20719936]
49. Rana R, Coulter S, Kinyamu H, Goldstein JA. Rbck1, an e3 ubiquitin ligase, interacts with and ubiquinates the human pregnane x receptor. Drug Metab Dispos. 2012; 41(2):398–405. [PubMed: 23160820]
50. Rochette-Egly C. Nuclear receptors: Integration of multiple signalling pathways through phosphorylation. Cell Signal. 2003; 15(4):355–366. [PubMed: 12618210]
51. Pondugula SR, Dong H, Chen T. Phosphorylation and protein-protein interactions in pxr-mediated cyp3a repression. Expert Opin Drug Metab Toxicol. 2009; 5(8):861–873. [PubMed: 19505191]
52. Sugatani J, Uchida T, Kurosawa M, Yamaguchi M, Yamazaki Y, Ikari A, Miwa M. Regulation of pregnane x receptor (pxr) function and ugt1a1 gene expression by posttranslational modification of pxr protein. Drug Metab Dispos. 2012; 40(10):2031–2040. [PubMed: 22829544]
53. Morgan ET, Goralski KB, Piquette-Miller M, Renton KW, Robertson GR, Chaluvadi MR, Charles KA, Clarke SJ, Kacevska M, Liddle C, Richardson TA, et al. Regulation of drug-metabolizing enzymes and transporters in infection, inflammation, and cancer. Drug Metab Dispos. 2008; 36(2): 205–216. [PubMed: 18218849]
54. Kim SK, Novak RF. The role of intracellular signaling in insulin-mediated regulation of drug metabolizing enzyme gene and protein expression. Pharmacol Ther. 2007; 113(1):88–120. [PubMed: 17097148]
55. Sayeed MM. Alterations in cell signaling and related effector functions in t lymphocytes in burn/trauma/septic injuries. Shock. 1996; 5(3):157–166. [PubMed: 8696979]
56. Abdel-Razzak Z, Loyer P, Fautrel A, Gautier JC, Corcos L, Turlin B, Beaune P, Guillouzo A. Cytokines down-regulate expression of major cytochrome p-450 enzymes in adult human hepatocytes in primary culture. Mol Pharmacol. 1993; 44(4):707–715. [PubMed: 8232220]
57. Muntane-Relat J, Ourlin JC, Domergue J, Maurel P. Differential effects of cytokines on the inducible expression of cyp1a1, cyp1a2, and cyp3a4 in human hepatocytes in primary culture. Hepatology. 1995; 22(4 Pt 1):1143–1153. [PubMed: 7557864]
58. Jover R, Bort R, Gomez-Lechon MJ, Castell JV. Down-regulation of human cyp3a4 by the inflammatory signal interleukin-6: Molecular mechanism and transcription factors involved. Faseb J. 2002; 16(13):1799–1801. [PubMed: 12354697]
59. Hines RN. Ontogeny of human hepatic cytochromes p450. J Biochem Mol Toxicol. 2007; 21(4): 169–175. [PubMed: 17936930]
60. Donato MT, Gomez-Lechon MJ, Jover R, Nakamura T, Castell JV. Human hepatocyte growth factor down-regulates the expression of cytochrome p450 isozymes in human hepatocytes in primary culture. J Pharmacol Exp Ther. 1998; 284(2):760–767. [PubMed: 9454825]
61. Gomez-Lechon MJ, Castelli J, Guillen I, O'Connor E, Nakamura T, Fabra R, Trullenque R. Effects of hepatocyte growth factor on the growth and metabolism of human hepatocytes in primary culture. Hepatology. 1995; 21(5):1248–1254. [PubMed: 7737630]
62. Greuet J, Pichard L, Ourlin JC, Bonfils C, Domergue J, Le Treut P, Maurel P. Effect of cell density and epidermal growth factor on the inducible expression of cyp3a and cyp1a genes in human hepatocytes in primary culture. Hepatology. 1997; 25(5):1166–1175. [PubMed: 9141435]

63. Braeuning A. Regulation of cytochrome p450 expression by ras- and beta-catenin-dependent signaling. Curr Drug Metab. 2009; 10(2):138–158. [PubMed: 19275549]
64. Shima N, Stolz DB, Miyazaki M, Gohda E, Higashio K, Michalopoulos GK. Possible involvement of p21/waf1 in the growth inhibition of hepg2 cells induced by hepatocyte growth factor. J Cell Physiol. 1998; 177(1):130–136. [PubMed: 9731753]
65. Sivertsson L, Edebert I, Palmertz MP, Ingelman-Sundberg M, Neve EP. Induced cyp3a4 expression in confluent huh7 hepatoma cells as a result of decreased cell proliferation and subsequent pregnane x receptor activation. Mol Pharmacol. 2013; 83(3):659–670. [PubMed: 23264496]
66. Zhu J, Li W, Mao Z. Cdk5: Mediator of neuronal development, death and the response to DNA damage. Mech Ageing Dev. 2011; 132(8–9):389–394. [PubMed: 21600237]
67. Min L, He B, Hui L. Mitogen-activated protein kinases in hepatocellular carcinoma development. Semin Cancer Biol. 2010; 21(1):10–20. [PubMed: 20969960]
68. Zassadowski F, Rochette-Egly C, Chomienne C, Cassinat B. Regulation of the transcriptional activity of nuclear receptors by the mek/erk1/2 pathway. Cell Signal. 2012; 24(12):2369–2377. [PubMed: 22906493]
69. Elias A, High AA, Mishra A, Ong SS, Wu J, Peng J, Chen T. Identification and characterization of phosphorylation sites within the pregnane x receptor protein. Biochem Pharmacol. 2013
70. Portbury AL, Ronnebaum SM, Zungu M, Patterson C, Willis MS. Back to your heart: Ubiquitin proteasome system-regulated signal transduction. J Mol Cell Cardiol. 2012; 52(3):526–537. [PubMed: 22085703]
71. Masuyama H, Hiramatsu Y, Kunitomi M, Kudo T, MacDonald PN. Endocrine disrupting chemicals, phthalic acid and nonylphenol, activate pregnane x receptor-mediated transcription. Mol Endocrinol. 2000; 14(3):421–428. [PubMed: 10707959]
72. Rubin DM, Coux O, Wefes I, Hengartner C, Young RA, Goldberg AL, Finley D. Identification of the gal4 suppressor sug1 as a subunit of the yeast 26s proteasome. Nature. 1996; 379(6566):655–657. [PubMed: 8628401]
73. Bossis G, Melchior F. Sumo: Regulating the regulator. Cell Div. 2006; 1(13)
74. Masuyama H, Inoshita H, Hiramatsu Y, Kudo T. Ligands have various potential effects on the degradation of pregnane x receptor by proteasome. Endocrinology. 2002; 143(1):55–61. [PubMed: 11751591]
75. Treuter E, Venteclef N. Transcriptional control of metabolic and inflammatory pathways by nuclear receptor sumoylation. Biochim Biophys Acta. 2010; 1812(8):909–918. [PubMed: 21172431]
76. Wang C, Tian L, Popov VM, Pestell RG. Acetylation and nuclear receptor action. J Steroid Biochem Mol Biol. 2011; 123(3–5):91–100. [PubMed: 21167281]
77. Buler M, Aatsinki SM, Skoumal R, Hakkola J. Energy sensing factors pgc-1alpha and sirt1 modulate pxr expression and function. Biochem Pharmacol. 2011; 82(12):2008–2015. [PubMed: 21933665]
78. Nakajima M, Yokoi T. Micrornas from biology to future pharmacotherapy: Regulation of cytochrome p450s and nuclear receptors. Pharmacol Ther. 2011; 131(3):330–337. [PubMed: 21565218]
79. Takagi S, Nakajima M, Mohri T, Yokoi T. Post-transcriptional regulation of human pregnane x receptor by micro-rna affects the expression of cytochrome p450 3a4. J Biol Chem. 2008; 283(15): 9674–9680. [PubMed: 18268015]
80. Wei Z, Chen M, Zhang Y, Wang X, Jiang S, Wang Y, Wu X, Qin S, He L, Zhang L, Xing Q. No correlation of hsa-mir-148a with expression of pxr or cyp3a4 in human livers from chinese han population. PLoS One. 2013; 8(3):e59141. [PubMed: 23527115]
81. Rieger JK, Klein K, Winter S, Zanger UM. Expression variability of adme-related micrornas in human liver: Influence of non-genetic factors and association with gene expression. Drug Metab Dispos. 201310.1124/dmd.113.052126
82. Staudinger JL, Lichti K. Cell signaling and nuclear receptors: New opportunities for molecular pharmaceuticals in liver disease. Mol Pharm. 2008; 5(1):17–34. [PubMed: 18159925]

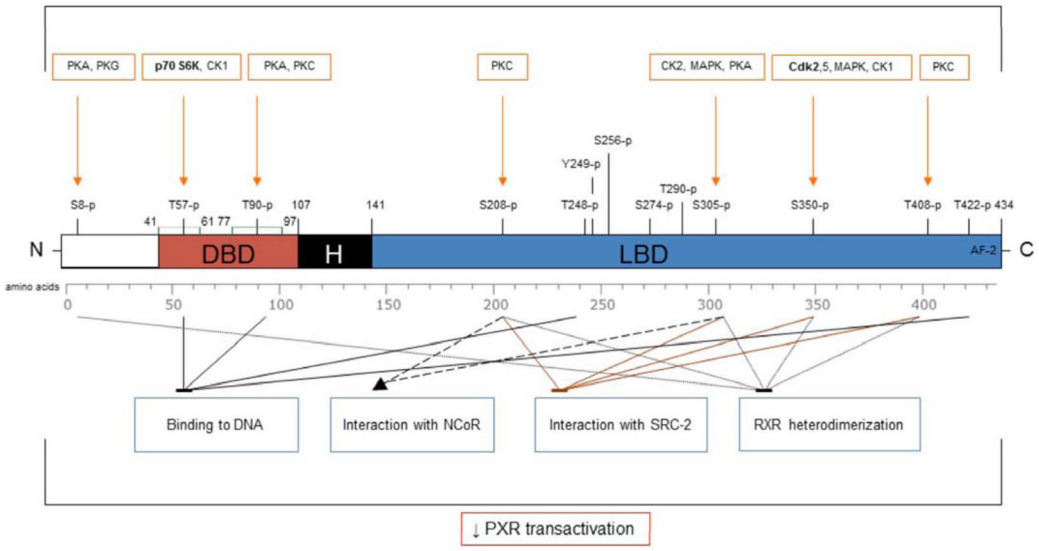

Fig. 1.

The N-terminal region of human PXR includes DNA-binding domain (DBD) which is connected to ligand-binding domain (LBD) and activation function 2 (AF2) situated on the C-terminal region by the hinge region (H).

Evolutionarily conserved zinc-finger motifs are highlighted by green color; *in silico* predictive phosphorylation sites for protein kinases (orange squares) in the human PXR are indicated by orange arrows [45]. The protein kinases by which specific phosphorylation sites within human PXR were confirmed to be important for their effect on PXR-mediated transcriptional activity are in bold.

The effects of site-specific phosphorylation of human PXR such as DNA binding, RXR dimerization and co-regulator interaction are depicted (blue squares; arrow means activation; stop bar means suppression).

Table 1

Summary of major PXR post-translational modifications and their effects on PXR-mediated transactivation of CYPs.

PXR modification	Site[1]	Enzyme	PXR-mediated mechanism	References
phosphorylation				
phosphorylation	unknown	PKC	↓ transcription; ↑ interaction with NCoR; ↓ ligand-dependent interaction with SRC-1	[38]
dephosphorylation	unknown	PP1/2A (inh.)	↓ transcription	
phosphorylation		Cdk2	↓ transcription	[39]
direct phosphorylation[2]	unknown	Cdk2/cyclin A, E		
phosphomimetic mutation	Ser350D		↓ transcription	
phosphorylation-deficient mutation	Ser350A		partial resistance to ↓ transcription by Cdk2	
unknown	unknown	Cdk2 (siRNA)	↑ expression	[40]
unknown	unknown	Cdk4 (siRNA)	↔ expression	
phosphorylation	unknown	Cdk5	↓ transcription	[41]
phosphorylation	unknown	Cdk5 (siRNA)	↑ transcription	
direct phosphorylation[2]	unknown	Cdk5/p35		
phosphorylation	unknown	p70 S6K	↓ transcription	[42]
direct phosphorylation[2]	unknown	p70 S6K		
phosphomimetic mutation	Thr57D		↓ transcription; × subcellular localization; ↔ SRC-1 interaction; ↓ DNA binding (ER6)	
phosphorylation-deficient mutation	Thr57A		partial resistance to ↓ transcription by p70S6K; ↔ subcellular localization; ↔ SRC-1 interaction, ↔ DNA binding	
phosphorylation	unknown	PKA	↑ transcription[3]; ↑ interaction with SRC-1, PBP	[43]
direct phosphorylation[2]	unknown	PKA		
phosphorylation	unknown	PKA	↓ transcription[4]; ↑ interaction with NCoR	[44]
phosphorylation	unknown	PKA	↑ threonine phophorylation[5]	
direct phosphorylation [2]	unknown	Cdk1, CK2, GSK3, PKA, PKC, p70 S6K		
phosphomimetic mutations	Ser8D		↓ transcription; ↔ DNA binding (ER6); ↓ RXRα heterodimerization;	[45]
	Ser208D		↓ transcription; ↔ DNA binding; ↓ RXRα heterodimerization; interaction with NCoR ↑; SRC-2↓	
	Ser305D		↓ transcription; ↔ DNA binding; ↓ RXRα heterodimerization; interaction with NCoR ↑; SRC-2↓	
	Ser350D		↓ transcription; ↔ DNA binding; ↓ RXRα heterodimerization; interaction with NCoR↔; SRC-2↓	

PXR modification	Site[1]	Enzyme	PXR-mediated mechanism	References
	Thr408D		↓ transcription; ↔ DNA binding; ↓ RXRα heterodimerization; interaction with NCoR↔; SRC-2↓; × subcellular localization	
	Thr57D		↓ transcription; ↓ DNA binding; ↔ RXRα heterodimerization	
	Thr90D		↔ transcription; ↓ DNA binding; ↔ RXRα heterodimerization	
phosphorylation-deficient mutations	Ser8A		↔ transcription; ↔ DNA binding; ↔ RXRα heterodimerization	
	Ser208A		↑ transcription; ↔ DNA binding; ↔ RXRα heterodimerization; interaction with NCoR↓; SRC-2↑	
	Ser305A		↔ transcription; ↔ DNA binding; ↔ RXRα heterodimerization; interaction with NCoR↑; SRC-2↑	
	Ser350A		↔ transcription; ↔ DNA binding; ↔ RXRα heterodimerization; interaction with NCoR↔; SRC-2↓	
	Thr408A		↓ transcription; ↔ DNA binding; ↔ RXRα heterodimerization; interaction with NCoR↑; SRC-2↓; × subcellular localization	
	Thr57A		↔ transcription; ↔ DNA binding; ↔ RXRα heterodimerization	
	Thr90A		↔ transcription; ↓ DNA binding; ↔ RXRα heterodimerization	
mutations (including phosphorylation-deficient mutations)	Thr248G, A,V,L,S		↓ transcription	[46]
phosphorylation-deficient mutations	Thr248A,V		SRC-1 ↓	
phosphomimetic mutations	Thr248D		↑ transcription; ↓ DNA binding (DR3); ↔ RXRα heterodimerization	[47]
	Tyr249D		↓ transcription; ↔ DNA binding; ↔ RXRα heterodimerization	
	Thr422D		↓ transcription; ↓ DNA binding; ↔ RXRα heterodimerization	
phosphorylation-deficient mutations	Thr248V		↓ transcription; ↓ DNA binding; ↔ RXRα heterodimerization	
	Tyr249F		↔ transcription; ↔ DNA binding; ↔ RXRα heterodimerization	
	Thr422A		↓ transcription; ↔ DNA binding; ↔ RXRα heterodimerization	
SUMOylation				
SUMOylation-SUMO-1, SUMO-2, SUMO-3 (*in vitro*)	unknown	E1; E2		[48]
SUMOylation-preferentially SUMO-3 (*in vivo*)	unknown	E2	↔ transcription	
ubiquitination				
ubiquitination	unknown	RBCK1	↓ transcription	[49]
ubiquitination ↑	unknown	PKA		[29]
ubiquitination ↑[6]	unknown		↓ transcription	

PXR modification	Site[1]	Enzyme	PXR-mediated mechanism	References
acetylation				
acetylation (*in vivo*)	unknown	unknown		[37]
deacetylation (*in vivo*)	unknown	SIRT1[7]		

A, alanine; D, aspartic acid; F, phenylalanine; G, glycine; L, leucine; Ser, S, serine; Thr, threonine; Y, Tyr, tyrosine; V, valine

[1] It is unclear whether amino acid residues within PXR which have been shown to be associated with phosphorylation-related functions are really phosphorylation sites for kinases;

[2] by *in vitro* kinase assay;

[3] mouse hepatocytes;

[4] rat and human hepatocytes;

[5] PXR exists as a phosphoprotein as detected by Western blot analysis;

[6] using 26S proteasome inhibitor (MG132);

[7] other HDAC(s) are assumed

↑: stimulation or strengthen; ↓: repression or weaken; ↔: no effect; ×: alteration

5. Development of 3,5-Dinitrobenzylsulfanyl-1,3,4-oxadiazoles and Thiadiazoles as Selective Antitubercular Agents Active Against Replicating and Nonreplicating Mycobacterium tuberculosis.

Karabanovich G, Zemanová J, **Smutný T**, Székely R, Šarkan M, Centárová I, Vocat A, Pávková I, Čonka P, Němeček J, Stolaříková J, Vejsová M, Vávrová K, Klimešová V, Hrabálek A, Pávek P, Cole ST, Mikušová K, Roh J. Development of 3,5-Dinitrobenzylsulfanyl-1,3,4-oxadiazoles and Thiadiazoles as Selective Antitubercular Agents Active Against Replicating and Nonreplicating Mycobacterium tuberculosis. (2016) J Med Chem., 59(6):2362-80.
(IF 2015: **5.589**)

One aim of this study was to estimate a toxicity of newly developed compounds with potential antituberculotic activity. To fulfill this aim, we used primary human hepatocytes and four different mammalian cell lines including hepatic HuH-7 and HepG2 cells besides others. The mitochondrial activity measured by MTS assay was chosen as a marker of a cell viability. Tested compounds revealed generally a low cellular toxicity with several exceptions.

Journal of Medicinal Chemistry

Article

pubs.acs.org/jmc

Development of 3,5-Dinitrobenzylsulfanyl-1,3,4-oxadiazoles and Thiadiazoles as Selective Antitubercular Agents Active Against Replicating and Nonreplicating *Mycobacterium tuberculosis*

Galina Karabanovich,[†] Júlia Zemanová,[‡] Tomáš Smutný,[†] Rita Székely,[⊥] Michal Šarkan,[‡] Ivana Centárová,[‡] Anthony Vocat,[⊥] Ivona Pávková,[§] Patrik Čonka,[†] Jan Němeček,[†] Jiřina Stolaříková,[∥] Marcela Vejsová,[†] Kateřina Vávrová,[†] Věra Klimešová,[†] Alexandr Hrabálek,[†] Petr Pávek,[†] Stewart T. Cole,[⊥] Katarína Mikušová,[‡] and Jaroslav Roh*[,†]

[†]Faculty of Pharmacy in Hradec Králové, Charles University in Prague, Heyrovského 1203, 50005 Hradec Králové, Czech Republic

[‡]Faculty of Natural Sciences, Department of Biochemistry, Comenius University in Bratislava, Mlynská dolina, Ilkovičova 6, 842 15 Bratislava, Slovakia

[§]Faculty of Military Health Sciences, Department of Molecular Pathology and Biology, University of Defence, Třebešská 1575, 50005 Hradec Králové, Czech Republic

[∥]Department of Bacteriology and Mycology, Regional Institute of Public Health, Partyzánské náměstí 7, 70200 Ostrava, Czech Republic

[⊥]Ecole Polytechnique Fédérale de Lausanne, Global Health Institute, CH-1015 Lausanne, Switzerland

Supporting Information

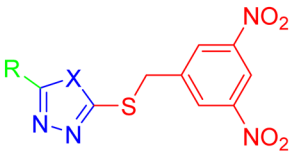

Antitubercular activity (MIC)
- *M.tb* CNCTC My 331/88 = **0.03 - 0.06 μM** (9 examples)
- active against MDR-TB and XDR-TB strains
- active against nonreplicating *M.tb.* (SS18b model)

High selectivity
- no activity against other bacteria and fungi
- low toxicity: IC_{50} (4 mammalian cell lines, isolated human hepatocytes)
- low genotoxicity/mutagenicity

ABSTRACT: Herein, we report the discovery and structure−activity relationships of 5-substituted-2-[(3,5-dinitrobenzyl)-sulfanyl]-1,3,4-oxadiazoles and 1,3,4-thiadiazoles as a new class of antituberculosis agents. The majority of these compounds exhibited outstanding in vitro activity against *Mycobacterium tuberculosis* CNCTC My 331/88 and six multidrug-resistant clinically isolated strains of *M. tuberculosis*, with minimum inhibitory concentration values as low as 0.03 μM (0.011−0.026 μg/mL). The investigated compounds had a highly selective antimycobacterial effect because they showed no activity against the other bacteria or fungi tested in this study. Furthermore, the investigated compounds exhibited low in vitro toxicities in four proliferating mammalian cell lines and in isolated primary human hepatocytes. Several in vitro genotoxicity assays indicated that the selected compounds have no mutagenic activity. The oxadiazole and thiadiazole derivatives with the most favorable activity/toxicity profiles also showed potency comparable to that of rifampicin against the nonreplicating streptomycin-starved *M. tuberculosis* 18b-Lux strain, and therefore, these derivatives, are of particular interest.

INTRODUCTION

Tuberculosis (TB) is a widespread infectious disease predominantly caused by *Mycobacterium tuberculosis* (*M.tb.*), which can be transmitted through the air as droplets and predominantly affects the lungs. Although there has been a slow decrease in new TB cases and TB-related deaths in recent years, the numbers of TB patients and TB-related deaths remain extremely high. According to the World Health Organization, an estimated 9.6 million new TB cases and 1.5 million TB-related deaths were reported worldwide in 2014.[1]

The application of first-line drugs (isoniazid (INH), rifampicin (RIF), pyrazinamide, and ethambutol) is an effective approach for treating TB caused by drug-susceptible *M.tb.* strains. This therapy leads to recovery in approximately 90% of patients. To cure drug-resistant *M.tb.* strains, second-line and third-line anti-TB drugs are required. Streptomycin, kanamycin (KAN), amikacin, capreomycin, viomycin, fluoroquinolones, *para*-aminosalicylic acid, cycloserine, terizidone, ethionamide,

Received: April 27, 2015
Published: March 5, 2016

DOI: 10.1021/acs.jmedchem.5b00608
J. Med. Chem. 2016, 59, 2362−2380

prothionamide, thioacetazone, and linezolid are second-line anti-TB drugs, whereas amoxicillin/clavulanic acid, imipenem/cilastatin, clarithromycin, and clofazimine are third-line anti-TB drugs.[2] Unfortunately, the majority of these medications are poorly tolerated when applied as part of a long-term TB chemotherapy regimen. Furthermore, they are often ineffective: only 50% of patients with multidrug-resistant TB (MDR-TB) have been successfully treated using these drugs.[1] Therefore, both the appearance and increasing spread of MDR-TB and the evolution of extensively drug-resistant (XDR-TB) strains have become a serious problem for current TB treatments. In 2014, 3.3% of new TB cases and 20% of previously treated cases were MDR-TB; an estimated 9.7% of these cases involved XDR-TB.[1]

Despite the introduction of two new compounds (delamanid[3] and bedaquiline[4,5]) to the repertoire of anti-TB therapies for drug-resistant strains of *M.tb.*, further development of antimycobacterial compounds with new mechanisms of action and that are active against MDR and XDR-TB is urgently needed.[2,6] Recently, several nitro group-containing inhibitors of mycobacterial decaprenylphosphoryl-β-D-ribofuranose 2′-oxidase (DprE1), which is involved in the synthesis of decaprenylphosphoryl arabinose, the only donor of arabinosyl residues for the biosynthesis of arabinan polymers in mycobacteria, have been extensively studied (Figure 1).[7,8]

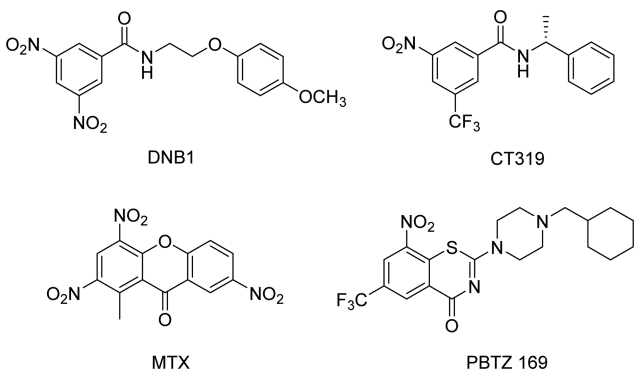

Figure 1. Structures of selected DprE1 inhibitors, including dinitrobenzamide DNB1,[9] its analogue CT319,[10] trinitroxanthone MTX,[10,11] and piperazinobenzothiazinone PBTZ 169.[12,13]

In our previous studies, benzazoles (**1**)[14−16] and 1,5-[17] and 2,5-disubstituted tetrazoles[18] (**2** and **3**, Figure 2) bearing 3,5-dinitrobenzylsulfanyl fragments were found to exhibit strong

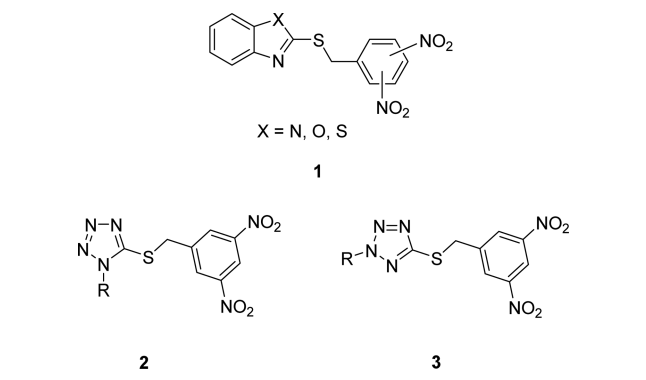

Figure 2. Dinitrobenzylsulfanyl benzimidazoles, benzoxazoles, and benzothiazoles **1** and 5-(3,5-dinitrobenzylsulfanyl)tetrazoles **2** and **3** as anti-TB lead compounds.

antimycobacterial activities with minimum inhibitory concentration (MIC) values of 1 μM (0.36−0.44 μg/mL) against drug-susceptible *M.tb.* and 0.25 μM (0.09−0.11 μg/mL) against six multidrug-resistant clinically isolated strains of *M.tb.* These results indicate that antimycobacterial 3,5-dinitrobenzylsulfanyl tetrazoles may not show cross-resistance to common anti-TB drugs. Moreover, the benzazole derivatives **1** and 5-(3,5-dinitrobenzylsulfanyl)tetrazole derivatives **2** and **3** exhibited selective antimycobacterial effects, as they were ineffective against four Gram-positive and four Gram-negative bacteria and eight fungal (five yeasts and three molds) strains and exhibited low cytotoxicity.[17,18]

In this work, we focused on 1,3,4-oxadiazole and 1,3,4-thiadiazole scaffolds as possible bioisosteric surrogates for 2,5-disubstituted tetrazole in lead compound **3**. Various compounds based on 1,3,4-oxadiazoles and 1,3,4-thiadiazoles, including 2-alkylsulfanyl derivatives, exhibit strong anti-TB effects.[19−23] An overview of several oxadiazole- and thiadiazole-based anti-TB compounds is shown in Figure 3.

Oxadiazole derivative **4** exhibited significant activity with MIC values of 0.1 μM against *M.tb.* H37Rv and 1.10 μM against INH-resistant *M.tb.*[24] Derivatives of 4-(5-pentadecyl/heptadecyl-1,3,4-oxadiazol-2-yl)pyridine (**5a**) bearing long, highly lipophilic alkyl chains presented MIC values of 0.35 and 0.65 μM against *M.tb.* H37Rv and were highly efficient against the drug-resistant strain CIBIN 112. Note that 4-(5-(3,5-dinitrophenyl)-1,3,4-oxadiazol-2-yl)pyridine (**5b**) had only weak potency.[25] 2-((5-(4-Methoxyphenyl)-1,3,4-oxadiazol-2-yl)sulfanyl)-*N*-phenethylacetamide (**6**) is an example of a highly efficient anti-TB derivative of 1,3,4-oxadiazole-5-thiol that showed an IC_{90} value of 0.38 μM (0.14 μg/mL). Substituted thiadiazole **7** with an IC_{90} of 0.62 μM (0.2 μg/mL) is another example of a highly efficient anti-TB derivative.[26] Among the substituted 1,3,4-thiadiazole-5-thiols with general structures based on **8**, compounds with MIC values as low as 1.1 μM (0.39 μg/mL) were found.[21,27−29]

The aims of this work were to synthesize a series of 2-alkyl/aryl-5-(dinitrobenzylsulfanyl)-1,3,4-oxadiazoles and 1,3,4-thiadiazoles as analogues of lead compound **3** and to investigate their structure−activity relationships with respect to anti-TB activity/cytotoxicity and selectivity. Furthermore, several trifluoromethyl-substituted and reduced analogues of the most active compounds were prepared, and their antimycobacterial activities were studied (Table 1).

RESULTS AND DISCUSSION

Synthesis of Oxadiazole and Thiadiazole Derivatives. 2-Alkyl/aryl-5-benzylsulfanyl-1,3,4-oxadiazoles (**9o**, **10d**, **10g**, **10l**, **10n**, **10o**, **10q**, **11b−q**, **15g**, **15i**, and **15o**) were synthesized according to the previously reported three-step approach depicted in Scheme 1.[30] The corresponding methyl esters (**19b−p**) were either prepared by Fischer esterification of carboxylic acid or were commercially available. The reaction of methyl esters **19b−p** with hydrazine hydrate in ethanol led to the formation of the corresponding acyl hydrazides **20b−p**, which were further reacted with carbon disulfide in basic ethanol under reflux to produce 2-substituted-1,3,4-oxadiazole-5-thiols **21b−p**. The synthesis of 2-(pyridin-4-yl)-1,3,4-oxadiazole-5-thiol (**21q**) was accomplished from INH **20q**. The alkylation of oxadiazoles **21b−q** in the presence of tetrabutylammonium bromide (TBAB) as a phase-transfer catalyst resulted in the formation of the target nitro-substituted 2-alkyl/aryl-5-benzylsulfanyl-1,3,4-oxadiazoles **9o**, **10d**, **10g**,

DOI: 10.1021/acs.jmedchem.5b00608
J. Med. Chem. 2016, 59, 2362−2380

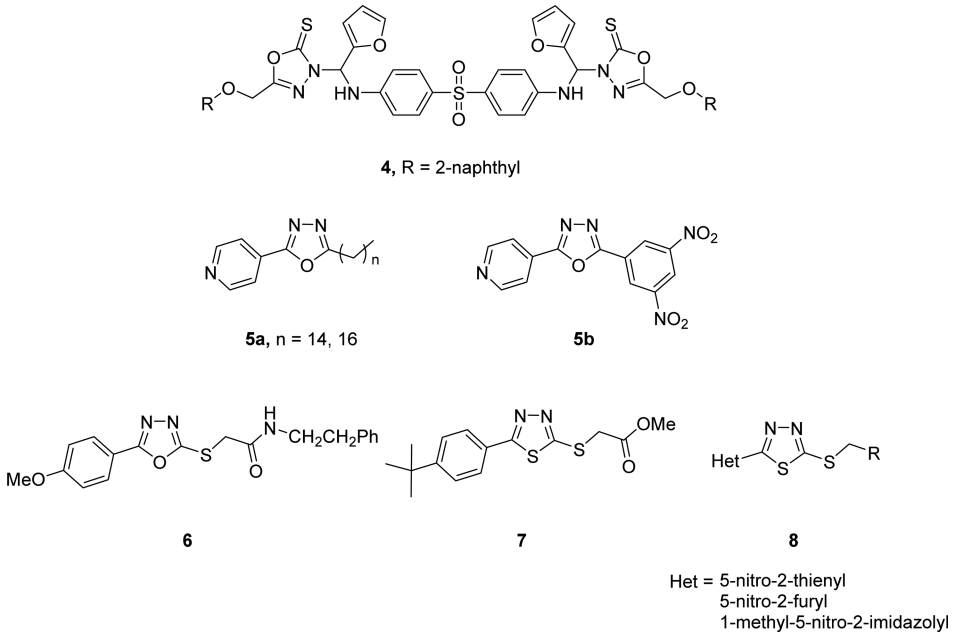

Figure 3. Structures of 1,3,4-oxadiazole (**4**, **5a**, and **6**) and 1,3,4-thiadiazole (**7** and **8**) derivatives with high antimycobacterial activities. Compound **5b** bearing a 3,5-dinitrophenyl moiety possessed only weak anti-TB activity.

Table 1. Nitro-Substituted 1,3,4-Oxadiazole and 1,3,4-Thiadiazole Derivatives Studied in This Work

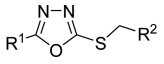

R^2 = 4-NO_2Ph: **9o**
R^2 = 2,4-$(NO_2)_2$Ph: **10d**, **10g**, **10l**, **10n**, **10o**, **10q**
R^2 = 3,5-$(NO_2)_2$Ph: **11a-q**
R^2 = 3-NO_2-5-CF_3Ph: **15g**, **15i**, **15o**
R^2 = 3-NH_2-5-NO_2Ph: **17o**
R^2 = 3,5-$(NH_2)_2$Ph: **18o**

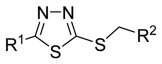

R^2 = 4-NO_2Ph: **12o**
R^2 = 2,4-$(NO_2)_2$Ph: **13d**, **13g**, **13o**
R^2 = 3,5-$(NO_2)_2$Ph: **14a**, **14d-g**, **14i-l**, **14n**, **14o**, **14q**
R^2 = 3-NO_2-5-CF_3Ph: **16g**, **16i**, **16o**

	a	b	c	d	e	f	g
R^1	CH_3	$CH_3(CH_2)_{10}$	cyclohexyl	Ph	2-ClPh	3-ClPh	4-ClPh
	h	i	j	k	l		m
R^1	2,4-Cl_2Ph	4-CH_3Ph	3,5-$(CH_3)_2$Ph	3-CH_3OPh	4-CH_3OPh		3,5-$(CH_3O)_2$Ph
		n	o	p			q
R^1		3-NO_2Ph	4-NO_2Ph	4-HOPh			4-pyridyl

Scheme 1. Synthesis of Nitro-Substituted 2-Alkyl/Aryl-5-benzylsulfanyl-1,3,4-oxadiazoles 9o, 10d, 10g, 10l, 10n, 10o, 10q, 11b–q, 15g, 15i, and 15o[a,b]

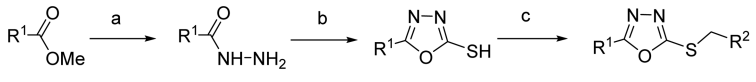

R^2 = 4-NO_2Ph: **9o**
R^2 = 2,4-$(NO_2)_2$Ph: **10d**, **10g**,**10l**, **10n**, **10o**, **10q**
R^2 = 3,5-$(NO_2)_2$Ph: **11b-q**
R^2 = 3-NO_2-5-CF_3Ph: **15g**, **15i**, **15o**

[a]Reagents and conditions: (a) hydrazine hydrate, EtOH, reflux, 4–48 h, 60–96%; (b) CS_2, KOH, EtOH, reflux, 6–44 h, 61–97%; (c) R^2CH_2Cl, NaOH, tetrabutylammonium bromide (TBAB), H_2O/CH_2Cl_2, rt, overnight, 45–96%. [b]A list of R^1 groups (a–q) can be found in Table 1.

10l, **10n**, **10o**, **10q**, **11b–q**, **15g**, **15i**, and **15o** in 45–96% yields.

2-[(3,5-Dinitrobenzyl)sulfanyl]-5-methyl-1,3,4-oxadiazole (**11a**) was prepared by reacting 5-[(3,5-dinitrobenzyl)sulfanyl]-1*H*-tetrazole (**23**) with acetic anhydride (Scheme 2).[31,32] The starting 5-[(3,5-dinitrobenzyl)sulfanyl]-1*H*-tetrazole (**23**) was prepared using Koguro's method.[33]

Unfortunately, this approach was unsuccessful for phenyl derivative **11d**. The reaction of **23** with benzoyl chloride proceeded with low yield, and a mixture of products was formed. Thus, **11d** was prepared using the standard procedure depicted in Scheme 1.

Thiadiazole derivatives (**12o**, **13d**, **13g**, **13o**, **14a**, **14d–g**, **14i–l**, **14n**, **14o**, **14q**, **16g**, **16i**, and **16o**) were synthesized as

DOI: 10.1021/acs.jmedchem.5b00608
J. Med. Chem. 2016, 59, 2362–2380

Scheme 2. Synthesis of 2-[(3,5-Dinitrobenzyl)sulfanyl]-5-methyl-1,3,4-oxadiazole (11a)[a]

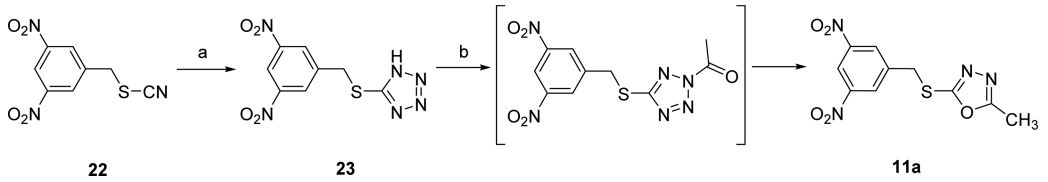

[a]Reagents and conditions: (a) NaN_3, Et_3NHCl, $PhCH_3$, 105 °C, 2 h, 68%; (b) $(CH_3CO)_2O$, microwave, 90 °C, 10 h, 60%.

Scheme 3. Synthesis of Nitro-Substituted 2-Alkyl/Aryl-5-benzylsulfanyl-1,3,4-thiadiazoles 12o, 13d, 13g, 13o, 14a, 14d–g, 14i–l, 14n, 14o, 14q, 16g, 16i, and 16o[a,b]

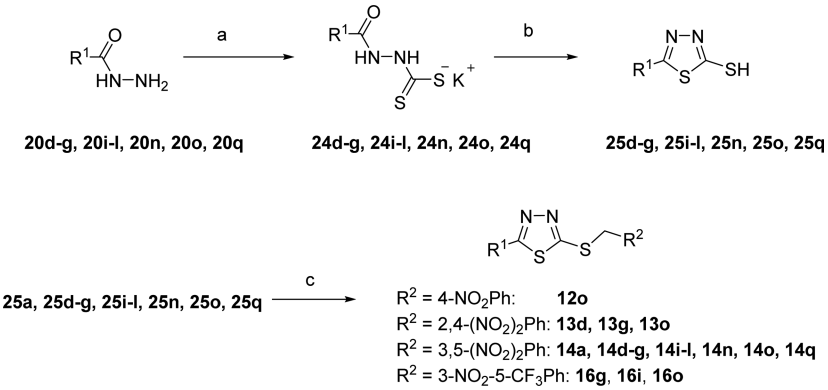

[a]Reagents and conditions: (a) CS_2, KOH, EtOH, rt, overnight; (b) H_2SO_4, 0 °C to rt, 4 h, 24–76%; (c) R^2CH_2Cl, NaOH, TBAB, H_2O/CH_2Cl_2, rt, overnight, 48–87%. [b]A list of R^1 groups (a-q) can be found in Table 1.

shown in Scheme 3.[34] Substituted benzohydrazides **20d–g**, **20i–l**, **20n**, **20o**, and **20q** were converted to the corresponding potassium 3-aroyl dithiocarbazates **24d–g**, **24i–l**, **24n**, **24o**, and **24q** in 72–96% yields. The dithiocarbazates were then cyclized using concentrated sulfuric acid to the corresponding 2-aryl-1,3,4-thiadiazole-5-thiols **25d–g**, **25i–l**, **25n**, **25o**, and **25q** in 24–76% yields. In some cases, this reaction resulted in low yields of **25**. Unfortunately, neutralization of the reaction mixture with aqueous ammonia[35] did not improve the yields. 2-Methyl-1,3,4-thiadiazole-5-thiol (**25a**) was commercially available. The alkylation of 2-substituted-1,3,4-thiadiazole-5-thiols **25a**, **25d–g**, **25i–l**, **25n**, **25o**, and **25q** in the presence of TBAB led to the formation of the target nitro-substituted 2-alkyl/aryl-5-benzylsulfanyl-1,3,4-thiadiazoles **12o**, **13d**, **13g**, **13o**, **14a**, **14d–g**, **14i–l**, **14n**, **14o**, **14q**, **16g**, **16i**, and **16o** in 48–87% yields.

The alkyl and benzyl halides used in the aforementioned approaches are commercially available, with the exception of 3-nitro-5-trifluoromethylbenzyl chloride (**29**), which was prepared via a three-step procedure starting from 3-trifluoromethylbenzoic acid (**26**) (Scheme 4).

The synthesis of reduced analogues **17o** and **18o** is depicted in Scheme 5. In the first step, 3,5-dinitrobenzyl chloride was reduced using an excess of tin(II) chloride dihydrate in ethanol.[36] The addition of 5-(4-nitrophenyl)-1,3,4-oxadiazole-2-thiol (**21o**) in THF to an aqueous solution of these partially a fully reduced ammonium salts followed by the addition of sodium carbonate (to pH 8–10) resulted in the formation of desired products **17o** and **18o**.

In Vitro Antimycobacterial Activity against Replicating *Mycobacterium* spp. All synthesized compounds were assessed for in vitro antimycobacterial activities against *M.tb.* (H37Rv) and against the nontuberculous mycobacterial species *Mycobactierium avium* CNCTC My 330/88, *Mycobacterium*

Scheme 4. Synthesis of 3-Nitro-5-trifluoromethylbenzyl Chloride 29[a]

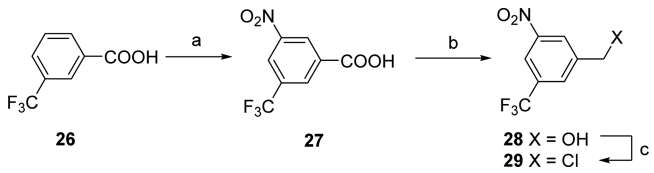

[a]Reagents and conditions: (a) H_2SO_4, HNO_3, 0–40 °C, 4 h, 91%; (b) BH_3, THF, −15 °C to rt, 24 h, 90%; (c) PCl_5, $CHCl_3$, 0 °C to reflux, 24 h, 91%.

kansasii CNCTC My 235/80, and the clinically isolated *M. kansasii* 6509/96. Selected compounds were assessed for in vitro antimycobacterial activities against six clinically isolated multidrug-resistant strains of *M.tb.* The antimycobacterial activities of the compounds were evaluated after incubation at 37 °C for 7/14/21 days for both strains of *M. kansasii* and after 14/21 days for the *M.tb.* and *M. avium* strains. The antimycobacterial activities are expressed as MICs (IC_{99}), which is the lowest concentration of a compound at which the inhibition of mycobacterial growth occurred. The first-line anti-TB drug INH was used as a reference compound.

The results of the in vitro antimycobacterial evaluation revealed that almost all compounds bearing the 3,5-dinitrobenzylsulfanyl moiety (**11b–q** and **14d–g**, **14i–l**, **14n**, **14o**, and **14q**) exhibited excellent activity against drug-susceptible *M.tb.* strains and against nontuberculous *M. kansasii* strains (Table 2).

The results confirmed that dinitrobenzylsulfanyl substitution is necessary for high antimycobacterial activity, which is consistent with our previous observations.[17,18] The 4-nitrobenzyl derivatives **9o** and **12o** exhibited the lowest anti-TB

DOI: 10.1021/acs.jmedchem.5b00608
J. Med. Chem. 2016, 59, 2362–2380

Scheme 5. Synthesis of Partially and Fully Reduced Derivatives 17o and 18o[a]

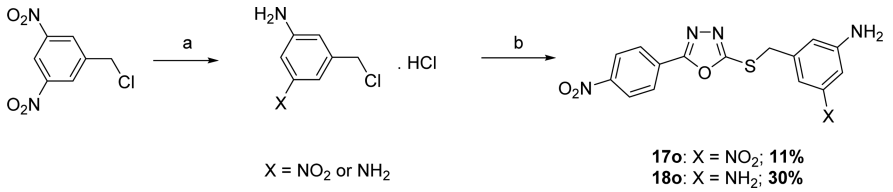

[a]Reagents and conditions: (a) $SnCl_2 \cdot 2H_2O$, EtOH, 10 min; (b) **21o**, Na_2CO_3, THF, rt, overnight.

effects in all cases. The positions of the two nitro groups substantially impacted the antimycobacterial activities of the prepared compounds. The antimycobacterial potencies of the 3,5-dinitro-substituted derivatives of series **11** and **14** were found to be considerably higher than those of the 2,4-dinitro-substituted derivatives of series **10** and **13**.

The highest activities against *M.tb.* were exhibited by the 1,3,4-oxadiazole derivatives **11c**, **11d**, **11f**, **11h**, **11i**, and **11j**, with MIC values of 0.03−0.06 μM (approximately 0.011−0.026 $\mu g.mL^{-1}$), and by the 1,3,4-thiadiazole derivatives **14d** and **14k**, with MIC values of 0.03−0.125 μM (approximately 0.012−0.06 $\mu g.mL^{-1}$). Nevertheless, almost all of the 3,5-dinitrobenzylsulfanyl derivatives of series **11** and **14** that were prepared and studied in this work possessed significantly higher activities than current first-line anti-TB drugs. Furthermore, selected compounds bearing 3,5-dinitrobenzylsulfanyl groups (**11d**, **11l**, **11o**, **14l**, **14g**, and **14o**) exhibited outstanding activities against all six MDR strains of *M.tb.*, with MIC values of 0.03−0.5 μM and no cross-resistance with any first- or second-line anti-TB drugs (Table 3).

Substituent R^1 in position 2 on the 1,3,4-oxadiazole and 1,3,4-thiadiazole cycles appears to have a negligible influence on the antimycobacterial activities of the investigated compounds. However, the R^1 substituent determines the physicochemical properties of the investigated compounds, as the remainder of the molecules remains unchanged. The low activity of 2-[(3,5-dinitrobenzyl)sulfanyl]-5-methyl-1,3,4-oxadiazole (**11a**) and its thiadiazole analogue (**14a**) against all four mycobacterial strains can be explained by the low lipophilicity of the methyl substituent R^1. The slightly lower activity of hydroxyphenyl derivative **11p** compared to the other derivatives of series **11** can be attributed to the same phenomenon.

The 2-alkyl/aryl-5-[(3,5-dinitrobenzyl)sulfanyl]-1,3,4-oxadiazoles of series **11** and 1,3,4-thiadiazoles of series **14** exhibited only moderate activities against highly resilient *M. avium* (MIC 4−62 μM). Nevertheless, clinically isolated *M. kansasii* 6509/96 and INH-resistant *M. kansasii* My 235/80 were susceptible to compounds from series **11** and **14**. Almost all compounds from both series were effective against these strains, with MIC values of 0.125−1 μM. The compounds from series **10** and **13** again appeared to be considerably less active than their 3,5-dinitro analogues.

The loss of the antimycobacterial activities of the partially and fully reduced derivatives **17o** and **18o** showed that the presence of both nitro groups is crucial for the high efficacies of the investigated compounds from series **11** and **14**. Because the lead compounds **11** and **14** showed structural similarities with the known DprE1 inhibitors DNB1[9] and MTX,[10,11] we replaced one nitro group with a trifluoromethyl group, such as in the structures of the DprE1 inhibitors PBTZ 169[8] and CT319.[10] However, trifluoromethyl analogues **15** and **16** were found to be inactive.

In Vitro Antimycobacterial Activity against Dormant Mycobacteria. The antimycobacterial activities of two selected compounds, **11i** and **14g**, were further evaluated against nonreplicating streptomycin (STR)-starved *M.tb.* strain 18b-Lux (SS18b-Lux) using a luciferase assay (Figure 4) and a standard resazurin reduction microplate assay (Supporting Information, Figure S2).[37] Both compounds showed equal or even better potency on the latent model SS18b than RIF. Furthermore, the SS18b-Lux assay also enabled us to monitor the time-dependent potency of the compounds. Here, we can conclude that **11i** and **14g** act on the dormant mycobacteria in a dose-dependent rather than time-dependent manner.

In Vitro Antibacterial and Antifungal Activities. To obtain basic insights regarding the selectivity of the inhibitory effects of the investigated compounds, the MIC values of compounds **10d**, **10g**, **10l**, **10o**, **11b**, **11d**, **11g−i**, **11k**, **11n**, **11o**, **13g**, **13o**, **14g**, **14l**, and **14o** against eight bacterial strains and eight fungal strains (five yeasts and three molds) were evaluated (Tables S1 and S2, see the Supporting Information). Interestingly, none of the compounds bearing 3,5-dinitrobenzyl or 2,4-dinitrobenzyl moieties exhibited antibacterial or antifungal activities (MIC values from >125 to >500 μM, depending on solubility), indicating that the molecular target of these compounds is exclusively mycobacterial.

In Vitro Effects of the Investigated Compounds on Cell Proliferation/Viability and Genotoxicity/Mutagenicity. First, we tested the effects of compounds **10d**, **10l**, **10o**, **11d**, **11f**, **11h**, **11i**, **11k**, **11l**, **11o**, **14d**, **14f**, **14g**, **14k**, **14l**, and **14o** on cellular viability using HuH7 (human hepatocellular carcinoma), HeLa (human cervical epithelioid carcinoma), and MDCKII-MDR1 (Madin−Darby canine kidney cells permanently expressing human efflux transporter MDR1) cell lines (Table 4). The data are presented as relative viability at a concentration of 20 μM compared to control vehicle-treated samples (100% viability). The results suggest that the 3,5-dinitrobenzylsulfanyl derivatives **11d**, **11f**, **11h**, **11i**, **11k**, **11l**, **11o**, **14d**, **14f**, **14g**, **14k**, **14l**, and **14o**, each of which possessed excellent anti-TB activity, produced limited negative effects on cellular viability in these three mammalian cell lines after 24 h of treatment at a concentration of 20 μM. Interestingly, compounds **11o** and **14o**, each bearing a third nitro group, produced no toxic effects even after 48 h of treatment. The remaining compounds, however, affected viability in at least one cell line each after 48 h of treatment. The 2,4-dinitrobenzylsulfanyl derivatives **10d**, **10l**, and **10o** produced insignificant negative effects on cellular viability following both 24 and 48 h of treatment.

In addition to these three model proliferating cell lines, we also studied the effects of compounds **11h**, **11i**, **11o**, **14g**, and **14k** on cell viability in primary human hepatocytes (Table 5). Importantly, none of the studied compounds were cytotoxic to hepatocytes after 48 h of treatment at a concentration of 20

DOI: 10.1021/acs.jmedchem.5b00608
J. Med. Chem. 2016, 59, 2362−2380

Table 2. In Vitro Antimycobacterial Activities of the Target Compounds from Series 9−18 Expressed as MICs (μM)

	14/21 days		7/14/21 days	
	M. tuberculosis My 331/88	*M. avium* My 330/88	*M. kansasii* My 235/80	*M. kansasii* 6509/96
9o	250/250	250/250	250/250/250	62/62/62
10d	2/4	>16/>16	4/8/16	2/8/8
10g	2/2	8/16	2/4/4	4/8/8
10l	0.5/1	4/4	2/8/16	2/8/16
10n	16/16	32/32	8/16/32	16/16/32
10o	2/2	>125/>125	2/4/8	2/4/8
10q	8/8	62/62	16/32/32	32/32/32
11a	4/8	500/500	4/8/16	16/16/32
11b	0.25/0.25	4/8	0.125/0.25/0.25	0.25/0.25/0.25
11c	≤0.03/≤0.03	nd	0.06/0.125/0.25	0.06/0.25/0.25
11d	0.06/0.06	16/32	0.5/1/1	0.5/1/2
11e	0.125/0.125	16/32	0.125/0.25/0.5	0.125/0.5/1
11f	≤0.03/0.06	16/16	0.125/0.25/0.5	0.125/0.5/1
11g	0.125/0.125	>125 >125	0.125/0.25/0.25	0.125/0.25/0.5
11h	≤0.03/0.06	16/32	0.125/0.5/0.5	0.125/0.25/0.5
11i	≤0.03/≤0.03	8/16	0.06/0.06/0.06	0.06/0.06/0.125
11j	0.06/0.06	>32/>32	0.25/0.5/1	0.5/1/2
11k	0.125/0.125	16/16	0.125/0.25/0.5	0.125/0.5/1
11l	0.125/0.125	16/32	0.125/0.25/0.25	0.125/0.25/0.5
11m	0.125/0.125	16/16	0.125/0.25/0.5	0.125/0.5/1
11n	0.125/0.125	16/16	0.25/0.5/0.5	0.5/1/2
11o	0.125/0.125	>125/>125	0.25/0.25/0.5	0.25/0.5/1
11p	1/1	62/62	4/8/16	4/8/16
11q	0.5/0.5	62/62	1/2/2	2/2/4
12o	62/62	250/250	250/250/250	62/62/62
13d	8/16	8/32	1/4/4	1/2/4
13g	2/4	4/8	1/2/4	1/2/4
13o	16/32	250/250	1/4/8	1/4/8
14a	4/4	125/125	4/4/8	8/8/16
14d	0.06/0.125	8/16	0.25/0.5/1	0.25/0.5/1
14e	0.125/0.125	16/>16	0.5/1/1	0.5/1/1
14f	0.125/0.125	8/16	0.25/1/1	0.25/0.5/0.5
14g	0.06/0.06	8/16	0.125/0.5/0.5	0.125/0.25/0.5
14i	0.125/0.125	>125/>125	0,5/0,5/1	0.5/1/2
14j	0.125/0.125	>16/>16	0.25/1/1	0.25/0.5/0.5
14k	≤0.03/0.06	8/16	0.25/0.5/0.5	0.25/0.5/0.5
14l	0.125/0.125	8/16	0.25/1/1	0.25/1/1
14n	0.125/0.125	>16/>16	0.25/1/1	0.5/1/1
14o	0.125/0.125	>16/>16	0.25/0.5/1	0.25/0.5/1
14q	0.125/0.125	>125/>125	0.5/1/1	0.5/1/1
15g	>32/>32	>500/>500	>32/>32/>32	>32/>32/>32
15i	>32/>32	>500/>500	>32/>32/>32	>32/>32/>32
15o	32/32	>500/>500	16/32/32	16/32/32
16g	>32/>32	>500/>500	>32/>32/>32	>32/>32/>32
16i	>32/>32	>500/>500	>32/>32/>32	>32/>32/>32
16o	>32/>32	>500/>500	>32/>32/>32	>32/>32/>32
17o	125/125	250/250	250/250/250	250/250/250
18o	250/250	250/250	250/250/250	250/250/250
INH	0.5/1	>250/>250	>250/>250/>250	4/4/4

μM. These results indicate that neither the compounds themselves nor their potential metabolites were cytotoxic to primary human hepatocytes. Furthermore, compounds **11i** and **14g** showed no toxic effect on HepG2 cells at the highest concentration tested (50 μM). Thus, the selectivity indices of these two compounds are higher than 500.

In our previous study, we showed that the 3,5-dinitrobenzylsulfanyl moiety, which is crucial for the high anti-TB activities of our compounds, is not a mutagenic carrier.[18] To further explore how this moiety contributes to the mutagenic effects caused by selected compounds, a 96-well microplate "fluctuation" version of the classical reverse mutation *Salmonella typhimurium* Ames Test was performed. We found that compounds **11f**, **11i**, **11k**, **14d**, **14g**, and **14k** produced no mutagenic effects on either strain TA98 or TA100 when used at a concentration of 30 μM. Reverse mutations were generated in at least one strain by compounds **11o** and **14o**, both of which harbor additional nitro groups in their molecular structures, as

DOI: 10.1021/acs.jmedchem.5b00608
J. Med. Chem. 2016, 59, 2362−2380

Table 3. In Vitro Antimycobacterial Activities of Compounds 11d, 11l, 11o, 14g, 14l, and 14o and of Selected Common Anti-TB Drugs against MDR Strains of *M.tb.*[a]

	MDR *M. tuberculosis* strains					
	234/2005	9449/2007	8666/2010	Praha 1	Praha 4	Praha 131
11d	≤0.03/0.06	0.06/0.06	≤0.03/0.06	0.06/0.06	≤0.03/0.06	≤0.03/0.06
11l	0.06/0.125	0.06/0.125	0.06/0.06	0.06/0.125	0.06/0.125	0.06/0.125
11o	0.06/0.125	0.06/0.125	0.06/0.06	0.06/0.125	0.06/0.125	0.06/0.125
14g	0.5/0.5	0.25/0.5	0.25/0.5	0.25/0.5	0.25/0.5	0.5/0.5
14l	0.125/0.25	0.125/0.25	0.06/0.125	0.125/0.25	0.125/0.25	0.125/0.25
14o	0.06/0.06	0.06/0.06	≤0.03/0.06	0.06/0.06	0.06/0.06	0.06/0.06
streptomycin	32 (R)	>32 (R)	>32 (R)	16 (R)	>32 (R)	>32 (R)
isoniazid	16 (R)	64 (R)	32 (R)	16 (R)	16 (R)	16 (R)
ethambutol	16 (R)	8 (S)	16 (R)	32 (R)	16 (R)	32 (R)
rifampin	>8 (R)	>8 (R)	>8 (R)	>8 (R)	>8 (R)	>8 (R)
ofloxacin	0.5 (S)	2 (S)	8 (R)	1 (S)	>16 (R)	16 (R)
gentamicin	0.25 (S)	1 (S)	2 (S)	1 (S)	0.5 (S)	>8 (R)
clofazimine	0.125 (S)	0.125 (S)	2 (R)	0.5 (R)	0.5 (R)	0.25 (S)
amikacin	0.5 (S)	0.5 (S)	2 (S)	0.5 (S)	1 (S)	>32 (R)

[a]The results are expressed as MICs (μM) after 14/21 days of incubation for the compounds and after 14 days of incubation for the anti-TB drugs. S: Strain susceptible to the given antibiotic drug. R: Strain resistant to the given antibiotic drug.

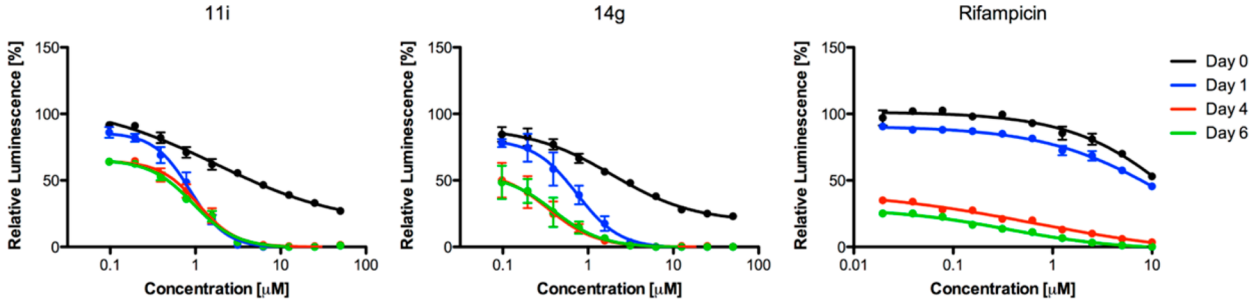

Figure 4. Assessment of compounds **11i**, **14g**, and RIF in the luciferase-based assay with SS18b-Lux. Relative luminescence: luminescence values normalized to the untreated control values.

Table 4. Cell Viability in Three Different Mammalian Cell Lines Determined by a Proliferation/Viability Cell Assay (MTS Assay) after Treatments with Test Compounds for 24 and 48 h[a]

	HuH7				HeLa				MDCKII-MDR1			
	24 h treatment		48 h treatment		24 h treatment		48 h treatment		24 h treatment		48 h treatment	
	IC_{50} (μM)	viability at 20 μM	IC_{50} (μM)	viability at 20 μM	IC_{50} (μM)	viability at 20 μM	IC_{50} (μM)	viability at 20 μM	IC_{50} (μM)	viability at 20 μM	IC_{50} (μM)	viability at 20 μM
10d	>20	99.5 ± 5.6	>20	92.8 ± 12.0	>20	97.7 ± 6.2	>20	112.9 ± 15.0	>20	69.6 ± 6.8	>20	73.3 ± 6.6
10l	>20	85.1 ± 8.6	>20	77.0 ± 7.3	>20	89.9 ± 5.8	>20	105.5 ± 7.8	>20	87.9 ± 15.1	>20	78.5 ± 16.3
10o	>20	107.3 ± 10.0	>20	99.6 ± 11.3	>20	90.1 ± 6.3	>20	117.0 ± 24.2	>20	85.2 ± 8.7	>20	119.8 ± 19.0
11d	>20	99.3 ± 5.5	>20	73.8 ± 10.9	>20	88.3 ± 7.4	nd	33.2 ± 10.1	>20	72.6 ± 14.3	nd	42.4 ± 9.9
11f	>20	97.9 ± 5.2	nd	45.9 ± 11.9	>20	81.9 ± 5.9	nd	34.6 ± 8.0	>20	93.3 ± 19.5	>20	57.9 ± 30.1
11h	>20	95.7 ± 5.7	nd	37.7 ± 8.5	>20	76.4 ± 4.9	nd	39.9 ± 9.4	>20	105.9 ± 8.6	nd	27.9 ± 20.5
11i	>20	100.9 ± 7.0	>20	53.1 ± 8.6	>20	87.2 ± 6.9	>20	118.1 ± 20.9	>20	98.0 ± 5.5	nd	48.5 ± 15.7
11k	>20	89.6 ± 2.3	nd	47.0 ± 8.4	>20	74.2 ± 14.0	4.1	16.4 ± 3.9	>20	104.7 ± 8.0	nd	10.5 ± 4.5
11l	>20	91.6 ± 6.8	nd	34.1 ± 5.4	>20	83.9 ± 8.4	nd	37.3 ± 5.7	>20	80.6 ± 17.1	10.6	14.5 ± 5.9
11o	>20	101.0 ± 6.4	>20	111.3 ± 18.7	>20	93.6 ± 8.9	>20	108.7 ± 10.8	>20	82.0 ± 10.5	>20	97.4 ± 11.9
14d	>20	84.3 ± 8.0	nd	36.3 ± 10.7	>20	78.5 ± 9.6	2.4	15.9 ± 4.7	>20	97.8 ± 8.5	3.1	7.3 ± 11.4
14f	>20	90.7 ± 7.5	nd	32.8 ± 9.2	>20	78.6 ± 4.3	2.6	16.8 ± 3.3	>20	107.6 ± 6.3	nd	48.6 ± 42.7
14g	>20	94.0 ± 7.0	nd	43.4 ± 18.5	>20	92.8 ± 7.4	>20	107.5 ± 26.1	>20	101.6 ± 43.8	>20	91.4 ± 7.9
14k	>20	86.3 ± 7.1	nd	33.0 ± 6.3	>20	71.2 ± 3.2	4.0	17.5 ± 3.7	>20	100.3 ± 6.5	6.4	18.5 ± 15.6
14l	>20	95.4 ± 4.9	>20	84.2 ± 9.3	>20	88.0 ± 5.9	4.4	27.1 ± 2.9	>20	101.4 ± 6.8	>20	60.0 ± 17.0
14o	>20	99.5 ± 8.4	>20	97.9 ± 5.0	>20	89.2 ± 5.2	>20	120.0 ± 29.3	>20	75.0 ± 15.2	>20	103.8 ± 11.3
RIF	>20	98.3 ± 25.1	>20	52.7 ± 18.4	>20	101.7 ± 5.4	>20	100.4 ± 8.1	>20	103.1 ± 9.1	>20	105.6 ± 7.5

[a]Vehicle (DMSO) and background (Triton X-100 0.9%; v/v, toxic control) controls of cell viability were set to be 100% and 0%, respectively. nd: not determined.

DOI: 10.1021/acs.jmedchem.5b00608
J. Med. Chem. 2016, 59, 2362−2380

Table 5. Cell Viabilities of Isolated Primary Human Hepatocytes and HepG2 Cells after a 48 h Treatment with Test Compounds at a Concentration of 20 μM for Primary Human Hepatocytes and 50 μM for HepG2 Cells

	primary human hepatocytes 48 h treatment		HepG2 48 h treatment	
	IC_{50} (μM)	viability at 20 μM	IC_{50} (μM)	viability at 50 μM
11h	>20	81.1 ± 5.8		
11i	>20	95.1 ± 8.6	>50	95.5 ± 1.3
11o	>20	106.9 ± 1.5		
14g	>20	101.8 ± 16.4	>50	98.5 ± 0.98
14k	>20	120.6 ± 5.9		
RIF	>20	123.2 ± 3.0		

well as by the 2,4-dinitrosubstituted derivative **10d** (Table 6). These results confirm that the 3,5-dinitrobenzyl moiety is not generally connected with either frame shift or base-exchange mutagenicity and that the investigated compounds bearing two nitro groups possess low mutagenicity.

Table 6. Evaluation of the Mutagenicity of Compounds 10d, 11d, 11f, 11i, 11k, 11o, 14d, 14g, 14k, and 14o via an Ames Fluctuation Assay Performed on *Salmonella typhimurium* TA100 and TA98 Strains at a Concentration of 30 μM[a]

	Ames fluctuation assay	
	TA100	TA98
sodium azide	+	nd
2-nitrofluorene	nd	+
10d	nd	+
11d	−	+
11f	−	−
11i	−	−
11k	−	−
11o	+	−
14d	−	−
14g	−	−
14k	−	−
14o	+	+

[a]−, negative mutagenicity; +, positive mutagenicity. nd, not determined. For all positive compounds, the statistical significance related to mutagenicity was set at 0.001.

On the basis of in silico ADMETox predictions (using ADMET Predictor, Simulation Plus Inc., Lancaster, CA), compound **14g** was selected for further genotoxicity studies. An in vitro mammalian cell micronucleus test was performed according to OECD guideline no. 487, and an in vitro mammalian chromosome aberration test was performed according to OECD guideline no. 473. Compound **14g** produced no genotoxic effects on human peripheral blood lymphocytes in either of the experiments, both with and without metabolic activation, at concentrations of 0.6−12 mM (250−5000 μg/mL).

Docking Studies. The selectivity of lead compounds of series **11** and **14** toward mycobacteria suggests the presence of a unique molecular target in this genus. Because they both possess structural similarities to 3,5-dinitrobenzamides (Figure 1),[9] a class of efficient DprE1 inhibitors, a docking experiment using DprE1[38,39] was performed with AutoDock Vina. The region selected for docking was represented by a box measuring 20 Å × 20 Å × 20 Å, which was centered at the N5 atom of the flavin group of the cofactor in DprE1. First, a 3-nitro-*N*-[(1*R*)-1-phenylethyl]-5-(trifluoromethyl) benzamide inhibitor that had been cocrystallized with DprE1 was docked into the enzyme to evaluate whether AutoDock Vina had the ability to reproduce its binding mode. The best scoring docked binding mode occupied the same space as the ligand in the crystal structure with an RMSD of 0.5 Å, confirming that AutoDock Vina is suitable for correctly identifying binding modes in this system. The best binding modes predicted for compounds **11i** and **14g** were similar (Supporting Information, Figure S1), with favorable binding energies of −9.2 and −8.6 kcal/mol, respectively.

Evaluation of the Effects of the Investigated Compounds on DprE1. The inhibition of DprE1 by compounds **11i** and **14g** was assessed by examining the incorporation of P[^{14}C]RPP into [^{14}C]decaprenylphosphoryl arabinose and its precursors accomplished by membrane and cell envelope enzyme fractions from *M. smegmatis* mc^{2}155, as previously described.[40] TLC analyses followed by autoradiography revealed that neither **11i** nor **14g** affected the biosynthesis of arabinan lipid precursors when used at concentrations of up to 0.6 mM (250 μg/mL) in the reaction mixture (Figure 5A). In addition, we performed [^{14}C]-acetate metabolic labeling of a model nonpathogenic strain *M.tb.* H37Ra grown in the presence of these compounds, along with the cultures treated with benzothiazinone BTZ-043.[12] On the basis of our experience, the suitable concentration of the compounds for examining their specific effects on metabolism is the one that results in the continued growth of the cultures after the addition of the compound and only modest (up to 40%) growth inhibition of the treated cultures compared to the control. For [^{14}C]-acetate metabolic labeling, we chose concentrations of 0.2 and 0.5 μg/mL for **11i** and **14g** and of 0.2 μg/mL for BTZ-043. Growth inhibition after 24 h of the drug treatment followed by 24 h of radiolabeling was approximately 12% for **14g** (0.5 μg/mL), 36% for **11i** (0.5 μg/mL), and 38% for BTZ-043 (0.2 μg/mL) (Supporting Information, Table S4). Analysis of the lipids extracted from the radiolabeled cells showed the typical profile of trehalose dimycolate (TDM) accumulation for BTZ-043, similar to the effects observed for ethambutol, which inhibits the synthesis of mycobacterial arabinans.[41] This phenotype was not observed in lipids extracted from cells treated with the investigated compounds (Figure 5B). These data suggest that despite favorable docking of **11i** and **14g** to the DprE1 structure, this enzyme is not the target of these compounds.

Radiolabeling of 11i- and 14g-Treated *M.tb.* H37Ra with [^{14}C]-Uracil and [^{14}C]-Methionine. To examine the potential effects of the studied drugs on the synthesis of nucleic acids and proteins, *M.tb.* H37Ra cultures were pretreated for 1 h with 1 μg/mL **11i** and **14g** followed by 24 h of incubation with [^{14}C]-uracil and [^{14}C]-methionine as tracers. RIF (0.05 μg/mL) was used as a control drug for the inhibition of the biosynthesis of RNA, and KAN (5 μg/mL) served as a control for the inhibition of proteosynthesis. Under these experimental conditions, the growth inhibition by **11i** was comparable to that of RIF and KAN; the effect of **14g** was less pronounced (Figure 6A; Supporting Information, Table S5). Although the presence of KAN in the culture strongly inhibited the incorporation of [^{14}C]-methionine into the cells, there was no defect in the [^{14}C]-uracil radiolabeling of the KAN-treated mycobacteria, confirming the known mode of action of this drug. In contrast, RIF reduced the incorporation of both [^{14}C]-uracil and [^{14}C]-

DOI: 10.1021/acs.jmedchem.5b00608
J. Med. Chem. 2016, 59, 2362−2380

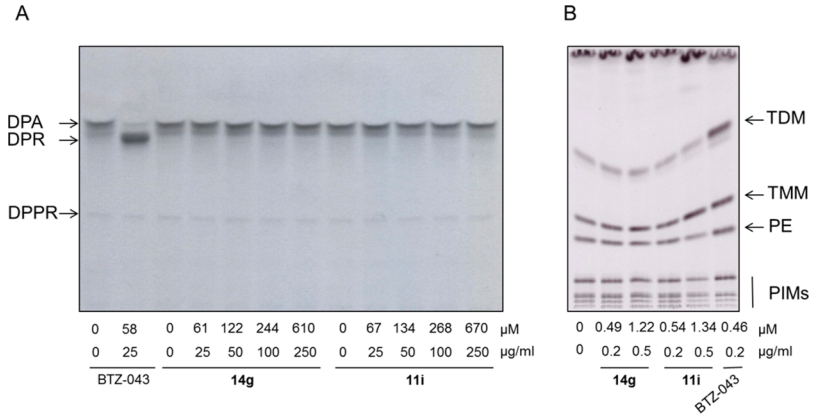

Figure 5. Investigation of the effects of **14g** and **11i** on DprE1. (A) Monitoring of cell-free synthesis of decaprenylphosphoryl arabinose in the presence of **14g** and **11i**. Reactions with P[^{14}C]RPP substrate were performed as described in the Experimental Section. A total of 25% of the extracted radiolabeled products were separated on a silica gel TLC plate, which was developed in $CHCl_3/CH_3OH$/concentrated NH_4OH/1 M ammonium acetate/H_2O (180:140:9:9:23, v/v). The plate was exposed to autoradiography film at −80 °C for 3 days. DPPR, decaprenylphosphoryl ribose-5-phosphate; DPR, decaprenylphosphoryl ribose; DPA, decaprenylphosphoryl arabinose. (B) TLC analysis of the lipids from [^{14}C]-acetate-labeled *M.tb.* H37Ra grown in the presence of **14g**, **11i**, or DprE1 inhibitor BTZ-043. Bacteria were pretreated with the drugs for 24 h, followed by 24 h of radiolabeling with [^{14}C]-acetate. Lipids were extracted and dissolved in $CHCl_3/CH_3OH$/concentrated NH_4OH/H_2O (65:25:0.5:3.6, v/v) in the ratio of 150 μL/OD_{600} 0.5. First, 5 μL of each sample were loaded on a silica gel TLC plate and separated in $CHCl_3/CH_3OH/H_2O$ (20:4:0.5, v/v). Then the plate was exposed to autoradiography film at −80 °C for 3 days. TDM, trehalose dimycolate; TMM, trehalose monomycolate; PE, phosphatidylethanolamine; PIMs, phosphatidylinositol mannosides.

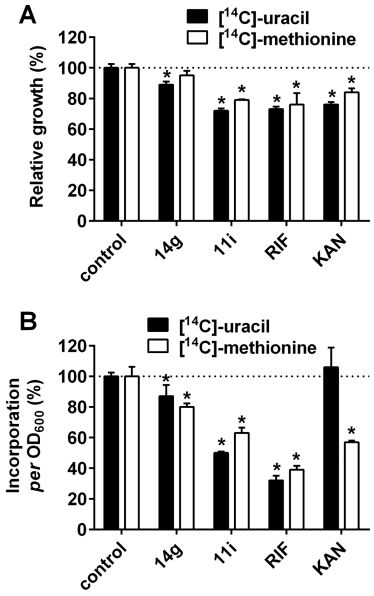

Figure 6. Metabolic labeling of *M.tb.* H37Ra with [^{14}C]-uracil and [^{14}C]-methionine. (A) Relative growth of the cultures treated with the investigated compounds in the following concentrations: **14g**, 1 μg/mL (2.5 μM); **11i**, 1 μg/mL (2.7 μM); RIF, 0.05 μg/mL (0.06 μM); and KAN, 5 μg/mL (10 μM). (B) Relative incorporation of [^{14}C]-uracil and [^{14}C]-methionine into the cells from drug-treated cultures described in A normalized to the same OD_{600} and expressed as a percentage of incorporation in untreated controls. The data in both panels represent the average values of triplicate samples with standard deviations. * indicates statistical significance against control at $p < 0.05$ (Two-Way ANOVA with Dunnett's multiple comparisons test).

methionine by 68% and 61%, respectively (Figure 6B; Supporting Information, Table S5). [^{14}C]-Methionine radiolabeling was very likely disturbed by RIF due to secondary effects of RNA synthesis inhibition on proteosynthesis. Similar trends were observed for compound **11i**, which caused a 50% inhibition of [^{14}C]-uracil incorporation into the cells and a 37% inhibition of [^{14}C]-methionine labeling. The incorporation of both tracers was also inhibited by compound **14g**, although to a lesser extent, 13% for [^{14}C]-uracil and 20% for [^{14}C]-methionine, probably due to the lower growth inhibition caused by **14g** compared to **11i** (Figure 6; Supporting Information, Table S5). The analogous effects observed for RIF and the investigated compounds imply that **14g** and **11i** could affect the synthesis of nucleic acids. This finding is consistent with their high activity against the nonreplicating *M.tb.* SS18b-Lux strain.

Chemical Stability, Human Microsomal Stability, and Solubility of Compounds 11i and 14g in aqueous media. Solutions of compounds **11i** and **14g** at concentrations of 100 μM in DMSO were stored at rt for 1 month. HPLC analysis showed no decomposition of either compound. Furthermore, compound **14g** was heated in DMSO (4 mg/mL) at 60 °C for 3 days under open-vessel conditions. After evaporation, the residue was subjected to ^{1}H NMR, and the spectrum was the same as that of pure compound **14g**.

Moreover, the stability of compounds **11i** and **14g** in DMSO was indirectly confirmed via the in vitro evaluation of their MICs against *M.tb*. Both compounds were dissolved in DMSO, and one aliquot of each solution was used to determine its MIC against *M.tb*. A second aliquot of each solution was stored at rt for 1 month and then used in the same way. Both experiments produced the same MIC values.

Because the in silico prediction indicates that the sulfur atom adjacent to the heterocycle in **11i** and **14g** is highly susceptible to metabolization by the CYP2D6 and CYP3A4 enzymes of cytochrome P450 (software ACD/I-Lab, ACD Lab.), we performed a microsomal stability assay. Microsomes can be used to determine the in vitro intrinsic clearance (CL_{int}) of a compound, which can be scaled up to the in vivo situation and used in the prediction of human clearance. On the basis of CL_{int}, compounds can be categorized into low-, medium-, or high-clearance compounds.[42]

The CL_{int} for **14g** was determined to be 29 μL/min/mg protein, and the CL_{int} for **11i** was determined to be 86 μL/

DOI: 10.1021/acs.jmedchem.5b00608
J. Med. Chem. 2016, 59, 2362−2380

min/mg protein. Thus, these compounds can be classified as compounds with medium and high clearance with respect to phase I metabolic deactivation.

All compounds of series **11** and **14** described in this work possess high lipophilicity. To determine their aqueous solubility, 20 mM stock solutions of compounds **11i** and **14g** in DMSO were prepared and added to water to obtain final DMSO concentrations (v/v) of 1% (200 μM of the investigated compound), 0.1% (20 μM of compound), and 0.01% (2 μM of compound). These aqueous samples of compounds **11i** and **14g** were slightly opalescent but highly stable (except for the highest concentration of 200 μM), as shown by HPLC analysis. To determine the actual solubility, the opalescent solutions were centrifuged at 10000 rpm for 10 min and the clear supernatants were analyzed. The solubilities of **11i** and **14g** in water with 0.01−1% DMSO ranged from 0.50 ± 0.05 to 0.76 ± 0.09 μM and from 0.54 ± 0.03 to 3.44 ± 0.74 μM, respectively. To determine the solubility in water without DMSO, both compounds were shaken with distilled water for 24 h, the suspensions were centrifuged at 10000 rpm for 10 min, and the clear supernatants were analyzed. The solubilities of **11i** and **14g** in water were 0.067 ± 0.008 and 0.030 ± 0.009 μM, respectively.

CONCLUSIONS

In this work, we found that 5-substituted 2-[(3,5-dinitrobenzyl)sulfanyl]-1,3,4-oxadiazoles (**11**) and 1,3,4-thiadiazoles (**14**) possess excellent activity against drug-susceptible and multidrug-resistant *M.tb.*, with no cross resistance with first- and second-line anti-TB drugs. The MIC values of the most active compounds against *M.tb.* were as low as 0.03 μM (approximately 0.011 μg/mL). Furthermore, these compounds exhibited excellent activity against the nonreplicating *M.tb.* strain SS18b-Lux. Our SAR study determined that 3,5-dinitro substitution has a crucial role in antimycobacterial activity: any changes to the positions or numbers of nitro groups led to a significant decrease in antimycobacterial activity. The 2,4-dinitrobenzylsulfanyl derivatives **10** and **13** possessed 10−100-fold lower antimycobacterial effects, and the 4-nitrobenzylsulfanyl analogues **9o** and **12o** practically lost activity. Because the relatively high variability of substituent R^1 on the oxadiazole/thiadiazole moieties does not negatively affect their antimycobacterial activities, further structural optimization of lead compounds **11** and **14** is possible. The main drawback of the reported compounds is their low solubility in aqueous media. This issue, together with relatively fast metabolic degradation, will be considered in further structural optimizations.

Interestingly, the replacement of one nitro group with a trifluoromethyl moiety resulted in compounds with diminished antimycobacterial activity. Although the 3,5-dinitrobenzylsulfanyl lead compounds **11** and **14** and their trifluoromethyl analogues **15** and **16** all showed structural similarities to known highly efficient inhibitors of DprE1, such as dinitrobenzamides[9] or benzothiazinones,[12,13] only the lead compounds **11** and **14** exhibited excellent antimycobacterial activities.

The antimycobacterial effects of the investigated compounds were selective, as they showed no growth inhibitory activity against other bacteria or against fungi and had low toxicity against proliferating cell lines and isolated human hepatocytes. Moreover, several genotoxicity and mutagenicity assays indicated that these nitro group-containing compounds have low mutagenicity. These results indicate that the reported compounds affect some specific mycobacterial system. Although docking experiments suggested that compounds **11i** and **14g** might inhibit DprE1, cell-free assays did not confirm this assumption. Nevertheless, metabolic radiolabeling experiments with [^{14}C]-acetate, [^{14}C]-uracil, and [^{14}C]-methionine showed that compound **11i** reduced the incorporation of both [^{14}C]-uracil and [^{14}C]-methionine by 50% and 37%, respectively, similar to RIF. These findings, together with the absence of cross-resistance with common anti-TB drugs including RIF, indicate that the investigated compounds possess a novel mechanism of action targeting the synthesis of mycobacterial nucleic acids.

5-Substituted-2-[(3,5-dinitrobenzyl)sulfanyl]-1,3,4-oxadiazoles (**11**) and 1,3,4-thiadiazoles (**14**) proved to be promising antitubercular agents, warranting further structural optimization and assessment both in vitro and in vivo.

EXPERIMENTAL SECTION

General. The structural identities of the prepared compounds were confirmed by ^{1}H NMR and ^{13}C NMR spectroscopy. Each of the reported compounds had ≥95% purity, as determined by elemental analysis. All chemicals used for synthesis were obtained from Sigma-Aldrich (Schnelldorf, Germany) and were used as received. TLC was performed on Merck aluminum plates with silica gel 60 F_{254}. Merck Kieselgel 60 (0.040−0.063 mm) was used for column chromatography. Melting points were recorded using a Büchi B-545 apparatus and are uncorrected. ^{1}H and ^{13}C NMR spectra were recorded using Varian Mercury Vx BB 300 and VNMR S500 NMR spectrometers. Chemical shifts were reported as δ values in parts per million (ppm) and were indirectly referenced to tetramethylsilane (TMS) via the solvent signal. The elemental analysis was conducted using an EA1110CE automatic microanalyzer (Fisons Instruments S.p.A., Milano, Italy). Electrospray ionization mass spectroscopy (ESI MS) experiments were performed using an LCQ Advantage Max (Thermo Finnigan, San Jose, USA) equipped with an ESI source. Mass spectra of the samples were obtained by direct injection of each sample in a CH_3CN:H_2O:HCOOH 50:50:0.1 (v/v) solvent system into the detector. HPLC-HRMS (ESI+) experiments were performed using an UltiMate3000 rapid separation liquid chromatography system with a Q-Exactive Plus mass spectrometer (Thermo Scientific, Bremen, Germany).

4-Nitrobenzyl chloride, 2,4-dinitrobenzyl chloride, 3,5-dinitrobenzyl chloride, and **29** were used as alkylating agents.

General Procedure for the Synthesis of Acyl Hydrazides (20b−p). An 80% solution of hydrazine hydrate (1.56 g, 1.52 mL, 25 mmol) was added dropwise to a solution of the methyl ester of corresponding carboxylic acid **19** (5 mmol) in EtOH (25 mL). The reaction mixture was refluxed for 4−48 h until completion, as determined by TLC. After cooling, water (7 mL) was added and the precipitated product was filtered and washed with a small amount of ethanol and water. In cases in which the product did not precipitate, it was necessary to evaporate approximately half of the solvent. Some acyl hydrazide derivatives are partially soluble in water. Therefore, NaCl was added to the filtrate, and a subsequent extraction with EtOAc was performed to obtain all of the product. Acyl hydrazides (**20b−p**) were obtained with sufficient purity to be used in further reactions without purification.

General Procedure for the Synthesis of 5-Substituted-1,3,4-oxadiazole-2-thiols (21b−q). Carbon disulfide (0.46 g, 0.36 mL, 6 mmol) was slowly added to a solution of corresponding acyl hydrazide (**20**) (2 mmol) and potassium hydroxide (0.11 g, 2 mmol) in EtOH (15 mL). The reaction mixture was refluxed for 6−44 h, depending on the R^1-substituent. Upon completion, the solvent was evaporated under reduced pressure and the residue was dissolved in water. The aqueous solution was acidified to pH 2 using hydrogen chloride. The product was filtered and washed with water to obtain a neutral pH. 2-Substituted-1,3,4-oxadiazole-5-thiols (**21b−q**) were obtained with sufficient purity to be used in further reactions without purification.

DOI: 10.1021/acs.jmedchem.5b00608
J. Med. Chem. 2016, 59, 2362−2380

General Procedure for the Synthesis of 2-Alkyl/Aryl-5-benzylsulfanyl-1,3,4-oxadiazoles (9o, 10d, 10g, 10l, 10n, 10o, 10q, 11b−q, 15g, 15i, 15o). A solution of an alkylating agent (1 mmol) and tetrabutylammonium bromide (0.016 g, 0.05 mmol) in CH_2Cl_2 (5 mL) was added to a solution of the corresponding 5-substituted-1,3,4-oxadiazole-2-thiol (**21**) (1.1 mmol) with sodium hydroxide (0.05 g, 1.25 mmol) in H_2O (5 mL). The reaction mixture was slowly stirred at room temperature overnight. Upon completion, the organic layer was separated, washed with water (2 × 7 mL), and dried over anhydrous sodium sulfate. The solvent was removed under reduced pressure, and the product was purified by column chromatography (mobile phase: hexane/EtOAc).

*2-(4-Nitrophenyl)-5-((4-nitrobenzyl)sulfanyl)-1,3,4-oxadiazole (**9o**).* 4-Nitrobenzyl chloride was used as an alkylating agent. Yield 82% as a white solid; mp 217−219 °C. ^{1}H NMR (500 MHz, DMSO) δ 8.40 (d, J = 8.8 Hz, 2H, Ar-*H*), 8.20 (t, J = 8.8 Hz, 4H, Ar-*H*), 7.79 (d, J = 8.4 Hz, 2H, Ar-*H*), 4.74 (s, 2H, SCH_2). ^{13}C NMR (126 MHz, DMSO) δ 164.53, 164.23, 149.32, 147.09, 145.02, 130.55, 128.62, 127.96, 124.78, 123.83, 35.05. Anal. Calcd for $C_{15}H_{10}N_4O_5S$: C, 50.28; H, 2.81; N, 15.64; S, 8.95. Found: C, 49.9; H, 2.72; N, 15.47; S, 9.26. MS (ESI): m/z 359.05 (M + H$^+$, 100%), 360.12 (20%).

*2-((2,4-Dinitrobenzyl)sulfanyl)-5-phenyl-1,3,4-oxadiazole (**10d**).* 2,4-Dinitrobenzyl chloride was used as an alkylating agent. Yield 82% as a light-beige solid; mp 137−138 °C. ^{1}H NMR (300 MHz, DMSO) δ 8.78 (d, J = 2.4 Hz, 1H, $(NO_2)_2$Ph-*H*), 8.57 (dd, J = 8.6, 2.4 Hz, 1H, $(NO_2)_2$Ph-*H*), 8.10 (d, J = 8.6 Hz, 1H, $(NO_2)_2$Ph-*H*), 7.97−7.88 (m, 2H, Ph-*H*), 7.66−7.51 (m, 3H, Ph-*H*), 4.93 (s, 2H, SCH_2). ^{13}C NMR (75 MHz, DMSO) δ 165.83, 162.76, 148.06, 147.27, 139.17, 134.33, 132.32, 129.61, 128.25, 126.64, 123.06, 120.75, 33.17. Anal. Calcd of $C_{15}H_{10}N_4O_5S$: C, 50.28; H, 2.81; N, 15.64; S, 8.95. Found: C, 50.38; H, 2.86; N, 15.81; S, 9.06. MS (ESI): m/z 358.91 (M + H$^+$, 100%), 359.96 (16%).

*2-(4-Chlorophenyl)-5-((2,4-dinitrobenzyl)sulfanyl)-1,3,4-oxadiazole (**10g**).* 2,4-Dinitrobenzyl chloride was used as an alkylating agent. Yield 65% as a yellow solid; mp 116−118 °C. ^{1}H NMR (300 MHz, acetone) δ 8.88 (d, J = 2.4 Hz, 1H, $(NO_2)_2$Ph-*H*), 8.58 (dd, J = 8.5, 2.4 Hz, 1H, $(NO_2)_2$Ph-*H*), 8.24 (d, J = 8.5 Hz, 1H, $(NO_2)_2$Ph-*H*), 7.99 (d, J = 8.6 Hz, 2H, ClPh-*H*), 7.61 (d, J = 8.6 Hz, 2H, ClPh-*H*), 5.03 (s, 2H, SCH_2). ^{13}C NMR (75 MHz, acetone) δ 166.08, 164.14, 148.55, 140.14, 138.24, 135.30, 130.35, 129.03, 128.97, 128.69, 123.19, 121.53, 34.09. Anal. Calcd for $C_{15}H_9ClN_4O_5S$: C, 45.87; H, 2.31; N, 14.26; S, 8.16. Found: C, 45.56; H, 2.68; N, 14.15; S, 8.51. MS (ESI): m/z 393.05 (M + H$^+$, 100%), 395.05 (40%), 394.08 (20%).

*2-((2,4-Dinitrobenzyl)sulfanyl)-5-(4-methoxyphenyl)-1,3,4-oxadiazole (**10l**).* 2,4-Dinitrobenzyl chloride was used as an alkylating agent. Yield 60% as a yellowish solid; mp 106−107 °C. ^{1}H NMR (300 MHz, DMSO) δ 8.77 (d, J = 2.4 Hz, 1H, $(NO_2)_2$Ph-*H*), 8.62−8.51 (m, 1H, $(NO_2)_2$Ph-*H*), 8.08 (d, J = 8.6 Hz, 1H, $(NO_2)_2$Ph-*H*), 7.86 (d, J = 8.4 Hz, 2H, MeOPh-*H*), 7.11 (d, J = 8.4 Hz, 2H, MeOPh-*H*), 4.91 (s, 2H, SCH_2), 3.83 (s, 3H, OCH_3). ^{13}C NMR (75 MHz, DMSO) δ 165.79, 162.30, 161.90, 148.04, 147.25, 139.24, 134.30, 128.52, 128.22, 120.74, 115.38, 115.04, 55.71, 33.18. Anal. Calcd for $C_{16}H_{12}N_4O_6S$: C, 49.48; H, 3.11; N, 14.43; S, 8.26. Found: C, 49.42; H, 3.29; N, 14.40; S, 8.62. MS (ESI): m/z 388.94 (M + H$^+$, 100%), 389.97 (18%).

*2-((2,4-Dinitrobenzyl)sulfanyl)-5-(3-nitrophenyl)-1,3,4-oxadiazole (**10n**).* 2,4-Dinitrobenzyl chloride was used as an alkylating agent. Yield: 45% as a brownish solid; mp 160−163 °C. ^{1}H NMR (300 MHz, DMSO) δ 8.79 (d, J = 2.4 Hz, 1H, $(NO_2)_2$Ph-*H*), 8.60−8.55 (m, 2H, Ar-*H*), 8.48−8.42 (m, 1H, Ar-*H*), 8.39−8.33 (m, 1H, Ar-*H*), 8.13 (d, J = 8.6 Hz, 1H, $(NO_2)_2$Ph-*H*), 7.89 (t, J = 8.1 Hz, 1H, NO_2Ph-*H*), 4.97 (s, 2H, SCH_2). ^{13}C NMR (75 MHz, DMSO) δ 164.33, 163.77, 148.39, 148.11, 147.31, 139.11, 134.41, 132.70, 131.55, 128.25, 126.64, 124.57, 121.19, 120.78, 33.18. Anal. Calcd for $C_{15}H_9N_5O_7S$: C, 44.67; H, 2.25; N, 17.36; S, 7.95. Found: C, 44.88; H, 2.53; N, 17.16; S, 8.03. MS (ESI): m/z 404.02 (M + H$^+$, 100%), 405.06 (22%).

*2-((2,4-Dinitrobenzyl)sulfanyl)-5-(4-nitrophenyl)-1,3,4-oxadiazole (**10o**).* 2,4-Dinitrobenzyl chloride was used as an alkylating agent. Yield 80% as a light-beige solid; mp 185−186 °C. ^{1}H NMR (500 MHz, DMSO) δ 8.78 (d, J = 2.6 Hz, 1H, $(NO_2)_2$Ph-*H*), 8.59 (dd, J = 8.5, 2.6 Hz, 1H, $(NO_2)_2$Ph-*H*), 8.40 (d, J = 8.8 Hz, 2H, NO_2Ph-*H*), 8.19 (d, J = 8.8 Hz, 2H, NO_2Ph-*H*), 8.13 (d, J = 8.5 Hz, 1H, $(NO_2)_2$Ph-*H*), 4.97 (s, 2H, SCH_2). ^{13}C NMR (126 MHz, DMSO) δ 164.46, 164.20, 149.35, 148.06, 147.31, 139.02, 134.38, 128.59, 128.27, 128.02, 124.77, 120.75, 33.15. Anal. Calcd for $C_{15}H_9N_5O_7S$: C, 44.67; H, 2.25; N, 17.36; S, 7.95. Found: C, 45.00; H, 2.42; N, 17.20; S, 8.15. MS (ESI): m/z 403.87 (M + H$^+$, 100%), 404.92 (20%).

*2-((2,4-Dinitrobenzyl)sulfanyl)-5-(pyridin-4-yl)-1,3,4-oxadiazole (**10q**).* 2,4-Dinitrobenzyl chloride was used as an alkylating agent. Yield 87% as a yellow solid; mp 107−108 °C. ^{1}H NMR (500 MHz, DMSO) δ 8.81 (d, J = 6.0 Hz, 2H, Py-*H*), 8.78 (d, J = 2.4 Hz, 1H, $(NO_2)_2$Ph-*H*), 8.58 (dd, J = 8.6, 2.4 Hz, 1H, $(NO_2)_2$Ph-*H*), 8.12 (d, J = 8.6 Hz, 1H, $(NO_2)_2$Ph-*H*), 7.87 (d, J = 6.0 Hz, 2H, Py-*H*), 4.96 (s, 2H, SCH_2). ^{13}C NMR (126 MHz, DMSO) δ 164.29, 164.24, 151.10, 148.06, 147.30, 138.99, 134.37, 130.14, 128.27, 120.74, 120.20, 33.12. Anal. Calcd for $C_{14}H_9N_5O_5S$: C, 46.80; H, 2.52; N, 19.49; S, 8.92. Found: C, 47.06; H, 2.77; N, 19.43; S, 9.26. MS (ESI): m/z 360.00 (M + H$^+$, 100%), 361.01 (18%).

*2-((3,5-Dinitrobenzyl)sulfanyl)-5-(undecyl)-1,3,4-oxadiazole (**11b**).* 3,5-Dinitrobenzyl chloride was used as an alkylating agent. Yield: 92% as a light-beige solid; mp 55−56 °C. ^{1}H NMR (500 MHz, DMSO) δ 8.78 (d, J = 2.2 Hz, 2H, $(NO_2)_2$Ph-*H*), 8.73 (t, J = 2.2 Hz, 1H, $(NO_2)_2$Ph-*H*), 4.72 (s, 2H, SCH_2), 2.76 (t, J = 7.5 Hz, 2H, OC(=N)CH_2), 1.64−1.55 (m, 2H, OC(=N)CH_2CH_2), 1.31−1.13 (m, 16H), 0.83 (t, J = 6.8 Hz, 3H, CH_3). ^{13}C NMR (126 MHz, DMSO) δ 168.43, 162.15, 148.04, 142.31, 129.76, 117.92, 34.19, 31.44, 29.11, 28.95, 28.85, 28.59, 28.38, 25.75, 24.64, 22.24, 14.08. Anal. Calcd for $C_{20}H_{28}N_4O_5S$: C, 55.03; H, 6.47; N, 12.83; S, 7.35. Found: C, 55.12; H, 6.18; N, 12.75; S, 7.29. MS (ESI): m/z 437.16 (M + H$^+$, 100%), 438.17 (24%).

*2-Cyclohexyl-5-((3,5-dinitrobenzyl)sulfanyl)-1,3,4-oxadiazole (**11c**).* 3,5-Dinitrobenzyl chloride was used as an alkylating agent. Yield 85% as a white solid; mp 112−114 °C. ^{1}H NMR (300 MHz, DMSO) δ 8.78 (d, J = 2.2 Hz, 2H, $(NO_2)_2$Ph-*H*), 8.73 (t, J = 2.2 Hz, 1H, $(NO_2)_2$Ph-*H*), 4.72 (s, 2H, SCH_2), 2.95−2.80 (m, 1H, OC(=N)C*H*), 1.98−1.84 (m, 2H, Cy-*H*), 1.74−1.55 (m, 3H, Cy-*H*), 1.51−1.12 (m, 5H, Cy-*H*). ^{13}C NMR (75 MHz, DMSO) δ 171.13, 162.03, 148.07, 142.39, 129.83, 118.01, 34.32, 34.18, 29.52, 25.24, 24.80. Anal. Calcd for $C_{15}H_{16}N_4O_5S$: C, 49.44; H, 4.43; N, 15.38; S, 8.80. Found: C, 49.61; H, 4.59; N, 15.43; S, 9.04. MS (ESI): m/z 365.10 (M + H$^+$, 100%), 366.13 (18%).

*2-((3,5-Dinitrobenzyl)sulfanyl)-5-phenyl-1,3,4-oxadiazole (**11d**).* 3,5-Dinitrobenzyl chloride was used as an alkylating agent. Yield 90% as a light-beige solid; mp 140−141 °C. ^{1}H NMR (300 MHz, acetone) δ 8.92 (d, J = 2.1 Hz, 2H, $(NO_2)_2$Ph-*H*), 8.86 (t, J = 2.1 Hz, 1H, $(NO_2)_2$Ph-*H*), 8.02−7.92 (m, 2H, Ph-*H*), 7.62−7.52 (m, 3H, Ph-*H*), 4.92 (s, 2H, SCH_2). ^{13}C NMR (75 MHz, acetone) δ 166.77, 163.63, 149.37, 143.19, 132.71, 130.49, 130.09, 127.28, 124.41, 118.70, 35.27. Anal. Calcd for $C_{15}H_{10}N_4O_5S$: C, 50.28; H, 2.81; N, 15.64; S, 8.95. Found: C, 50.42; H, 3.09; N, 15.52; S, 9.19. MS (ESI): m/z 358.97 (M + H$^+$, 100%), 360.00 (18%).

*5-(2-Chlorophenyl)-2-((3,5-dinitrobenzyl)sulfanyl)-1,3,4-oxadiazole (**11e**).* 3,5-Dinitrobenzyl chloride was used as an alkylating agent. Yield 84% as a light-beige solid; mp 105−106 °C. ^{1}H NMR (300 MHz, DMSO) δ 8.84 (d, J = 2.1 Hz, 2H, $(NO_2)_2$Ph-*H*), 8.74 (t, J = 2.1 Hz, 1H, $(NO_2)_2$Ph-*H*), 7.91 (dd, J = 7.7, 1.7 Hz, 1H, ClPh-*H*), 7.73−7.45 (m, 3H, ClPh-*H*), 4.82 (s, 2H, SCH_2). ^{13}C NMR (75 MHz, DMSO) δ 163.69, 163.64, 148.11, 142.16, 133.51, 131.82, 131.36, 131.30, 129.90, 128.01, 122.19, 118.06, 34.36. Anal. Calcd for $C_{15}H_9ClN_4O_5S$: C, 45.87; H, 2.31; N, 14.26; S, 8.16. Found: C, 45.58; H, 2.62; N, 14.07; S, 8.35. MS (ESI): m/z 392.96 (M + H$^+$, 100%), 394.96 (34%), 393.96 (18%).

*5-(3-Chlorophenyl)-2-((3,5-dinitrobenzyl)sulfanyl)-1,3,4-oxadiazole (**11f**).* 3,5-Dinitrobenzyl chloride was used as an alkylating agent. Yield 73% as a light-orange solid; mp 128−129 °C. ^{1}H NMR (300 MHz, DMSO) δ 8.96−8.64 (m, 3H, $(NO_2)_2$Ph-*H*), 7.97−7.84 (m, 2H, ClPh-*H*), 7.72−7.53 (m, 2H, ClPh-*H*), 4.83 (s, 2H, SCH_2). ^{13}C NMR (75 MHz, DMSO) δ 164.49, 163.49, 148.10, 142.27, 134.23, 132.05, 131.56, 129.89, 126.11, 125.27, 124.98, 118.03, 34.22. Anal. Calcd for $C_{15}H_9ClN_4O_5S$: C, 45.87; H, 2.31; N, 14.26; S, 8.16. Found:

DOI: 10.1021/acs.jmedchem.5b00608
J. Med. Chem. 2016, 59, 2362−2380

C, 46.12; H, 2.68; N, 14.10; S, 8.39. MS (ESI): m/z 393.03 (M + H^+, 100%), 395.02 (36%), 394.06 (20%).

*5-(4-Chlorophenyl)-2-((3,5-dinitrobenzyl)sulfanyl)-1,3,4-oxadiazole (**11g**).* 3,5-Dinitrobenzyl chloride was used as an alkylating agent. Yield 66% as a yellow solid; mp 186−187 °C (with decomposition). ^{1}H NMR (500 MHz, $CDCl_3$) δ 8.97 (t, J = 2.1 Hz, 1H, $(NO_2)_2$Ph-*H*), 8.74 (d, J = 2.1 Hz, 2H, $(NO_2)_2$Ph-*H*), 7.91 (d, J = 8.7 Hz, 2H, ClPh-*H*), 7.48 (d, J = 8.7 Hz, 2H, ClPh-*H*), 4.67 (s, 2H, SCH_2). ^{13}C NMR (126 MHz, $CDCl_3$) δ 165.70, 162.33, 148.57, 140.82, 138.35, 129.54, 129.33, 127.95, 121.58, 118.43, 34.90. Anal. Calcd for $C_{15}H_9ClN_4O_5S$: C, 45.87; H, 2.31; N, 14.26; S, 8.16. Found: C, 46.02; H, 2.28; N, 14.41; S, 8.39. MS (ESI): m/z 392.99 (M + H^+, 100%), 394.99 (40%), 394.03 (20%).

*5-(2,4-Dichlorophenyl)-2-((3,5-dinitrobenzyl)sulfanyl)-1,3,4-oxadiazole (**11h**).* 3,5-Dinitrobenzyl chloride was used as an alkylating agent. Yield 72% as a white solid; mp 137−138 °C. ^{1}H NMR (300 MHz, DMSO) δ 8.84 (d, J = 2.0 Hz, 2H, $(NO_2)_2$Ph-*H*), 8.74 (t, J = 2.0 Hz, 1H, $(NO_2)_2$Ph-*H*), 7.95 (d, J = 8.5 Hz, 1H, Cl_2Ph-*H*), 7.88 (d, J = 2.0 Hz, 1H, Cl_2Ph-*H*), 7.62 (dd, J = 8.5, 2.0 Hz, 1H, Cl_2Ph-*H*), 4.82 (s, 2H, SCH_2). ^{13}C NMR (75 MHz, DMSO) δ 163.81, 163.03, 148.10, 142.10, 137.39, 132.89, 132.47, 130.92, 129.89, 128.31, 121.19, 118.06, 34.33. Anal. Calcd for $C_{15}H_8Cl_2N_4O_5S$: C, 42.17; H, 1.89; N, 13.11; S, 7.51. Found: C, 42.38; H, 2.05; N, 13.03; S, 7.65. MS (ESI): m/z 427.03 (M + H^+, 100%), 429.01 (70%), 428.06 (18%).

*2-((3,5-Dinitrobenzyl)sulfanyl)-5-(4-methylphenyl)-1,3,4-oxadiazole (**11i**).* 3,5-Dinitrobenzyl chloride was used as an alkylating agent. Yield 86% as a yellow solid; mp 151−153 °C. ^{1}H NMR (300 MHz, DMSO) δ 8.84 (d, J = 2.1 Hz, 2H, $(NO_2)_2$Ph-*H*), 8.73 (t, J = 2.1 Hz, 1H, $(NO_2)_2$Ph-*H*), 7.81 (d, J = 8.1 Hz, 2H, MePh-*H*), 7.36 (d, J = 8.1 Hz, 2H, MePh-*H*), 4.81 (s, 2H, SCH_2), 2.37 (s, 3H, CH_3). ^{13}C NMR (75 MHz, DMSO) δ 165.70, 162.55, 148.09, 142.47, 142.34, 130.09, 129.87, 126.54, 120.31, 118.02, 34.24, 21.29. Anal. Calcd for $C_{16}H_{12}N_4O_5S$: C, 51.61; H, 3.25; N, 15.05; S, 8.61. Found: C, 51.60; H, 3.47; N, 14.97; S, 8.95. MS (ESI): m/z 373.05 (M + H^+, 100%), 374.07 (18%).

*5-(3,5-Dimethylphenyl)-2-((3,5-dinitrobenzyl)sulfanyl)-1,3,4-oxadiazole (**11j**).* 3,5-Dinitrobenzyl chloride was used as an alkylating agent. Yield 78% as a white solid; mp 175−176 °C. ^{1}H NMR (300 MHz, DMSO) δ 8.86 (d, J = 2.1 Hz, 2H, $(NO_2)_2$Ph-*H*), 8.73 (t, J = 2.1 Hz, 1H, $(NO_2)_2$Ph-*H*), 7.51 (s, 2H, Me_2Ph-*H*), 7.22 (s, 1H, Me_2Ph-*H*), 4.81 (s, 2H, SCH_2), 2.32 (s, 6H, CH_3). ^{13}C NMR (75 MHz, DMSO) δ 165.78, 162.70, 148.09, 142.42, 138.94, 133.67, 129.89, 124.12, 122.88, 118.03, 34.21, 20.84. Anal. Calcd for $C_{17}H_{14}N_4O_5S$: C, 52.85; H, 3.65; N, 14.50; S, 8.30. Found: C, 52.53; H, 3.49; N, 14.34; S, 8.45. MS (ESI): m/z 387.05 (M + H^+, 100%), 388.07 (20%).

*2-((3,5-Dinitrobenzyl)sulfanyl)-5-(3-methoxyphenyl)-1,3,4-oxadiazole (**11k**).* 3,5-Dinitrobenzyl chloride was used as an alkylating agent. Yield 96% as a white solid; mp 142−143 °C. ^{1}H NMR (300 MHz, DMSO) δ 8.84 (d, J = 2.1 Hz, 2H, $(NO_2)_2$Ph-*H*), 8.73 (t, J = 2.1 Hz, 1H, $(NO_2)_2$Ph-*H*), 7.52−7.38 (m, 3H, MeOPh-*H*), 7.20−7.13 (m, 1H, MeOPh-*H*), 4.82 (s, 2H, SCH_2), 3.82 (s, 3H, OCH_3). ^{13}C NMR (75 MHz, DMSO) δ 165.50, 163.01, 159.80, 148.08, 142.27, 130.86, 129.87, 124.20, 118.89, 118.30, 118.03, 111.32, 55.62, 34.25. Anal. Calcd for $C_{16}H_{12}N_4O_6S$: C, 49.48; H, 3.11; N, 14.43; S, 8.26. Found: C, 49.26; H, 3.30; N, 14.30; S, 8.49. MS (ESI): m/z 389.05 (M + H^+, 100%), 390.09 (20%).

*2-((3,5-Dinitrobenzyl)sulfanyl)-5-(4-methoxyphenyl)-1,3,4-oxadiazole (**11l**).* 3,5-Dinitrobenzyl chloride was used as an alkylating agent. Yield 88% as a white solid; mp 131−133 °C. ^{1}H NMR (300 MHz, DMSO) δ 8.83 (d, J = 2.1 Hz, 2H, $(NO_2)_2$Ph-*H*), 8.72 (t, J = 2.1 Hz, 1H, $(NO_2)_2$Ph-*H*), 7.86 (d, J = 8.8 Hz, 2H, MeOPh-*H*), 7.09 (d, J = 8.8 Hz, 2H, MeOPh-*H*), 4.80 (s, 2H, SCH_2), 3.83 (s, 3H, OCH_3). ^{13}C NMR (75 MHz, DMSO) δ 165.58, 162.26, 162.10, 148.08, 142.35, 129.86, 128.47, 118.02, 115.39, 114.98, 55.71, 34.29. Anal. Calcd for $C_{16}H_{12}N_4O_6S$: C, 49.48; H, 3.11; N, 14.43; S, 8.26. Found: C, 49.58; H, 3.30; N, 14.41; S, 8.61. MS (ESI): m/z 389.03 (M + H^+, 100%), 390.06 (18%).

*5-(3,5-Dimethoxyphenyl)-2-((3,5-dinitrobenzyl)sulfanyl)-1,3,4-oxadiazole (**11m**).* 3,5-Dinitrobenzyl chloride was used as an alkylating agent. Yield 81% as a white solid; mp 140−141 °C. ^{1}H NMR (300 MHz, DMSO) δ 8.83 (d, J = 2.1 Hz, 2H, $(NO_2)_2$Ph-*H*), 8.72 (t, J = 2.1 Hz, 1H, $(NO_2)_2$Ph-*H*), 7.01 (d, J = 2.3 Hz, 2H, $(MeO)_2$Ph-*H*), 6.71 (t, J = 2.3 Hz, 1H, $(MeO)_2$Ph-*H*), 4.82 (s, 2H, SCH_2), 3.80 (s, 6H, OCH_3). ^{13}C NMR (75 MHz, DMSO) δ 165.47, 163.06, 161.12, 148.08, 142.23, 129.85, 124.62, 118.01, 104.33, 104.18, 55.78, 34.23. Anal. Calcd for $C_{17}H_{14}N_4O_7S$: C, 48.80; H, 3.37; N, 13.39; S, 7.66. Found: C, 48.89; H, 3.55; N, 13.36; S, 8.02. MS (ESI): m/z 419.04 (M + H^+, 100%), 420.06 (22%).

*2-((3,5-Dinitrobenzyl)sulfanyl)-5-(3-nitrophenyl)-1,3,4-oxadiazole (**11n**).* 3,5-Dinitrobenzyl chloride was used as an alkylating agent. Yield 82% as a light-pink solid; mp 122−124 °C. ^{1}H NMR (300 MHz, DMSO) δ 8.86 (d, J = 2.1 Hz, 2H, $(NO_2)_2$Ph-*H*), 8.74 (t, J = 2.1 Hz, 1H, $(NO_2)_2$Ph-*H*), 8.58 (t, J = 2.0 Hz, 1H, NO_2Ph-*H*), 8.46−8.33 (m, 2H, NO_2Ph-*H*), 7.87 (t, J = 8.1 Hz, 1H, NO_2Ph-*H*), 4.85 (s, 2H, SCH_2). ^{13}C NMR (75 MHz, DMSO) δ 164.14, 163.96, 148.36, 148.12, 142.21, 132.66, 131.48, 129.92, 126.59, 124.58, 121.10, 118.05, 34.29. Anal. Calcd for $C_{15}H_9N_5O_7S$: C, 44.67; H, 2.25; N, 17.36; S, 7.95. Found: C, 44.69; H, 2.52; N, 17.39; S, 8.21. MS (ESI): m/z 403.93 (M + H^+, 100%), 404.95 (20%).

*2-((3,5-Dinitrobenzyl)sulfanyl)-5-(4-nitrophenyl)-1,3,4-oxadiazole (**11o**).* 3,5-Dinitrobenzyl chloride was used as an alkylating agent. Yield: 70% as a yellow solid; mp 198−200 °C (with decomposition). ^{1}H NMR (500 MHz, DMSO) δ 8.87 (d, J = 2.1 Hz, 2H, $(NO_2)_2$Ph-*H*), 8.74 (t, J = 2.1 Hz, 1H, $(NO_2)_2$Ph-*H*), 8.38 (d, J = 8.8 Hz, 2H, NO_2Ph-*H*), 8.20 (d, J = 8.8 Hz, 2H, NO_2Ph-*H*), 4.85 (s, 2H, SCH_2). ^{13}C NMR (126 MHz, DMSO) δ 164.40, 164.30, 149.33, 148.11, 142.12, 129.92, 128.61, 127.98, 124.70, 118.08, 34.27. Anal. Calcd for $C_{15}H_9N_5O_7S$: C, 44.67; H, 2.25; N, 17.36; S, 7.95. Found: C, 44.28; H, 2.39; N, 17.68; S, 8.19. MS (ESI): m/z 403.99 (M + H^+, 100%), 405.10 (18%).

*2-((3,5-Dinitrobenzyl)sulfanyl)-5-(4-hydroxyphenyl)-1,3,4-oxadiazole (**11p**).* A solution of 5-(4-hydroxyphenyl)-1,3,4-oxadiazole-2-thiol (**19p**) (0.18 g, 0.93 mmol), 3,5-dinitrobenzyl chloride (0.167 g, 0.77 mmol), and triethylamine (0.1 g, 1 mmol) in acetonitrile (5 mL) was refluxed for 3 h. After completion, the solvent was evaporated under reduced pressure. The crude product was dissolved in EtOAc (20 mL) and washed with 5% sodium carbonate (2 × 15 mL) and water (1 × 20 mL). The organic layer was separated and dried over anhydrous sodium sulfate. The solvent was removed under reduced pressure, and the product was purified by column chromatography (mobile phase: hexane/EtOAc, 6:1). Yield 93% as a yellowish solid; mp 185−187 °C. ^{1}H NMR (500 MHz, DMSO) δ 10.31 (s, 1H, O*H*), 8.83 (d, J = 2.1 Hz, 2H, $(NO_2)_2$Ph-*H*), 8.73 (t, J = 2.1 Hz, 1H, $(NO_2)_2$Ph-*H*), 7.74 (d, J = 8.7 Hz, 2H, HOPh-*H*), 6.90 (d, J = 8.7 Hz, 2H, HOPh-*H*), 4.78 (s, 2H, SCH_2). ^{13}C NMR (126 MHz, DMSO) δ 165.82, 161.65, 161.02, 148.07, 142.40, 129.82, 128.58, 118.00, 116.27, 113.77, 34.29. MS (ESI): m/z 374.99 (M + H^+, 100%), 376.00 (18%).

*2-((3,5-Dinitrobenzyl)sulfanyl)-5-(pyridin-4-yl)-1,3,4-oxadiazole (**11q**).* 3,5-Dinitrobenzyl chloride was used as an alkylating agent. Yield 95% as a beige solid; mp 140−141 °C. ^{1}H NMR (500 MHz, DMSO) δ 8.86 (d, J = 2.1 Hz, 2H, $(NO_2)_2$Ph-*H*), 8.78 (d, J = 6.1 Hz, 2H, Py-*H*), 8.73 (t, J = 2.1 Hz, 1H, $(NO_2)_2$Ph-*H*), 7.86 (d, J = 6.1 Hz, 2H, Py-*H*), 4.84 (s, 2H, SCH_2). ^{13}C NMR (126 MHz, DMSO) δ 164.41, 164.10, 151.04, 148.09, 142.10, 130.12, 129.91, 120.15, 118.05, 34.24. Anal. Calcd for $C_{14}H_9N_5O_5S$: C, 46.80; H, 2.52; N, 19.49; S, 8.92. Found: C, 46.28; H, 2.74; N, 19.30; S, 9.19. MS (ESI): m/z 360.04 (M + H^+, 100%), 361.04 (18%).

Synthesis of 2-((3,5-Dinitrobenzyl)sulfanyl)-5-methyl-1,3,4-oxadiazole (11a). *3,5-Dinitrobenzyl Thiocyanate (**22**).* 3,5-Dinitrobenzyl chloride (0.5 g, 2.31 mmol) with potassium thiocyanate (0.34 g, 3.45 mmol) was stirred in DMF (8 mL) at 100 °C for 2 h. Upon completion, the reaction mixture was diluted with EtOAc (25 mL) and the organic layer was washed with water (2 × 20 mL). The organic solvent was dried over anhydrous sodium sulfate and evaporated. The crude product was crystallized from CH_3CN/H_2O. Yield: 82% as a yellowish solid; mp 120−121 °C (lit.[17] mp 120−121 °C). ^{1}H NMR (500 MHz, acetone) δ 8.95 (t, J = 2.1 Hz, 1H, $(NO_2)_2$Ph-*H*), 8.82 (d, J = 2.1 Hz, 2H, $(NO_2)_2$Ph-*H*), 4.74 (s, 2H, CH_2). ^{13}C NMR (126 MHz, acetone) δ 149.66, 141.82, 130.29,

DOI: 10.1021/acs.jmedchem.5b00608
J. Med. Chem. 2016, 59, 2362−2380

119.37, 111.87, 36.31. Anal. Calcd for $C_8H_5N_3O_4S$: C, 40.17; H, 2.11; N, 17.57; S, 13.40. Found: C, 40.15; H, 2.06; N, 17.42; S, 13.53.

*5-((3,5-Dinitrobenzyl)sulfanyl)-1H-tetrazole (**23**).* 3,5-Dinitrobenzyl thiocyanate (**22**) (0.47 g, 1.95 mmol) was added to a suspension of sodium azide (0.14 g, 2.15 mmol) and triethylammonium chloride (0.3 g, 2.15 mmol) in toluene (10 mL), and the reaction mixture was heated at 105 °C for 2 h. Upon completion, the reaction mixture was diluted with EtOAc (15 mL) and washed with water (2 × 20 mL). The aqueous layer was acidified by HCl, and the formed precipitate was filtered and washed to a neutral pH. Yield 68% as a white solid; mp 151−152 °C (lit.[17] mp 151−152 °C). ^{1}H NMR (500 MHz, DMSO) δ 8.75 (t, J = 2.1 Hz, 1H, $(NO_2)_2$Ph-*H*), 8.71 (d, J = 2.1 Hz, 2H, $(NO_2)_2$Ph-*H*), 4.75 (s, 2H, CH_2). ^{13}C NMR (126 MHz, DMSO) δ 148.09, 142.46, 129.7, 126.96, 117.92, 34.39. Anal. Calcd for $C_8H_6N_6O_4S$: C, 34.04; H, 2.14; N, 29.78; S, 11.36. Found: C, 34.06; H, 2.1; N, 29.46; S, 11.34.

*2-((3,5-Dinitrobenzyl)sulfanyl)-5-methyl-1,3,4-oxadiazole (**11a**).* A solution of 5-((3,5-dinitrobenzyl)sulfanyl)-1*H*-tetrazole (**23**) (0.2 g, 0.71 mmol) in acetic anhydride (4 mL) was heated to 90 °C for 10 h under microwave irradiation. Upon completion, the acetic anhydride was removed under reduced pressure, and the residue was dissolved in EtOAc (15 mL) and washed with 2% aqueous NaOH (2 × 15 mL) and water (1 × 20 mL). The product was purified by column chromatography (mobile phase: hexane/EtOAc, 3:1). Yield: 60% as a yellowish solid; mp 104−106 °C. ^{1}H NMR (500 MHz, acetone) δ 8.85 (s, 3H, $(NO_2)_2$Ph-*H*), 4.81 (s, 2H, SCH_2), 2.45 (s, 3H, CH_3). ^{13}C NMR (126 MHz, acetone) δ 166.23, 163.04, 149.31, 143.18, 130.41, 118.62, 35.08, 10.71. Anal. Calcd for $C_{10}H_8N_4O_5S$: C, 40.54; H, 2.72; N, 18.91; S, 10.82. Found: C, 40.21; H, 2.49; N, 18.65; S, 11.21. MS (ESI): m/z 296.97 (M + H$^+$, 100%), 398.02 (14%).

*2-(4-Chlorophenyl)-5-((3-nitro-5-(trifluoromethyl)benzyl)-sulfanyl)-1,3,4-oxadiazole (**15g**).* 3-Nitro-5-trifluoromethylbenzyl chloride (**29**) was used as an alkylating agent. Yield: 76% as a white solid; mp 115−116.5 °C. ^{1}H NMR (500 MHz, DMSO) δ 8.72 (s, 1H, Ar-*H*), 8.39 (s, 2H, Ar-*H*), 7.94 (d, J = 8.5 Hz, 2H, ClPh-*H*), 7.63 (d, J = 8.5 Hz, 2H, ClPh-*H*), 4.78 (s, 2H, SCH_2). ^{13}C NMR (126 MHz, DMSO) δ 164.66, 163.03, 148.08, 141.74, 136.76, 132.05 (q, J = 3.6 Hz), 130.22 (q, J = 33.4 Hz), 129.47, 128.16, 127.82, 122.84 (q, J = 272.8 Hz), 121.75, 119.61 (q, J = 3.9 Hz), 34.23. HRMS (ESI+) calcd for $(C_{16}H_9ClF_3N_3O_3S + H)^+$ m/z: 416.0078 (100.0%), 418.0049 (32.0%), 417.0112 (17.3%); found 416.0075 (100%), 418.0044 (36%), 417.0107 (18%).

*2-((3-Nitro-5-(trifluoromethyl)benzyl)sulfanyl)-5-(p-tolyl)-1,3,4-oxadiazole (**15i**).* 3-Nitro-5-trifluoromethylbenzyl chloride (**29**) was used as an alkylating agent. Yield 86% as a white solid; mp 91−93 °C. ^{1}H NMR (500 MHz, DMSO) δ 8.72 (t, J = 1.9 Hz, 1H, Ar-*H*), 8.39 (s, 2H, Ar-*H*), 7.80 (d, J = 8.0 Hz, 2H, MePh-*H*), 7.36 (d, J = 8.0 Hz, 2H, MePh-*H*), 4.77 (s, 2H, SCH_2), 2.37 (s, 3H, CH_3). ^{13}C NMR (126 MHz, DMSO) δ 165.50, 162.33, 148.08, 142.23, 141.86, 132.03 (q, J = 3.5 Hz), 130.23 (q, J = 32.8 Hz), 129.83, 127.80, 126.29, 122.84 (q, J = 272.8 Hz), 120.10, 119.58 (q, J = 3.9 Hz), 34.23, 21.13. HRMS (ESI+) calcd for $(C_{17}H_{12}F_3N_3O_3S + H)^+$ m/z: 396.0624 (100.0%), 397.0658 (18.4%); found 396.0622 (100%), 397.0654 (18%).

*2-((3-Nitro-5-(trifluoromethyl)benzyl)sulfanyl)-5-(4-nitrophenyl)-1,3,4-oxadiazole (**15o**).* 3-Nitro-5-trifluoromethylbenzyl chloride (**29**) was used as an alkylating agent. Yield 78% as a yellowish solid; mp 145−147 °C. ^{1}H NMR (500 MHz, DMSO) δ 8.74 (s, 1H, Ar-*H*), 8.42−8.39 (m, 2H, Ar-*H*), 8.37 (dd, J = 8.8, 2.2 Hz, 2H, NO_2Ph-*H*), 8.18 (dd, J = 8.8, 2.6 Hz, 2H, NO_2Ph-*H*), 4.81 (s, 2H, SCH_2). ^{13}C NMR (126 MHz, DMSO) δ 164.22, 164.07, 149.11, 148.08, 141.63, 132.11 (q, J = 3.6 Hz), 130.24 (q, J = 33.2 Hz), 128.39, 127.87, 127.73, 124.45, 122.84 (q, J = 273.0 Hz), 119.65 (q, J = 3.8 Hz), 34.23. HRMS (ESI+) calcd for $(C_{16}H_9F_3N_4O_5S + H)^+$ m/z: 427.0319 (100.0%), 428.0352 (17.3%); found 427.0313 (100%), 428.0345 (18%).

General Procedure for the Synthesis of Potassium 3-Aroyl Dithiocarbazates (24d−g, 24i−l, 24n, 24o, 24q). Carbon disulfide (0.3 g, 0.24 mL, 4 mmol) was added dropwise to a solution of the corresponding benzohydrazide (**20**) (2 mmol) and potassium hydroxide (0.22 g, 4 mmol) in ethanol (10 mL). The reaction mixture was stirred at room temperature overnight and then Et_2O (5 mL) was added. The precipitate was filtered, washed with ether, and dried. Products were formed at 72−97% yields and were used without further purification or characterization.

General Procedure for the Synthesis of 2-Aryl-1,3,4-thiadiazole-5-thiols (25d−g, 25i−l, 25n, 25o, 25q). Potassium 3-aroyl dithiocarbazate (1.5 mmol) was added in small portions to concentrated sulfuric acid (3 mL) at 0 °C under vigorous stirring. The reaction mixture was stirred for 4 h in an ice bath and then poured into cold water (10 mL). The precipitated product was filtered and dissolved in an aqueous solution of sodium hydroxide. The insolubilities were filtered, the solution was acidified with HCl, and 1,3,4-thiadiazole-5-thiol (**25d−g**, **25i−l**, **25n**, **25o**, **25q**) was filtered and washed with water.

General Procedure for the Synthesis of 2-Alkyl/Aryl-5-benzylsulfanyl-1,3,4-thiadiazoles (12o, 13d, 13g, 13o, 14a, 14d−g, 14i−l, 14n, 14o, 14q, 16g, 16i, 16o). A solution of an alkylating agent (1 mmol) and tetrabutylammonium bromide (0.016 g, 0.05 mmol) in CH_2Cl_2 (5 mL) was added to a solution of the corresponding 1,3,4-thiadiazole-5-thiol (**25**) (1.1 mmol) with sodium hydroxide (0.05 g, 1.25 mmol) in H_2O (5 mL). The reaction mixture was slowly stirred at room temperature overnight. Upon completion, the organic layer was separated, washed with water (2 × 7 mL), and dried over anhydrous sodium sulfate. The solvent was removed under reduced pressure, and the product was purified by column chromatography (mobile phase: hexane/EtOAc).

*2-(4-Nitrophenyl)-5-((4-nitrobenzyl)sulfanyl)-1,3,4-thiadiazole (**12o**).* 4-Nitrobenzyl chloride was used as an alkylating agent. Yield 87% as a yellowish solid; mp 175−176 °C. ^{1}H NMR (500 MHz, DMSO) δ 8.34 (d, J = 8.8 Hz, 2H, Ar-*H*), 8.20 (d, J = 8.7 Hz, 2H, Ar-*H*), 8.14 (d, J = 8.8 Hz, 2H, Ar-*H*), 7.77 (d, J = 8.7 Hz, 2H, Ar-*H*), 4.78 (s, 2H, SCH_2). ^{13}C NMR (126 MHz, DMSO) δ 166.48, 166.38, 148.85, 147.01, 144.91, 134.88, 130.56, 128.88, 124.75, 123.82, 36.63. Anal. Calcd for $C_{15}H_{10}N_4O_4S_2$: C, 48.12; H, 2.69; N, 14.96; S, 17.13. Found: C, 48.3; H, 2.62; N, 14.74; S, 17.28. MS (ESI): m/z 375.05 (M + H$^+$, 100%), 376.08 (18%).

*2-((2,4-Dinitrobenzyl)sulfanyl)-5-phenyl-1,3,4-thiadiazole (**13d**).* 2,4-Dinitrobenzyl chloride was used as an alkylating agent. Yield 48% as a white solid; mp 137−139 °C. ^{1}H NMR (300 MHz, DMSO) δ 8.76 (d, J = 2.4 Hz, 1H, $(NO_2)_2$Ph-*H*), 8.54 (dd, J = 8.5, 2.4 Hz, 1H, $(NO_2)_2$Ph-*H*), 8.09 (d, J = 8.5 Hz, 1H, $(NO_2)_2$Ph-*H*), 7.90−7.83 (m, 2H, Ph-*H*), 7.58−7.47 (m, 3H, Ph-*H*), 4.99 (s, 2H, SCH_2). ^{13}C NMR (75 MHz, DMSO) δ 169.02, 163.69, 148.23, 147.12, 139.30, 134.33, 131.70, 129.69, 129.26, 128.12, 127.72, 120.71, 34.17. Anal. Calcd for $C_{15}H_{10}N_4O_4S_2$: C, 48.12; H, 2.69; N, 14.96; S, 17.14. Found: C, 48.11; H, 2.64; N, 15.24; S, 16.74. MS (ESI): m/z 374.96 (M + H$^+$, 100%), 375.98 (18%).

*2-(4-Chlorophenyl)-5-((2,4-dinitrobenzyl)sulfanyl)-1,3,4-thiadiazole (**13g**).* 2,4-Dinitrobenzyl chloride was used as an alkylating agent. Yield 70% as a yellow solid; mp 159−160 °C. ^{1}H NMR (300 MHz, DMSO) δ 8.76 (d, J = 2.4 Hz, 1H, $(NO_2)_2$Ph-*H*), 8.53 (dd, J = 8.6, 2.4 Hz, 1H, $(NO_2)_2$Ph-*H*), 8.08 (d, J = 8.6 Hz, 1H, $(NO_2)_2$Ph-*H*), 7.89 (d, J = 8.5 Hz, 2H, ClPh-*H*), 7.59 (d, J = 8.5 Hz, 2H, ClPh-*H*), 4.99 (s, 2H, SCH_2). ^{13}C NMR (75 MHz, DMSO) δ 167.81, 164.19, 148.22, 147.11, 139.24, 136.28, 134.31, 129.74, 129.39, 128.10, 120.69, 34.15. Anal. Calcd for $C_{15}H_9ClN_4O_4S_2$: C, 44.07; H, 2.22; N, 13.70; S, 15.69. Found: C, 44.31; H, 2.42; N, 13.85; S, 15.38. MS (ESI): m/z 409.03 (M + H$^+$, 100%), 411.03 (42%), 410.07 (20%).

*2-((2,4-Dinitrobenzyl)sulfanyl)-5-(4-nitrophenyl)-1,3,4-thiadiazole (**13o**).* 2,4-Dinitrobenzyl chloride was used as an alkylating agent. Yield 54% as a yellow solid; mp 187−189 °C (with decomposition). ^{1}H NMR (300 MHz, DMSO) δ 8.77 (d, J = 2.4 Hz, 1H, $(NO_2)_2$Ph-*H*), 8.53 (dd, J = 8.6, 2.4 Hz, 1H, $(NO_2)_2$Ph-*H*), 8.34 (d, J = 8.8 Hz, 2H, NO_2Ph-*H*), 8.15 (d, J = 8.8 Hz, 2H, NO_2Ph-*H*), 8.11 (d, J = 8.6 Hz, 1H, $(NO_2)_2$Ph-*H*), 5.03 (s, 2H, SCH_2). ^{13}C NMR (75 MHz, DMSO) δ 167.18, 166.04, 149.33, 148.62, 147.54, 139.23, 135.18, 134.60, 129.24, 128.28, 124.97, 120.87, 34.72. Anal. Calcd for $C_{15}H_9N_5O_6S_2$: C, 42.96; H, 2.16; N, 16.70; S, 15.29. Found: C, 43.59; H, 2.09; N, 17.1; S, 15.07. MS (ESI): m/z 419.96 (M + H$^+$, 100%), 420.99 (20%).

DOI: 10.1021/acs.jmedchem.5b00608
J. Med. Chem. 2016, 59, 2362−2380

*2-((3,5-Dinitrobenzyl)sulfanyl)-5-methyl-1,3,4-thiadiazole (**14a**).* 3,5-Dinitrobenzyl chloride was used as an alkylating agent. Yield 62% as a yellowish solid; mp 119−121 °C. ^{1}H NMR (500 MHz, DMSO) δ 8.77 (d, J = 1.9 Hz, 2H, $(NO_2)_2$Ph-*H*), 8.71 (t, J = 1.9 Hz, 1H, $(NO_2)_2$Ph-*H*), 4.8 (s, 2H, SCH_2), 2.64 (s, 3H, CH_3). ^{13}C NMR (125 MHz, DMSO) δ 166.36, 163.54, 148.06, 142.39, 129.75, 117.88, 35.41, 15.40. Anal. Calcd for $C_{10}H_8N_4O_4S_2$: C, 38.46; H, 2.58; N, 17.94; S, 20.53. Found: C, 38.61; H, 2.68; N, 17.97; S, 20.76. MS (ESI): m/z 313.06 (M + H$^+$, 100%), 314.08 (15%).

*2-((3,5-Dinitrobenzyl)sulfanyl)-5-phenyl-1,3,4-thiadiazole (**14d**).* 3,5-Dinitrobenzyl chloride was used as an alkylating agent. Yield 66% as a yellow solid; mp 119−120 °C. ^{1}H NMR (300 MHz, DMSO) δ 8.81 (d, J = 2.1 Hz, 2H, $(NO_2)_2$Ph-*H*), 8.72 (t, J = 2.1 Hz, 1H, $(NO_2)_2$Ph-*H*), 7.91−7.82 (m, 2H, Ph-*H*), 7.60−7.47 (m, 3H, Ph-*H*), 4.88 (s, 2H, SCH_2). ^{13}C NMR (75 MHz, DMSO) δ 168.76, 163.94, 148.10, 142.23, 131.63, 129.79, 129.66, 129.26, 127.70, 117.92, 35.69. Anal. Calcd for $C_{15}H_{10}N_4O_4S_2$: C, 48.12; H, 2.69; N, 14.96; S, 17.13. Found: C, 48.06; H, 2.89; N, 15.15; S, 17.40. MS (ESI): m/z 375.03 (M + H$^+$, 100%), 376.06 (18%).

*2-(2-Chlorophenyl)-5-((3,5-dinitrobenzyl)sulfanyl)-1,3,4-thiadiazole (**14e**).* 3,5-Dinitrobenzyl chloride was used as an alkylating agent. Yield 52% as a yellow solid; mp 112−113 °C. ^{1}H NMR (300 MHz, acetone) δ 8.93−8.82 (m, 3H, $(NO_2)_2$Ph-*H*), 8.23−8.15 (m, 1H, ClPh-*H*), 7.67−7.47 (m, 3H, ClPh-*H*), 5.00 (s, 2H, SCH_2). ^{13}C NMR (75 MHz, acetone) δ 165.92, 164.88, 149.36, 143.29, 133.11, 132.76, 131.66, 131.49, 130.48, 129.32, 128.63, 118.57, 36.56. Anal. Calcd for $C_{15}H_9ClN_4O_4S_2$: C, 44.07; H, 2.22; N, 13.70; S, 15.69. Found: C, 44.49; H, 2.21; N, 13.53; S, 15.38. MS (ESI): m/z 408.98 (M + H$^+$, 100%), 410.97 (40%), 410.08 (20%).

*2-(3-Chlorophenyl)-5-((3,5-dinitrobenzyl)sulfanyl)-1,3,4-thiadiazole (**14f**).* 3,5-Dinitrobenzyl chloride was used as an alkylating agent. Yield 51% as a light-beige solid; mp 96−97 °C. ^{1}H NMR (300 MHz, acetone) δ 8.88 (d, J = 2.2 Hz, 2H, $(NO_2)_2$Ph-*H*), 8.84 (t, J = 2.2 Hz, 1H, $(NO_2)_2$Ph-*H*), 7.94−7.91 (m, 1H, ClPh-*H*), 7.86−7.80 (m, 1H, ClPh-*H*), 7.60−7.50 (m, 2H, ClPh-*H*), 4.98 (s, 2H, SCH_2). ^{13}C NMR (75 MHz, acetone) δ 168.14, 165.06, 149.37, 143.23, 135.56, 132.42, 131.95, 131.90, 130.45, 127.78, 127.07, 118.57, 36.58. Anal. Calcd for $C_{15}H_9ClN_4O_4S_2$: C, 44.07; H, 2.22; N, 13.70; S, 15.69. Found: C, 44.39; H, 2.52; N, 13.78; S, 15.49. MS (ESI): m/z 409.05 (M + H$^+$, 100%), 411.03 (38%), XY (20%).

*2-(4-Chlorophenyl)-5-((3,5-dinitrobenzyl)sulfanyl)-1,3,4-thiadiazole (**14g**).* 3,5-Dinitrobenzyl chloride was used as an alkylating agent. Yield 67% as a yellow solid: mp 175−176 °C. ^{1}H NMR (300 MHz, acetone) δ 8.88 (d, J = 2.1 Hz, 2H, $(NO_2)_2$Ph-*H*), 8.85 (t, J = 2.1 Hz, 1H, $(NO_2)_2$Ph-*H*), 7.93 (d, J = 8.6 Hz, 2H, ClPh-*H*), 7.57 (d, J = 8.6 Hz, 2H, ClPh-*H*), 4.98 (s, 2H, SCH_2). ^{13}C NMR (75 MHz, acetone) δ 167.58, 164.46, 148.11, 142.20, 136.24, 129.80, 129.73, 129.40, 128.14, 117.94, 35.69. Anal. Calcd for $C_{15}H_9ClN_4O_4S_2$: C, 44.07; H, 2.22; N, 13.70; S, 15.69. Found: C, 44.21; H, 2.21; N, 13.40; S, 15.33. MS (ESI): m/z 409.05 (M + H$^+$, 100%), 411.09 (38%), 410.14 (20%).

*2-((3,5-Dinitrobenzyl)sulfanyl)-5-(4-methylphenyl)-1,3,4-thiadiazole (**14i**).* 3,5-Dinitrobenzyl chloride was used as an alkylating agent. Yield 59% as a light-beige solid; mp 120−121 °C. ^{1}H NMR (500 MHz, $CDCl_3$) δ 8.87 (t, J = 2.1 Hz, 1H, $(NO_2)_2$Ph-*H*), 8.65 (d, J = 2.1 Hz, 2H, $(NO_2)_2$Ph-*H*), 7.65 (d, J = 8.1 Hz, 2H, MePh-*H*), 7.21−7.15 (m, 2H, MePh-*H*), 4.68 (s, 2H, SCH_2), 2.33 (s, 3H, CH_3). ^{13}C NMR (126 MHz, $CDCl_3$) δ 169.53, 161.51, 148.50, 141.95, 141.67, 129.91, 129.30, 127.65, 126.69, 118.09, 35.87, 21.49. Anal. Calcd for $C_{16}H_{12}N_4O_4S_2$: C, 49.47; H, 3.11; N, 14.42; S, 16.51. Found: C, 49.46; H, 3.31; N, 14.51; S, 16.62. MS (ESI): m/z 389.10 (M + H$^+$, 100%), 390.14 (18%).

*2-(3,5-Dimethylphenyl)-5-((3,5-dinitrobenzyl)sulfanyl)-1,3,4-thiadiazole (**14j**).* 3,5-Dinitrobenzyl chloride was used as an alkylating agent. Yield 62% as a light-beige solid; mp 115−116 °C. ^{1}H NMR (500 MHz, DMSO) δ 8.81 (d, J = 2.2 Hz, 2H, $(NO_2)_2$Ph-*H*), 8.71 (t, J = 2.2 Hz, 1H, $(NO_2)_2$Ph-*H*), 7.46 (s, 2H, Me_2Ph-*H*), 7.16 (s, 1H, Me_2Ph-*H*), 4.86 (s, 2H, SCH_2), 2.31 (s, 6H, CH_3). ^{13}C NMR (126 MHz, DMSO) δ 168.95, 163.56, 148.05, 142.23, 138.95, 133.03, 129.78, 129.12, 125.29, 117.88, 35.65, 20.83. Anal. Calcd for $C_{14}H_9N_5O_4S_2$: C, 50.74; H, 3.51; N, 13.92; S, 15.93. Found: C, 50.71; H, 3.46; N, 13.77; S, 16.06. MS (ESI): m/z 403.08 (M + H$^+$, 100%), 404.11 (22%).

*2-((3,5-Dinitrobenzyl)sulfanyl)-5-(3-methoxyphenyl)-1,3,4-thiadiazole (**14k**).* 3,5-Dinitrobenzyl chloride was used as an alkylating agent. Yield 78% as a white solid; mp 142−143 °C. ^{1}H NMR (300 MHz, DMSO) δ 8.81 (d, J = 2.1 Hz, 2H, $(NO_2)_2$Ph-*H*), 8.72 (t, J = 2.1 Hz, 1H, $(NO_2)_2$Ph-*H*), 7.53−7.31 (m, 3H, MeOPh-*H*), 7.19−7.03 (m, 1H, MeOPh-*H*), 4.87 (s, 2H, SCH_2), 3.81 (s, 3H, OCH_3). ^{13}C NMR (75 MHz, DMSO) δ 168.55, 164.07, 159.87, 148.09, 142.24, 130.90, 130.45, 129.79, 120.29, 117.93, 117.48, 112.29, 55.58, 35.69. Anal. Calcd for $C_{16}H_{12}N_4O_5S_2$: C, 47.52; H, 2.99; N, 13.85; S, 15.86. Found: C, 47.27; H, 2.88; N, 13.75; S, 15.95. MS (ESI): m/z 405.06 (M + H$^+$, 100%), 406.09 (24%).

*2-((3,5-Dinitrobenzyl)sulfanyl)-5-(4-methoxyphenyl)-1,3,4-thiadiazole (**14l**).* 3,5-Dinitrobenzyl chloride was used as an alkylating agent. Yield 76% as a yellow solid; mp 165−167 °C. ^{1}H NMR (300 MHz, DMSO) δ 8.80 (d, J = 2.1 Hz, 2H, $(NO_2)_2$Ph-*H*), 8.71 (t, J = 2.1 Hz, 1H, $(NO_2)_2$Ph-*H*), 7.79 (d, J = 8.9 Hz, 2H, MeOPh-*H*), 7.05 (d, J = 8.9 Hz, 2H, MeOPh-*H*), 4.85 (s, 2H, SCH_2), 3.81 (s, 3H, OCH_3). ^{13}C NMR (75 MHz, DMSO) δ 168.55, 162.65, 161.84, 148.07, 142.31, 129.76, 129.35, 121.78, 117.89, 115.02, 55.66, 35.71. Anal. Calcd for $C_{16}H_{12}N_4O_5S_2$: C, 47.52; H, 2.99; N, 13.85; S, 15.86. Found: C, 47.38; H, 2.88; N, 13.83; S, 15.90. MS (ESI): m/z 405.09 (M + H$^+$, 100%), 406.12 (22%).

*2-((3,5-Dinitrobenzyl)sulfanyl)-5-(3-nitrophenyl)-1,3,4-thiadiazole (**14n**).* 3,5-Dinitrobenzyl chloride was used as an alkylating agent. Yield 61% as a light-brown solid; mp 158−160 °C (with decomposition). ^{1}H NMR (300 MHz, DMSO) δ 8.83 (d, J = 2.1 Hz, 2H, $(NO_2)_2$Ph-*H*), 8.72 (t, J = 2.1 Hz, 1H, $(NO_2)_2$Ph-*H*), 8.59 (t, J = 2.0 Hz, 1H, NO_2Ph-*H*), 8.36 (dd, J = 8.3, 2.3 Hz, 1H, NO_2Ph-*H*), 8.32−8.24 (m, 1H, NO_2Ph-*H*), 7.82 (t, J = 8.0 Hz, 1H, NO_2Ph-*H*), 4.90 (s, 2H, SCH_2). ^{13}C NMR (75 MHz, DMSO) δ 166.59, 165.57, 148.42, 148.11, 142.11, 134.03, 131.40, 130.65, 129.83, 125.84, 121.77, 117.96, 35.71. Anal. Calcd for $C_{15}H_9N_5O_6S_2$: C, 42.96; H, 2.16; N, 16.70; S, 15.29. Found: C, 43.14; H, 2.30; N, 17.02; S, 15.41. MS (ESI): m/z 420.05 (M + H$^+$, 100%), 421.04 (20%).

*2-((3,5-Dinitrophenyl)sulfanyl)-5-(4-nitrophenyl)-1,3,4-thiadiazole (**14o**).* 3,5-Dinitrobenzyl chloride was used as an alkylating agent. Yield 80% as a light-beige solid; mp 209−210 °C. ^{1}H NMR (500 MHz, DMSO) δ 8.83 (s, 2H, $(NO_2)_2$Ph-*H*), 8.73 (s, 1H, $(NO_2)_2$Ph-*H*), 8.34 (d, J = 9.0 Hz, 2H, NO_2Ph-*H*), 8.15 (d, J = 9.0 Hz, 2H, NO_2Ph-*H*), 4.91 (s, 2H, SCH_2). ^{13}C NMR (126 MHz, DMSO) δ 166.63, 166.19, 148.89, 148.11, 142.07, 134.87, 129.83, 128.93, 124.77, 117.97, 35.69. Anal. Calcd for $C_{15}H_9N_5O_6S_2$: C, 42.96; H, 2.16; N, 16.70; S, 15.29. Found: C, 42.85; H, 2.25; N, 16.38; S, 15.12. MS (ESI): m/z 420.04 (M + H$^+$, 100%), 421.00 (18%).

*2-((3,5-Dinitrobenzyl)sulfanyl)-5-(pyridine-4-yl)-1,3,4-thiadiazole (**14q**).* 3,5-Dinitrobenzyl chloride was used as an alkylating agent. Yield 66% as a light-beige solid; mp 193−194 °C. ^{1}H NMR (500 MHz, DMSO) δ 8.83 (d, J = 2.1 Hz, 2H, $(NO_2)_2$Ph-*H*), 8.77−8.70 (m, 3H, $(NO_2)_2$Ph-*H*, Py-*H*), 7.84 (d, J = 6.1 Hz, 2H, Py-*H*), 4.91 (s, 2H, SCH_2). ^{13}C NMR (126 MHz, DMSO) δ 166.67, 166.17, 151.06, 148.11, 142.06, 136.13, 129.82, 121.45, 117.96, 35.69. Anal. Calcd for $C_{14}H_9N_5O_4S_2$: C, 44.79; H, 2.42; N, 18.66; S, 17.08. Found: C, 45.04; H, 2.61; N, 18.70; S, 17.10. MS (ESI): m/z 376.07 (M + H$^+$, 100%), 377.06 (18%).

*2-(4-Chlorophenyl)-5-((3-nitro-5-(trifluoromethyl)benzyl)-sulfanyl)-1,3,4-thiadiazole (**16g**).* 3-Nitro-5-trifluoromethylbenzyl chloride (**29**) was used as an alkylating agent. Yield 63% as a white solid; mp 92−94 °C. ^{1}H NMR (500 MHz, DMSO) δ 8.69 (t, J = 1.9 Hz, 1H, Ar-*H*), 8.38 (s, 1H, Ar-*H*), 8.35 (s, 1H, Ar-*H*), 7.88 (d, J = 8.6 Hz, 2H, ClPh-*H*), 7.59 (d, J = 8.6 Hz, 2H, ClPh-*H*), 4.84 (s, 2H, SCH_2). ^{13}C NMR (126 MHz, DMSO) δ 167.37, 164.18, 148.07, 141.62, 136.01, 132.04 (q, J = 3.4 Hz), 130.21 (q, J = 33.4 Hz), 129.49, 129.14, 127.92, 127.77, 122.84 (q, J = 273.0 Hz), 119.50 (q, J = 3.8 Hz), 35.72. HRMS (ESI+) calcd for $(C_{16}H_9ClF_3N_3O_2S_2 + H)^+$ m/z: 431.9850 (100.0%), 433.9820 (32.0%), 432.9883 (17.3%); found 431.9839 (100%), 433.9806 (36%), 432.9869 (18%).

*2-((3-Nitro-5-(trifluoromethyl)benzyl)sulfanyl)-5-(p-tolyl)-1,3,4-thiadiazole (**16i**).* 3-Nitro-5-trifluoromethylbenzyl chloride (**29**) was

DOI: 10.1021/acs.jmedchem.5b00608
J. Med. Chem. 2016, 59, 2362−2380

used as an alkylating agent. Yield 72% as a white solid; mp 107−109 °C. ^{1}H NMR (500 MHz, DMSO) δ 8.68 (s, 1H, Ar-*H*), 8.38 (s, 1H, Ar-*H*), 8.34 (s, 1H, Ar-*H*), 7.75 (d, *J* = 8.1 Hz, 2H, MePh-*H*), 7.33 (d, *J* = 8.1 Hz, 2H, MePh-*H*), 4.82 (s, 2H, SCH_2), 2.35 (s, 3H, CH_3). ^{13}C NMR (126 MHz, DMSO) δ 168.67, 163.10, 148.19, 141.72, 141.54, 132.04 (q, *J* = 3.9 Hz), 130.23 (q, *J* = 33.4 Hz), 127.77, 127.69, 127.40, 122.64 (q, *J* = 272.8 Hz), 119.54, 119.49 (q, *J* = 3.9 Hz), 35.95, 21.14. HRMS (ESI+) calcd for ($C_{17}H_{12}F_3N_3O_2S_2$ + H)$^+$ *m*/*z*: 412.0396 (100.0%), 413.0429 (18.4%); found 412.0391 (100%), 413.0422 (19%).

*2-((3-Nitro-5-(trifluoromethyl)benzyl)sulfanyl)-5-(4-nitrophenyl)-1,3,4-thiadiazole (**16o**).* 3-Nitro-5-trifluoromethylbenzyl chloride (**29**) was used as an alkylating agent. Yield 61% as a yellowish solid; mp 153−155 °C. ^{1}H NMR (300 MHz, $CDCl_3$) δ 8.58 (s, 1H, Ar-*H*), 8.40 (s, 1H, Ar-*H*), 8.33 (d, *J* = 8.8 Hz, 2H, NO_2Ph-*H*), 8.12 (s, 1H, Ar-*H*), 8.05 (d, *J* = 8.8 Hz, 2H, NO_2Ph-*H*), 4.78 (s, 2H, SCH_2). ^{13}C NMR (75 MHz, $CDCl_3$) δ 166.51, 164.72, 149.12, 148.44, 140.23, 135.06, 132.57 (q, *J* = 34.2 Hz), 131.71 (q, *J* = 3.5 Hz), 128.50, 127.24, 124.51, 122.58 (q, *J* = 271.2 Hz), 120.19 (q, *J* = 3.8 Hz), 36.11. HRMS (ESI+) calcd for ($C_{16}H_9F_3N_4O_4S_2$ + H)$^+$ *m*/*z*: 443.0090 (100.0%), 444.0124 (17.3%); found 443.0085 (100%), 444.0116 (18%).

Synthesis of Partially or Fully Reduced Derivatives 17o and 18o. A yellow solution of 3,5-dinitrobenzyl chloride (0.217 g, 1 mmol) and tin(II) chloride dihydrate (1.6 g, 7 mmol) in ethanol (10 mL) was stirred under reflux for 10 min. Upon completion, the solvent was evaporated under reduced pressure, and water (5 mL) was added to form a dense mass that was then washed with EtOAc (2 × 10 mL). Then **21o** (0.245 g, 1.1 mmol) in THF (7 mL) was added to the aqueous layer, followed by the addition of sodium carbonate to reach pH 8−10. The reaction mixture was stirred at room temperature overnight. Upon completion, the reaction mixture was washed with EtOAc (2 × 15 mL). The organic layer was separated, dried over anhydrous Na_2SO_4, and evaporated. Products were purified by column chromatography (mobile phase: EtOAc/hexane/Et_3N, 50:25:1).

*3-Nitro-5-(((5-(4-nitrophenyl)-1,3,4-oxadiazol-2-yl)thio)methyl)-aniline (**17o**).* Yield 11% as a yellow solid. R_f (EtOAc/hexane/Et_3N, 50:25:1) 0.81. ^{1}H NMR (300 MHz, acetone) δ 8.41 (d, *J* = 9.0 Hz, 2H, NO_2Ph-*H*), 8.25 (d, *J* = 9.0 Hz, 2H, NO_2Ph-*H*), 7.60 (t, *J* = 1.8 Hz, 1H, Ar-*H*), 7.42 (t, *J* = 2.2 Hz, 1H, Ar-*H*), 7.23 (t, *J* = 1.9 Hz, 1H, Ar-*H*), 4.62 (s, 2H, SCH_2). ^{13}C NMR (75 MHz, acetone) δ 165.69, 165.11, 150.77, 150.38, 150.29, 140.11, 129.92, 128.45, 125.22, 121.03, 112.14, 108.10, 36.33. Anal. Calcd for $C_{15}H_{11}N_5O_5S$: C, 48.26; H, 2.97; N, 18.76; S, 8.59. Found: C, 48.1; H, 2.58; N, 18.5; S, 8.61.

*5-((3,5-Diaminobenzyl)sulfanyl)-2-(4-nitrophenyl)-1,3,4-oxadiazol (**18o**).* Yield 30% as a light-brown solid. R_f (EtOAc/hexane/Et_3N, 50:25:1) 0.48. ^{1}H NMR (300 MHz, DMSO) δ 8.40 (d, *J* = 8.9 Hz, 2H, NO_2Ph-*H*), 8.22 (d, *J* = 8.9 Hz, 2H, NO_2Ph-*H*), 5.87 (d, *J* = 2.0 Hz, 2H, $(NH_2)_2$Ar-*H*), 5.76−5.70 (m, 1H, $(NH_2)_2$Ar-*H*), 4.81 (s, 4H, NH_2), 4.30 (s, 2H, SCH_2). ^{13}C NMR (75 MHz, DMSO) δ 164.11, 149.89, 149.48, 136.72, 129.00, 128.59, 125.04, 103.85, 99.62, 37.27. Anal. Calcd for $C_{15}H_{13}N_5O_3S$: C, 52.47; H, 3.82; N, 20.40; S, 9.34. Found: C, 52.19; H, 3.62; N, 20.28; S, 9.61.

In Vitro Antimycobacterial Assay. The in vitro antimycobacterial activity of the prepared compounds was evaluated against mycobacterial strains *Mycobacterium tuberculosis* CNCTC My 331/88, *M. kansasii* CNCTC My 235/80, and *M. avium* CNCTC My 330/88 from the Czech National Collection of Type Cultures (CNCTC) and against the clinically isolated strains *M. kansasii* 6509/96, *M. tuberculosis* 234/2005, *M. tuberculosis* 9449/2007, *M. tuberculosis* 8666/2010, *M. tuberculosis* Praha 1, *M. tuberculosis* Praha 4, and *M. tuberculosis* Praha 131. Basic suspensions of the mycobacterial strains were prepared according to a 1.0 McFarland standard. From the basic suspensions, subsequent dilutions of each strain were made: *M. tuberculosis*, 10^{-3}; *M. avium*, 10^{-5}; and *M. kansasii*, 10^{-4}. The appropriate dilutions of the strains were prepared, and 0.1 mL was added to each well of a collection of microtiter plates containing the compounds.

The activities of the compounds were determined via the micromethod for the determination of the minimum inhibitory concentration in Šula's semisynthetic medium (SEVAC, Prague). Compounds **9o**, **12o**, **17o**, and **18o**, which were expected to have low activities, were dissolved in dimethyl sulfoxide and added to the medium at concentrations of 1000, 500, 250, 125, 62, 32, 16, 8, 4, 2, and 1 μmol/L. The remaining compounds were dissolved in dimethyl sulfoxide and added to the medium at concentrations of 32, 16, 8, 4, 2, 1, 0.5, 0.25, 0.125, 0.06, and 0.03 μmol/L in the assays using the *M.tb.* and *M. kansasii* strains and at concentrations of 1000, 500, 250, 125, 62, 32, 16, 8, 4, 2, and 1 μmol/L in the assay using the *M. avium* strain. MICs, defined as the lowest concentration of a compound at which mycobacterial growth inhibition occurred (the concentration that inhibited >99% of the mycobacterial population), were determined after incubation at 37 °C for 7/14/21 days for both strains of *M. kansasii* and after 14/21 days for the *M. tuberculosis* and *M. avium* strains. INH was used as a prototype drug.

SS18b-LUX Assay As a Latent Tuberculosis Model. 18b-Lux strain was grown in 7H9 medium with acetate (0.1% final concentration) supplemented with 10% albumin-NaCl, 0.05% Tween 80, and 50 μg/mL streptomycin (STR). Hygromycin B (HYG) (50 μg/mL) was added to the 18b-Lux cultures. Non-replicating STR-starved 18b-Lux (SS18b-Lux) was generated as follows. 18b-Lux was grown to the mid logarithmic phase in STR- and HYG-containing medium and was washed three times in phosphate-buffered saline (PBS) containing 0.05% Tween 80 (PBST). The final bacterial pellets were resuspended in medium without STR and were frozen in 15% glycerol at −80 °C. Two weeks prior to the experiment, fresh cultures were taken in medium without STR and kept between OD_{600} = 0.2−0.5 until they stopped replicating.

OD = 0.1 SS18b-Lux cells were plated together with the compound on white 96-well plates in 100 μL of assay volume and incubated at 37 °C. Luminescence was recorded 5 min, 1 day, 4 days, and 6 days after the addition of compounds using a Tecan Infinite M200 microplate reader. The same plate was then used for evaluating the potency of the compounds through a resazurin reduction microplate assay (REMA). Then 10 μL of 0.025% (w/v) resazurin was added to the wells and incubated overnight. The fluorescence was measured (excitation, 560 nm; emission, 590 nm; gain, 70) using a Tecan Infinite M200 microplate reader.[37]

In Vitro Antibacterial and Antifungal Assays. To assess the antibacterial and antifungal activities of the synthesized compounds in vitro, a broth microdilution method was used. The set of tested fungi included five yeasts and yeast-like organisms (*Candida albicans* ATCC 44859 (CA), *Candida tropicalis* 156 (CT), *Candida krusei* E28 (CK), *Candida glabrata* 20/I (CG), and *Trichosporon asahii* 1188 (TA)) and three molds (*Aspergillus fumigatus* 231 (AF), *Absidia corymbifera* 272 (AC), and *Trichophyton mentagrophytes* 445 (TM)). The procedure was performed with 2-fold dilutions of the investigated compounds in RPMI-1640 medium buffered to pH 7.0 with 0.165 mol of 3-morpholinopropane-1-sulfonic acid. The compounds were dissolved in DMSO, and the final concentrations of the compounds ranged from 500 to 0.488 μM (due to solubility limits, the final concentrations of some compounds ranged from only 250 or 125 to 0.488 μM). Drug-free controls were included. The MIC was defined as an 80% or greater (for yeasts and yeast-like organisms, IC_{80}) or 50% or greater (for molds, IC_{50}) reduction of fungal growth compared with the control. The MIC values were determined after 24 and 48 h of static incubation at 35 °C. For *T. mentagrophytes*, the final MICs were determined after 72 and 120 h of incubation. Fluconazole and amphotericin B were used as prototype drugs.

The set of tested bacteria included four strains of Gram-positive cocci (*Staphylococcus aureus* ATCC 6538 (SA), methicillin-resistant *Staphylococcus aureus* H 5996/08 (MRSA), *Staphylococcus epidermidis* H 6966/08 (SE), and *Enterococcus faecalis* J 14365/08 (EF)) and four strains of Gram-negative rods (*Escherichia coli* ATCC 8739 (EC), *Klebsiella pneumoniae* D 11750/08 (KP), *Klebsiella pneumoniae* (a producer of extended-spectrum β-lactamases) (ESBL) J 14368/08 (KP-E), and *Pseudomonas aeruginosa* ATCC 9027 (PA)). The concentration range was the same as that used for the aforementioned fungi. Mueller−Hinton broth was used as a culture medium when testing the bacteria. The MIC was defined as a 95% or greater reduction of growth compared with the control. The MIC values were

DOI: 10.1021/acs.jmedchem.5b00608
J. Med. Chem. 2016, 59, 2362−2380

determined after 24 and 48 h of static incubation at 35 °C. Vancomycin was used as a prototype drug for Gram-positive cocci, and gentamicin was used as a prototype drug for Gram-negative rods.

Docking Studies. *Preparation of Ligands.* The three-dimensional structures of compounds **11i** and **14g** were constructed and optimized using CORINA.[43] The output file format was converted into the AutoDock Vina[44] compliant pdbqt format by MGLTools.[45]

Preparation of Receptor. The crystal structure of *M.tb.* oxidoreductase DprE1 (PDB 4FDO) was used as a receptor for molecular docking. All ligands, with the exception of water molecules, were removed from the structure. Hydrogen atoms were added to the receptors using PyMOL Molecular Graphic System, version 1.5.0.4, Schrödinger, LLC. Gasteiger charges and AutoDock atom types were assigned to receptors by MGLTools.

In Vitro Cell Proliferation/Viability Assay (MTS Assay). *Cell Lines and Culture Conditions.* HeLa cells (human cervical epithelioid carcinoma) and MDCKII-MDR1 cells (Madin−Darby canine kidney cells permanently expressing human efflux transporter MDR1) were cultivated in Dulbecco's Modified Eagle's Medium (DMEM) supplemented with 10% (v/v) fetal bovine serum (FBS) and 1% (v/v) nonessential amino acids. HuH7 cells (human hepatocellular carcinoma) were maintained in DMEM with 10% (v/v) fetal bovine serum (FBS). HeLa and HuH7 cells were purchased from the European Collection of Cell Cultures (ECACC, Salisbury, UK), and MDCKII-MDR1 cells were received as a gift from Dr. A. H. Schinkel (NKI, Amsterdam, The Netherlands).

The cells were seeded into 96-well cultivation plates (10×10^3 cells per well) 24 h prior to treatment. Then the cells were exposed to the test compounds for either 24 or 48 h at a concentration of 20 μM. Stock solutions of the test compounds were prepared in DMSO solvent at a concentration of 20 mM (the final concentration of DMSO in the culture did not exceed 0.1% v/v).

Primary human hepatocytes were obtained from Biopredic (Rennes, France) (batch HEP220797). The cells were isolated from liver tissue (66-year-old Caucasian female) and seeded into 96-well cultivation plates. The cells were cultivated in "maintenance" medium overnight, and then the medium was replaced by "use" medium according to the manufacturer's protocol. They were treated with selected test compounds for 48 h in "use" medium at a concentration of 20 μM.

Cell Proliferation/Viability Assay. A CellTiter 96AQ$_{ueous}$One Solution cell proliferation assay (Promega, Madison, WI, USA) was performed to evaluate the toxicity of the test compounds in vitro in the three mammalian cell lines and primary human hepatocytes. The method is based on the colorimetric determination of MTS tetrazolium ([3-(4,5-dimethylthiazol-2-yl)-5-(3-carboxymethoxyphenyl)-2-(4-sulfophenyl)-2*H*-tetrazolium] bioreduction into colored formazan by viable cells. Formazan production is thus proportional to the number of viable cells. All experiments were conducted according to the manufacturer's protocol. Briefly, the cells were treated with either the test compounds or the vehicle alone (DMSO) for either 24 or 48 h in Opti-MEM reduced-serum medium (Life Technologies) to avoid potential binding of the test compounds to serum proteins. At the end of the treatment, 20 μL of MTS reagent was added directly to each culture well and further cultivated for 1.5 h. Finally, the absorbance of converted formazan was recorded at 490 nm using a plate reader (BioTec Synergy 2, Winooski, VT, USA). In the toxic control, Triton X-100 (0.9% v/v) was added to the cells 45 min before the addition of the MTS reagent. The relative viabilities of cells treated either with the vehicle (DMSO, 0.1%) or Triton X were set to 100% and 0%, respectively. The results were expressed as relative cell viability at a concentration of 20 μM. All experiments were performed in triplicate and repeated at least three times.

HepG2 Assay. HepG2 cells were cultured in Dulbecco's Modified Eagle's Medium (DMEM) supplemented with 10% (v/v) fetal bovine serum (FBS) at 37 °C and 5% CO_2. Prior to the experiment, the cells were washed with PBS and then trypsinized. Lifted cells were washed twice with PBS, resuspended in fresh medium, and separated on a 40 μm cell strainer. Two thousand cells per well were plated on a transparent 384-well plate together with the compounds in a final volume of 50 μL. The cells were incubated at 37 °C and 5% CO_2 for 2 days, and then 5 μL of 0.025% (w/v) resazurin was added to the wells. After overnight incubation, the fluorescent signal was monitored using a Tecan Infinite M200 microplate reader at 590 nm.

Ames Fluctuation Assay. The mutagenic activities of the selected compounds were detected using the commercially available Muta-ChromoPlate bacterial strain kit (ebpi, Mississauga, Ontario, Canada), which is a 96-well microplate version of the *Salmonella typhimurium* Ames Test. The test was performed and evaluated according to the manufacturer's instructions. The final concentration of the tested compounds was 30 μM (the highest concentration that enables full solubility and that showed no cytotoxicity in mammalian cell lines). *Salmonella typhimurium* tester strains TA 98 (detection of frame shift mutagens) and TA 100 (detection of base-exchange mutations) were used. The compounds were dissolved in DMSO, and the final concentration of DMSO in the entire reaction mixture was 0.1%. The following standard direct-acting mutagens were used as positive controls: sodium azide for use with strain TA100 (final amount of 0.5 μg) and 2-nitrofluorene for use with strain TA98 (final amount of 30 μg). A blank plate was used as a sterility control, and plates of each strain without any test compounds were used as spontaneous mutation controls (background controls).

Cell-Free Assays. P[^{14}C]RPP incorporation into [^{14}C]-decaprenylphosphoryl arabinose and its precursors was tested with a mixture of membrane and cell envelope enzyme fractions from *M. smegmatis* mc^{2}155. Compounds **14g** and **11i** were added as DMSO solutions to the reaction mixtures; the DMSO concentration in each of the reaction mixtures, including the control reactions, was 3.125% (v/v). A combined 300 μg of membrane and 500 μg of cell envelope protein was incubated with 15000 dpm of P[^{14}C]RPP and DMSO or DMSO solution of the compound in 80 μL of the reaction mixture for 1 h at 37 °C, and radiolabeled lipid products were extracted with $CHCl_3/CH_3OH$ (2:1, v/v) and analyzed by TLC on a silica gel TLC plate (Merck) and autoradiography using Biomax MR1 film (Kodak) following previously reported procedures.[40]

Metabolic Labeling. For [^{14}C]-acetate radiolabeling, *M.tb.* H37Ra was grown statically at 37 °C in 7H9-ADC-Tween 80 medium to OD_{600} 0.182. Then the culture was divided into 20 mL aliquots to which the compounds dissolved in DMSO were added to final concentrations of 0.2 μg/mL and 0.5 μg/mL for both **11i** and **14g** and 0.2 μg/mL for BTZ-043, and the incubation continued with shaking. The DMSO concentration in each culture, including the control, was 1%. After 24 h, OD_{600} was measured, and then three 2 mL portions of each culture were removed to Falcon tubes and [1,2-^{14}C]-acetate (American Radiolabeled Chemicals, specific activity 106 mCi/mmol) was added at a final concentration of 0.5 μCi/mL. After 24 h of incubation, OD_{600} was measured again, and the radiolabeled mycobacteria were harvested by centrifugation at 4500*g* for 15 min at 4 °C. The lipids were extracted with $CHCl_3/CH_3OH$ (1:2, v/v) at 56 °C for 1.5 h, followed by extraction with $CHCl_3/CH_3OH$ (2:1, v/v) at 56 °C for 1.5 h. The organic extracts were combined, dried under a stream of N_2 at rt, and subjected to a biphasic separation with $CHCl_3/CH_3OH/H_2O$ (4:2:1, v/v). The bottom organic phase was recovered, dried under a stream of N_2 at rt, and dissolved in $CHCl_3/CH_3OH$/concentrated NH_4OH/H_2O (65:25:0.5:3.6, v/v) in the ratio of 150 μL/OD_{600} 0.5. Aliquots of 5 μL of each sample were loaded on a silica gel TLC plate (Merck) and separated in $CHCl_3/CH_3OH/H_2O$ (20:4:0.5, v/v). The plate was exposed to Biomax MR1 film (Kodak) at −80 °C for 3 days.

For [^{14}C]-uracil and [^{14}C]-methionine radiolabeling, *M.tb.* H37Ra was grown as described above until the OD_{600} reached 0.300. The culture was divided into 20 mL portions, which were treated with 1 μg/mL **11i** and **14g**, 0.05 μg/mL RIF, and 5 μg/mL KAN for 1 h with shaking. Then, six 1 mL aliquots were removed, of which three were radiolabeled with [2-^{14}C]-uracil (American Radiolabeled Chemicals, specific activity of 53 mCi/mmol) at a final concentration of 0.1 μCi/mL and the next three with 0.2 μCi/mL of L-[methyl-^{14}C]-methionine (American Radiolabeled Chemicals, specific activity 55 mCi/mmol). After 24 h of radiolabeling, OD_{600} was measured, the cells were harvested by centrifugation at 14000*g* for 10 min at 4 °C and the

DOI: 10.1021/acs.jmedchem.5b00608
J. Med. Chem. 2016, 59, 2362−2380

radioactivity in the cell pellets was quantified by scintillation spectrometry.

Microsomal Stability Assay. Microsomes pooled from 50 donors (catalogue no. HMMCPL, Human Microsomes, 50 donors) to minimize the effect of interindividual variability were purchased from Life Technologies (now ThermoFisher Scientific, Walham, MA) and were processed according to the manufacturer's protocol for microsomal stability assays. The concentration of test compounds in the assays was 3 μM, and the microsome concentration was 0.5 mg/mL in 500 μL of phosphate buffer at pH 7.4. Briefly, 458 μL of 100 mM buffer, 5 μL of a stock solution of compounds **11i** or **14g** in DMSO, and 12.5 μL of microsomes (20 mg/mL) were combined and preincubated in a water bath for 5 min. Then the reaction was initiated by adding 25 μL of 20 mM NADPH and incubated at 37 °C with gentle agitation. The reaction was terminated by adding 500 μL of AcCN, centrifuged at approximately 3000 rpm for 5 min, and the supernatant was analyzed using HPLC. The sampling time points were 0, 30, or 60 min. Samples without NADPH cofactor (60 min only) were used as controls.

Solubility in Aqueous Media. First, 50 μL of a 20 mM stock solution of compound **11i** or **14g** in DMSO was added to 4950 μL of water, 5 μL of a 20 mM stock solution of compound **11i** or **14g** in DMSO was added to 4995 μL of water, and 1 μL of a 20 mM stock solution of compound **11i** or **14g** in DMSO was added to 9999 μL of water to obtain solutions in aqueous DMSO with final DMSO concentrations of 1% (200 μM of compound), 0.1% (20 μM of compound), and 0.01% (2 μM of compound), respectively. All solutions were then centrifuged at 10000 rpm for 10 min, and the clear supernatants were analyzed. All experiments were repeated 6−8 times.

Compounds **11i** and **14g** were shaken in distilled water (0.2 mg/mL) for 24 h at rt. The suspensions were centrifuged at 10000 rpm for 10 min, and the clear supernatants were analyzed using HPLC. All experiments were repeated four times.

HPLC Analysis. The samples were analyzed using a Shimadzu Prominence instrument (Shimadzu, Kyoto, Japan) consisting of LC-20AD pumps with a DGU-20A3 degasser, an SIL-20A HT autosampler, a CTO-20AC column oven, an SPD-M20A diode array detector, and a CBM-20A communication module. The data were analyzed using LCsolutions 1.22 software.

Compounds **11i** and **14g** were analyzed using a Discovery HS C18 150−4.6 mm column with 5 μm particles (Supelco Analytical, Sigma-Aldrich, Schnelldorf, Germany) at 30 °C. A mobile phase composed of water/acetonitrile 3:7 (v/v) at a flow rate of 1.5 mL/min was used. The samples were monitored at 265 nm for **11i** and 300 nm for **14g**. The retention times of **11i** and **14g** were 2.9 and 4.5 min, respectively. The calibration curves were linear in the range of 0.1−20 μM.

■ ASSOCIATED CONTENT

Supporting Information

The Supporting Information is available free of charge on the ACS Publications website at DOI: 10.1021/acs.jmedchem.5b00608.

In vitro antibacterial activities of selected compounds expressed as MIC, in vitro antifungal activities of selected compounds expressed as MIC, metabolic labeling with [^{14}C]-acetate, metabolic labeling with [^{14}C]-uracil and [^{14}C]-methionine, best binding modes of studied compounds docked into DprE1, assessment of compounds **11i**, **14g**, and RIF in the resazurin reduction microplate assay with SS18b-Lux, in silico effective human jejunum permeability study; characterization data of intermediates (PDF)

Molecular formula strings (CSV)

■ AUTHOR INFORMATION

Corresponding Author

*Phone: +420 495 067 339. Fax: +420 495 067 166. E-mail: jaroslav.roh@faf.cuni.cz.

Author Contributions

The manuscript was written through the contributions of all authors. All authors have given approval to the final version of the manuscript.

Notes

The authors declare no competing financial interest.

■ ACKNOWLEDGMENTS

This work was supported by the Czech Science Foundation project 14-08423S, the European Community's Seventh Framework Programme (MM4TB, grant 260872), and the Slovak Research and Development Agency (contract no. DO7RP-0015-11, K.M.). G.K., J.N., and T.S. thank Charles University in Prague (SVV 260 062 and 260 064). P.C. thanks the European Social Fund and the state budget of the Czech Republic, project no. CZ.1.07/2.3.00/30.0061. We thank Dr. Vadim Makarov (Bakh Institute of Biochemistry, Russian Academy of Science, Moscow, Russia) for providing BTZ-043.

■ ABBREVIATIONS USED

ADC, albumin, dextrose, catalase; ADME, absorption, distribution, metabolism, excretion; CNCTC, Czech National Collection of Type Cultures; DMEM, Dulbecco's Modified Eagle's Medium; DMSO, dimethyl sulfoxide; DprE1, decaprenylphosphoryl-β-D-ribose 2′-oxidase; DPPR, decaprenylphosphoryl ribose-5 phosphate; DPR, decaprenylphosphoryl ribose; DPA, decaprenylphosphoryl arabinose; INH, isoniazid; KAN, kanamycin; MDR, multidrug-resistant; MIC, minimum inhibitory concentration; MTS, [3-(4,5-dimethyl-2-yl)-5-(3-carboxymethoxyphenyl)-2-(4-sulfophenyl)-2*H*-tetrazolium; RMSD, root-mean-square deviation; R_f, retention factor; SDS, sodium dodecyl sulfate; RIF, rifampicin; TB, tuberculosis; TBAB, tetrabutylammonium bromide; THF, tetrahydrofuran; TLC, thin layer chromatography; XDR, extensively drug-resistant

■ REFERENCES

(1) *Global Tuberculosis Report 2015*; World Health Organization: Geneva, 2015; http://www.who.int/tb.

(2) Zumla, A.; Nahid, P.; Cole, S. T. Advances in the development of new tuberculosis drugs and treatment regimens. *Nat. Rev. Drug Discovery* **2013**, *12*, 388−404.

(3) Gler, M. T.; Skripconoka, V.; Sanchez-Garavito, E.; Xiao, H. P.; Cabrera-Rivero, J. L.; Vargas-Vasquez, D. E.; Gao, M. Q.; Awad, M.; Park, S. K.; Shim, T. S.; Suh, G. Y.; Danilovits, M.; Ogata, H.; Kurve, A.; Chang, J.; Suzuki, K.; Tupasi, T.; Koh, W. J.; Seaworth, B.; Geiter, L. J.; Wells, C. D. Delamanid for Multidrug-Resistant Pulmonary Tuberculosis. *N. Engl. J. Med.* **2012**, *366*, 2151−2160.

(4) Diacon, A. H.; Pym, A.; Grobusch, M.; Patientia, R.; Rustomjee, R.; Page-Shipp, L.; Pistorius, C.; Krause, R.; Bogoshi, M.; Churchyard, G.; Venter, A.; Allen, J.; Palomino, J. C.; De Marez, T.; van Heeswijk, R. P. G.; Lounis, N.; Meyvisch, P.; Verbeeck, J.; Parys, W.; de Beule, K.; Andries, K.; Mc Neeley, D. F. The Diarylquinoline TMC207 for Multidrug-Resistant Tuberculosis. *N. Engl. J. Med.* **2009**, *360*, 2397−2405.

(5) Kakkar, A. K.; Dahiya, N. Bedaquiline for the treatment of resistant tuberculosis: Promises and pitfalls. *Tuberculosis* **2014**, *94*, 357−362.

(6) Beena; Rawat, D. S. Antituberculosis Drug Research: A Critical Overview. *Med. Res. Rev.* **2013**, *33*, 693−764.

DOI: 10.1021/acs.jmedchem.5b00608
J. Med. Chem. 2016, 59, 2362−2380

(7) Mikusova, K.; Makarov, V.; Neres, J. DprE1 - from the Discovery to the Promising Tuberculosis Drug Target. *Curr. Pharm. Des.* **2014**, *20*, 4379−4403.
(8) Makarov, V.; Lechartier, B.; Zhang, M.; Neres, J.; van der Sar, A. M.; Raadsen, S. A.; Hartkoorn, R. C.; Ryabova, O. B.; Vocat, A.; Decosterd, L. A.; Widmer, N.; Buclin, T.; Bitter, W.; Andries, K.; Pojer, F.; Dyson, P. J.; Cole, S. T. Towards a new combination therapy for tuberculosis with next generation benzothiazinones. *EMBO Mol. Med.* **2014**, *6*, 372−383.
(9) Christophe, T.; Jackson, M.; Jeon, H. K.; Fenistein, D.; Contreras-Dominguez, M.; Kim, J.; Genovesio, A.; Carralot, J. P.; Ewann, F.; Kim, E. H.; Lee, S. Y.; Kang, S.; Seo, M. J.; Park, E. J.; Skovierova, H.; Pham, H.; Riccardi, G.; Nam, J. Y.; Marsollier, L.; Kempf, M.; Joly-Guillou, M. L.; Oh, T.; Shin, W. K.; No, Z.; Nehrbass, U.; Brosch, R.; Cole, S. T.; Brodin, P. High Content Screening Identifies Decaprenyl-Phosphoribose 2′ Epimerase as a Target for Intracellular Antimycobacterial Inhibitors. *PLoS Pathog.* **2009**, *5*, e1000645.
(10) Trefzer, C.; Rengifo-Gonzalez, M.; Hinner, M. J.; Schneider, P.; Makarov, V.; Cole, S. T.; Johnsson, K. Benzothiazinones: Prodrugs That Covalently Modify the Decaprenylphosphoryl-beta-D-ribose 2′-epimerase DprE1 of Mycobacterium tuberculosis. *J. Am. Chem. Soc.* **2010**, *132*, 13663−13665.
(11) Schaper, K. J.; Pickert, M.; Frahm, A. W. Substituted xanthones as antimycobacterial agents Part 3: QSAR investigations. *Arch. Pharm.* **1999**, *332*, 91−102.
(12) Makarov, V.; Manina, G.; Mikusova, K.; Mollmann, U.; Ryabova, O.; Saint-Joanis, B.; Dhar, N.; Pasca, M. R.; Buroni, S.; Lucarelli, A. P.; Milano, A.; De Rossi, E.; Belanova, M.; Bobovska, A.; Dianiskova, P.; Kordulakova, J.; Sala, C.; Fullam, E.; Schneider, P.; McKinney, J. D.; Brodin, P.; Christophe, T.; Waddell, S.; Butcher, P.; Albrethsen, J.; Rosenkrands, I.; Brosch, R.; Nandi, V.; Bharath, S.; Gaonkar, S.; Shandil, R. K.; Balasubramanian, V.; Balganesh, T.; Tyagi, S.; Grosset, J.; Riccardi, G.; Cole, S. T. Benzothiazinones Kill Mycobacterium tuberculosis by Blocking Arabinan Synthesis. *Science* **2009**, *324*, 801−804.
(13) Trefzer, C.; Skovierova, H.; Buroni, S.; Bobovska, A.; Nenci, S.; Molteni, E.; Pojer, F.; Pasca, M. R.; Makarov, V.; Cole, S. T.; Riccardi, G.; Mikusova, K.; Johnsson, K. Benzothiazinones Are Suicide Inhibitors of Mycobacterial Decaprenylphosphoryl-beta-D-ribofuranose 2′-Oxidase DprE1. *J. Am. Chem. Soc.* **2012**, *134*, 912−915.
(14) Klimesova, V.; Koci, J.; Pour, M.; Stachel, J.; Waisser, K.; Kaustova, J. Synthesis and preliminary evaluation of benzimidazole derivatives as antimicrobial agents. *Eur. J. Med. Chem.* **2002**, *37*, 409−418.
(15) Koci, J.; Klimesova, V.; Waisser, K.; Kaustova, J.; Dahse, H. M.; Mollmann, U. Heterocyclic benzazole derivatives with antimycobacterial in vitro activity. *Bioorg. Med. Chem. Lett.* **2002**, *12*, 3275−3278.
(16) Klimesova, V.; Koci, J.; Palat, K.; Stolarikova, J.; Dahse, H. M.; Mollmann, U. Structure-Activity Relationships of 2-Benzylsulfanyl-benzothiazoles: Synthesis and Selective Antimycobacterial Properties. *Med. Chem.* **2012**, *8*, 281−292.
(17) Karabanovich, G.; Roh, J.; Smutný, T.; Němeček, J.; Vicherek, P.; Stolaříková, J.; Vejsová, M.; Dufková, I.; Vávrová, K.; Pávek, P.; Klimešová, V.; Hrabálek, A. 1-Substituted-5-[(3,5-Dinitrobenzyl)-sulfanyl]-1*H*-Tetrazoles and Their Isosteric Analogs: A New Class of Selective Antitubercular Agents Active against Drug-Susceptible and Multidrug-Resistant Mycobacteria. *Eur. J. Med. Chem.* **2014**, *82*, 324−340.
(18) Karabanovich, G.; Roh, J.; Soukup, O.; Pávková, I.; Pasdiorová, M.; Tambor, V.; Stolaříková, J.; Vejsová, M.; Vávrová, K.; Klimešová, V.; Hrabálek, A. Tetrazole Regioisomers in the Development of Nitro Group-Containing Antitubercular Agents. *MedChemComm* **2015**, *6*, 174−181.
(19) Maddry, J. A.; Ananthan, S.; Goldman, R. C.; Hobrath, J. V.; Kwong, C. D.; Maddox, C.; Rasmussen, L.; Reynolds, R. C.; Secrist, J. A.; Sosa, M. I.; White, E. L.; Zhang, W. Antituberculosis activity of the molecular libraries screening center network library. *Tuberculosis* **2009**, *89*, 354−363.
(20) Bakal, R. L.; Gattani, S. G. Identification and development of 2,5-disubstituted oxadiazole as potential candidate for treatment of XDR and MDR tuberculosis. *Eur. J. Med. Chem.* **2012**, *47*, 278−282.
(21) Foroumadi, A.; Soltani, F.; Moallemzadeh-Haghighi, H.; Shafiee, A. Synthesis, in vitro-antimycobacterial activity and cytotoxicity of some alkyl alpha-(5-aryl-1,3,4-thiadiazole-2-ylthio)acetates. *Arch. Pharm.* **2005**, *338*, 112−116.
(22) Ahsan, M. J.; Samy, J. G.; Khalilullah, H.; Nomani, M. S.; Saraswat, P.; Gaur, R.; Singh, A. Molecular properties prediction and synthesis of novel 1,3,4-oxadiazole analogues as potent antimicrobial and antitubercular agents. *Bioorg. Med. Chem. Lett.* **2011**, *21*, 7246−7250.
(23) Macaev, F.; Rusu, G.; Pogrebnoi, S.; Gudima, A.; Stingaci, E.; Vlad, L.; Shvets, N.; Kandemirli, F.; Dimoglo, A.; Reynolds, R. Synthesis of novel 5-aryl-2-thio-1,3,4-oxadiazoles and the study of their structure-anti-mycobacterial activities. *Bioorg. Med. Chem.* **2005**, *13*, 4842−4850.
(24) Ali, M. A.; Shaharyar, M. Oxadiazole mannich bases: Synthesis and antimycobacterial activity. *Bioorg. Med. Chem. Lett.* **2007**, *17*, 3314−3316.
(25) Navarrete-Vazquez, G.; Molina-Salinas, G. M.; Duarte-Fajardo, Z. V.; Vargas-Villarreal, J.; Estrada-Soto, S.; Gonzalez-Salazar, F.; Hernandez-Nunez, E.; Said-Fernandez, S. Synthesis and antimycobacterial activity of 4-(5-substituted-1,3,4-oxadiazol-2-yl)pyridines. *Bioorg. Med. Chem.* **2007**, *15*, 5502−5508.
(26) Ananthan, S.; Faaleolea, E. R.; Goldman, R. C.; Hobrath, J. V.; Kwong, C. D.; Laughon, B. E.; Maddry, J. A.; Mehta, A.; Rasmussen, L.; Reynolds, R. C.; Secrist, J. A.; Shindo, N.; Showe, D. N.; Sosa, M. I.; Suling, W. J.; White, E. L. High-throughput screening for inhibitors of Mycobacterium tuberculosis H37Rv. *Tuberculosis* **2009**, *89*, 334−353.
(27) Foroumadi, A.; Asadipour, A.; Mirzaei, M.; Karimi, J.; Emami, S. Antituberculosis agents. V. Synthesis, evaluation of in vitro antituberculosis activity and cytotoxicity of some 2-(5-nitro-2-furyl)-1,3,4-thiadiazole derivatives. *Farmaco* **2002**, *57*, 765−769.
(28) Foroumadi, A.; Kiani, Z.; Soltani, F. Antituberculosis agents VIII: Synthesis and in vitro antimycobacterial activity of alkyl α-[5-(5-nitro-2-thienyl)-1,3,4-thiadiazole-2-ylthio] acetates. *Farmaco* **2003**, *58*, 1073−1076.
(29) Foroumadi, A.; Sakhteman, A.; Sharifzadeh, Z.; Mohammadhosseini, N.; Hemmateenejad, B.; Moshafi, M. H.; Vosooghi, M.; Amini, M.; Shafiee, A. Synthesis, antituberculosis activity and QSAR study of some novel 2-(nitroaryl)-5-(nitrobenzylsulfinyl and sulfonyl)-1,3,4-thiadiazole derivatives. *Daru J. Pharm. Sci.* **2007**, *15*, 218−226.
(30) Zarghi, A.; Faizi, M.; Shafaghi, B.; Ahadian, A.; Khojastehpoor, H. R.; Zanganeh, V.; Tabatabai, S. A.; Shafiee, A. Design and synthesis of new 2-substituted-5-(2-benzylthiophenyl)1,3,4-oxadiazoles as benzodiazepine receptor agonists. *Bioorg. Med. Chem. Lett.* **2005**, *15*, 3126−3129.
(31) Disli, A.; Salman, M. Synthesis of some new 5-substituted 1*H*-tetrazoles. *Russ. Russ. J. Org. Chem.* **2009**, *45*, 151−153.
(32) Efimova, Y. A.; Artamonova, T. V.; Koldobskii, G. I. Tetrazoles: LIII. Microwave-Activated Acylation of 5-Substituted Tetrazoles. *Russ. J. Org. Chem.* **2008**, *44*, 1345−1347.
(33) Koguro, K.; Oga, T.; Mitsui, S.; Orita, R. Novel synthesis of 5-substituted tetrazoles from nitriles. *Synthesis* **1998**, *1998*, 910−914.
(34) Baron, M.; Wilson, C. V. 2-Substituted-1,3,4-Oxa and Thia-Diazoline-5-Thiones. *J. Org. Chem.* **1958**, *23*, 1021−1023.
(35) Wei, M. X.; Feng, L.; Li, X. Q.; Zhou, X. Z.; Shao, Z. H. Synthesis of new chiral 2,5-disubstituted 1,3,4-thiadiazoles possessing gamma-butenolide moiety and preliminary evaluation of in vitro anticancer activity. *Eur. J. Med. Chem.* **2009**, *44*, 3340−3344.
(36) Gutsche, C. D.; See, K. A. Calixarenes 0.27. Synthesis, Characterization, and Complexation Studies of Double-Cavity Calix 4 Arenes. *J. Org. Chem.* **1992**, *57*, 4527−4539.
(37) Vocat, A.; Hartkoorn, R. C.; Lechartier, B.; Zhang, M.; Dhar, N.; Cole, S. T.; Sala, C. Bioluminescence for Assessing Drug Potency

DOI: 10.1021/acs.jmedchem.5b00608
J. Med. Chem. 2016, 59, 2362−2380

against Nonreplicating Mycobacterium tuberculosis. *Antimicrob. Agents Chemother.* **2015**, *59*, 4012−4019.
(38) Neres, J.; Pojer, F.; Molteni, E.; Chiarelli, L. R.; Dhar, N.; Boy-Rottger, S.; Buroni, S.; Fullam, E.; Degiacomi, G.; Lucarelli, A. P.; Read, R. J.; Zanoni, G.; Edmondson, D. E.; De Rossi, E.; Pasca, M. R.; McKinney, J. D.; Dyson, P. J.; Riccardi, G.; Mattevi, A.; Cole, S. T.; Binda, C. Structural Basis for Benzothiazinone-Mediated Killing of Mycobacterium tuberculosis. *Sci. Transl. Med.* **2012**, *4*, 150ra121.
(39) Batt, S. M.; Jabeen, T.; Bhowruth, V.; Quill, L.; Lund, P. A.; Eggeling, L.; Alderwick, L. J.; Futterer, K.; Besra, G. S. Structural basis of inhibition of Mycobacterium tuberculosis DprE1 by benzothiazinone inhibitors. *Proc. Natl. Acad. Sci. U. S. A.* **2012**, *109*, 11354−11359.
(40) Mikusova, K.; Huang, H. R.; Yagi, T.; Holsters, M.; Vereecke, D.; D'Haeze, W.; Scherman, M. S.; Brennan, P. J.; McNeil, M. R.; Crick, D. C. Decaprenylphosphoryl arabinofuranose, the donor of the D-arabinofuranosyl residues of mycobacterial arabinan, is formed via a two-step epimerization of decaprenylphosphoryl ribose. *J. Bacteriol.* **2005**, *187*, 8020−8025.
(41) Mikusova, K.; Slayden, R. A.; Besra, G. S.; Brennan, P. J. Biogenesis of the Mycobacterial Cell-Wall and the Site of Action of Ethambutol. *Antimicrob. Agents Chemother.* **1995**, *39*, 2484−2489.
(42) Obach, R. S. Prediction of human clearance of twenty-nine drugs from hepatic microsomal intrinsic clearance data: An examination of in vitro half-life approach and nonspecific binding to microsomes. *Drug Metab. Dispos.* **1999**, *27*, 1350−1359.
(43) Renner, S.; Schwab, C. H.; Gasteiger, J.; Schneider, G. Impact of conformational flexibility on three-dimensional similarity searching using correlation vectors. *J. Chem. Inf. Model.* **2006**, *46*, 2324−2332.
(44) Trott, O.; Olson, A. J. AutoDock Vina: Improving the Speed and Accuracy of Docking with a New Scoring Function, Efficient Optimization, and Multithreading. *J. Comput. Chem.* **2010**, *31*, 455−461.
(45) Sanner, M. F. Python: A programming language for software integration and development. *J. Mol. Graph. Modell.* **1999**, *17*, 57−61.

DOI: 10.1021/acs.jmedchem.5b00608
J. Med. Chem. 2016, 59, 2362−2380

U1. Human induced hepatocyte-like cells as alternative model for evaluation of herb-induced liver injury.

Tomáš Smutný, Riina Harjumäki, Liisa Kanninen, Marjo Yliperttula, Petr Pávek, Yan-Ru Lou. Human induced hepatocyte-like cells as alternative model for evaluation of herb-induced liver injury. (*preparing manuscript, yet unpublished data*)

The administration of herbal medicines is sometimes associated with safety concerns such as HILI. Since hepatotoxic phytochemicals-derived from herbs have not been broadly evaluated on the current *in vitro* hepatocyte models such iHep cells, we aimed at the toxicological assessment of HILI using iHep cells in our preparing manuscript.

To meet our aim, we chose several hepatotoxicans with different modes of toxicity such as saikosaponin D, monocrotaline, deoxycalyciphylline B, and triptolide employing MTS and LDH assays.

Saikosaponin D revealed both higher reduction of mitochondrial activity and LDH leakage (suggesting membrane damage) on iHep cells than HepG2 cells. Triptolide resulted in dose-dependent cytotoxicity in iHep cells. However, no alteration of viability markers was found for the treatment with monocrotaline and deoxycalyciphylline B in both cell models.

9. Discussion

Despite the tremendous progress in development of liver *in vitro* models in several past years, most works in this scientific field depict proof of concept studies and suggest the future course rather than introduce a current valid tool applicable for drug development (Roth and Singer 2014). Before a new model can be approved and incorporated into official guidelines, it has to go through a complex validation process. The procedure requires a time-consuming comparison of results among different laboratories (Ranganatha and Kuppast 2012). Although we are victims of breathtaking advancement in analytical methods, it is worth to emphasise that data captured from *in vitro* models can provide as much valid information as a model closely resembles *in vivo* state. Hence, the progress of analytical methods has to go side by side with development of better *in vitro* models (Roth and Singer 2014).

In this thesis, I focused on three main aims. First, I and my collaborators attempted to identify small molecules for the improvement of metabolic capacity of *in vitro* liver cell models. Since DMEs are poorly expressed in most *in vitro* hepatocyte systems, we also dealt with post-transcriptional and post-translational modifications of NRs implicated in the regulation of DMEs, which could at least partially stand behind this phenomenon. Eventually, we attempted to assess the risk of DILI/HILI of new candidate drugs and phytochemicals using *in vitro* liver cell models. Our results will be discussed in next three sections, which correspond to these three main aims.

- **Small molecules**

Small molecules have been proofed to be an efficient tool to mitigate some roadblocks associated with using *in vitro* liver models. Small molecules were shown to maintain expression of DMEs in sandwich-cultured hepatocytes (Kienhuis et al. 2007). They also allow to induce proliferation of primary human hepatocytes (Shan et al. 2013). In stem cell research, they were used for a somatic cell reprogramming functioning as pluripotency gene activators, self-renewal modulators and reprogramming boosters (Feng et al. 2009). Additionally, inhibitors of MEK and GSK3 signaling supported

the promotion of fully competent iPSCs from somatic cells (Feng et al. 2009). Furthermore, several compounds identified by Shan and colleagues promoted maturation of human iHep cells (Shan et al. 2013).

The identification of new small molecules raises the possibility to replace expensive growth factors (Chiang et al. 2013) and reduce variation between batches. One of goals of this field might be to develop a "chemical-only cocktail", which could e.g. reprogram somatic cells (Feng et al. 2009) or restore of the full repertoire of hepatocyte functions in liver cancer cell lines including DMEs.

Following this aim, we identified MEK1/2 inhibitors as potent activators CYP3A subfamily genes in commonly used hepatocellular carcinoma cell line HepG2. These data are of critical importance since CYP3A4 isoform transforms about 30-50% of all clinically used drugs and is known to be poorly expressed in HepG2 cells and other liver models (Smutny et al. 2014). In another study, we found several compounds derived from 2-(3-methoxyphenyl)quinazoline to be "pan-xenosensors" ligands. Since xenosensors such as PXR, CAR, VDR and AhR control the gene regulation of DMEs, we could hypothesize that these compounds are boosters of DME expression in *in vitro* liver models (Smutny et al. 2016).

- **Post-transcriptional and post-translational modifications of NRs involved in a regulation of DMEs**

Insufficient expression of DMEs such as CYPs in both liver cancer cell lines and iHep cells continues to be the problem limiting their application as a suitable surrogate of primary human hepatocytes. One reason is that we do not fully understand mechanisms responsible for CYP expression. The regulation of DMEs is very complex and dictated by the orchestration of various factors such as NRs.

It was reported that the post-transcriptional modification realized by miRNAs can influence expression and activity of DMEs as excellently reviewed elsewhere (Nakajima and Yokoi 2011). In our prediction analysis, we tried to list potential miRNAs targeting key NRs involved in CYP3A4 regulation using four *in silico* programs. We showed that expression of genes encoding PXR, CAR, VDR, HNF4α, RXRα, SHP and GR could potentially be affected by many miRNAs. We and others proposed a potential

contribution of miRNA-mediated regulation of NRs in CYP3A4 variability (Smutny et al. 2015; Takagi et al. 2008). We also suggested that some miRNAs may function as master regulators of NRs since they were predicted to target more than three genes (Smutny et al. 2015). Several reports have been already published demonstrating the impact of miRNAs on DME expression (Mohri et al. 2010; Pan et al. 2009; Takagi et al. 2008). Therefore, we can speculate here that the approaches based on affecting miRNAs (e.g. inhibition) involved in NRs regulation could be adopted to increase expression of NRs with the subsequent increase of DME expression.

PXR and other NRs are regulated not only by the direct ligand binding but they are also subjects of post-translational modifications controlled by cell singling pathways. PXR was shown to be modified by phosphorylation, SUMOylation, ubiquitination and acetylation which in turn alter CYP expression (Smutny et al. 2013).

Based on above noted facts, it emerges clear that better knowledge about the regulatory network controlling DME expression can lead to such cell manipulations which will pay a way to more relevant *in vitro* liver cell models.

- **DILI**

Primary human hepatocytes are wildly accepted as a "gold" standard. They display the highest **sensitivity** in the detection of DILI as assessed by cell-electrode impedance (42% on average; defined as a fraction of truly hepatotoxic compounds predicted by cells from all tested positives; n=16 human hepatotoxic drugs) (Gerets et al. 2012). As further shown, primary human hepatocytes substantially exceeded commonly used human liver cell line HepG2, which revealed a weak sensitivity (6.3%); however, neither primary hepatocytes reached an ideal sensitivity (80-100%). Human liver HepaRG cells appear to be a promising *in vitro* liver cell model, as cells possess high metabolic capacity and CYP inducibility. HepaRG cells gave a surprisingly poor sensitivity in terms of the DILI detection (12.5%), proposing that high metabolic capacity is not necessarily associated with higher sensitivity to predict hepatotoxic compounds. The **specificity** defined as a fraction of non-hepatotoxic compounds predicted by model system to all tested negatives was 100% in this report (Gerets et al. 2012). Similarly, another comprehensive study (n=300 compounds) assigned 50-60% sensitivity and 0-5% false-positive rate to human hepatocytes to detect DILI as determined by measuring

cellular imaging parameters such as reactive oxygen species, mitochondrial membrane potential and intracellular GSH (Xu et al. 2008). With respect to DILI prediction, non-dividing primary hepatocytes are less sensitive to compounds which can potentially alter the cell cycle compared to proliferating cell lines which further supports the superiority of primary hepatocytes (Xu et al. 2008).

The important aspect of *in vitro* toxicity studies is to choose clinically relevant concentration, which can help to discern safer drug candidates. In the work by Gerets and colleagues, the LC_{50} cut-off value distinguishing toxic drugs was set arbitrary to be less than 10 μM (Gerets et al. 2012). Other authors defined maximal tested concentration, a threshold between safe versus toxic compound, as 100-fold of maximum plasma concentration (C_{max}) value reached after single oral-dose administration at a therapeutic dose in humans. Uncertainty scaling factor 100 is a product of three partial factors. Factor sixfold is for a population variability in C_{max} from an average, which encompasses genetic and epigenetic factors altering clearance of the compound. Next factor sixfold represents the higher exposition of the liver to a drug via the portal vein after *per os* administration. Finally, factor threefold reflects the concentration variability of drug resulted from drug-drug and food-drug interactions and potential accumulation of drug after repeated dose (Xu et al. 2008). Such adjustment of safety margin was also considered in another study, where HepG2 cells were employed for prediction of DILI. This work showed that the change of toxicity cut-off over 1-fold, 30-fold and 100-fold of C_{max} value resulted in 4.6%, 39.4% and 67.9% sensitivity, respectively as well as 100%, 90.3% and 75% specificity, respectively. As expected, improved sensitivity leads to decrease in specificity. Relatively good specificity (90.3%) was acquired when 30-fold C_{max} cut-off was used compared to 75% specificity for 100-fold C_{max} (Lin and Will 2012).

Another question is whether target organ-related cell lines can more accurately detect specific organ toxicities. To answer this, Lin and Will evaluated a large array of compounds (n=273 hepatotoxic, 191 cardiotoxic, 85 nephrotoxic and 72 non-toxic) using three different cell lines such as HepG2 (hepatocellular carcinoma), H9c2 (embryonic myocardium), and NRK-52E (kidney proximal tubule) by ATP assay. The authors concluded that different cell lines showed the similar value in detection of general cytotoxicity but the evaluation towards specific organ toxicity does not seem feasible. In other words, prediction efficacy to detect hepatotoxicity using liver-specific HepG2

cells is relatively equal to the efficacy of non-liver specific H9c2 or NRK-52E cells (Lin and Will 2012).

Furthermore, basic cytotoxic endpoints e.g. mitochondrial functions or reduced GSH may hardly predict organ specific toxicity since they are basic reactions of cells on the toxic compound-mediated insult (Lin and Will 2012). It is expected that a toxicology will shift more towards mechanism-based evaluation in future.

In our recent work (Karabanovich et al. 2016), we aimed to study a toxicity of newly synthesized compounds used as potential antituberculotics. Primary human hepatocytes considered as a standard of *in vitro* liver models were used to assess toxicity among promising drug candidates. Moreover, other models such cervical HeLa, liver HuH7 and HepG2 and canine kidney MDCKII-MDR1 cell lines were also used. Maximal tested concentration cut-off was arbitrary set to be 20 μM (taking account of compound solubility). The mitochondrial activity was analyzed as a marker of a cell viability. As revealed from results, most compounds appeared to be non-toxic. However, it was only preliminary screening and more investigation is needed to confirm the safety of these compounds. Used models predicted rather a single cell type toxicity than tissue toxicity because they omitted distinct cell type interactions. The measured parameter like mitochondrial activity is too simple to distinguish specific organ toxicity. Nevertheless, we believe that a current approach enables to remove some highly toxic entities in initial stage of preclinical development.

iHep cells have been suggested as an effective model for toxicological screening. In our preparing manuscript, we deal with the evaluation of HILI on iHep cells and further comparison with commonly used hepatocellular HepG2 cells and primary hepatocytes. For this evaluation, we used several hepatotoxic phytochemicals with different mode of toxicity to validate model sensitivity. Cell viability was estimated by mitochondrial activity (measured by MTS assay) as well as LDH leakage reflecting membrane damage. Saikosaponin D showed higher toxicity in iHep cells than HepG2 cells. Triptolide revealed dose-dependent cytotoxicity in iHep cells. However, no impact on viability markers was found for the treatment with monocrotaline and deoxycalyciphylline B. According to our knowledge, this is first report evaluating the herb-derived hepatotoxicans on an iHep cell model. Such analysis can bring a reference point for tracking of a position of currently available iHep cells for toxicological applications.

10. Future perspectives

It is unrealistic to anticipate that either primary hepatocytes or iHep cells will retain all their properties in simple 2D environment. To reach ultimate goal represented by development of a fully competent *in vivo*-like liver cell model, it will be necessary to combine several strategies at once. Recently, a complex approach was used to yield iHep cells employing stage-specific transduction of hepatocyte transcription factors (FOXA2 and HNF1α) and treatment with soluble factors. To promote hepatocyte maturation, the cells were transferred onto specifically designed plates (Nanopillar Plate) resulting in 3D spheroid formations. Moreover, spheroids were further overlaid by Matrigel. Such iHep cells showed the close resemblance with cultured primary hepatocytes (Takayama et al. 2013).

Thus, to discover optimal hepatic cellular model in future, we should consider pharmaceutical, cellular and molecular biology, technology and medical chemistry expertise.

11. Oral presentations

The Sanofi Prize for Pharmacy, Prague, Czech Republic, 2016

Novel hepatocyte cellular models for drug development

Interdisciplinary seminar for young pharmacologists and toxicologists "Květinův den", Brno, Czech Republic, 2016

Novel hepatocyte cellular models for drug development

5th postgradual and 3rd postdoctoral conference, Faculty of Pharmacy, Charles University, 2015

Novel class of activators of pharmacologically important nuclear receptors

4th postgradual and 2nd postdoctoral conference, Faculty of Pharmacy, Charles University, 2014

In silico identification of microRNAs predicted to target nuclear receptors and other transcription factors involved in the regulation of drug metabolism enzymes

XXVII. Xenobiochemic symposium, Pavlov, Czech Republic, 2013

The effect of cell signaling pathways on function of Pregnane X receptor

3rd postgradual and 1st postdoctoral conference, Faculty of Pharmacy, Charles University, 2013

Mitogen-activated protein kinase kinase 1 and 2 (MEK1 and 2) inhibitor upregulates gene expression of CYP3A subfamily members in hepatocellular carcinoma cells

12. Conference posters

21st International Symposium on Microsomes and Drug Oxidations

Davis, California, USA, 2. - 6. 10. 2016

Human induced pluripotent stem cell-derived hepatocytes as an *in vitro* liver cell model for the evaluation of herb-induced liver injury

20th International Symposium on Microsomes and Drug Oxidations

Stuttgart, Germany, 18. - 22. 5. 2014

U0126, a mitogen-activated protein kinase kinase 1 and 2 (MEK1 and 2) inhibitor, selectictively up-regulates main isoforms of CYP3A subfamily via a pregnane X receptor (PXR) in HepG2 cells

10th International ISSX Meeting

Toronto, Ontario, Canada, 29. 9. - 3. 10. 2013

The effect of ERK signaling pathway inhibition on Pregnane X receptor (PXR)-mediated CYP3A sub-family genes expression

19th International Symposium on Microsomes and Drug Oxidations, 12th European Regional ISSX Meeting

Noordwijk aan Zee, The Netherlands, 17. - 21. 6. 2012

Complex effects of dietary phytochemical sulforaphane on CYP3A4 gene expression

13.Abbreviations

ABC	ATP-binding cassette
ADMET	Absorption, distribution, metabolism, excretion, and toxicity
AFP	Alpha-fetoprotein
AhR	Aryl hydrocarbon receptor
ARNT	Aryl hydrocarbon receptor nuclear translocator
BCRP	Breast cancer resistance protein
BSEP	Bile salt export pump
C/EBPs	CCAAT/enhancer-binding proteins
CAR	Constitutive androstane receptor
CITCO	6-(4-Chlorophenyl)imidazo[2,1-*b*][1,3]thiazole-5-carbaldehyde-*O*-(3,4-dichlorobenzyl)oxime
CYPs	Cytochromes P450
DDIs	Drug-drug interactions
DILI	Drug-induced liver injury
DMEs	Drug-metabolizing enzymes
ECM	Extracellular matrix
ERK	Extracellular signal-regulated protein kinase
ESCs	Embryonic stem cells
EST	Embryonic stem cell test
GR	Glucocorticoid receptor
GSH	Glutathione
GSK3	Glycogen synthase kinase-3
GSTs	Glutathione S-transferases
HCC	Hepatocellular carcinoma
hERG	human Ether-à-go-go-related gene
HILI	Herb-induced liver injury
HNF4α	Hepatocyte nuclear factor 4 α
HUVECs	Human umbilical vein endothelial cells
iHep cells	induced Hepatocyte-like cells
iPSCs	induced Pluripotent stem cells

LDH	Lactate dehydrogenase
MAPKs	Mitogen-activated protein kinases
MDR1	Multidrug resistance protein 1
MEK	Mitogen-activated protein kinase kinase
miRNAs	microRNAs
MNT	Micronucleus test
MRP2	Multidrug resistance-associated protein 2
NADP	Nicotinamide adenine dinucleotide phosphate
NAPQI	N-acetyl-p-benzoquinone imine
NATs	N-acetyltransferases
NRs	Nuclear receptors
NSAID	Non-steroidal anti-inflammatory drug
OATPs	Organic anion transporting polypeptides
OATs	Organic anion transporters
OCTs	Organic cation transporters
PEG	poly(ethylene glycol)
PHEMA	poly(hydroxyethyl methacrylate)
PS cells	Pluripotent stem cells
PVA	poly(vinyl alcohol)
PXR	Pregnane X receptor
ROS	Reactive oxygen species
RXRα	Retinoid X receptor α
SHP	Small heterodimer partner
SLC	Solute carrier
SULTs	Sulfotransferases
TCDD	2,3,7,8-tetrachlorodibenzo-p-dioxin
UGTs	UDP-glucuronosyltransferases
VDR	Vitamin D receptor